A GRAVITY STUDY
IN THE
AMISK LAKE AREA
SASKATCHEWAN

A Thesis

Submitted to the Faculty of Graduate Studies

in Partial Fulfilment of the Requirements

for the Degree of

Doctor of Philosophy

in the Department of Geological Sciences

University of Saskatchewan

by

D.~~J.~~ Don John Gendzwill

Saskatoon, Saskatchewan

July, 1968

A GRAVITY STUDY IN THE AMISK LAKE AREA SASKATCHEWAN

Don J. Gendzwill

ABSTRACT

A gravity and density study of a Precambrian greenstone belt has been made near Flin Flon in the Amisk Lake area of Saskatchewan. Approximately 800 gravity stations were read in the three hundred square mile area and 1585 density determinations were made on bedrock samples taken from a one hundred square mile portion of the area. The gravity field and rock densities are strongly correlated with the different rocks which underlie the region. The density variations associated with the outcropping rock units need extend to various depths less than five kilometers to account for all the gravity relief (29 milligals) observed in the area. Below these depths lies a fairly uniform, low density rock with composition possibly approaching that of granite. Surface seismic measurements and well log velocity and density measurements also indicate the existence of low density material at depth.

Three new interpretation techniques are presented for the quantitative interpretation of gravity anomalies associated with outcropping rock units. The gravity effect of a right rectangular prism is shown to be directly proportional to its width. This fact has been used to develop a set of characteristic curves which permit the interpretation of the depth to the bottom of such a prism whose top is at zero depth. The expression for the gravity effect of the sloping step model has been used to generate characteristic curves for that model whose top is at zero depth. A

mathematical expression has been developed for the gravity effect of a gradational density contrast between two semi-infinite slabs. Type curves and interpretation charts are presented for this model. Fortran IV computer programs which were used in the computations are listed in an appendix.

Rock densities were found to depend almost entirely on their mineral content. Porosity of these igneous and metamorphic rocks is negligible and, to the depths considered, pressure and temperature effects are also negligible. The lightest rock is the Phantom Lake granite (2.656 $\pm$ .017 gm/cc) and the heaviest is the Ruth Lake meta-gabbro (3.042 $\pm$ .066 gm/cc). The mean density of all the samples is 2.862 gm/cc.

The gravity interpretation shows the Reynard Lake granodioritic pluton to be sheet-like in its southern part, the depth to the bottom being about 1000 meters in some places. The northern part of the Mystic Lake granodioritic pluton may be even shallower. The sheet-like portions of the plutons are underlain by basic volcanic or intrusive rock which is in turn underlain by the low density, possibly granitic, rock at depth. Several large basic and ultra-basic dikes and sills lie in a downbuckling of Amisk volcanic rocks east of Amisk Lake. This assemblage extends to a maximum depth of almost five kilometers in the southern part of the area and somewhat lesser depths to the north. Elsewhere, rocks of the Amisk group are about three kilometers deep.

Several rock units not recognized in the detailed geological mapping have been indicated by the geophysical work. These include a possible fine grained basic intrusion between Amisk and Mosher Lakes, an acidic intrusion

near Denare Beach, a basic intrusion under Comeback Bay and one or more large basic to ultrabasic intrusions extending more than ten miles in the center of Amisk Lake.

Some of these interpretations may be interesting from an economic standpoint since both basic intrusions and granodiorite bodies have been thought to be related to ore deposits. In particular, the underside of the sheet-like portions of the granodiorites may be shallow enough to explore with detailed geophysical work and drilling. Also, the existence of previously unrecognized basic intrusions should encourage exploration of these areas with detailed geological and geophysical work and drilling.

ACKNOWLEDGMENTS

The Saskatchewan Research Council has provided the financial and material support necessary for the completion of this thesis. The author has been in the employ of the Saskatchewan Research Council, Physics Division, while doing all of the work described herein, and he gratefully acknowledges the assistance and facilities provided through the Physics Division, and the encouragement of Dr. T.P. Pepper, Head of the Physics Division.

Dr. K.B. Burke of the Department of Geological Sciences, University of Saskatchewan, acted as advisor for this thesis. His assistance and advice on many aspects of the work has been extremely valuable.

Dr. A.R. Byers, Head of the Department of Geological Sciences, and chairman of the thesis committee, has provided much advice and assistance, especially concerning the geology of the Amisk Lake region.

Dr. J.R. Smith of the Geology Division, Saskatchewan Research Council, made available a large number of rock samples which he collected in the East Amisk area. He has also contributed much to the author's knowledge through many long and interesting discussions of the geology of the Amisk Lake area.

The manuscript was typed by Mrs. F. Elvin, Miss Rose Fidgett and Miss Sheila Latsay and the figures were drafted by Richard Reich and Carlos Sardinha, all of the Saskatchewan Research Council.

" 'Cause you never can tell

What goes on down below!

"This pool <u>might</u> be bigger

Than you or I know!"

Dr. Seuss, 1947

McELLIGOT'S POOL

Random House, N.Y.

TABLE OF CONTENTS

TABLE OF CONTENTS (Continued)

TABLE OF CONTENTS (Continued)

LIST OF ILLUSTRATIONS

LIST OF ILLUSTRATIONS (Continued)

LIST OF TABLES

1. INTRODUCTION

1. The Amisk Lake study

The object of this study was to advance the art of gravity interpretation as applied to the study of Precambrian geology, and to investigate a particular area, the Amisk Lake area, with the gravity method. The potential field of a gravitating body is a function of its depth of burial but if a body is large and has a density sufficiently different from the surrounding material, a measurable gravity anomaly results. Gravity measurements therefore are well suited to determine the approximate size, shape, and depth of large geological bodies such as granitic batholiths, sedimentary basins, and large basic intrusive bodies. Gravity measurements have also been used to detect small features such as metallic orebodies or caves provided the depth is not too great.

In the Amisk Lake area, both basic intrusive rocks and granitic intrusive rocks may be related to important mineral deposits (Stockwell, 1960; Smith, 1964, p. 29). An investigation of the depth and shape of such parent rocks would therefore have both theoretical and economic interest. This approach, the use of geophysics to find suitable environments for deeply buried ore deposits, is discussed in the following quotation which underscores the object of this study:

> "Scientific prospecting for metals, which is only about two decades old, has been eminently successful. Geophysicists have probably made the major contribution to this success, in general, on the basis of very limited

> research funds. But research, so far, has been aimed at detection of deposits at shallow depths. Metal exploration now requires geophysics aimed at finding suitable environments, often deeply buried, in which new mining fields may occur. Techniques already developed in oil exploration will be generally suitable".

This statement was made by C.J. Sullivan, President, Kennco Explorations, (Canada) Limited in an address to the Mining Luncheon of the 35th Annual Convention of the Society of Exploration Geophysicists in Dallas, Texas, November 16, 1965.

At the initiation of this study, similar thoughts were considered. Within this thesis are presented the gravity survey, a study of rock densities, new techniques of gravity interpretation and a consideration of geologic, seismic, well logging, and magnetic evidence. These data are combined into an interpretation of the structure and nature of the rocks at depth.

1.2 Similar gravity studies

Detailed gravity and density studies of geological formations and structure have been attempted since relatively portable gravity measuring devices were built. The first publication of a gravity study of igneous and metamorphic rocks is that by Zavaritsky (1924) who describes the use of a pendulum in 1900-1903 to investigate the gravity effect of a platinum bearing gabbro-peridotite massif in the Nijne-Tagilsk region of the Ural mountains. Later, Zavaritzky (1928) used a pendulum and Eötvös torsion balance to further investigate the basic massif. The next important publications were also in the U.S.S.R. Nikoforov et al. (1927 and 1928) and

Alexandrov (1931) published results of pendulum and torsion balance surveys in the Krivoy Rog district. Reich (1931) found negative anomalies associated with the granites of Finland. Sorokin (1934) published a review article of gravimetric methods in prospecting for ores in the U.S.S.R. The first English language publication is by Chamberlin (1935) who investigated the Black Hills-Bighorn-Beartooth region of the Rocky Mountains. Haalk (1932) developed one of the first useful gravimeters. Other gravimeters were rapidly developed and, because of their portability and ease of reading, they became widely used before 1940.

A bibliography is given in Section 1.3. These are selected papers describing gravity and density studies of local and regional geology, mostly where the bedrock is igneous and metamorphic rocks of Precambrian age. The list excludes papers on oil prospecting or those dealing wholly with geodetic and isostatic studies. Some of the listed papers are of particular interest.

Grant et al. (1965) presented a study of the Red Lake greenstone belt in northwest Ontario. He interpreted the greenstones to lie in a basin-like form within the surrounding, lower density gneisses and granitic rocks. According to Grant, the maximum depth of the greenstones is seven kilometers.

In his regional study of northern Ontario and Manitoba, Innes (1960) estimates minimum depths for some greenstones. A greenstone belt near Lake of the Woods is estimated to be at least four kilometers deep at one place and six kilometers at another, lying within low density gneisses.

An area of gneisses near Parry Sound, Ontario was studied by Oldham (1954). Oldham found that dense hornblende gneisses in a basin-like structure extended to depths of fourteen kilometers. If he had considered the possibility of large bodies of amphibolite or other rocks with density close to 3.0 gm/cc, he might have calculated a lesser depth for the hornblende gneisses.

Smithson (1963) studied the Bamble group of metasediments in southern Norway. He found the Bamble group to vary in thickness from 0.5 to 7 kilometers. Several granitic intrusions penetrate the entire thickness of Bamble rocks. Below the dense metasediments, the granitic intrusions are indistinguishable from the gneisses on the basis of density. The granites are considered to be remobilized portions of the gneissic basement.

Bott and Smithson (1967) present a study of a number of granite batholiths. They find that some Precambrian granites are thin or lenticular in shape. Other granites are 5 to 15 kilometers in thickness and might be correctly regarded as batholiths in their form. They conclude that forcible intrusion and piecemeal stoping separately or in combination may have been the mechanism for the emplacement of many granitic plutons. If stoping was important, then a local thickening of the low density crust would also be necessary to compensate for the sunken mass of the stoped material, otherwise positive gravity anomalies would surround granitic plutons. The lack of positive anomalies adjacent to granitic plutons argues against the "basic front" required by granitization theories.

1.3 Bibliography

Alexandrov, S., 1931, Results of Gravity Observations in Krivoy Rog in 1928: Transactions of the Geological and Prospecting Service of U.S.S.R. Leningrad, no. 36, p. 135-139.

Andreev, B.A., 1938, Geological Significance of the Gravity Map of Karelia, of Finland, and of the Leningrad Region: Central Geological Service, Geophysic, no. 7, p. 1-26, Leningrad.

Bacon, L.O., 1957, Relationship of Gravity to Geologic Structure in Michigan's Upper Peninsula: In Snelgrove, A.K. and Others, Geological Exploration, Michigan College of Mining and Technology, Inst. Lake Superior Geology, p. 54-58.

Bacon, L.O. and Wyble, D.O., 1952, Gravity Investigations in the Iron River Crystal Falls Mining District of Michigan: Mining Engineering, v. 4, no. 10, p. 973-979.

Barnes, V. and Romberg, F., 1943, Gravity and Magnetic Observations on Iron Mountain Magnetite Deposit, Llano County, Texas: Geophysics, v. 8, no. 1, p. 32-45.

Barnes, V.E., Romberg, F.E. and Anderson, W.A., 1954, Correlation of Gravity and Magnetic Observations with the Geology of Blanco and Gillespie Counties Texas: International Geol. Cong., Algiers 19th Sess., Comptes Rendus, Sec. 9, fasc. 9, p. 151-162.

Bean, R.J., 1953, Relation of Gravity Anomalies to the Geology of Central Vermont and New Hampshire: Geol. Soc. America Bull., v. 64, no. 5, p. 509-538.

Boronin, V.P., 1960, Fundamental Features of the Internal Structure of the Precambrian Crystalline Basement of the Tatar ASSR According to the Data of Gravity and Magnetic Surveys: Akad. Nauk SSSR, Doklady, v. 132, no. 2, p. 417-420.

Bott, M.H.P. and Smithson, S.B., 1967, Gravity Investigations of Subsurface Shape and Mass Distributions of Granite Batholiths: Geological Society of America Bull.,v. 78, no. 7, p. 859-878.

Chamberlin, R.T., 1935, Geologic Analysis of the Gravity Anomalies for the Black Hills-Bighorn-Beartooth Region: Bulletin of the Geological Society of America, Washington, v. 46, no. 3, p. 393-408.

Elders, W.A., 1963, On the Form and Mode of Emplacement of the Herefoss Granite: Norges Geologiske Undersøkelse, no. 214, p. 5-52, Universitetsforlaget, Oslo.

Fitzpatrick, M.M., 1950, A Gravitational Study of the Clare River Syncline Area, Ontario: Royal Soc. Canada, Trans. 3rd Series, v. 44, sect. 4, p. 21-34.

Frantti, G.E., 1956, Geophysical Investigations in the Central Portion of Michigan's Upper Peninsula: Mining Engineering, v. 8, no. 1, p. 70-72.

Frost, A., McIntire, R., Papenfus, E., and Weiss, O., 1946, The Discovery and Prospecting of a Potential Gold Field near Odendaalsrust in the Orange Free State, Union of South Africa: Chem. Met. Min. Soc. South Africa Journal, v. 47, no. 3, p. 107-141, Johannesburg.

Garland, G.D., 1950, Interpretations of Gravimetric and Magnetic Anomalies on Traverses in the Canadian Shield in Northern Ontario: Dominion Observatory, Ottawa, Pubs., v. 16, no. 1.

Garland, G.D., 1953, Gravity Measurements in the Maritime Provinces: Dominion Observatory, Ottawa, Pubs., v. 16, no. 7, p. 275.

Garland, G.D., 1955, Gravity Measurements Over the Cumberland Basin, N.S.: The Canadian Mining and Metallurgical Bulletin, v. 48.

Grant, F.S., Gross, W.H., and Chinnery, M.A., 1965, The Shape and Thickness of an Archean Greenstone Belt by Gravity Methods: Canadian Journal of Earth Sciences, v. 2, no. 5, p. 418-424.

Grosse, S., 1958, Results of Regional Gravity Surveys in the Western Erzgebirge: Zeitschr. Geophysik, v. 24, no. 4/5, p. 321-325.

Hinze, W.J., 1959, A Gravity Investigation of the Baraboo Syncline Region: Jour. Geology, v. 67, no. 4, p. 417-446.

Innes, M.J.S., 1960, Gravity and Isostasy in Northern Ontario and Manitoba: Dominion Observatory, Ottawa, Pubs., v. 21, no. 6.

Innes, M.J.S., 1957, Gravity and Isostasy in Central Quebec: Am. Geophys. Union Trans., v. 38, no. 2, p. 156-165.

Knapman, W.H., 1955, A Gravity Survey in the Peake and Denison Ranges: In the Geology of the Peake and Denison Region, South Australia Dept. Mines and Geol. Survey, Rept. Inv., no. 6, p. 17-23.

Kopayev, V.V. and Pavlovskiy, V.I., 1957, A Test of the Application of Gravimetry to the Study of the Geologic Structure of the Crystalline Basement in the Central Portion of the Kursk Magnetic Anomaly: Razvedka i Okrana nedr, no. 7, p. 38-46.

Kopf, Manfred, 1963, Density Determinations on Rocks of the Eastern Erzgebirge: Freiberger Forshungshefte, C 144, p. 5-36.

Kopf, Manfred, 1961, Density Values of Rocks of the Erzgebirge and Adjacent Regions: Zeitschr. Angew. Geologie, v. 7, no. 6, p. 301-302.

Kopf, Manfred, Grosse, Siegfried, and Sonntag, Klaus, 1961, Density Determination on Rocks of the Western Erzgebirge: Freiberger Forshungshefte, C 110, p. 5-53.

Krinari, A.I. and Salikov, A.G., 1959, Data for the Study of the Density of Rocks of the Paleozoic of Tatary and the Nature of the Gravity Anomalies: Akad. Nauk, SSSR Kazan Filial Izv. Ser. Geol. Nauk, no. 7, p. 423-432.

Longwell, C.R., 1936, Geological Interpretation of Gravity Anomalies in Connecticut and Massachusetts: Geol. Soc. America Preliminary list of titles and abstracts of papers offered at the 49th Ann. Meeting, Cincinnati.

Medvedev, V. Ya. and Stepanov, P.P., 1960, Density Characteristic of Ancient Units of the West Part of the Tien Shan: Sovetskaya Geologiya, no. 10, p. 81-98.

Miller, A.H. and Innes, M.J.S., 1953, Applications of Gravimeter Observations to the Determination of the Mean Density of the Earth and of Rock Densities in Mines: Dominion Observatory, Ottawa, Pubs., v. 16, no. 4.

Miller, A.H., and Innes, M.J.S., 1955, Gravity in the Sudbury Basin and Vicinity: Dominion Observatory, Ottawa, Pubs., v. 18, no. 2, p. 11-43.

Moiseyenko, F.S., 1965, Density of Rocks and Some Problems of its Study (with English Summ.): Akad. Nauk SSSR Sibirskoye Otdeleniye, Geologiya Geofizika, no. 8, p. 50-65.

Nikiforov, P. Ghirin, S. Terentiev, A. and Veshniakov, N., 1927, Gravimetric Researches of Ferruginous Quartzites in the Region of Krivoy Rog: Bulletin of the Institute of Practical Geophysics, no. 3, Leningrad, p. 322-385.

Nikiforov, P.M., Ghirin, S.K. and Uspensky, G.D., 1928, Gravimetric Prospecting of Ferriferous Quartzites in the District of Krivoy Rog: Bulletin of the Institute of Practical Geophysics, Leningrad, no. 4, p. 315-326.

Oelsner, Christian, 1963, Results of Gravity Measurements in the Eastern Erzgebirge: Frieberger Forshungshefte C 144, p. 37-82.

Oganisyan, S.S., 1955, On the Density of Rocks of Armenia: Akad. Nauk, Armyan. S.S.R., Isv. Ser. Geol. i. Geog. Nauk, v. 11, no. 3, p. 55-62.

Oldham, C.H.G., 1954, The Correlation Between Precambrian Rock Densities and Bouguer Gravity Near Parry Sound, Ontario: Geophysics, v. 19, No. 1, p. 76.

Pavlov, Yu. A. and Parfenov, L.M., 1965, Density Characteristics of Some Metamorphic and Magmatic Formations of the Eastern Sayan: Akad. Nauk. SSSR Sibirskoye Otdeleniye, Geologiya i Geofizika, no. 7, p. 105-108.

Riech, H., 1931, The Importance of Finnish Gravity Measurements for Applied Geophysics: Gerlands Beitrage Zur Geophysik Erganzungshafte fur Angewandte Geophysik, Leipzig, v. 2, no. 1, p. 1-13.

Romberg, F. and Barnes, V.E., 1948, Correlation of Gravity Observations with the Geology of the Coal Creek Serpentine Mass, Blanco and Gillespie Counties Texas (Abs.): Geophysics, v. 13, no. 3, p. 499.

Romberg, F. and Barnes, V.E., 1944, Correlation of Gravity Observations with the Geology of the Smoothingiron Granite Mass, Llano County, Texas: Geophysics, v. 9, no. 1, p. 79-93.

Saxov, S., 1956, A Gravity Survey of the Vicinity of Ottawa: Dominion Observatory, Ottawa, Pubs., v. 18, no. 11.

Sharapov, I.P., 1966, On the Statistical Distribution of the Density of Ore-Bearing Rocks: Izvestia Physics of the Solid Earth, Trans. by Amer. Geoph. Union, no. 5.

Shustova, L. Ye, 1963, Density of the Rocks of Northeastern Part of the Baltic Crystalline Shield: Geofiz. Razvedka, no. 13, p. 72-81.

Smithson, S.B., 1963, A Gravity Investigation of two Precambrian Granites in South Norway: Norges Geologiske Undersøkelse, no. 214, p. 53-140, Universitetsforlaget, Oslo.

Sorokin, L.V., 1934, Application of Gravimetric Methods in Prospecting for Ores in the U.S.S.R.: Transactions of the 7th Conference of the Baltic Geodetic Commission, Leningrad, no. 6, p. 19-25.

Tanner, J.G. and Uffen, R.J., 1960, Gravity Anomalies in the Gaspé Peninsula, Quebec: Dominion Observatory, Ottawa, Pubs., v. 21, no. 5.

Tanner, J.G., 1961, General Characteristics of the Gravity Field in West Central Quebec: Dominion Observatory, Ottawa, Pubs., Gravity Map Series, 1-4.

Tanner, J.G. and McConnell, R.K., 1964, The Gravity Anomaly Field in the Ungava Region of Northern Quebec: Dominion Observatory, Ottawa, Pubs., Gravity Map Series, 5-6.

Thiel, E., 1956, Correlation of Gravity Anomalies with the Keweenawan Geology of Wisconsin and Minnesota: Geol. Soc. America Bull., v. 67, no. 8, p. 1079-1100.

Verem'yev, P.S., 1965, Use of Geophysical Observations in Characterizing the Migmatization of Precambrian Rocks: Akad. Nauk Ukrayin. RST. Heol. Zhur, v. 25, no. 6, p. 76-82.

Weiss, O., 1957, Geophysical Surveys Discover Stilfontein Gold Mine in South Africa: in Methods and Case Histories in Mining Geophysics (Canada), 6th Commonwealth Mining and Metall. Cong., p. 341-345.

Welch, G.J., 1941, Geophysical Study of the Douglas Fault, Pine County, Minn.: Jour, Geology, v. 49, no. 4, p. 408-413.

Wilson, H.D.B. and Brisbin, W.C., 1961, Regional Structure of the Thompson-Moak Lake Nickel Belt: Canadian Mining and Metallurgical Bulletin, v. 54, p. 815-822.

Woollard, G.P. and Steenland, N.C., 1946, Gravity and Magnetic Survey of Cortlandt Complex (Abstract): Geol. Soc. America Bull., v. 57, no. 12, pt. 2, p. 1246.

Woollard, G.P., 1941, Geologic Correlation of Areal Gravitational and Magnetic Studies in New Jersey and Vicinity: Geol. Soc. America Bull., v. 52, no. 12, pt. 2, p. 1942.

Zavaritsky, A.N., 1928, Primary Platinum Deposits of the Urals: Comité Géologique de l'U.S.S.R. Materiaux pour la géologie générale et appliquée, no. 3, Leningrad, p. 1-56.

Zavaritsky, A.N., 1924, Problems of Gravimetrical Investigations in the Region of Nijne - Tagilsk in the Urals: Gorny Journal, Moscow, no. 9-10.

2. THE AMISK LAKE AREA

2.1 Reason for investigation

The Amisk Lake area was chosen as a site for this gravity investigation for several reasons:

1) The entire area was mapped in detail by Byers and Dahlstrom (1954) and Byers et al. (1965). Several problems which were not satisfactorily resolved in the geological studies were thought suitable for study by geophysical means. These include the definition of the shape and depth of acidic and basic intrusions in the area, and the depth of volcanic and sedimentary rocks.
2) It was thought that the variety of rock types in the area would produce large gravity anomalies because the range in density was expected to be large.
3) Systematic sampling of the bedrock in the area east of Amisk Lake had been done by Smith (1964). These samples were available for density determinations.
4) The area is readily accessible from good roads and short water routes.

2.2 Location and topography

The Amisk Lake area (Figure 2.1) is in northeastern Saskatchewan, adjacent to the Manitoba border and immediately south and west of the town

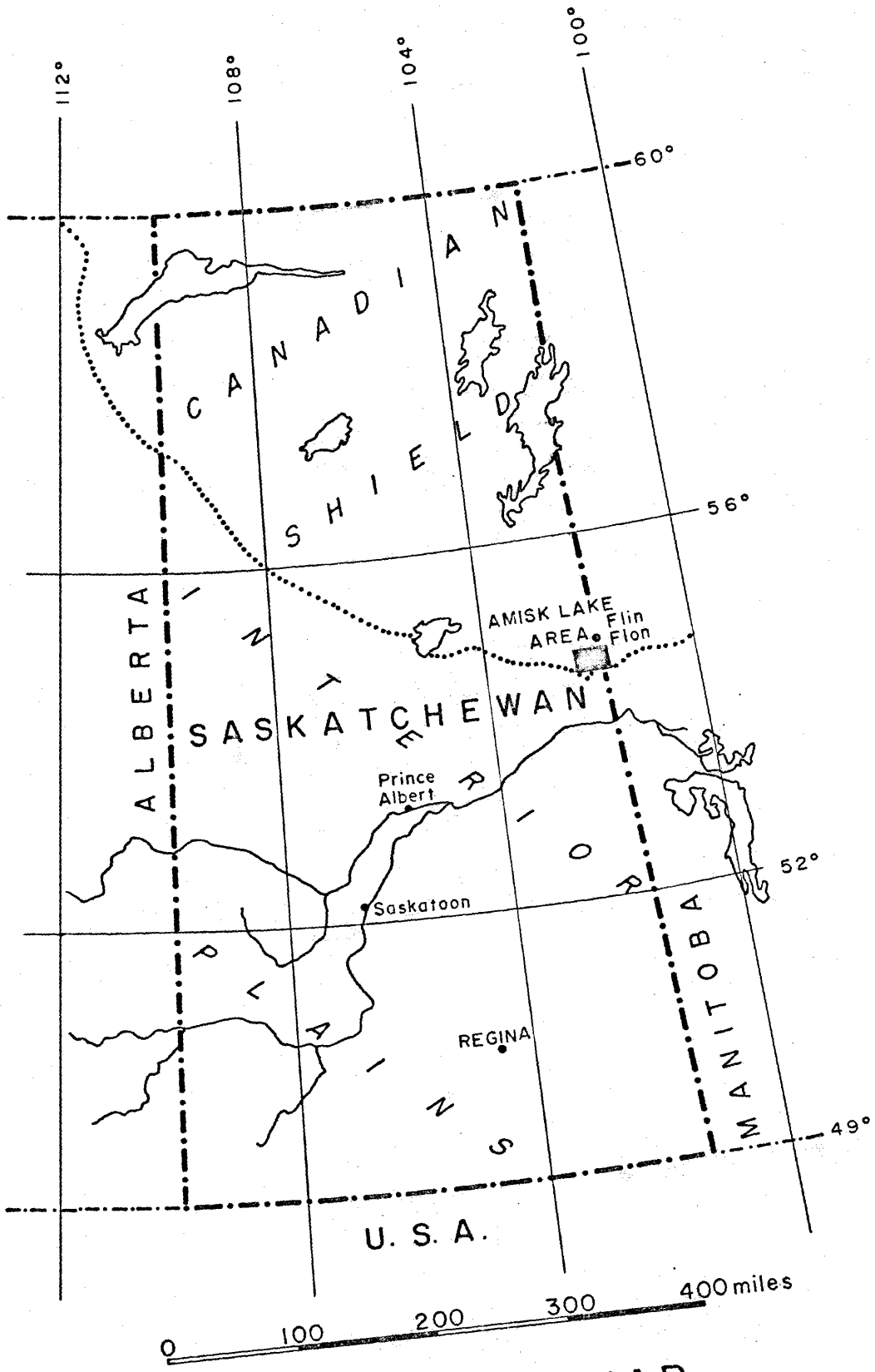

LOCATION MAP *Figure 2.1*

Drawn by
C. S.

of Flin Flon. The map area described in this report extends from latitude 54° 33.8' to 54° 47.3' north and from longitude 101° 50.9' to 102° 23.1' west. The dimensions of the area depicted on the map are 21.9 miles east - west by 15.3 miles north - south.

The topography is locally quite rugged but there is not much total relief. Steep-sided, rocky ridges are separated by swamps and lakes. The largest lake is Amisk Lake, locally known as Beaver Lake, which is about 22 miles long and 12 miles wide. Most of the lakes, including Amisk Lake, are dotted with numerous islands. The maximum depth of the lakes is generally less than 30 feet except for certain portions of Amisk Lake which exceed 115 feet in depth (Saskatchewan Department of Natural Resources, no date). Thick forest composed mostly of spruce, birch, poplar and various willows covers most of the land surface.

2.3 Mineral industry

The chief industry in the area is the Hudson Bay Mining and Smelting Company mines and smelter. The Flin Flon mine, which straddles the inter-provincial border, was discovered in 1914 and production commenced in 1930. By the end of 1963, the mine had produced approximately 53,200,000 tons of ore, averaging 0.085 oz. gold per ton, 1.30 oz. silver per ton, 2.23 percent copper and 4.57 percent zinc (Byers et al., 1965, p. 90). The life of the mine is now known because the ore body has been delimited. The Coronation mine, east

of Table Lake, was operated from 1960 to 1965, when ore reserves were exhausted. This ore body produced 1,412,861 tons of ore whose average grade was 4.25% Cu, (Cairns, 1967). The Birch Lake mine, near the south end of Birch Lake, was opened in 1957 and operated until 1960, when ore reserves were exhausted. The Birch Lake ore body produced 300,819 tons of ore whose average grade was 6.41% Cu. (Hudson Bay Mining and Smelting Co. Annual Reports, 1957, 1958, 1959, 1960.) The Flexar mine, at the north end of Birch Lake, is now being developed.

A number of gold showings exist in the area. Four of the deposits have produced some gold. The Phantom property lies at the south end of Phantom Lake. During exploration of this property in 1960, sample shipments from the vein amounted to 13 tons, which yielded 9.78 oz. gold and 4.87 oz. silver, (Byers et al. 1965). The Newcore deposit, located on the east side of Douglas Lake, produced some gold and arsenic before 1948. In 1949, reserves were 49,000 tons averaging 0.458 oz. gold per ton (ibid.). The Henning Maloney property, near the south end of Bootleg Lake, produced several shipments of gold ore in 1940. This mine was closed in 1941 (ibid.). The Prince Albert deposit, on the northwest side of Amisk Lake, was mined in 1937, 1940, 1941, and 1942. Total production amounted to 5,832 tons, which yielded 4,882.4 oz. gold and 837.1 oz. silver (Byers and Dahlstrom, 1954).

2.4 Access

Access to much of the area is by road from the town of Flin Flon. An all-weather gravel highway (No. 167) extends from Flin Flon to the village of

Denare Beach on the east shore of Amisk Lake, thence south along the shore to the south end of Amisk Lake. A branch extends from a point about 3 miles northeast of Denare Beach southward to the Coronation Mine, passing the Birch Lake minesite and Flexar mine. A railroad track joins the Coronation Minesite to Flin Flon. Much of the rest of the area is served by water routes. Amisk Lake, with its many islands, covers much of the west half of the area. Meridian Creek, from Meridian Lake, through Bootleg, Wekach, Mystic, and Table Lakes provides an excellent canoe route, with two portages, in the east half. The larger, remaining lakes provide access to smaller parts of the area.

3. GEOLOGICAL SKETCH

The geology of the area has been investigated by a number of people. Byers and Dahlstrom (1954) and Byers et al. (1965) give the most detailed account of the geology of the entire area. The following brief account is based mainly on these two reports. On the basis of density characteristics of the various rocks, the writer has grouped some of the rock types that are distinguished in the reports of Byers et al. (1954 and 1965).

Three geological maps are included. The Regional Geology, Flin Flon Area (Fig. 3.1) has been compiled from maps published by the Saskatchewan Department of Mineral Resources, and the Geological Survey of Canada. This map is intended to show the regional geological setting of the area. The more detailed map, General Geology of the Amisk Lake Area (Fig. 3.2), has been simplified from the 1 inch to $\frac{1}{2}$ mile maps of Byers and Dahlstrom (1954) and Byers et al. (1965). Except where specified otherwise, the following descriptions refer to this map. The structural map (Fig. 3.3) shows the major faults and folds in the Amisk Lake area.

3.1 Amisk Group

The oldest rocks in the area are the Precambrian volcanic lavas, and pyroclastic and sedimentary rocks of the Amisk group. On the basis of density they have been divided into basic and acidic units. The basic rocks are largely andesitic to basaltic lavas and pyroclastic rocks, with only minor

amounts of dacitic to rhyolitic rocks. The acidic rocks consist largely of dacitic lavas and dacite breccia, interlayered with minor agglomerate, tuff, rhyolite, trachyte, and andesite. Because of their similar density, acidic pyroclastic rocks and the Amisk sediments are included with the acidic rocks.

Rocks of the Amisk group have been totally metamorphosed to the greenschist facies or to the epidote amphibolite facies. With increase in the grade of metamorphism, the basic lavas grade through all stages of recrystallization until they form simple metamorphic amphibolites indistinguishable from many of the amphibolites in the Kisseynew group of gneisses (Byers and Dahlstrom, 1954, p. 26). In the basic lavas, the original feldspar has been altered to a mixture of epidote, zoisite, chlorite, sericite, and carbonate and any that remains is predominantly oligoclase. Hornblende is always present and is partly to completely chloritized (ibid). The alteration is significant for gravity interpretation because the density of epidote and zoisite ($\approx$3.3 gm/cc) is greater than the density of the original feldspar ($\approx$2.65 gm/cc) and conversely, the density of chlorite ($\approx$2.7 gm/cc) is less than the density of the original hornblende ($\approx$3.2 gm/cc). The acidic lavas and clastic and pyroclastic rocks are also metamorphosed, the original minerals having been partly or completely altered. For convenience, the rocks have been named according to their original composition, e.g. basalt and andesite, or more accurately, metabasalt and meta-andesite.

Basic volcanic rocks (marked with V's on Fig. 3.2) underlie much of the central and eastern portions of the map area. A potassium-argon date for a sample of biotite from this rock taken from the 1,050 level of the Coronation Mine is 1,930 m.y. (Wanless et al., 1965, p. 72). Acidic volcanic rocks (marked with P's on Fig. 3.2) are most common in the western part of the map area and make up a smaller proportion of the volcanic rocks in the central and eastern parts of Amisk Lake. Greywacke and argillite of the Amisk group crop out in a belt extending from the north end of Amisk Lake to the north edge of the map area. Pyroclastic rocks, with interbedded lavas and minor intrusions, extend in an irregular belt from Mystic to Wilson Lakes and make up some of the islands in Amisk Lake. The total thickness of the Amisk group is estimated in the order of 21,000 feet, made up of 10,000 feet of basic volcanic rocks, 7,000 feet of acidic to intermediate flows and breccias and 4,000 feet of clastic sediments (Byers and Dahlstrom, 1954, p. 25).

Amisk rocks are mainly steeply to vertically dipping and isoclinally folded. A series of anticlines and synclines with steep to vertical axial planes, and northerly strike in the southern part, swinging northwest in the northern part have been defined by the geological mapping (op. cit.), and are shown in Fig. 3.3. Some major anticlinal folds are occupied by large granodiorite intrusions (op. cit., p. 75).

3.2 Missi series

Conglomerate, arkose and greywacke of the Missi Series crop out north of Amisk Lake, in the northeast corner of the map area, and in a few small isolated patches not shown on the map. The sediments were derived from the underlying Amisk group. An estimated minimum thickness for the Missi Series in this area is 5,000 feet (op. cit., p. 37). A conglomerate lies at the base, and in several thinner horizons higher in the series, grading upward into arkose and greywacke. An unconformity exists between the Amisk and Missi deposits with angular discordance observed at some, but not all, exposed contacts. In most places the Missi rocks are in fault contact with, or intruded by, surrounding rocks. The Missi rocks north of Amisk Lake are folded isoclinally into the Magdalen Lake syncline (Fig. 3.3) whose axial plane strikes northwest, dips vertically to steeply southwest, and plunges northwest in the map area. The Missi rocks are metamorphosed and, north of the map area, grade into the more highly metamorphosed gneisses of the Kisseynew group (op. cit., p. 50).

3.3 Kisseynew group

Gneisses of the Kisseynew group underlie the northern part of the area covered by the regional geology map (Fig. 3.1). Biotite gneiss and

biotite garnet gneiss are the most abundant rocks of the Kisseynew group. Other gneisses characterized by hornblende, garnet, or pyroxene are common. Amphibolite, quartzite, granulite, and gneissic conglomerate are also found in the group. Byers et al. (1965) conclude that the Kisseynew gneisses are the more highly metamorphised equivalents of Amisk and Missi strata. The hornblende gneisses and amphibolites represent the basic volcanic rocks of the Amisk group, while the biotite gneisses, quartzite, granulite and gneissic conglomerate represent the Amisk acidic volcanic rocks and sediments, Missi arkose and greywacke, and Missi conglomerate.

Kisseynew rocks are intruded by a large number of acidic plutons, usually in a very intimate lit-par-lit fashion. Injection gneisses thus formed are found near the boundaries of large granitic intrusions. Pegmatite intrusions are very common in Kisseynew rocks, but uncommon elsewhere in the area. The gneisses are highly deformed and recrystallized, and detailed structural analysis has not yet been attempted.

3.4 Basic intrusions

Intermediate, basic and ultrabasic sills and dikes (diagonal dashed line, Fig. 3.2) have been intruded into the Amisk rocks and some are also found cutting Missi strata. Pyroxenite, peridotite, and serpentinite, although undifferentiated on the map, are found in continuous belt along the islands and east shores of Table Lake and Ruth Lake. Ultrabasic rocks crop out also

on the southeast shore of Cable Lake, the islands of Mosher Lake, and south east of the east bay of Wolverine Lake. Smith (1964) suggests from aeromagnetic evidence that the west half of the basic intrusion which extends northward from Cable Lake may be underlain by ultrabasic rocks at no great depth.

The basic intrusive rocks lying between Amisk and Mystic Lakes range from meta-diorite to meta-gabbro in composition. Wohlberg (1964) indicates that the body lying east of Ruth and Table Lakes was originally composed of pyroxene and calcic bytownite. Other basic intrusions are mainly meta-gabbro and porphyritic meta-gabbro.

The structure of the basic intrusions is massive in some places and gneissic in others. Wohlberg (op. cit.) considers the zoning in the Ruth Lake sill to be primary and from this concludes that the sill was intruded before regional deformation had ended.

The Boundary Intrusions are a related group of rocks, mainly basic in composition. They are the youngest basic intrusions in the area and are contemporaneous with the Phantom Lake granite. Only the largest of these is shown on the map at the north end of Phantom Lake. It is composed mostly of peridotite.

3.5 Acidic intrusions

The acidic intrusive rocks (denoted by X's on Fig. 3.2) include a wide

variety of compositions, structural settings, and ages. Numerous minor porphyritic dikes and sills intrude the Amisk rocks and in some areas, notably the Hannay Bay area and the central eastern part of Missi Island, constitute more than 50 per cent of the bulk of the rock. Some of the islands of the east channel of Amisk Lake are composed largely of porphyritic intrusions. "Quartz-eye" diorite underlies the southern part of the southwest peninsula and the north central part of Missi Island, but is undifferentiated from the porphyritic intrusions on the map. "Quartz-eye" diorite also outcrops in several locations in Comeback Bay and between Table Lake and Amisk Lake, and cuts both Amisk and Missi rocks.

Granodiorite forms large intrusive masses underlying much of the area. They are generally elongated parallel to the regional structure and show concordant relationships to the country rocks. They are considered to be syntectonic with the major regional deformation and occupy anticlinal positions. One pluton, the Reynard Lake mass, which extends from Mystic Lake to the north edge of the area, is a zoned structure with a core (outlined on the map) of porphyritic microcline granodiorite. Surrounding the core is a discontinuous zone of biotite granodiorite, enclosed by a contaminated border zone. The contaminated border zone is a heterogeneous complex of volcanic, sedimentary, granodioritic and other intrusive rocks. Angular

inclusions of country rock and of the intrusive rocks themselves are abundant. Contacts with volcanic rocks are sharp, but contacts with basic intrusions are sometimes difficult to define because many of the rocks of the contaminated border zone are essentially foliated amphibolites, closely similar to the amphibolitic intrusion west of Mystic Lake (Smith, 1964). A potassium-argon age for biotite from the Reynard Lake pluton is 1,705 ± 80 million years (Lowden et al. 1963, p. 66), which is typical of the Hudsonian orogeny.

The Mystic Lake pluton, which lies largely between Kaminis and Mystic Lakes, is not as well defined as the Reynard Lake mass. It consists mostly of hornblende granodiorite with variable quantities of mafic minerals and quartz. Some parts of the Mystic Lake pluton near its west boundary consist of quartz diorite.

A portion of the Annabel Lake pluton is in the map area northeast of Meridian Lake. It consists of relatively uniform, foliated, relatively mafic rich, hornblende granodiorite (Smith, 1964). A portion of the Wolf Lake mass, mainly biotite granodiorite, lies on the west edge of the map area, northwest of Oddan Lake. Albite granite forms a small boss-like intrusion, north of Stitt Lake. The Neagle Lake intrusion occupies the northwest corner of the map area. This intrusion, and the two smaller intrusions between it and Amisk Lake, are post-tectonic in age. The Neagle Lake body is largely

granodiorite but ranges from granodiorite to gabbro in composition. Stockwell (1961) gives a potassium-argon date of 1,730 ± 80 million years for biotite from this body.

The Phantom Lake granite underlies the southern part, and southwest shore, of Phantom Lake and intrudes Amisk rocks and the Mystic Lake pluton. It is composed of low density, pink to reddish, porphyritic microcline granite. It is outlined on the map to distinguish it from the Mystic Lake pluton. The Phantom Lake granite intrudes, and is intruded by, the Boundary Intrusions. Wanless et al. (1965, p. 80) give a potassium-argon age for biotite from Phantom Lake granite of 1,865 ± 65 m.y.

3.6 Phanerozoic rocks

Flat-lying, Ordovician dolomite and sandstone overlie the older Precambrian rocks along the southern edge of the map area. Unconsolidated Pleistocene glacial deposits are irregularly distributed over all older formations.

3.7 Faults

Many faults cut the Precambrian rocks in this area. The major ones are indicated on the structural map, Fig. 3.3. The Ross Lake fault, which

is in the extreme northeast corner of the map area, is the most prominent fault (in its area) and has been traced by geological mapping for over 25 miles. Left-hand strike slips have been estimated at 600 feet, 850 feet, and 1,750 feet in three different places, all with the east side moving up with respect to the west.

The Cliff Lake fault, a mile or two east of the map area, is a reverse fault with dip slip of at least 3,000 feet, and the east side thrust up and to the west.

The Creighton Creek fault and the Triangle Lake fault are both just north of the northeast corner of the map area. These faults also show left hand strike slip and reverse, dip slip, with the east side moving up and to the north.

The Annabel Lake fault, an east-striking fault several miles north of the map area, has drag folds near it, indicating the north side to have moved up, and to the southwest, with respect to the south side.

The West Channel fault zone through the west channel of Amisk Lake is indicated to have a reverse oblique movement, shown by tension fractures and drag folds. The west block, or hanging wall, has been moved up and to the southeast.

The above named faults are those listed by Byers et al. (1954 and 1965) with the sense or amount of movement defined.

The MacDonald Creek fault, which forms the southwest contact of the block of Missi sediments, north of Amisk Lake, must have a large, dip slip, with the west side moved up since it has cut out the entire basal conglomerate, about 600 feet thick, of the Missi series in the Magdalen Lake syncline. Similarly, the positions of the Mosher Lake fault and the Wilson Lake fault, which form parts of the northeast contact of the same unit of Missi rocks, suggest that the northeast walls of these two faults have moved up with respect to the southwest walls, at least where the faults cut Missi rocks, although the movement has not been suffieient, in these cases, to remove entirely the basal Missi conglomerate.

In spite of the lack of direct evidence for these inferred movements, there are two reasons to suggest them. Firstly, the suggested movements would have preserved the existing Missi sediments from erosion. Secondly, if the west block had been moved down along the MacDonald Creek fault, we should expect to find the missing Missi rocks somewhere along the downthrow side. Only one small patch of Missi conglomerate appears southwest of the MacDonald fault and it has been preserved there by local down faulting, consistent with the suggested movement up of the west side of the major fault.

A number of faults have been mapped along the eastern islands and shore of Amisk Lake, more or less in line with the MacDonald Creek and

Mosher Lake faults, but no movements have been determined for these. Numerous other faults occur in the area but no data have been reported as to their individual movements or possible cumulative movement. Froese (1963) shows that the joints and minor faults in the Coronation Mine area are the result of a local compressional force oriented in an ENE by WSW azimuth. Most of the movements are strike-slip, with very little dip-slip component. It is assumed that they do not cancel the movements on the faults described above.

It is likely that these faults, combined with the deformation of the Magdalene Lake syncline, are responsible for the preservation of the Missi sediments. A continuation of the fault pattern, combined with the deformation of the Denare Beach syncline may have moved the Amisk rocks downward, increasing the total depth of volcanic rocks East of Amisk Lake. Gravity anomalies discussed later, support this theory.

4. PREVIOUS GEOPHYSICAL INVESTIGATIONS

4.1 Regional gravity

The Dominion Observatory is currently conducting a program of gravity measurements in Canada (Tanner, 1967).

Bouguer gravity values at stations established within the area of National Topographic series map sheets 63L-9, 10, 15, 16 and 63K - 11, 12, 13, 14 are shown in Figure 4.1, Regional Gravity Map. These data were supplied by the Dominion Observatory (McConnell, 1966, Written Communication).

The station interval (approximately 8 miles) on this map is generally too broad to be useful in detailed geological studies, especially in comparison with the regional geology map. Nevertheless several interesting features are indicated. The prominent gravity high east of Amisk Lake is related to basic intrusive and extrusive igneous rocks. The gravity high north east of Flin Flon may be related to a series of basic and ultrabasic intrusive rocks described by Bateman and Harrison (1945). A broad anomaly south of Hanson Lake in the western part of the map suggests that the Amisk rocks of that area, mapped by Byers (1957), may extend southward under the sedimentary cover for some distance. Southwest of Athapapuskow Lake, an area of basic volcanics, mapped by Tanton (1941), is covered by a gravity high which extends southward over the sedimentary rocks. More detailed gravity surveys in these areas could indicate the extent of the greenstones. Other gravity highs and lows are probably related to basic and

acidic igneous rocks, but some well-defined geological units are not reflected in the gravity anomaly map, because the gravity station spacing is too broad.

The mean Bouguer anomaly for the 136 stations plotted on the map is -39.7 milligals. The mean Free Air anomaly is -4.9 milligals and the mean elevation is 1,027 feet. Innes (1960, p. 323) gives anomaly values for northern Ontario and Manitoba, the large area investigated by him, which includes the Flin Flon region. He also gives a chart showing the various gravity anomalies compared to mean elevations for different parts of his area. The following table compares the various gravity anomalies for northern Ontario and Manitoba with those for the Flin Flon region.

Table 4.1

Comparison of the gravity anomalies in the Flin Flon area with those in Northern Ontario and Manitoba (Innes, 1960)

	N. Ont. and Man.	Shore of Hudson Bay	Elevation 1027 N. Ont. and Man.	Flin Flon Region
Mean Bouguer	-39.6	-36.8	-39.2	-39.7
Mean Free Air	- 7.1	-31.5	- 4.3	- 4.9
Mean Isostatic (Hayford)	-11.3	-34.8	- 7.5	- 6.0
Mean Elevation	909		1,027	1,027
No. of stations	857		--	136

The gravity field in the Flin Flon area is generally similar to that for comparable elevation (1,027 ft.) in Northern Ontario and Manitoba. A mean isostatic anomaly of -34.8 milligals is found near the shore of Hudson Bay and Innes (1960) attributes this to incomplete isostatic adjustment following deglaciation. The anomaly indicates that Hudson Bay may yet have about 800 feet to rise isostatically (op. cit., p. 326). In the Flin Flon area, the mean isostatic anomaly is only -6.0 milligals which is smaller than that found near Hudson Bay and smaller even than the mean for Northern Ontario and Manitoba. This implies that the isostatic adjustment is nearly complete for the Flin Flon area compared to the shore of Hudson Bay or the intervening regions.

According to Jeffreys (1962), large isostatic anomalies with dimensions of up to 50 kilometers can easily be supported by the strength of the crust and small anomalies may persist over much larger areas. Therefore it is problematical whether or not the -6.0 milligal anomaly in the Flin Flon area represents any possible future isostatic movement.

4.2 Aeromagnetic maps

The Department of Mines and Natural Resources of Manitoba, the Department of Mineral Resources of Saskatchewan and the Geological Survey of the Department of Energy, Mines and Resources of Canada have published aeromagnetic maps of the Flin Flon area. Figure 4.2 is a compilation by the Saskatchewan Research Council of portions of maps 2454G Flin Flon 63 K/13, 2453G Athapapapuskow Lake 63 K/12, 4606G Denare Beach 63 L/9, and 4596G Annabel Lake 63 L/16.

Magnetic data shown on this map were obtained in aircraft flying at a nominal height of 1,000 feet above the land surface, along the flight lines shown which are generally ½ mile apart. A more detailed aeromagnetic map is also available for the area east of Amisk Lake (Map 1028G, Coronation Mine Area).

The total field intensity on the map varies from 60,400 gammas to 62,900 gammas. Magnetic values in the eastern part of the map are referred to an arbitrary base (about 2,000 gammas). To convert these to total field values 58,700 should be added to each contour number.

The variations in the magnetic intensity shown on the map are mainly caused by magnetic minerals, chiefly magnetite which is a minor constituent in many rocks. Basic and ultrabasic igneous rocks usually contain more magnetite than acidic igneous rocks or sedimentary rocks, but this is not universally true and many exceptions are found. In general, it is impossible to identify the source of a magnetic anomaly, unless the anomaly can be correlated with a known rock unit.

In the Amisk Lake area, some of the magnetic anomalies can be correlated with mapped rock units. The most prominent anomalies are a series of "highs" which parallel the east shore of Amisk Lake, and extend in a northeasterly direction to Phantom Lake. A second prominent anomaly occupies the center of Amisk Lake, extending south from Missi island. The series of anomalies are associated with ultrabasic rocks and basic dikes and sills east of Amisk Lake, on islands in the center of Amisk Lake, and with the Boundary Intrusions in the Phantom Lake area.

On the basis of the magnetic anomaly, Smith (1964) has suggested that ultrabasic rocks occur at no great depth in the basic intrusive rock which outcrops on the eastern shore of Amisk Lake. The magnetic anomaly in central Amisk Lake strongly suggests that the central and deepest portions of Amisk Lake also are underlain by basic or ultrabasic rocks such as outcrop on some of the islands. The anomaly in the southern part of Phantom Lake suggests that a Boundary Intrusion may lie under the water, more or less as a continuous unit with the intrusions of the northern part of the lake. Stockwell (1960) points out that the Phantom Lake (Kaminis) granite intrudes a Boundary Intrusion on the east shore of Phantom Lake. In the southern part of the lake, this granite forms the western shore and some islands. Therefore the granite may form an intrusive contact with the Boundary rock under the southern part of the lake. Other anomalies are associated with basic segregations of larger acidic intrusive units, such as the quartz diorite portions of the Mystic Lake pluton.

The Missi sediments are also characterized by distinctive magnetic anomalies. These anomalies can be traced continuously to the west and north into areas underlain by Kisseynew gneisses, thereby supporting the conclusion of Byers and Dahlstrom (1954) that the Kisseynew rocks are more highly metamorphosed equivalents of Amisk and Missi strata.

4.3 Seismic investigations from the surface

Figure 4.3 is an enlarged version of a chart published by Volarovich et al. (1967) using data on magmatic rocks from Kazhakistan and incorporating results of Birch (1964). This diagram shows that the compressional wave velocity of rocks increases with both pressure and density of the rock, as is well known. The rate of increase of velocity of a rock with a particular density may be estimated from this chart. Pressures up to 10 kilobars have a negligible effect on the density of most igneous and metamorphic rocks (Clark, 1966).

The Geological Survey of Canada (Whitham, 1967, p. 36) has carried out reflection and refraction studies to distances of 20 miles, near Flin Flon. A velocity of 19,500 feet per sec (5.94 km/sec) was observed with at least four reflection events, the deepest at four seconds.

Hall and Brisbin (1965) and Burke (1968) have conducted large scale seismic refraction studies in the Flin Flon area, using the abandoned and flooded North Star mine at Thompson Lake, Manitoba for a shot point. Thompson Lake, about 12 miles east of Flin Flon, is in an area of Amisk volcanic rocks similar to those surrounding Amisk Lake. Hall's and Brisbin's profile extends southward to Mafeking, Manitoba, but Burke's profile lies along the Hanson Lake road, west of the shot point, passing immediately north of Amisk Lake. The first three of Burke's six recording sites are shown on Figure 3.1, Regional Geology.

Hall and Brisbin (1965) give the following results for the area immediately south of Thompson Lake:

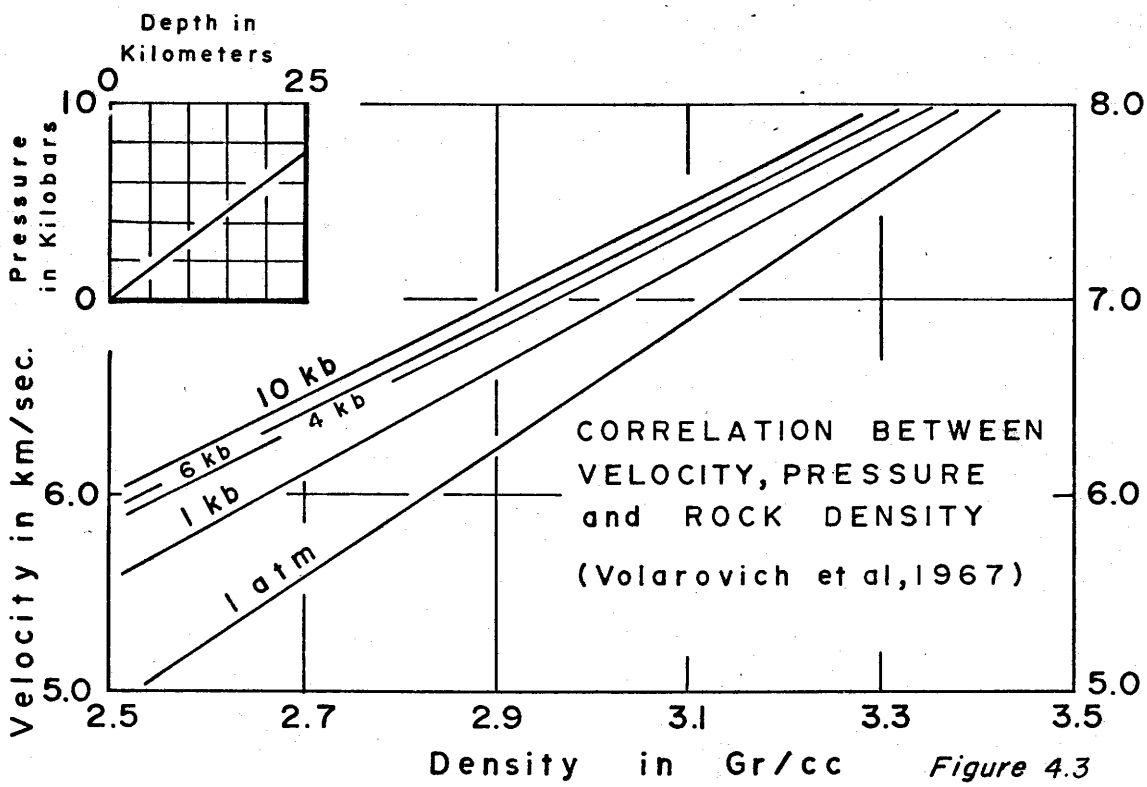

Figure 4.3

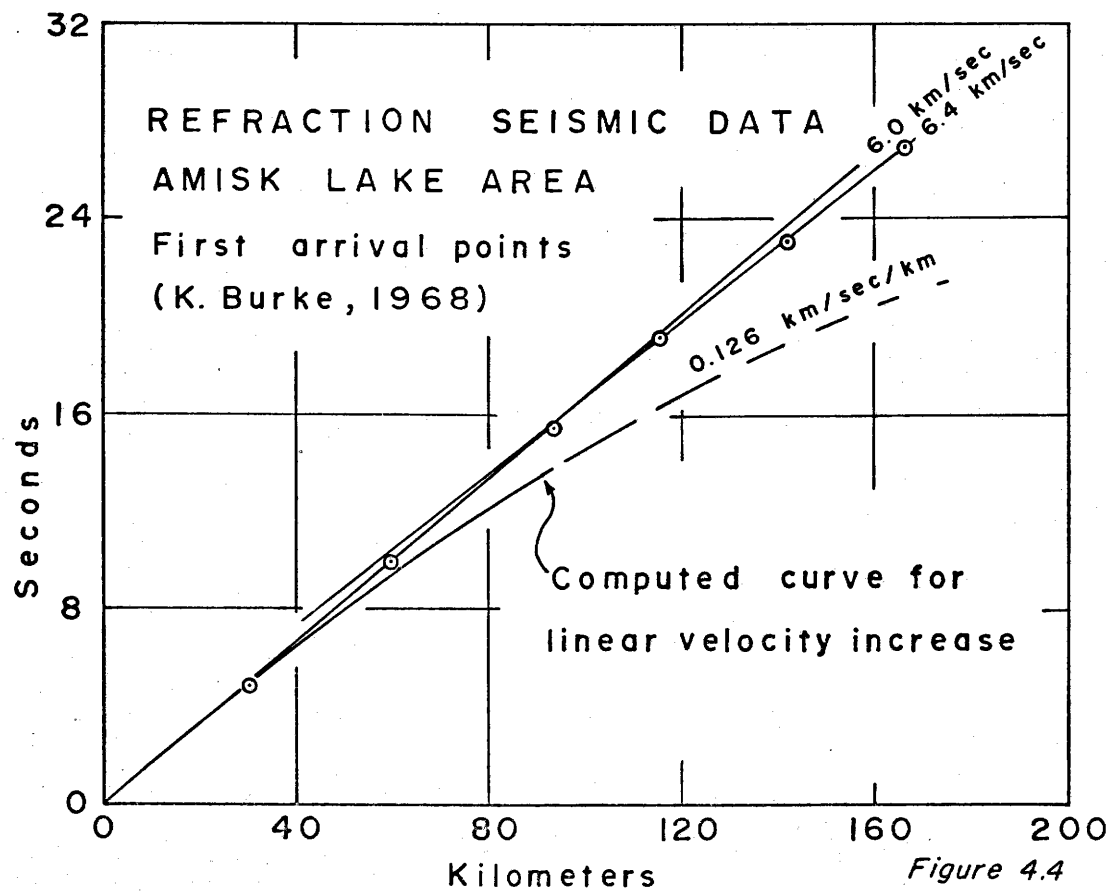

Figure 4.4

Table 4.2

	P wave Velocity	Density	Depth to Top
"Granitic" Layer	6.15 ± .05 km/sec	2.82 gm/cc	0
"Basaltic" Layer	6.65 ± .10 km/sec	2.95 gm/cc	15.5 ± 1 km
Upper Mantle	7.90 ± .10 km/sec	3.34 gm/cc	34 ± 1 km

The "basaltic" layer and upper mantle rise to shallower depths further south in the vicinity of the Churchill - Superior block boundary.

Burke (1968) lists the following data for the Hanson Lake road profile.

Table 4.3

	P Wave Velocity	Depth to Top
Layer I	6.0 km/sec	0
Layer II	6.4 km/sec	10 km
Upper Mantle	8.0 km/sec	~40 km

Figure 4.4 is a plot of the distances and first arrival times of the Hanson Lake road profile. Also plotted is the expected time of arrival if the velocity were to increase downward at the rate of 0.126 km/sec per kilometer depth. This rate is interpolated from figure 4.3, assuming a density of 2.86 for the near surface rocks. It should be noticed that the second layer velocity of 6.4 km/sec would be exceeded at a depth of about 3.2 km, at the assumed rate of increase.

According to Volarovich et al. (op. cit.), the largest change in velocity due to pressure occurs in the low pressure range, 0 to 4 kilobars, because of compaction and closing of fractures in the rock. Observed velocities in the two seismic profiles are constant to depths of 10 and 15 km. Evidently, some factor other than pressure alone is acting to maintain the velocity at a constant value. A decrease in the bulk density with corresponding changes in the elastic moduli of the rocks at depth could produce the observed effect.

Velocities of 6.0 to 6.15 km/sec at pressures in excess of 1,000 bars are characteristic of certain varieties of low density rock (Clark, 1966, p. 198).

The following table is extracted from a larger one. It lists some rocks with velocity of 6.00 km/sec or less at 1,000 bars pressure as given by Clark (op. cit.).

Table 4.4

Rock	Density gm/cc	Velocity km/sec. 1,000 bars	2,000 bars
Serpentinite (Thetford, Quebec)	2.601	5.67	5.73
Granite, Westerly, R.I.	2.619	5.84	5.97
Granite, Stone Mt., Ga.	2.625	5.94	6.16
Granite, Chelmsford, Mass.	2.626	5.91	6.09
Gneiss, Pelham, Mass.	2.643	5.91	6.06
Quartz Monzonite Porterville, Cal.	2.644	5.95	6.07
Sandstone, Catskill, N.Y.	2.659	5.27	5.44
Prophyllite ("lava")	2.662	4.73	5.02
Graywacke, New Zealand	2.679	5.76	5.87
Graywacke, Quebec	2.705	5.92	6.04
Slate, Medford, Mass.	2.734	5.79	5.91
Granodiorite Gneiss Bethlehem, N.H.	2.758	5.95	6.07

A variety of rocks is listed in the table. Although other rocks of low density have higher velocities, none of the high density rocks listed by Clark (op. cit.) have low velocities. Thus, low density is a necessary, but not sufficient, condition for low velocity.

In the Amisk Lake area, granite, granodiorite, and quartz diorite, all low density rocks, have been observed to intrude the older, denser, lavas, presumably after rising from unknown depths. Therefore, it is likely that the low seismic velocity observed to depths of 10 km is due to the widespread presence at depth of low density, acidic rock.

4.4 Geophysical well logs

During the winter of 1965-66, a series of bore holes were drilled in the JXWS drilling project near the R.C.A.F. Joint Experimental Weather Station near Flin Flon. The drilling project was carried out by Defence Construction (1951) Ltd. with technical assistance provided by the Geological Survey of Canada. Schlumberger of Canada Ltd. provided well logging service in the deep (10,060 feet) bore hole "A". Copies of the logs, core and cutting samples, were provided to the Saskatchewan Research Council through Dr. C.H. Smith of the Geological Survey of Canada. A description of the drilling project and the geology was written by Findlay (1966).

JXWS borehole "A" was collared at 54°43.25' N. latitude and 101°59.75 W longitude.

Figure 4.5 is a location sketch. The site is within the microcline porphyry core zone of the Reynard Lake granodiorite pluton. The hole was drilled through the core zone and a section of biotite granodiorite, finishing in the "contaminated border zone" of the pluton.

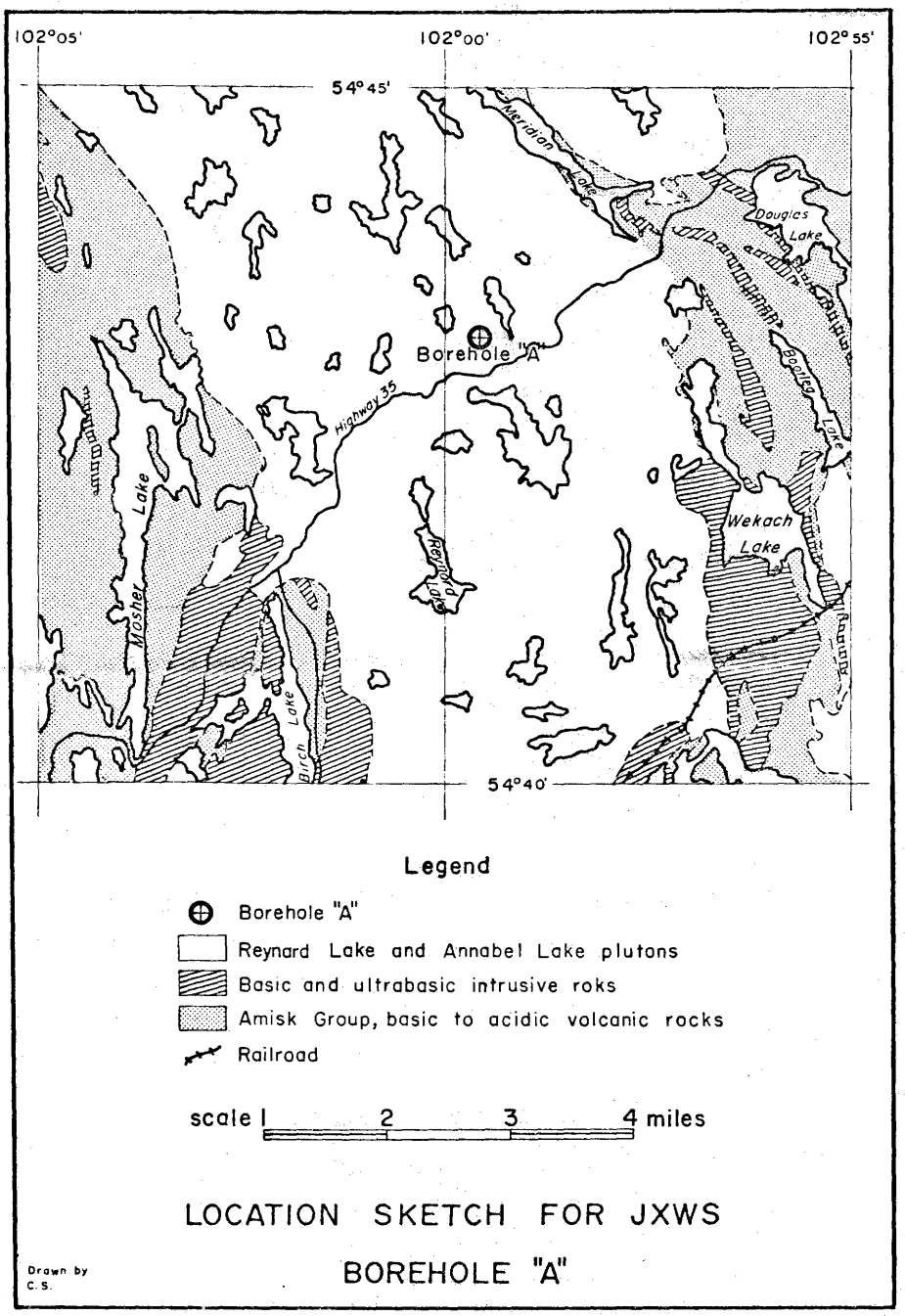
102°05'
102°00'
102°55'
54°45'
54°40'
Meridian Lake
Douglas Lake
Borehole "A"
Highway 35
Mosher Lake
Reynard Lake
Birch Lake
Wekach Lake
Legend
Borehole "A"
Reynard Lake and Annabel Lake plutons
Basic and ultrabasic intrusive roks
Amisk Group, basic to acidic volcanic rocks
Railroad
scale 1 2 3 4 miles
LOCATION SKETCH FOR JXWS
BOREHOLE "A"
Drawn by C.S.

Figure 4.5

Findlay (1966) summarizes the geology of JXWS as follows:

0 - 860 feet	Granodiorite, in part quartz monzonite, minor quartz diorite
860 - 7,570 "	Mainly quartz diorite and leucocratic quartz diorite, minor granodiorite
7,570 - 10,060 "	Mainly mafic quartz diorite and quartz diorite

Contacts are broadly transitional and thus their positions are only approximate. Compositional layering is indicated in cutting samples and cores. Small granitic or aplitic dikes are fairly common, and dark green, chlorite-rich, schist fragments are common throughout the section.

The three broad groupings are equivalent to Byer's et al.(1954) and (1965) terminology as follows:

0	-	860	feet	Porphyritic microcline granodiorite
860	-	7,570	"	Biotite Granodiorite
7,570	-	10,060	"	Contaminated Border Zone

Ten different geophysical logs were run in the hole. These are tabulated below.

Table 4.5

1. Bulk Density Log
2. Caliper Log
3. Gamma Ray Log
4. Sonic Interval Transit Time Log
5. Seismic Reference Service Geophysical Log
6. Neutron Log
7. Directional Log
8. Continuous Dipmeter Log
9. Cement Bond Log
10. Depth Determination Log

Figure 4.6 is an abbreviated version of the density log, the seismic interval velocity log and the average velocity log. The interval velocity log represents a measured velocity at each sample point. The average velocity is derived from the integral of the interval velocity log and represents the apparent velocity that would be observed if a seismic pulse travelled from the datum level to a single detector at any particular level. The density log measures the apparent bulk density of the formation with a gamma radiation technique. The other logs are not relevant to this work.

A low velocity was measured in the upper few feet of the hole. There is about three feet of overburden at the hole site (Findlay, 1966) but this is not sufficient to account for the velocity anomaly. There must also be a "weathered"zone in the granodiorite which may extend as deep as a hundred feet, since the first velocity plotted at 100 feet depth is anomalously low. Alteration in the granodiorite at surface is not present, or else quite minor (Byers et al. 1965, p. 35) so the "weathered zone" is not a chemically weathered zone but is related to something else, possibly fractures in the rock due to the action of frost.

The interval velocity log shows a general decrease from about 200 feet to about 3,200 feet and thereafter increases except for local variations. There appears to be a step increase in the velocity at the contact between leuco-quartz diorite and the denser mafic quartz diorite at about 7,200 feet. The velocities appear to be approximately linear along three segments so straight line fits by the least squares method were made for these segments, excluding a few

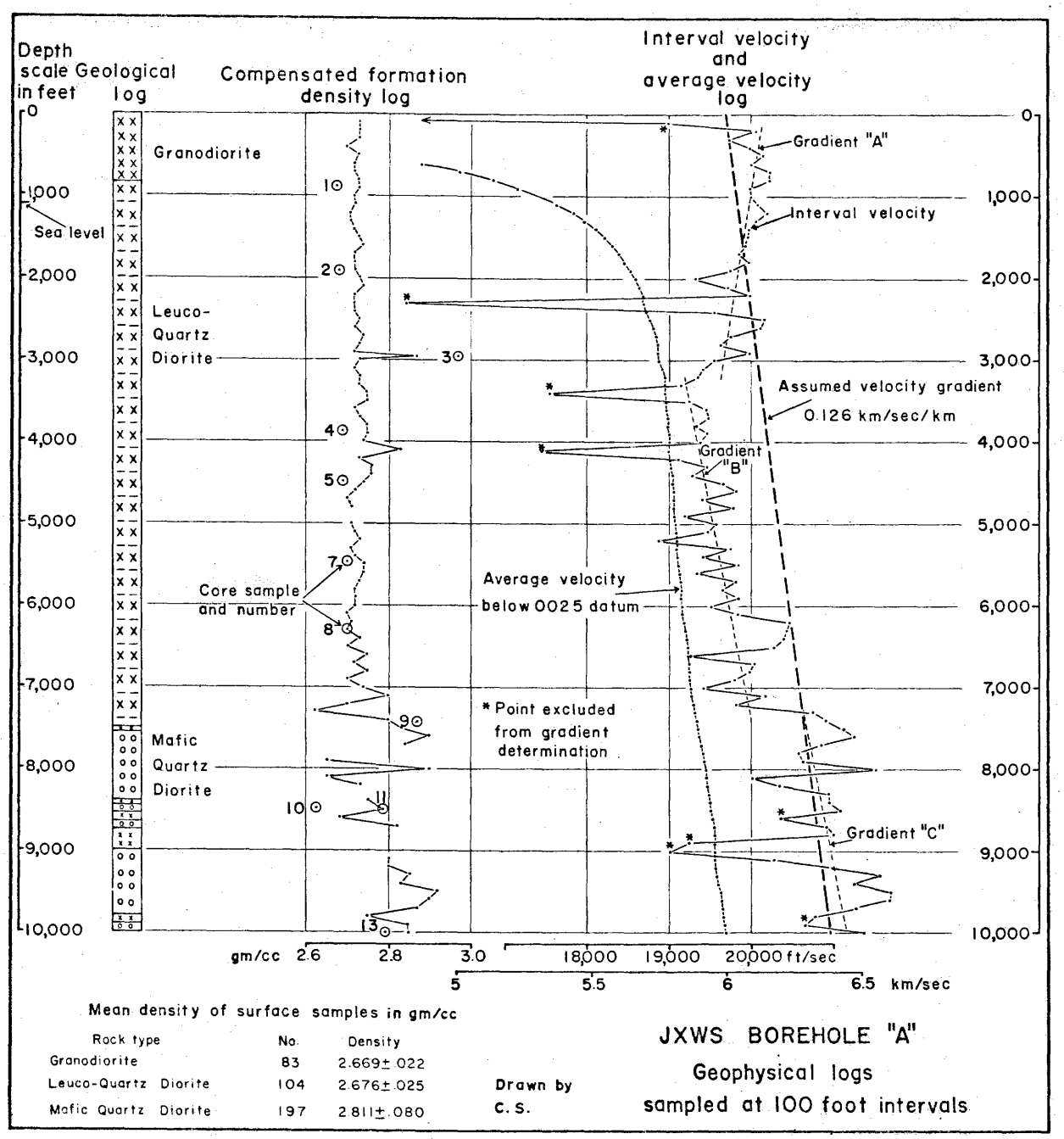
Depth scale in feet
Geological log
Compensated formation density log
Interval velocity and average velocity log
Granodiorite
Leuco-Quartz Diorite
Mafic Quartz Diorite
Sea level
Gradient "A"
Interval velocity
Assumed velocity gradient
0.126 km/sec/km
Gradient "B"
Average velocity below 0025 datum
Core sample and number
* Point excluded from gradient determination
Gradient "C"
gm/cc
ft/sec
km/sec
Mean density of surface samples in gm/cc
Rock type | No. | Density
Granodiorite | 83 | 2.669± .022
Leuco-Quartz Diorite | 104 | 2.676± .025
Mafic Quartz Diorite | 197 | 2.811± .080
Drawn by C. S.
JXWS BOREHOLE "A"
Geophysical logs
sampled at 100 foot intervals

Figure 4.6

widely divergent points and several low values due to quartz diorite in the mafic quartz diorite section.

Table 4.6

	From	To	Slope km/sec/km	Intercept
Gradient "A"	200	3,200	-.163	20,160
"B"	3,200	7,200	.19	18,580
"C"	7,200	10,000	.204	19,220

Also shown on the sketch is the 0.126 km/sec/km gradient interpolated from figure 4.3 in section 4.3.

Gradient "B" and gradient "C" have about the right size and sense to be attributed to the pressure effect on velocity. The opposite sense of gradient "A" is unexplained.

In the lower part of the hole, the interval velocity exceeds 6.0 km/sec, more than the velocity observed by Burke (1968) to a depth of 10 km, and more than the 5.94 km/sec reported by Whitham (1967). A maximum velocity of 6.71 km/sec was reached in mafic quartz diorite. The velocity of the leuco-quartz diorite, if extrapolated to 10,000 feet, is 6.24 km/sec.

The pressure effect on velocity of igneous rocks is important to a pressure of about 4 kilobars (Volarovitch et al., 1967). The pressure at 10,000 feet depth in rock is only about 1 kilobar, therefore, the velocity

should continue to increase with depth if the rock type remains the same. Since the velocities at 10,000 feet for both mafic quartz diorite and leuco-quartz diorite rocks exceed the velocity observed in deep seismic sounding, it must be concluded that the rock type changes with depth. Laboratory measurements on rocks indicate that certain types of granite or granite gneiss have the necessary properties.

Eleven core samples from various depths and cutting samples at 10 foot intervals were supplied for analysis. The densities of the core samples were measured in the laboratory and are listed below.

Table 4.7

Sample No.	Depth	Description	Density
1	988.7 - 989.0	Quartz Diorite	2.668
2	1901.5 - 1901.9	Quartz Diorite	2.679
3	2949.1 - 2949.5	Chlorite biotite schist	2.969
4	3866.8 - 3856.0	Leuco-Quartz Diorite	2.689
5	4495.3 - 4495.6	Leuco-Quartz Diorite	2.690
7	5471.5 - 5471.9	Quartz Diorite	2.700
8	6294.0 - 6294.4	Quartz Diorite	2.700
9	7409.7 - 7410.1	Mafic Quartz Diorite	2.868
10	8496.5 - 8496.7	Granitic Dike	2.624
11	8498.0 - 8498.2	Mafic Quartz Diorite	2.789
13	10003.5 - 10003.8	Mafic Quartz Diorite	2.794

The cutting samples are largely in granular and powdered form. They have been partially oxidized and contaminated by drilling mud and metal filings. No densities were, therefore, determined for the cutting samples.

The data is plotted on figure 4.6 with the Schlumberger log densities sampled at the 100 foot intervals. The density log is relatively constant for the upper 7,000 feet of granodiorite and quartz diorite fluctuating between 2.70 and 2.76 gr/cc except for a few jumps, as at 2,950 feet which represents a chlorite schist inclusion. Below 7,500 feet, the rock has been termed mafic quartz diorite and is equivalent to the contaminated border zone of the Reynard Lake Pluton at surface. The mafic rock is denser and more variable than the acidic rock.

The log densities are consistently higher than the sample densities measured in the laboratory. In the upper part of the hole the difference is about .045 gm/cc. A porosity of 4.5% could account for the difference if it is assumed that the rock in place is saturated with water and the laboratory samples are dry. However, igneous and metamorphic rocks are characteristically low in porosity. In one attempt to measure it, (c.f. section 5.4), very little porosity was detected in Amisk Lake area rocks.

Fracture due to strain release could also account for the difference if it is assumed that a rock expands and fractures when taken from its place at great depth. Several of the core samples were, in fact, broken into disks perpendicular to the core axis. In this case, a fracture porosity of 1.7% would be adequate to explain the difference in density. However, the density

log shows no gradient that could be interpreted as the effect of pressure closing the fractures and controlling density. The interval velocity log suggests fractures at depths less than 100 feet but there is no corresponding change in the density log because the fractures are probably coarse and widely spaced so as not to affect surface samples or most log values. The core sample densities from great depth seem to be in even better agreement with the log than the shallow samples, opposite to what might be expected.

Since the method of density determinations in the laboratory is simple and was checked several times, the calibration of the density log is suspected to cause the error.

The gamma-gamma density log is affected by a number of variables (Tittman and Wahl, 1965), (Danes, 1960). These are listed below with their relative effects.

Table 4.8

VARIABLE	EFFECT ON MEASURED DENSITY
Borehole rugosity	Decrease
Mudcake	Increase or Decrease
Large Borehole Diameter	Decrease
Rock Chemistry	Decrease for most igneous rocks
Photoelectric Absorption	Increase

Since the apparent log density is too large in the granodiorite and leuco-quartz diorite sections of the hole, either the mudcake is incorrectly compensated, or photoelectric absorption effects are important. Danes (1960) points out that the photoelectric effect for 0.1 Mev gamma rays in iron is larger than the Compton effect. The calibration of the density log assumes Compton scattering only, and as common igneous minerals such as hornblende and biotite contain iron, this may be an important factor.

5. ROCK DENSITIES

The gravitational potential of a mass M is:

$$U_{(x,y,z)} = G \int_V \frac{\rho(v)dV}{r}$$

where U is the potential due to M at a point (x,y,z)

G is the gravitational constant = 6.670×10^{-8} cgs

V is the volume of the mass

dV is a differential volume element of M

r is scalar distance from dV to the point (x,y,z)

$\rho(v)$ is the density function of V

Density appears directly in the equation of gravitational potential and in most of the formulas derived from it. The amplitude of gravity anomalies varies directly in proportion to the density of gravitating bodies.

Density is defined as mass per unit volume of a substance and is expressed as grams per cubic centimeter in the C.G.S. system. Specific gravity is the ratio of the weight of a certain volume of substance to the weight of an equal volume of water at 4°C (Hodgman, 1956, p. 2798, 2831). Pure water, at 3.98°C and one atmosphere pressure has a density of 0.999973 grams per cubic centimeter (op. cit. p. 1964), therefore density and specific gravity are almost numerically equal.

5.1 Factors causing density variations

Rock densities at shallow depth are a function of three main variables: the densities of the constituent minerals, the porosity of the rock, and the density of the fluid filling the pore spaces. These are related according to the following formula:

$$\rho = \rho_g - \phi(\rho_g - \rho_f)$$

where ρ = bulk density of the rock

ρ_g = weighted mean grain density

ρ_f = weighted mean density of fluid filling the pores

ϕ = total porosity of the rock.

Although the formula is simple, in practice it is difficult to apply, mainly because total porosity and measurable porosity are usually different. Furthermore porosity is affected by the related factors of pressure, depth of burial, compaction, and age. The fluid in the pores could be one or more types of gas, fresh water, brine, crude oil, or any combination of these. Figure 5.1 shows the effect of depth of burial on a shale and a sandstone.

The porosity of most igneous and metamorphic rocks is low compared to that of most sedimentary rocks. Micro fractures, fractures and vesicles contribute porosity to some igneous and metamorphic rocks. Daly (1933, p.52) gives the following table of rock porosities in per cent:

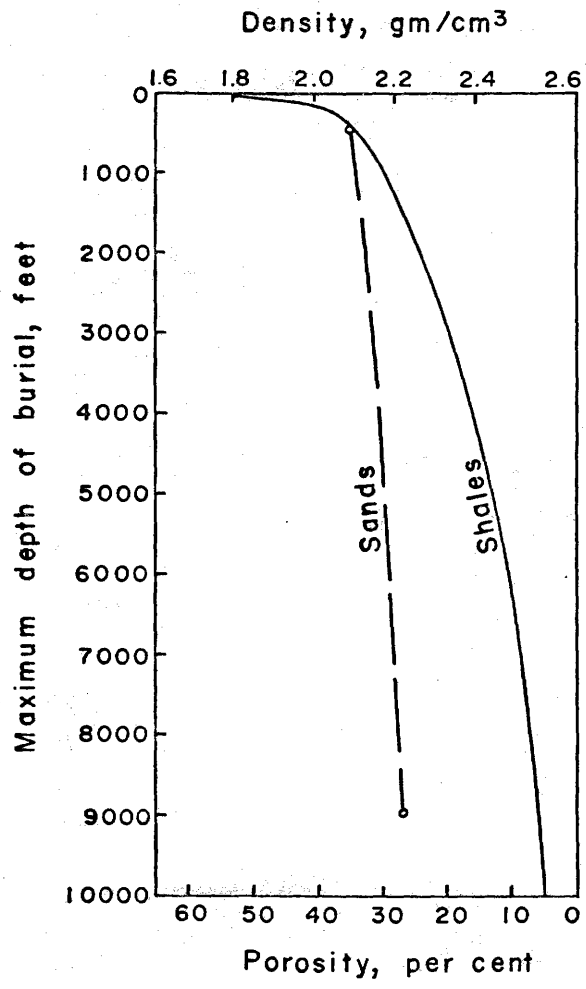

Density and porosity as functions of depth of burial in sands and shales. Yungul (1961)

Drawn by C.S.

Figure 5.1

Table 5.1

Rock	No. of Samples	Range of Porosity %
Granite	5	0.3 - 2.6
Gabbro	1	3.0
Basalt	2	0.4 - 0.5
Diabase	3	0.2 - 1.2
Gneiss	3	2.5 - 4.4
Marble	12	0.4 - 1.8
Limestone	9	1.0 - 20.0
Sandstone	13	1.9 - 22.0

Rocks of the Amisk Lake area are not the same as in Daley's table above. An experiment to detect porosity in 56 samples, found very little porosity (section 5.2).

Some common rock forming minerals found in the Amisk Lake area are listed below with their densities as given by Dana (1953).

Table 5.2

Mineral	Density
Serpentine	2.50 - 2.65 gm/cc
Microcline	2.54 - 2.57
Orthoclase	2.56 - 2.58
Albite	2.60 - 2.62
Chlorite	2.65 - 2.78
Quartz	2.653- 2.660
Biotite	2.7 - 3.1
Muscovite	2.76 - 3
Calcite	2.710
Anorthite	2.74 - 2.76
Dolomite	2.8 - 2.9
Tremolite	2.9 - 3.2
Actinolite	3 - 3.2
Hornblende	3.05 - 3.47
Enstatite	3.1 - 3.3
Garnet	3.15 - 4.3
Apatite	3.17 - 3.23
Augite	3.19
Diopside	3.2 - 3.38
Zoisite	3.25 - 3.37
Epidote	3.25 - 3.5
Olivine	3.27 - 3.37

Mineral	Density	
Hypersthene	3.4 - 3.5	gm/cc
Sphene	3.4 -3.56	
Ilmenite	4.5 - 5	
Pyrrhotite	4.58 - 4.64	
Zircon	4.68 - 4.70	
Pyrite	4.95 - 5.10	
Magnetite	5.168- 5.180	

Theoretical rock densities based on mineral densities and the observed mineral content have been found to agree closely with laboratory determined rock densities for some Amisk Lake area rocks (section 5.4).

The mineral composition of igneous and metamorphic rocks is very complex, with variations occurring for many reasons. Gravity differentiation in a single thick lava flow, for example, may result in composition ranging from granodiorite to norite (Turner and Verhoogen, 1951, p. 231). Metamorphism further complicates the matter. If rocks are subjected to conditions of temperature, pressure and non-uniform stress, different from those under which they initially formed, the mineral assemblage recrystallizes to equilibrate to the new conditions. The rate of recrystallization depends on a number of factors, generally progressing faster with higher temperature and pressure. If fluids can penetrate the rock, then various materials may be introduced or removed from the rock. Transfer of material, of course, permits gross changes in bulk chemical composition.

These variables cause significant differences, not only between different rock types but also within rock types. Chemical analyses of 20 samples of rock from the Coronation Mine area range in composition from andesite to a rock more basic than average basalt (Froese, 1963). All 20 samples came from the Ruth, Birch and Stitt Lake basic lavas which were classed as one unit for density correlation. Therefore, there is a range of density associated with each rock type, and various rock types may overlap in their density range. Nevertheless, rock types with sufficiently different composition may be characterized by significantly different mean density.

Temperature and pressure have a relatively small effect on the density of igneous and metamorphic rocks, at least in the upper few kilometers of the crust of the earth. The temperature co-efficient of volume expansion for some rocks is given by Clark (1966, p. 94) in the following table. The units are cc/cc/°C.

Table 5.3

Rock Type	Number of Determinations	Average Volume Expansion Co-efficient $\alpha = \frac{1}{V}\frac{\Delta V}{\Delta T}$
Granites and rhyolites	21	$24 \pm 9 \times 10^{-6}$
Andesites and diorites	4	21 ± 6
Basalts, gabbros and diabases	10	16.2 ± 3
Sandstones	10	30 ± 6
Quartzites	2	33
Limestones	20	32 ± 12
Marbles	9	21 ± 6
Slates	3	27 ± 3

The reader is cautioned against placing too high a reliance on these values. There is uncertainty whether the numbers represent true thermal co-efficients or composite effects with both thermal expansion and fracture porosity being important. Skinner (in Clark, op. cit., p. 77) suggests that for rocks, weighted averages of the co-efficients of the component minerals should be used. Two such theoretical calculations are made below for granite and gabbro.

Table 5.4

Granite 20°C	Mineral Volume Proportion	α	$\Sigma \alpha$
Quartz	15%	34×10^{-6}	5.1
Microcline	30%	7	2.1
Oligoclase	40%	12	4.8
Hornblende	15%	23	3.4
Total	100%		$15.4 \times 10^{-6} °C^{-1}$
Granite 400°C			
Quartz	15%	69×10^{-6}	10.4
Microcline	30%	17	5.1
Oligoclase	40%	17	6.8
Hornblende	15%	28	4.2
Total	100%		$26.5 \times 10^{-6} °C^{-1}$
Gabbro 20°C			
Andesine	50%	13×10^{-6}	6.5
Augite	50%	18	9.0
Total	100%		$15.5 \times 10^{-6} °C^{-1}$

Figure 5.2 is a chart of some data given by Clark (1966, p. 150, 169). It represents the volume compressibilities of a number of rocks which were compressed while enclosed. Some of the same specimens, when unenclosed, exhibit volume compressibilities between 1.25 and 3.3 cc/cc/megabar at one atmospheric pressure. This is

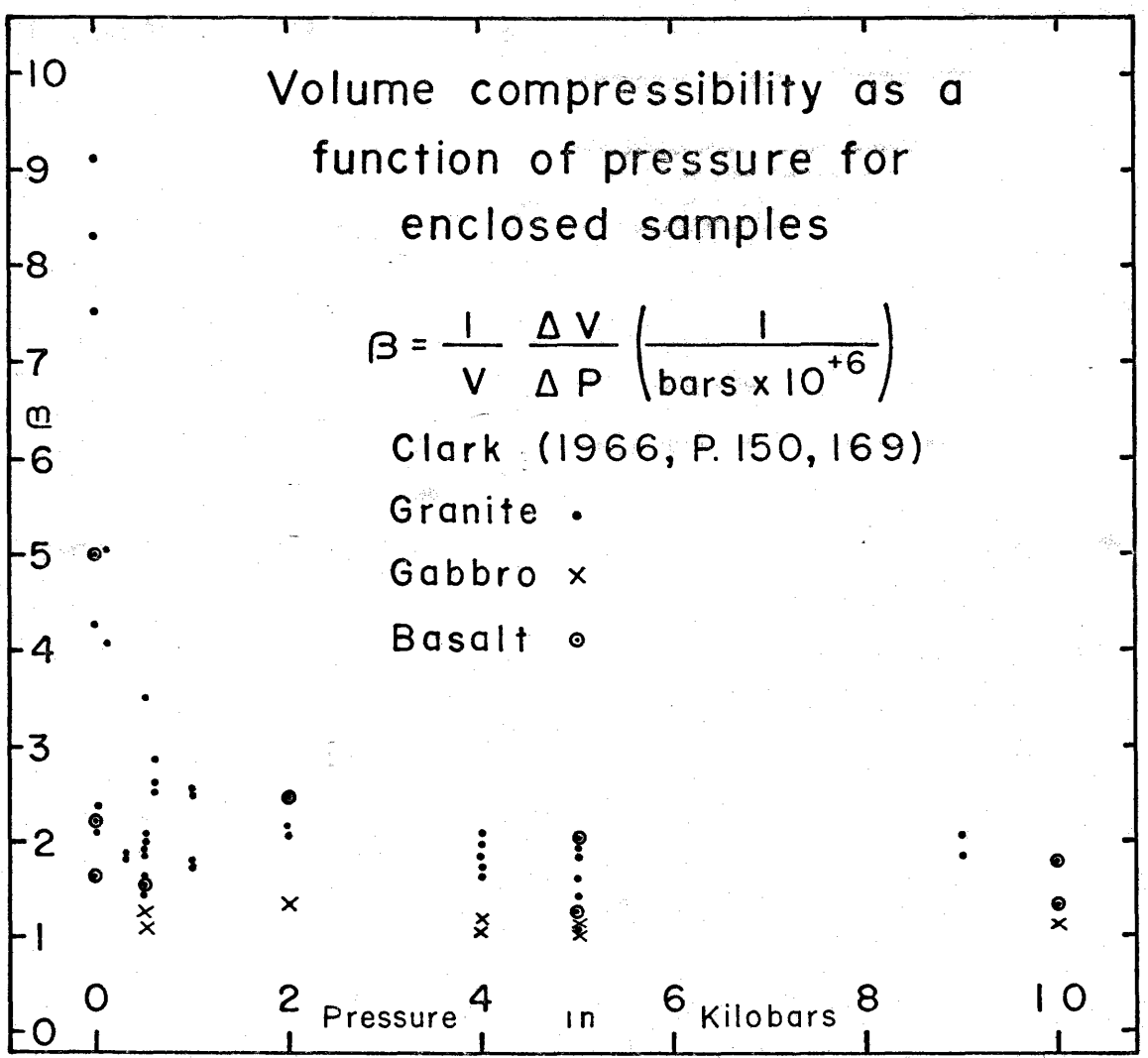
Volume compressibility as a function of pressure for enclosed samples
$\beta = \frac{1}{V} \frac{\Delta V}{\Delta P} \left(\frac{1}{\text{bars} \times 10^{+6}} \right)$
Clark (1966, P. 150, 169)
Granite •
Gabbro ×
Basalt ⊙
β
10
9
8
7
6
5
4
3
2
1
0
0
2
4
6
8
10
Pressure in Kilobars
Drawn by C.S.

Figure 5.2

much lower than some of the values obtained when enclosed. At higher pressures, the two methods of measurement yield more similar results.

These data indicate that temperature and pressure have a relatively small effect on igneous rocks at depths of a few kilometers. A sample calculation is listed below.

Table 5.5

Depth km	α 1/°C	T °C	ΔV_T	$\frac{\beta}{1}$ megabars	P bars	ΔV_P	$\Sigma\Delta V$ cc	Rock Density gm/cc
0	15.4	0	0	5.0	0	0	1.00	2.6800
1.9	16.0	23	.00037	2.5	500	-.00187	.99850	2.6840
3.7	16.6	44	.00035	2.2	1,000	-.00117	.99766	2.6863
7.5	17.9	90	.00082	1.9	2,000	-.00205	.99641	2.6897
14.9	20.3	179	.00181	1.8	4,000	-.00370	.99446	2.6949
18.7	21.6	224	.00119	1.8	5,000	-.00180	.99369	2.6970
33.6	26.5	404	.00477	1.8	9,000	-.00720	.99099	2.7044
			.00931			-.01779		

α is the temperature co-efficient of expansion

T is the temperature in °C

ΔV_T is the change in volume due to each temperature increment

β is the pressure co-efficient of compaction

P is the pressure in bars

ΔV_P is the change in volume due to each pressure increment

$\Sigma\Delta V$ is the total volume change to each depth.

A granitic rock is assumed.

The temperature gradient is 12°C/km for the Flin Flon area (Clark, 1966, p. 489).

The liquid and glassy phase of rock is less dense than the corresponding crystalline phase. Daly (1933, p. 48) cites values obtained

by Day, Sosman, and Hostetter (1914) as reproduced in the following table.

Table 5.6a

Palisade diabase	At 20°C	At 1200°C
Specific gravity, crystalline	2.975	2.89
Specific volume, crystalline	0.336	0.346
Specific gravity, glassy	2.761	2.603
Specific volume, glassy	0.362	0.384

Douglas (1907), quoted in Daly (1933) also gives densities of crystalline rocks and their corresponding glasses.

Table 5.6b

	Specific Gravity of Crystalline Rock	Specific Gravity of Glass	Per Cent Change
Granite, Shap Falls	2.656	2.446	7.90
Granite, Peterhead	2.630	2.376	9.66
Syenite, Plauensher Grand	2.724	2.560	6.02
Tonalite, New Zealand	2.765	2.575	6.87
Diorite, Guernsey	2.833	2.680	5.40
Diorite, Markfield	2.880	2.710	5.90
Gabbro, Carrock Fell	2.940	2.791	5.07
Olivine dolerite, Clee Hills	2.889	2.775	3.95
Dolerite, Rowley Rag	2.800	2.640	5.71
Dolerite, Whin Sill	2.925	2.800	4.27

It should be noted that the data cited above are for rocks measured under laboratory conditions and on a laboratory time scale. In particular, the temperature and pressure co-efficients of expansion have been measured over a relatively short time, but rocks in the depths of the earth have been exposed to extreme conditions for many millions of years. It is known that over a long period, rocks behave in ways that are not readily apparent from short term examinations. The rheid flow of salt and granite are good examples. Therefore, the data on physical properties of rocks are always

somewhat tenuous when applied to the earth and especially so when extrapolated to conditions not yet investigated in the laboratory. The laboratory measurements are, however, the best available in most cases, and it is necessary to use them until better data are obtained. To do otherwise is mere speculation.

5.2 Porosity of Amisk Lake area rocks

In an attempt to detect porosity of Amisk Lake area rocks, 56 specimens were soaked in water for 24 months. The rocks had been collected from surface outcrop in 1960, 1961, and 1962 and had been stored in a warm, dry place until 1965. They were weighed in May, 1965, then covered with water, removing them only to be weighed, until May, 1967. The variation in the density of these rocks is shown in Table 5.8. The variation in the volumes of the samples is listed in Table.5.9. The volumes and weights of some samples may vary because of chips which might have broken off in handling. The mean values for all samples are listed below.

Table 5.7

	May 1965	Aug. 1965	May 1966	May 1967
Mean Weight grams	341.91	342.42	342.21	342.18
Mean Density gm/cc	2.833	2.832	(2.825)	2.831
Mean Volume cc	120.69	120.91	(121.14)	120.87
Water Density gm/cc	0.9960	0.9960	0.9931	0.9954

The water density is used in the calculation of the rock volume and density. The May 1966 water density is lower than any others and the rock volumes and densities are systematically low and high respectively with respect to the other determinations, as might be expected if the water density is in error. Therefore, the densities and volumes determined in 1966 are not reliable and the data has been included only for the sake of completeness.

The sample weights, of course, are independent of the water density. The mean sample weight shows a slight increase (0.51 grams) on the second weighing, thereafter, it slightly decreases. The initial increase is interpreted as the effect of absorbed water, the later weight loss is probably the result of the loss of chips of rock, broken off while handling them.

The mean density of each of the rock types listed in Table 5.8 shows a slight decrease in density after the first three months of soaking. This is accompanied in each case by a slight increase in the mean volumes, Table 5.9, suggesting that the loss in density is due to expansion caused by oxidation and/or hydration of some minerals.

After 21 additional months of soaking the mean densities of Amisk and Missi rocks show a further slight decrease, but the densities of the microcline and hornblende rocks increase slightly. These later changes in density do not have any consistent relationship to changes in volume, perhaps because the rock samples lost some volume due to breakage when being handled.

Using the mean values, 120.69 cubic centimeters of rock absorbed 0.51 grams of water in the first three months. Ignoring the increase in volume, this indicates a partial porosity of 0.4%. The accuracy of this figure is very much in doubt because the method of determination is not precise and the meaning of the volume increase is not clear. It may be said that the porosity of Amisk Lake area rocks is low, certainly less than, and probably much less than one per cent.

Table 5.8

Densities of soaked samples

grams per cubic centimeter

Sample No.	May 1965	Aug. 1965	May 1966	May 1967
Microcline Granodiorite and Biotite Granodiorite				
299	2.641	2.640	2.630	2.638
300	2.647	2.643	2.638	2.647
301	2.673	2.667	2.660	2.663
302	2.665	2.651	2.657	2.664
303	2.668	2.669	2.661	2.667
304	2.671	2.665	2.662	2.671
305	2.672	2.671	2.665	2.673
Mean	2.662	2.658	(2.653)	2.660
Hornblende granodiorite and contaminated border zone				
468	2.876	2.872	2.873	2.879
469	3.012	3.009	3.008	3.014
470	2.905	2.903	2.903	2.906
471	2.791	2.786	2.788	2.791
472	2.731	2.725	2.725	2.734
473	2.769	2.780	2.775	2.787
474	2.794	2.793	2.792	2.796
478	2.792	2.784	2.786	2.788
479	2.789	2.788	2.782	2.793
480	2.831	2.830	2.826	2.829
481	2.777	2.779	2.774	2.778
484	2.903	2.901	2.895	2.904
485	3.019	3.019	3.014	3.020
306	2.776	2.778	2.759	2.769
307	2.819	2.812	2.810	2.814
308	2.728	2.728	2.720	2.735
309	2.857	2.863	2.855	2.863
Mean	2.833	2.832	(2.828)	2.835

Table 5.8 (Continued)

Sample No.	May 1965	Aug. 1965	May 1966	May 1967
Amisk group mainly basic lavas southeast of Flin Flon				
467	2.778	2.776	2.772	2.783
475	3.039	3.026	3.024	3.029
477	2.991	2.984	2.984	2.989
483	3.008	2.987	2.987	2.989
1406	2.677	2.661	2.651	2.659
1407	2.803	2.809	2.798	2.807
1408	3.061	3.055	3.047	3.050
1409	2.826	2.820	2.815	2.818
1411	2.960	2.962	2.954	2.961
1413	3.041	3.043	3.030	3.040
1414	2.956	2.952	2.944	2.950
1415	2.871	2.868	2.859	2.865
1416	2.999	2.996	2.992	2.998
1454	2.807	2.807	2.799	2.803
1455	2.923	2.927	2.921	2.930
1456	2.922	2.909	2.901	2.907
1458	3.046	3.047	3.038	3.052
1459	2.918	2.913	2.920	2.917
1460	2.669	2.669	2.665	2.669
1463	2.899	2.896	2.882	2.877
1464	2.855	2.857	2.846	2.853
1596	2.752	2.753	2.745	2.750
Mean	2.900	2.896	(2.890)	2.895

Table 5.8 (Continued)

Sample No.	May 1965	Aug. 1965	May 1966	May 1967
		Basic intrusive rock		
466	2.798	2.797	2.793	2.803
476	3.029	3.024	3.024	3.032
1457	2.891	2.884	2.879	2.882
1461	2.860	2.856	2.852	2.859
1462	3.058	3.058	3.052	3.057
Mean	2.927	2.924	(2.920)	2.927
		Missi sedimentary rocks		
1595	2.745	2.740	2.734	2.743
1597	2.703	2.698	2.689	2.697
1598	2.658	2.643	2.644	2.641
1599	2.669	2.670	2.663	2.667
1600	2.635	2.641	2.637	2.636
Mean	2.682	2.678	(2.673)	2.677

Table 5.9

Volumes of soaked samples

cubic centimeters

Sample No.	May 1965	Aug. 1965	May 1966	May 1967
Microcline granodiorite and biotite granodiorite				
299	143.80	143.94	144.44	144.06
300	113.60	113.93	114.12	113.61
301	109.85	110.21	110.47	110.41
302	119.88	120.78	120.43	120.88
303	153.61	153.56	154.06	153.72
304	52.86	53.06	53.07	52.86
305	158.92	159.03	159.46	159.09
Mean	121.79	122.07	122.29	122.09
Hornblende granodiorite and contaminated border zone				
468	76.08	76.19	76.20	76.05
469	222.24	222.54	222.63	222.11
470	153.11	153.31	153.41	153.19
471	162.90	163.35	163.27	163.05
472	92.24	92.57	92.54	92.27
473	142.42	143.02	143.30	142.80
474	148.13	148.39	148.44	148.18
478	62.74	62.97	62.94	62.86
479	143.10	143.22	143.58	142.69
480	138.68	138.75	139.08	138.88
481	112.87	112.95	113.16	112.94
484	123.84	124.01	124.27	123.86
485	168.89	168.92	169.13	168.86
306	94.93	94.75	95.56	95.19
307	93.48	93.67	93.78	93.67
308	86.33	86.34	86.65	86.50
309	38.10	37.85	37.92	37.85
Mean	121.18	121.34	121.52	121.23

Table 5.9 (Continued)

Sample No.	May 1965	Aug. 1965	May 1966	May 1967
Amisk group mainly basic lavas southeast of Flin Flon				
467	153.66	153.81	154.09	153.59
475	69.42	69.77	69.84	69.72
477	59.42	59.58	59.65	59.55
483	73.96	74.54	74.56	74.50
1406	123.28	124.29	124.79	124.46
1407	140.11	139.80	140.35	139.93
1408	153.66	153.91	154.33	154.29
1409	127.83	128.06	128.35	128.22
1411	101.80	101.68	102.01	101.78
1413	86.39	86.29	86.69	86.53
1414	85.49	85.59	85.85	85.77
1415	127.56	127.71	128.15	127.93
1416	157.32	157.47	157.72	157.42
1454	183.55	183.78	184.30	183.94
1455	87.04	86.94	87.13	86.90
1456	107.88	108.41	108.69	108.49
1458	122.94	122.94	123.35	122.76
1457	58.41	58.68	58.39	58.13
1460	87.65	87.65	87.81	87.96
1463	32.23	33.28	33.43	33.53
1464	63.35	63.30	63.56	63.44
1496	100.10	100.20	100.51	100.34
Mean	104.68	104.89	105.16	104.96

Table 5.9 (Continued)

Sample No.	May 1965	Aug. 1965	May 1966	May 1967
		Basic intrusive rock		
466	71.99	72.04	72.16	71.93
476	135.74	136.04	136.05	135.66
1457	273.19	273.96	274.43	274.16
1461	254.38	254.86	255.14	254.47
1462	231.47	231.37	231.77	231.58
Mean	193.34	193.65	193.91	193.56
		Missi sedimentary rocks		
1595	102.53	102.81	103.02	102.66
1597	107.93	108.48	108.76	108.44
1598	81.33	82.37	82.19	81.85
1599	156.97	157.12	157.60	157.27
1600	126.40	126.90	127.01	126.65
Mean	115.03	115.54	115.72	115.37

5.3 Rock sample densities

A large number of samples of rock was collected from the area east of Amisk Lake by Smith (1964) and his assistants during 1960-1962 for geochemical analysis. Fig.5.3 shows the locations of the samples. Each sample was freshly broken on all, or all but one, of its sides. These rocks were collected as nearly as possible on a $\frac{1}{4}$ mile grid and each sample chosen to represent the most abundant rock type at each locale. Thin beds, local variations, intrusive dikes and sills, etc., were excluded from the sampling. In the northeast part of the map area, some acidic rocks were deliberately excluded. The unweighted mean density of the samples therefore may not be characteristic of the bulk density of the rock in this area (Smith, oral communication, 1968). Actual densities would tend to be somewhat lighter than is apparent from the laboratory measurements.

The densities of 1585 rock samples were determined in the laboratory. Most of the samples weigh between 200 and 500 grams.

Density measurements were made using a water displacement technique. A Fisher Scientific Company triple beam balance was used for all measurements. This balance has a capacity of 1610 grams and can be read directly to 0.1 grams. It was calibrated using standard weights. Rocks were weighed when in air and when submersed in a tank of water. The porosity and permeability of these rocks is very low so that no particular precautions were observed to account for porosity. Distilled water or tap water, let stand for several days, was used to reduce gas bubbles. The density of the water was

determined by weighing a sample whose volume was determined in a volumetric flask. The water density at room temperature ranged from 0.9975 to 0.9945 gr/cc. Pure water at 20.0°C has a density of 0.998203 gm/cc (Hodgman, 1956, p. 1971). The difference is due to dissolved gas remaining in the water in the tank, and impurities introduced when rocks were weighed in the water. The water was changed frequently and its density determined daily during the course of the rock density measurements.

The rock densities were calculated with the University of Saskatchewan IBM 7040 Computer using the following formulas:

Volume = (Dry weight - submersed weight)/water density.

Density = Dry weight/Volume.

The results were output in both line printed and punched card form. Each card contains the sample number, the dry weight, the weight immersed, the volume, and the density. A second set of cards supplied by the Saskatchewan Research Council Geology Division contains the sample number, the coded geological identification, the concentration in parts per million of copper, nickel, and zinc in the sample, and map co-ordinates. A third set of cards contains the sample number, geological identification, co-ordinates, metal concentrations, and density.

The Table of Densities(Table 5.10) summarizes the correlation of density and rock type. The rock type is listed, followed by the number of samples, the mean density and the standard deviation. There are 31 rock types listed. The mean density of the 1585 samples is 2.862 gm/cc.

Table 5.10

TABLE OF DENSITIES

	Number of Samples	Mean Density gm/cc
Ordovician Sediments	none	
Precambrian		
Intrusive Rocks		
Acidic Intrusive Rocks		
Phantom Lake Granite	34	2.656 ± .017
Reynard Lake Microcline Granodiorite	83	2.669 ± .022
Reynard Lake Biotite Granodiorite	104	2.676 ± .025
Reynard Lake Border Zone	197	2.811 ± .080
Mystic Lake Pluton	176	2.789 ± .077
Annabel Lake Pluton	21	2.791 ± .057
"Quartz-Eye" Diorite	24	2.727 ± .112
Grey Diorite	33	2.925 ± .078
Basic Intrusive and Ultrabasic Rocks		
a) Ultrabasic Rocks		
Serpentinites	25	2.728 ± .101
Undifferentiated Ultrabasic Rocks	4	2.833 ± .118
Meta Pyroxenite and Peridotite	5	2.988 ± .054
Boundary Intrusion	10	2.956 ± .095
b) Basic Intrusive Rocks		
Wolverine Lake, east side of	15	3.033 ± .043
Cable Lake to Amisk Lake	33	3.004 ± .075
Table Lake, west side of	76	2.956 ± .076
Ruth Lake, east side of	41	3.042 ± .066
Schist Lake, west of West Arm	9	3.001 ± .062
Wekach Lake	98	2.974 ± .084

TABLE OF DENSITIES (continued)

	Number of Samples	Mean Density gm/cc
Missi Series		
Arkose	5	2.682 ± .043
Amisk Group		
Acidic to Intermediate Volcanic and Pyroclastic Rocks		
Lava, East and North of Wekach Lake	11	2.707 ± .036
Lava, West and South of Wekach Lake	14	2.719 ± .041
Tuff, West and South of Wekach Lake	7	2.738 ± .025
Tuff, East and North of Wekach Lake	7	2.756 ± .032
Basic Volcanic and Pyroclastic Rocks		
Tuff & Agglomerate, West & South of Wekach Lake	10	2.868 ± .110
Tuff & Agglomerate, East & North of Wekach Lake	25	2.902 ± .098
a) Lava, Greenschist Facies		
(Eastern Islands and Shore Amisk Lake)	185	2.918 ± .108
(Schist, Phantom, and Douglas Lakes)	161	2.936 ± .096
b) Lava, Epidote-Amphibolite Facies		
(Konuto Lake Unit)	35	2.932 ± .062
(Ruth, Birch and Stitt Lake Unit)	57	2.939 ± .084
(South of Wekach Lake)	22	2.979 ± .058
c) Lava (Mosher, Wolverine Lakes)	58	2.961 ± .085

The densities of the rock samples are proportional to the basicity of the rock, with the notable exception of serpentinite. The lightest and most uniform rock is the Phantom Lake Granite and the heaviest is the Ruth Lake Sill, a meta-gabbro. The densities listed are, in general, consistent with other published lists of density, Innes (1960), Jakosky (1950, page 264), Clark (1966, p. 198).

Figure 5.4 shows areas of similar rock density with superimposed Bouguer contours. Some density groupings fall into well defined patterns, especially the extreme values. Most of the low density areas can be readily correlated with acidic intrusive rocks, whereas most of the high density areas can be correlated with basic intrusive rock (fig. 3.2, Geological Map). Many of the isolated low density samples were taken from acidic dikes or serpentinite bodies.

A further correlation exists between the Bouguer anomalies, the large basic and acidic intrusive rock units, and the broader density groupings. An exception to this is seen in the area immediately west of Mosher Lake, where a prominent gravity maximum exists, together with a density maximum, but no large basic intrusion. However, ultrabasic rocks outcrop on the islands of Mosher Lake, and a small meta-gabbro body has been mapped within the density anomaly. Since these features are contiguous with large basic intrusions between Amisk and Ruth Lakes, they suggest that a similar intrusion may exist at a shallow depth west of Mosher Lake, or that rocks mapped as volcanics may be fine-grained meta-gabbros.

5.4 Rock densities calculated from mineral content

Mineral composition of various rock samples from the Amisk Lake area have been given by several authors. Some are listed below with the calculated densities based on the volume percentage of the minerals. Mineral densities are taken from Dana (1953). Some of the sample compositions are only estimates, hence, ranges are listed and the exact percentages were chosen arbitrarily so as to make 100%. Below each calculated density is listed the measured density of samples of the equivalent rock type as given in Table 5.10.

Table 5.11

Granodiorite (Reynard Lake Pluton?), Byers and Dahlstrom (1954, p. 59)

Oligoclase	50 - 65%	(.60) x 2.64 =	1.584
Quartz	15 - 25%	(.22) x 2.66 =	.585
Microcline	5 - 15%	(.12) x 2.56 =	.307
Biotite	1 - 10%	(.06) x 2.95 =	.177
Hornblende	0 - 10%	0	
		1.00	2.653
Reynard Lake Core Zone		83 samples	2.669 ± .022

Quartz-eye diorite, Byers and Dahlstrom (1954, p. 55)

Oligoclase	65 - 85%	(.80) x 2.64 =	2.112
Quartz	10 - 20%	(.15) x 2.66 =	0.398
Biotite	2 - 10%	(.05) x 2.95 =	0.148
		1.00	2.658
"Quartz-Eye" diorite		24 samples	2.727 ± .112

Mafic Quartz Diorite, Sample C-12 JXWS Borehole, Depth 10,002.5, Findlay (1966)

Quartz	14.8% x 2.66	0.394
Plagioclase	62.2% x 2.66	1.654
Biotite and Chlorite	18.3% x 2.85	0.522
Hornblende	3.8% x 3.26	0.124
Magnetite and Pyrite	0.6% x 5.17	0.031
Saussurite	0.3% x 3.30	0.010
	100.0%	2.735
Sample 13 10,003.6 ft JXWS		2.794
Reynard Lake Border Zone	197 Samples	2.811 ± .080

Basalt, Sample F60-91, Froese (1963, p. 78)

Quartz	6.5% x 2.66	0.173
Plagioclase (An 30)	31.8% x 2.65	0.842
Hornblende	61.0% x 3.26	1.988
Magnetite	0.7% x 5.17	0.036
	100.0%	3.039
Ruth, Birch, Stitt Lake Unit	57 Samples	2.939 ± .084

Andesite, Sample F60 - 95, Froese (1963, p. 78)

Quartz	10.9% x 2.66	0.290
Plagioclase (An 33)	36.9% x 2.66	0.982
Hornblende	42.3% x 3.26	1.379
Epidote	9.5% x 3.37	0.320
Calcite	0.4% x 2.71	0.008
	100.0%	2.979
Ruth, Birch, Stitt Lake Unit	57 Samples	2.939 ± .084

Pyroclastic hornblende - feldspar porphyry of basalt composition, Sample M13-12, Froese (1963, p. 80)

Quartz	3.9% x 2.66	0.104
Plagioclase (An 35)	30.0% x 2.66	0.798
Hornblende	62.0% x 3.26	2.020
Biotite	4.1% x 2.95	0.012
	100.0%	2.934
Basic Tuff and Agglomerate	10 Samples	2.868 ± .110

Granodiorite, Mystic Lake Pluton, Eckstrand (1962)

Plagioclase (An 35)	34 - 40%	(0.39) x 2.66	1.037
Microcline	7 - 25%	(0.16) x 2.56	0.410
Myrmekite	1 - 3%	(0.02) x 2.65	0.053
Quartz	7 - 15%	(0.12) x 2.66	0.319
Hornblende	10 - 20%	(0.16) x 3.26	0.522
Biotite	0 - 15%	(0.08) x 2.95	0.236
Chlorite	0 - 10%	(0.05) x 2.70	0.135
Iron Oxide	0 - 1%	0	
Epidote	0 - 5%	(0.02) x 3.37	0.067
		1.00	2.779
Mystic Lake Pluton		176 Samples	2.789 ± .077

Comparison of these calculated densities with the Table of Densities (p. 10 and 11) shows that each value is within the density range listed for the corresponding rock type except for the basalt. The basalt and andesite samples came from the "Ruth, Birch and Stitt Lake Unit" of the density table. The pyroclastic rock came from the "Tuff and Agglomerate, West and South of Wekach Lake" unit. The value for the basalt sample is only slightly outside the listed range (3.039 vs. 3.023) and, therefore, the overall comparison is fairly good.

5.5 Gravimetric density determinations

The gravity meter may be used to estimate density of rocks by measuring the gravity effect of a hill or valley, or by measuring the gravity variations in a mine shaft. This method utilizes a fundamental property of mass, i.e. its gravitational attraction, to calculate density, but requires high accuracy in the measurements and calculations.

Several density profiles over hills using the method of Nettleton (1939) were attempted. Unfortunately in the Amisk Lake area this method does not produce satisfactory results. The major problem is that large density changes occur within short distances and much of the topography is related to variations in the bulk density of the rocks. Figure 5.5 illustrates the effect of lateral density variations. This profile was made on the road,

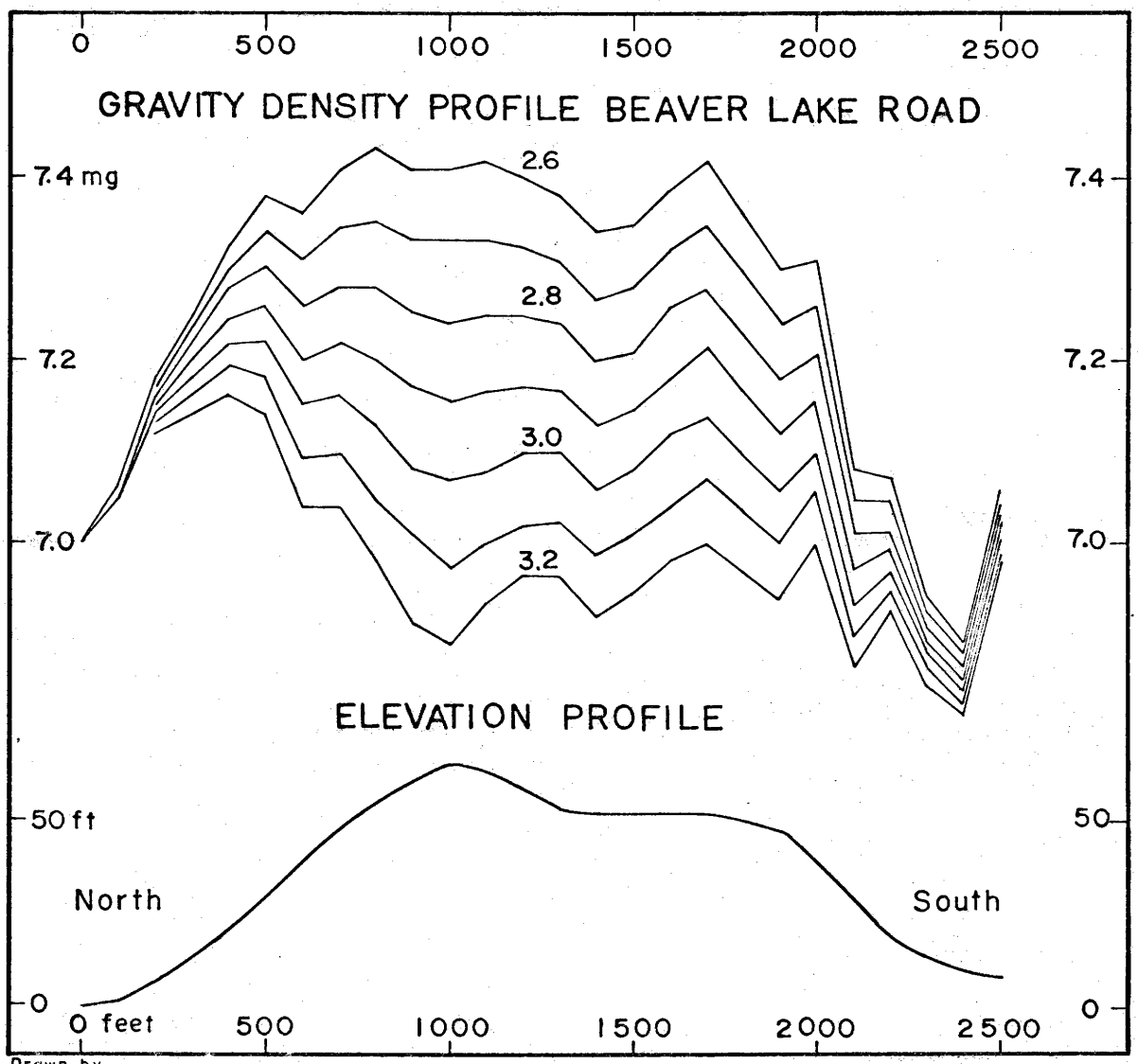
0
500
1000
1500
2000
2500
GRAVITY DENSITY PROFILE BEAVER LAKE ROAD
7.4 mg
7.2
7.0
2.6
2.8
3.0
3.2
7.4
7.2
7.0
ELEVATION PROFILE
50 ft
0
North
South
50
0
0 feet
500
1000
1500
2000
2500
Drawn by
C.S.

Figure 5.5

south of Denare Beach, in an area where rock sample densities range from about 2.9 to 3.0. The profiles with assumed densities of 2.8 and 2.9 seem to reflect the hilltop topography least, but the 3.1 profile best removes the effect of the entire hill. A distinct positive anomaly exists on the north slope, and a distinct negative anomaly exists on the south slope of the hill, causing uncertainty in the interpretation. No other suitable hill with as much elevation relief was found in the area.

Elegant improvements of Nettletons method have been devised by Grant and Elsaharty (1962), Jung (1959), and Parasnis (1952). Grant's method requires that the Bouguer gravity map be convoluted with the topographic map, producing a density function of the map area. These methods are not applicable to the survey reported here since most of the stations were read at few constant elevations, the lake levels. In many cases, significant density variations occur under the water of large lakes, but since the gravity stations at lake level do not vary in elevation, and the lake depths are unknown, it is impossible to relate the topographic density effect to elevation.

Hammer (1950) was one of the earliest to measure rock density in situ with underground gravity measurements. He discovered a puzzling discrepancy between his gravity meter determinations and Jolly balance measurements on rock samples from the Pittsburgh Plate Glass Company's limestone mine at Barberton, Ohio. McCulloh (1965) was able to show 18 years later, by re-occupying the same stations that Hammer's Gulf gravimeter had an error in calibration of nearly 12 percent. After correcting for the error, all measurements

were in essential agreement. The methods of Hammer (1950) and McCulloh (1965) were adapted by Gendzwill (1967) in southern Saskatchewan and also used in the Amisk Lake area.

In 1966, the Flexar mine at Birch Lake was under development. The shaft had been sunk to a depth of 1134 feet, with shaft stations cut at 325, 650, and 1050 feet. Very little horizontal development existed at the time of the survey, therefore, little gravity correction was required for the gravity effects of mine openings. Gravity readings were taken in the shaft (fig. 5.6) to obtain a value for rock density with the following results:

Table 5.12

Station	Gravity	Corrections		Δg	Elevation feet	Δg/Δz mg/ft	Density gm/cc
		Terrain	Mine				
surface	28.46	.04	.04	28.54	1035.0		
						24.75	2.712
325	36.63	.08	-.13	36.58	710.2		
						21.88	2.826
650	43.71	.10	-.13	43.68	385.7		
						22.02	2.820
1050	52.21	.11	.20	52.52	-15.7		

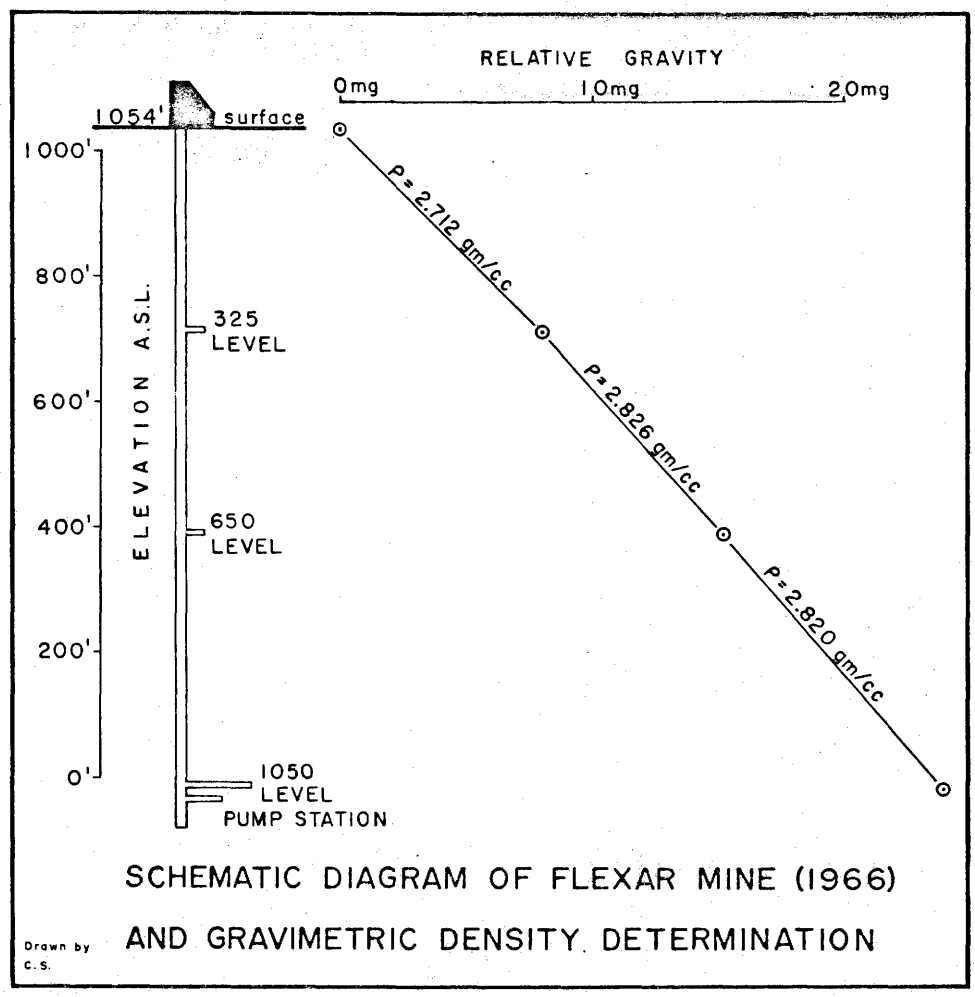
RELATIVE GRAVITY
0mg
1.0mg
2.0mg
1054'
surface
1000'
800'
600'
400'
200'
0'
ELEVATION A.S.L.
325
LEVEL
650
LEVEL
1050
LEVEL
PUMP STATION
ρ = 2.712 gm/cc
ρ = 2.826 gm/cc
ρ = 2.820 gm/cc
SCHEMATIC DIAGRAM OF FLEXAR MINE (1966)
AND GRAVIMETRIC DENSITY DETERMINATION
Drawn by
C.S.

Figure 5.6

Froese (1963) indicates the Flexar Mine area is underlain by basic volcanic flow rock. A dike complex of acidic feldspar porphyry crops out near the head frame. No detailed geological description of the mine is available. Densities of surface rock samples in the area have a mean value of 2.939 $\pm$ .084 gm/cc. The gravimetrically determined densities appear to be consistent with the picture of basic volcanic rock cut by varying amounts of acidic dike rock, with more acidic dikes in the part of the mine above the 325 level than below.

Unfortunately, this example cannot be taken as typical of basic volcanic Amisk rock, since most areas do not have large acidic dikes in them, although small dikes are common. Furthermore, the shaft measurements may be influenced by the large meta-gabbro intrusion to the west and the granodiorite to the east of the mine.

6. GRAVITY MEASUREMENTS

The Newtonian formula for gravitational attraction is:

$$F = G\, m\, m_1 / r^2$$

where F is the force in dynes

G is the gravity constant 6.670×10^{-8} c.g.s.

m and m_1 are the masses in grams of two small bodies

r is the distance between the bodies in centimeters.

r must be much larger than the dimensions of m or m_1.

It is often more convenient to think of the acceleration of a small test mass, m_1, due to the gravity field of a large mass, m. This acceleration is usually termed g.

$$g = F/m_1 = G\, m/r^2$$

The units of g are cm/sec/sec or gal in honor of Galileo. In most geophysical work, the gal is too large for convenient use so a smaller unit, the milligal, abbreviated mg is used.

$$1 \text{ mg} = 10^{-3} \text{ gal}$$

To determine the gravity effect of a finite body, Newton's formula must be integrated over the entire volume of the body.

$$g = G \int_V \frac{f(\rho)\cos\theta}{r^2} \, dv$$

where $f(\rho)$ is the density function

V is the volume of the body

dv is the volume element of integration

θ is the angle between r and some reference direction (usually vertical) in which the gravity effect is computed

r is the distance from dv to the point where g is calculated.

This equation has been solved for a number of simple geometrical forms. Complicated forms are very difficult or impossible to determine and usually are solved by breaking them up into several simpler forms.

The gravity field of the earth and the flattening of the spheroid was first determined by Clairaut (1743). Garland (1965) presents a development of the International Gravity Formula as adopted by the International Union of Geodesy and Geophysics in 1931.

$$g_o = 978.049(1 + .0052884 \sin^2\theta - 0.0000059 \sin^2 2\theta) \text{ cm/sec/sec}$$

where θ is the latitude and g_o is the theoretical gravity on the surface of a reference ellipsoid.

Although recent gravity measurements have led to revised formulae, the one presented here is still used as the standard for gravity reductions.

Variations in terrestrial gravity are caused by a number of factors. Most texts in elementary geophysics discuss these variations and the methods of measurement. See, for example, Dobrin (1952), Nettleton (1940) or Parasnis (1962). The two factors which cause the largest variations in the total gravity field on the surface of the earth are latitude and elevation. The variation with latitude is a result of the axipetal acceleration and shape of the rotating earth. The variation with elevation is due to the "square of the distance" term which appears in the denominator of the Newtonian formula for gravitational attraction, and the attraction of the slab of earth between the gravimeter and some datum elevation. The accuracy of modern gravimeters is such that changes of a few inches in elevation or about 50 feet in latitude cause measurable effects. Therefore, the effect of the elevation and latitude must be determined before the gravity values can be used for geological interpretation. Hills and valleys near the measurement point also have a perceptible effect. Tidal forces cause measurable changes in gravity.

Furthermore, the characteristics of gravimeters slowly change with time due to gradual relaxation of springs and fatigue of materials.

Only after the effect of all these factors has been compensated, can the relatively small gravity anomaly due to geological density variations, be studied.

6.1 Elevations and co-ordinates

Elevations were taken with rod and level along the roads in the area. Lake levels were also established by levelling thereby providing good elevations for all points along the shores. The Hudson Bay Mining and Smelting Company provided a grade profile for elevations along the Coronation Mine railroad. For points away from roads or lakeshores, an American Paulin Surveying "Terra" Altimeter was used in conjunction with a Belfort recording barograph to correct for barometric variations. Both instruments are readable to one foot elevation. In tests on known elevation points, the altimeter achieved an accuracy of $\pm$ 3 feet. Absolute elevations were obtained from points established by the Topographical Survey of the Department of Mines and Technical Surveys (now the Department of Energy, Mines, and Resources). Accuracy of elevations varies from 0.1 foot on roads, to 0.5 foot on lakeshores, to several feet for barometric points. The maximum and minimum elevations recorded are 1138.9 feet, on the road from Schist Lake to Flin Flon, and 958 feet, on Schist Lake. The elevation of Amisk Lake was 969.8 feet in July, 1965.

Latitude and longitude were determined by scaling the co-ordinates of points of observation from the geological maps published by Byers *et al.* (1954)

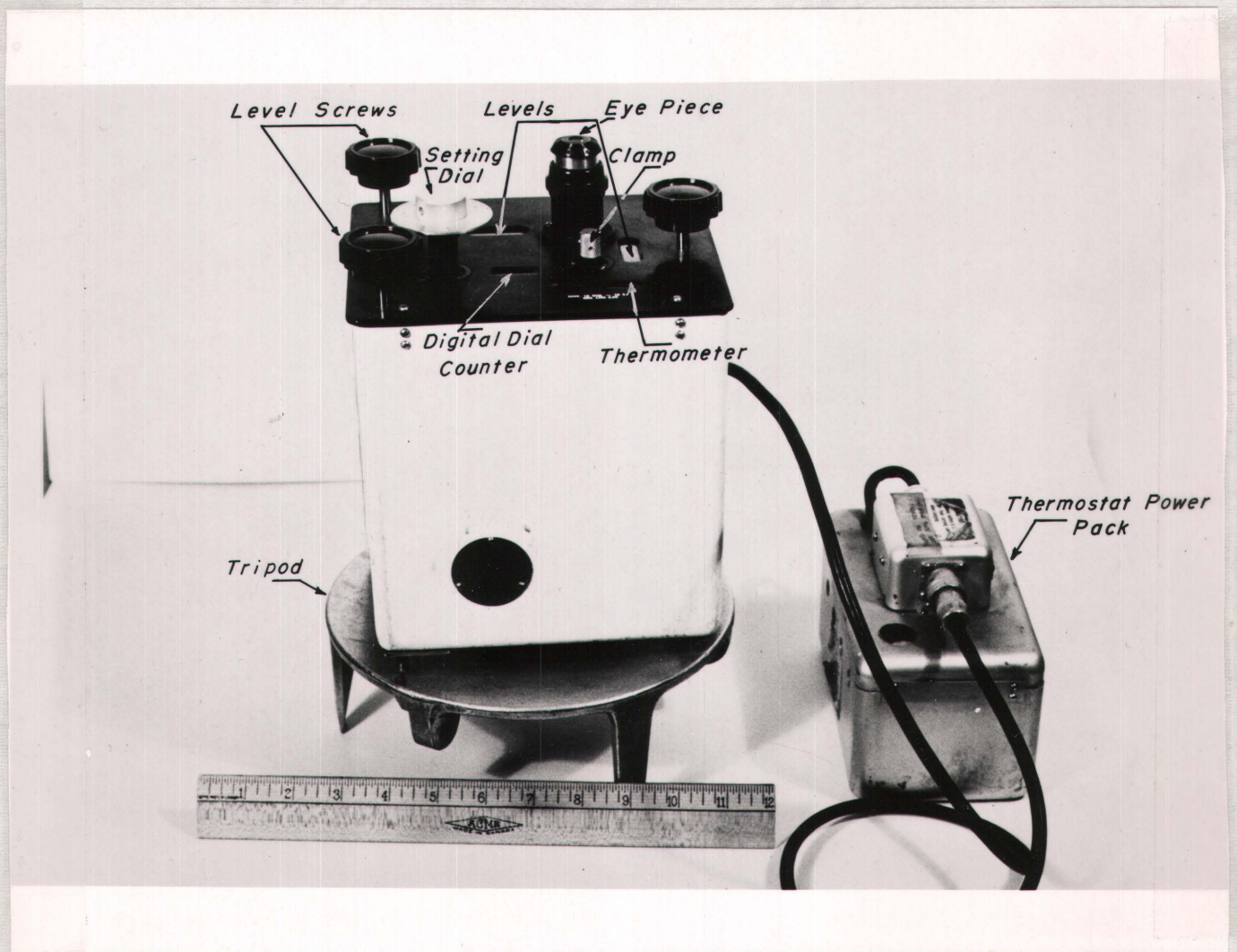

Figure 6.1

LACOSTE ROMBERT GRAVITY METER

and 1965), scale 1 inch to $\frac{1}{2}$ mile. The observation points were plotted on the maps by dead reckoning during the course of the survey. The co-ordinates were scaled to a precision of 0.01 inch from an arbitrary origin. The latitude and longitude of the origin are: lat. 54°35'N, long. 102°9.33'W. Factors such as errors in dead reckoning and map scale might cause errors of about 0.1 inch on the map or 264 feet on the ground.

6.2 The gravimeter

The gravity survey was carried out with a LaCoste-Romberg, Model G, Geodetic gravimeter, serial No. 52. This instrument has a reading range of over 7000 milligals and a reading accuracy of ± 0.01 milligal according to the manufacturer's specifications. The meter is thermostatically controlled to a constant temperature of 50°C.

Figure 6.1 is a photograph of the instrument resting on its tripod. The battery power pack for the thermostat is connected. Projecting from the top of the case are three levelling screws, the eye-piece, the clamp, and the setting dial. Recessed into the top of the case are two level bubbles, the digital dial counter, and the thermometer.

A simplified diagram of the basic meter is shown in Figure 6.2. The system consists of a mass on the end of a horizontal beam, the latter supported by a zero-length spring. The shock eliminating springs form a floating pivot thus eliminating any friction in the moving system. Since the gravity responsive

PRINCIPLE OF OPERATION

LA COSTE-ROMBERG GRAVIMETER

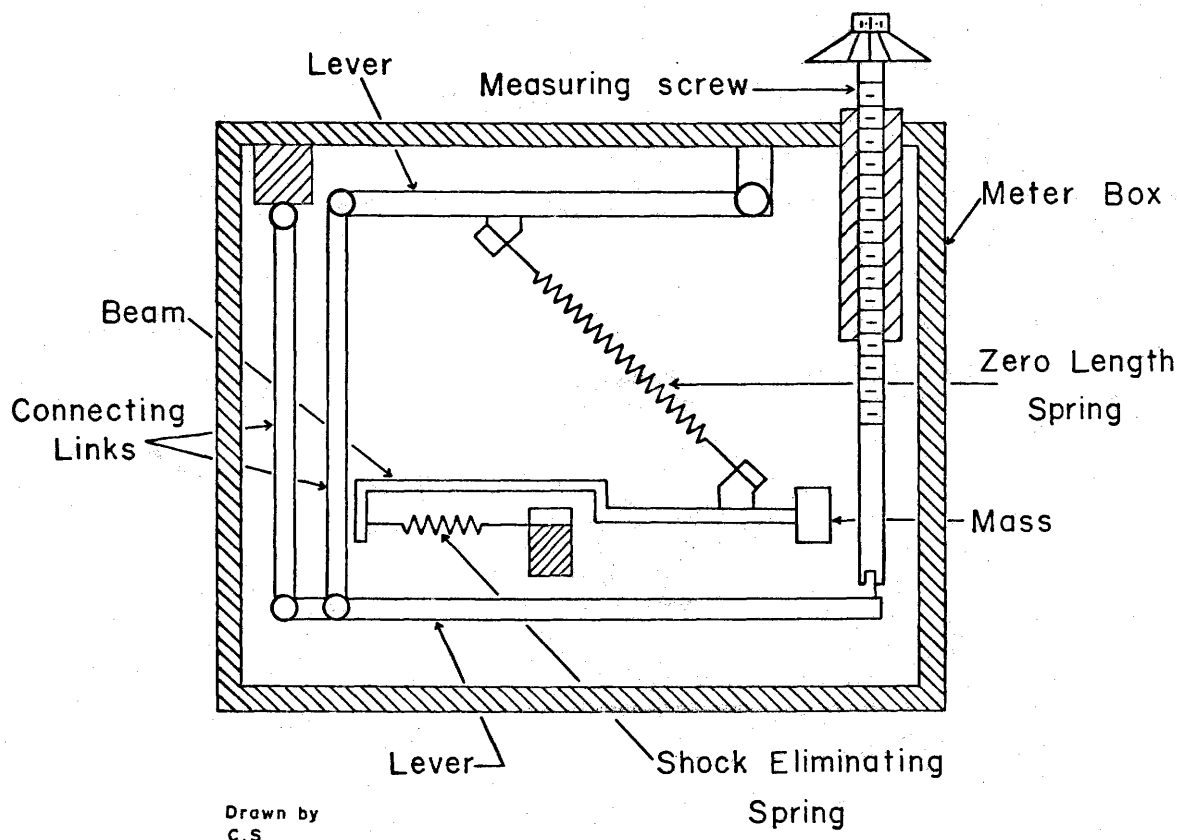

Figure 6.2

parts are completely suspended by springs, the instrument will withstand any shock that does not damage the housing that supports it. The levers and measuring screw shown in the diagram serve as the measuring system.

The gravimeter is calibrated between known gravity values. The calibration factors depend only on the quality of the measuring screw and levers; they do not depend upon any type of weak auxiliary springs. For this reason, the calibration factors of LaCoste and Romberg meters do not change perceptibly with time. This eliminates any need for frequent checks of calibration.

LaCoste (1934) described the principle of the zero length spring as applied to seismographs. The principle applies equally well to gravimeters since both seismographs and gravimeters measure acceleration. The zero-length spring is a spring wound in such a way that the coils are in tension when fully closed and the amount of tension is proportional to the length of the spring.

Referring to Figure 6.3, it is required to calculate the torque about the pivot "D". The torque due to the mass m is:

$$T_m = -g\ m\ b \sin\theta$$

where g is the gravitational acceleration

The torque due to the spring is:

$$T_s = K(FC)(DG)$$

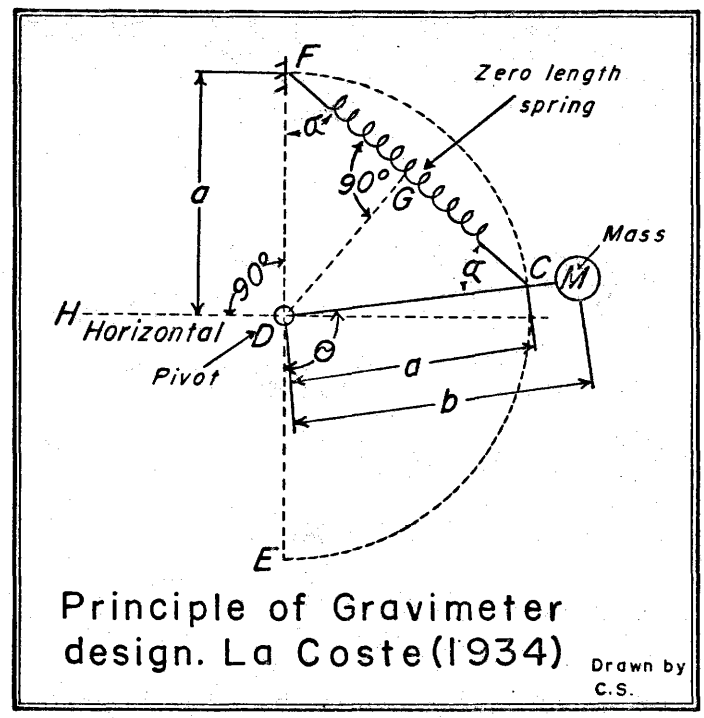

Principle of Gravimeter design. La Coste (1934)

Drawn by C.S.

Figure 6.3

where K is the spring constant

$FC = FG + GC = 2(a \cos \alpha)$

$DG = a \sin \alpha$

$T_s = 2Ka^2 \sin \alpha \cos \alpha = Ka^2 \sin 2\alpha$

but from geometrical considerations, $2\alpha = \theta$, therefore

$$T_s = Ka^2 \sin \theta$$

The total torque about D is

$$T_o = T_s + T_m = (Ka^2 - g\,mb) \sin \theta$$

If $Ka^2 = gmb$, then $T_o = 0$ for all values of θ, and the period is infinite.

If $g = g_o + \Delta g$

$T_o = (Ka^2 - (g_o + \Delta g)mb) \sin \theta$

$= (Ka^2 - g_o mb) \sin \theta - \Delta gmb \sin \theta$

where g_o is a gravity value initially assumed.
But $\Delta gmb \sin \theta = 0$ only if $\Delta g = 0$ or $\theta = 0$. Therefore, the mechanism is theoretically unstable for any small departure from the gravity value assumed in the design. In practice, the beam is brought back to the null position by adjusting the position of the spring.

A table of calibration factors over the entire range of the instrument is given by the manufacturers. The calibration was verified by measurements between Primary Gravity Stations of the Canadian National Network at Regina, Saskatoon and Prince Albert, in 1964 and 1966. The results corrected for tidal variations and instrument drift are listed below.

TABLE 6.1

Gravimeter Calibration

Station	Meter Reading	Tide & Drift Correction	Corrected Reading	Gravity Value of National Network Station (milligals)
Regina, 1964 9143-55	4448.22	.10	4448.32	980957.56
Saskatoon, 1964 9910-58	4618.54	.0	4618.54	981135.47
Prince Albert, 1964 9120-57	4705.43	.04	4705.47	981226.20
Saskatoon, 1966 9910-58	4634.44	0	4634.44	981135.47
Prince Albert, 1966 9120-57	4721.41	0	4721.41	981226.20

Using these values, scale factors were calculated and are listed here with the equivalent manufacturer's factors for each range.

Range	Computed (mg/div)	Manufacturers (mg/div)
Regina - Saskatoon 1964	1.0452	1.0465
Saskatoon - Prince Albert, 1964	1.0437	1.04480
Saskatoon - Prince Albert, 1966	1.0432	1.04480

The total range of gravity in the area surveyed is 21.57 scale divisions on the LaCoste-Romberg instrument. Using the two factors in the above table for 1966, the following results are obtained:

Computed factor	1.0432	x 21.57	=	22.502
Manufacturer's factor	1.0448	x 21.57	=	22.536
Difference				.034 milligals

In view of the range of the gravity anomaly in the Amisk Lake area, the computed values were considered to be not significantly different from the manufacturer's values and, therefore, the manufacturer's list of scale factors was accepted for this survey.

Instrumental drift of the LaCoste-Romberg gravimeter is very low, amounting to an increase of 16 milligals in two years. Compare the 1964 and 1966 readings at Station 9120-57 (Prince Albert).

On a shorter time scale, however, the drift is more erratic and readings do not repeat much better than $\pm$ 0.05 milligal. Figure 6.4 shows a series of readings at the same station, taken by two operators, over a period of one hour on May 4, 1964. The meter was picked up and relevelled after each reading.

The variations shown are due, in part, to a difficulty in reading the

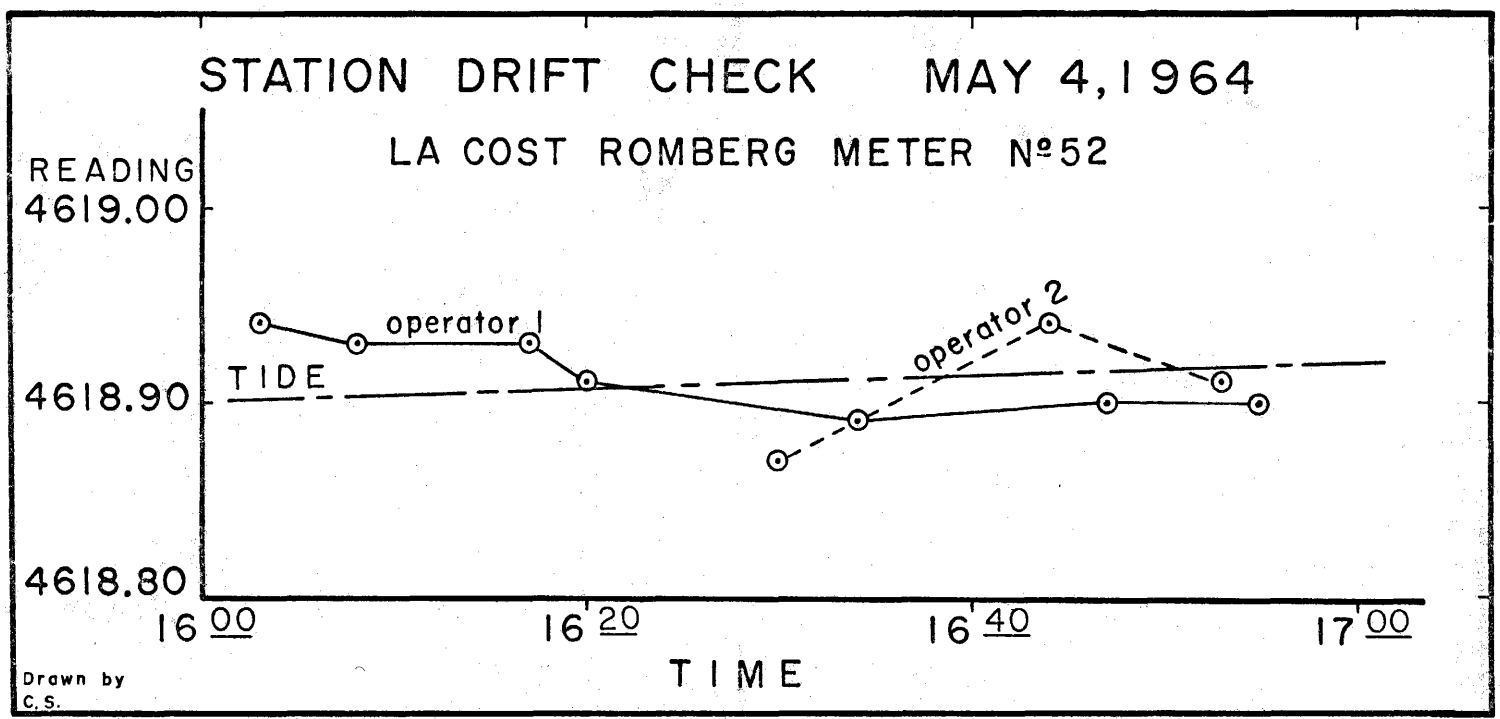
STATION DRIFT CHECK MAY 4, 1964
LA COST ROMBERG METER Nº52
READING
4619.00
4618.90
4618.80
operator 1
operator 2
TIDE
16 00
16 20
16 40
17 00
TIME
Drawn by
C.S.

Figure 6.4

instrument. In the viewing field of the eyepiece of the instrument, the operator must bring two parallel lines into contact by careful adjustment of the setting dial (Figure 6.1). Both lines have a certain thickness but the edges of the lines are blurred, making it difficult to repeat the setting exactly.

Tidal variations are generally not large, reaching a maximum of about o.3 milligals/day.

The term tare, as used by Woollard (1963, p. 27), refers to a sudden irreversible shift in the scale reading of an instrument, often caused by a physical shock. A tare of about 0.24 milligals was observed once, when transporting the meter in a small outboard powered boat (Figure 6.5). Certain vibration frequencies and intensities in the range produced by small engines have been known to cause tares (LaCoste, oral communication, 1966).

6.3 Gravity adjustments and calculations

Gravity surveys must be adjusted for various errors arising in the survey, such as those described above. A single gravity traverse should begin and end at a station whose gravity value is known. Any difference between the initial and final reading (drift) is usually distributed among all intermediate stations as a linear function of time. However, when an interpreter attempts to combine different traverses, or even different surveys, difficulties may be encountered. Stations which are common to both surveys usually have different values and the values do not always differ by constant amounts. The usual method of handling

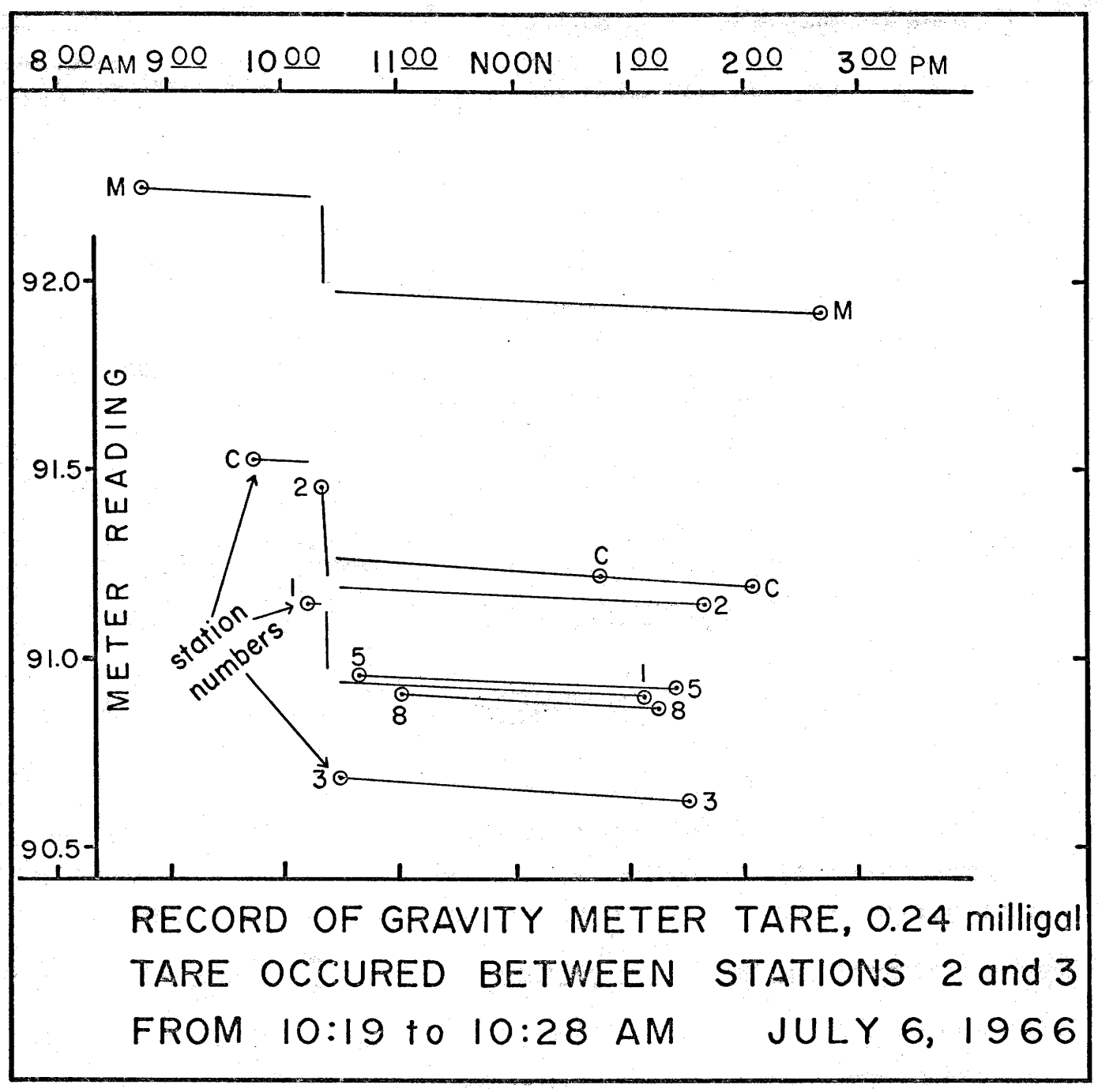
8 00 AM 9 00 10 00 11 00 NOON 1 00 2 00 3 00 PM
92.0
91.5
91.0
90.5
METER READING
station numbers
M
C
2
1
5
8
3
RECORD OF GRAVITY METER TARE, 0.24 milligal
TARE OCCURED BETWEEN STATIONS 2 and 3
FROM 10:19 to 10:28 AM JULY 6, 1966

Figure 6.5

these errors is to assume that they are random and adjust them by a least squares technique. This is accomplished by solving a set of linear equations, in a manner analogous to electric circuit problems (Gibson, 1941). This technique is well suited to geophysical surveys where loops or traverses are laid out in a well defined pattern. In the Amisk Lake area the complex system of traverses was not well suited to Gibson's method.

The procedure actually used is as follows:

1) Each station occupied in two or more different traverses is listed at the head of a page. Other base stations to which the above station ties directly are listed below with each observed gravity difference.

2) Certain values are assumed to be correct. (The Dominion Observatory Stations).

3) A tentative gravity value for each base station tied to "correct" values is calculated.

4) The tentative "correct" values of Step 3) are inserted into all lists and recalculated.

5) The calculation is repeated until no further change occurs.

Gibson (1941) points out that any solution of a circuit problem is a least squares solution, if the sum of the observational differences about each circuit is zero, and if the sum of the corrections at each point is zero. The method outlined above satisfies this criterion, since in each traverse

(circuit), the sum of observational differences about the circuit is set initially to zero by the drift correction. As each value is altered to satisfy an adjoining traverse, it does not disturb the balance in the first loop because the corrections are equal but of opposite sign.

A synthetic example was prepared to illustrate this procedure (See Table 6.2). A set of gravity stations was assumed with the observed differences as follows:

	A	B	C	D	E
A		0.00			18.01
B	0.00		7.52	15.58	17.98
C		-7.52		8.10	
D			-15.58		2.42
E	-18.01	-17.98			

Stations A and C are assumed correct with values 78.00 and 70.50. Station B, tied to both A and C, is estimated. B and C are then used to estimate D. In the third step, A, B, and D are used to estimate E. In the second iteration, the first estimates of B, D, and E are used to improve the estimates. The third iteration introduces no significant changes.

Except for the adjustment procedure described above, survey corrections were made in a conventional manner. Values of gravity were calculated with respect to the Flin Flon area control stations, established by the Dominion Observatory. The effects of tide, instrumental drift, elevation,

TABLE 6.2

NETWORK ADJUSTMENT

First Iteration				Second Iteration				Third Iteration			
Station B				**Station B**				**Station B**			
Sta	G	ΔG	G_B	Sta	G	ΔG	G_B	Sta	G	ΔG	G_B
A	78.00	.00	78.00	A	78.00	.00	78.00	A	78.00	.00	78.00
C	70.50	7.52	78.02	C	70.50	7.52	78.02	C	70.50	7.52	78.02
D				D	62.415	15.58	77.995	D	62.415	15.58	77.995
E				E	60.005	17.98	77.985	E	60.00167	17.98	77.98167
First Mean B = 78.01				Second Mean B = 78.00				Third Mean B = 78.00084			
Station D				**Station D**				**Station D**			
Sta	G	ΔG	G_D	Sta	G	ΔG	G_D	Sta	G	ΔG	G_D
B	78.01	-15.58	62.43	B	78.00	-15.58	62.42	B	78.00084	-15.58	62.42084
C	70.50	- 8.10	62.40	C	70.50	- 8.10	62.40	C	70.50	- 8.10	62.40
E				E	60.005	2.42	62.425	E	60.00167	2.42	62.42167
First Mean D = 62.415				Second Mean D = 62.415				Third Mean D = 62.41417			
Station E				**Station E**				**Station E**			
Sta	G	ΔG	G_E	Sta	G	ΔG	G_E	Sta	G	ΔG	G_E
A	78.00	-18.01	59.99	A	78.00	-18.01	59.99	A	78.00	-18.01	59.99
B	78.01	-17.98	60.03	B	78.00	-17.98	60.02	B	78.00084	-17.09	60.02084
D	62.415	- 2.42	59.995	D	62.415	- 2.42	59.995	D	62.41417	- 2.42	59.99417
First Mean E = 60.005				Second Mean E = 60.00167				Third Mean E = 60.00491			

and latitude were computed and subtracted from the observed reading to obtain the Bouguer anomaly. A preliminary map was hand calculated during the course of the survey, but the final reductions were made with the aid of the University of Saskatchewan IBM 7040 computer. The effect of tide and drift is discussed earlier.

The elevation correction is composed of two parts, the free air correction and the Bouguer correction. A density of 2.67 gm/cc was used for the Bouguer correction, in order to be consistent with the practice of the Dominion Observatory, and the correction was made to sea level. Since the average density of rocks in the Amisk Lake area is 2.82 gm/cc, instead of 2.67 gm/cc, and the elevation is generally 1000 feet, the Bouguer anomaly should, in theory, have approximately

$$(2.82-2.67) \times 1000 \times 0.01276 = 1.91 \text{ milligals}$$

constantly subtracted from all values, where 0.01276 is the factor for the gravity effect of an infinite slab of uniform thickness (Grant and West, 1965 p. 238). Since a total of 181 feet of local relief was observed in the area, local variations of

$$(2.82 - 2.67) \times 181 \times 0.01276 = 0.35 \text{ milligals}$$

may be due to the choice of a non-typical density. Since the first effect is constant, and the second effect is small, they were both ignored. The free air

gravity gradient in the Flin Flon region is 0.09445 milligals/foot and this was combined with the Bouguer effect to give the total gravity elevation correction, where e is elevation,

$$(0.09445 - 2.67 \times 0.01276) \times e = 0.06038\ e \text{ mg}$$

The effect of latitude is expressed by the International Gravity Formula (c.f. page 83). The value determined from this formula is subtracted from the elevation-corrected gravity to yield the residual Bouguer anomaly. For approximate calculations, the formula $w = 1.307 \sin 2\theta$ is used, where w is the correction in milligals/mile. At the latitude of Amisk Lake (54°40'), this amounts to 1.233 milligals/mile.

Accurate topographic maps are not available. Care was taken to read the gravimeter well removed from steep slopes or cliffs. Because the station spacing was broad, and a contour interval of 1 milligal was desired, it is believed that neglect of the terrain correction is justified. The terrain is locally rugged and irregular but the total relief is only 181 feet for all stations and most of this range is found in the northeast corner of the map area.

Figure 6.6 shows computed terrain effects for some topographical features with density 2.67 gm/cc. Thirty feet of local terrain relief is fairly typical of the Amisk Lake area.

Of the three cases shown in Figure 6.6 the maximum effect is for a vertical cliff. A reading at the edge or base of the cliff would be 0.5 milligals

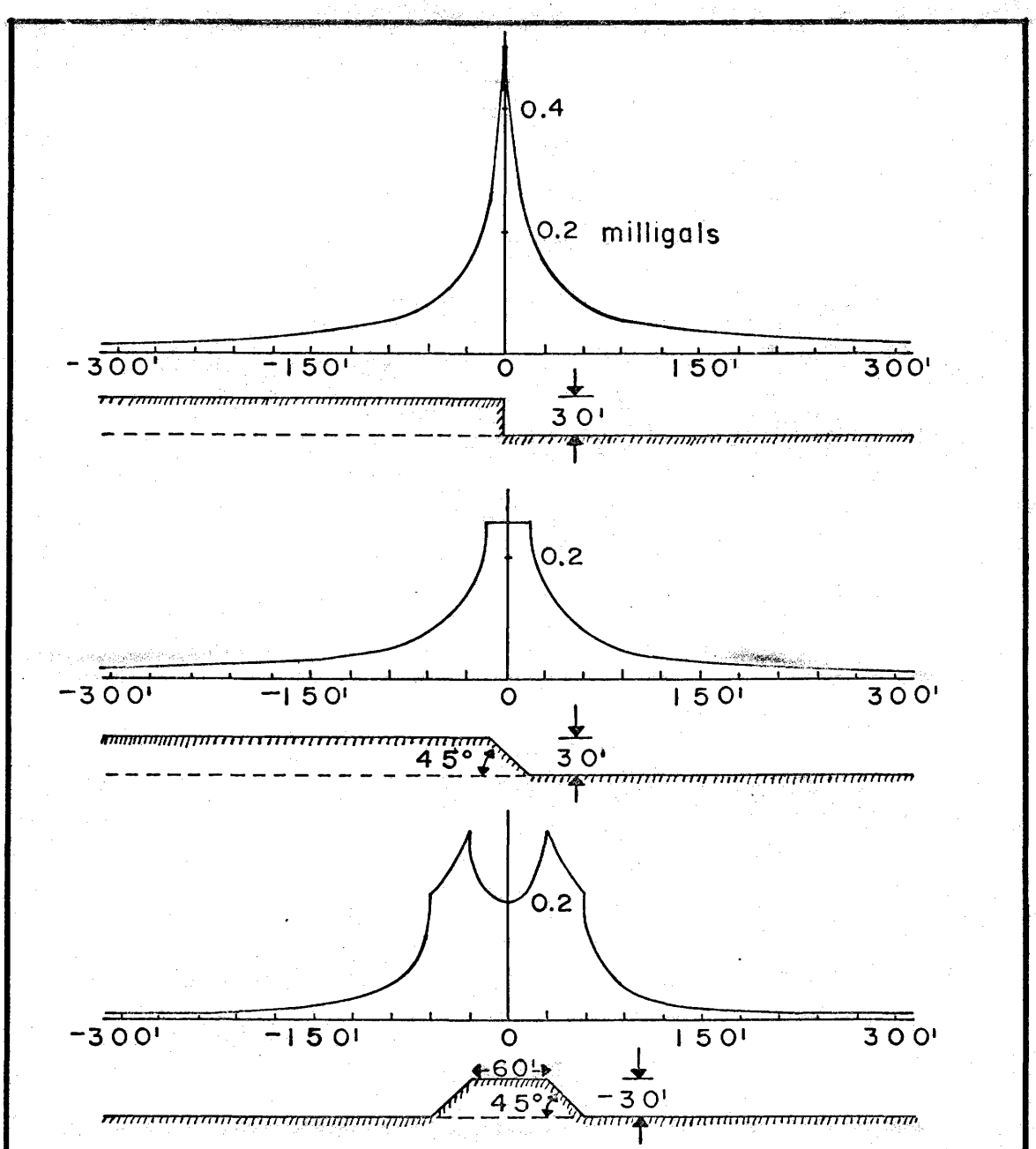

GRAVITATIONAL TERRAIN EFFECTS OF TWO DIMENSIONAL TOPOGRAPHIC FEATURES from HUBBERT (1948)

Drawn by C.S.

Figure 6.6

too low. A reading 100 feet from the cliff would be 0.05 milligals too low. Gravity readings in the Amisk Lake area were placed as far as possible from such features so that their effect is quite small. More important, and more difficult to assess, is the effect of a sloping cliff. Many gravity readings were located on lakeshores where the lake bottom sloped down at an unknown angle to an unknown depth. The sloping cliff thus formed has a gravity effect somewhat less than that shown in Fig. 6.6, (0.26 mg) because the presence of the lake water reduces the density contrast. If the rock density is 2.67 gm/cc the effect is:

$$\Delta g = 0.26 \text{ mg} \frac{2.67 - 1.00}{2.67} = 0.16 \text{ mg}$$

Errors in the relative gravity values of this survey may be due to a number of variables as listed below. Errors in reading the gravity meter amount to ± 0.05 mg, (page 100). Errors in elevation amount to ± 0.5 feet for readings referenced to lake elevations, (page 90). Errors in latitude may be about ± 264 feet, (page 91) and terrain effects may be about 0.16, (page 108). If all effects are additive this results in:

Reading error	± 0.05 mg
Elevation ± 0.5 x 0.06 mg/ft	± 0.03 mg
Latitude ± 264 ft x .000233 mg/ft	± 0.06 mg
Terrain	+ 0.16 mg
	+ 0.30 mg or - 0.14 mg

Most values of Bouguer anomaly should, therefore, have an error of no more than 0.30 milligals with respect to other values in the area.

6.4 The gravity map

A station spacing of about $\frac{1}{2}$ mile was desired, but the terrain prevented this in some areas, while much closer spacing was achieved in other localities. A total of 840 gravity stations were read in an area of about 200 square miles.

The results are shown in Figure 6.7, Bouguer Gravity Map of the Amisk Lake Area. Extreme Bouguer values of -12.7 milligals maximum and -41.8 milligals minimum were found in the area, a total range of 29.1 milligals. The gravity map is dominated by a pronounced gravity "high" which is centered along a zone through Table, Konuto, and Mosher Lakes. The anomaly falls off rapidly towards the north end of Wolverine Lake. This anomaly has a broad flank extending to the west shore of Mystic Lake, and a finger extends northeast through Wekach Lake. The anomaly is directly correlated with the outcrop area of basic and ultrabasic dikes and sills. A smaller gravity high is found over the ultrabasic Boundary Intrusion at the north end of Phantom Lake.

Pronounced gravity minima occur over most of the mappable acidic igneous intrusive rocks in the area. The gravity field displays a continuous decrease from east to west across Amisk Lake. This may be associated with the acidic volcanic rocks becoming more abundant towards the west side of the lake.

7. METHODS OF INTERPRETATION

A great variety of interpretation techniques have been developed through the years that gravity surveys have been used. However, most of these techniques have been designed to interpret anomalies due to buried sources. In particular, there is no published method for handling a gradational density contrast. In this chapter are presented derivations and characteristic curves for three new interpretation methods. The new methods provide means of interpreting:

1) The outcropping right rectangular prism
2) The gradational density contrast
3) The outcropping sloping step model.

In addition to the new methods presented, a number of published interpretation techniques have been used. These include the inequalities of Smith (1960) for estimating the limiting depths of gravitating bodies, the solid angle formulae and charts of Nettleton (1942) for estimating the gravity effect of two dimensional bodies, and the gravity effect of a right rectangular prism derived and programmed by Nagy (1966).

The initial procedure in interpretation is to inspect the Bouguer map and note the degree of correlation with the various outcropping rock types. Anomalies are then interpreted quantitatively to estimate the size, shape, density and depth of their causative bodies. Using these estimates, a series of geological models are postulated and their gravity effects computed. The computed gravity effects are compared with the observed gravity anomalies.

If a comparison is good and the model can be explained in geological terms, while not being contradictory to other geophysical evidence, then the interpretation is accepted.

Two papers recently listed (1966) in Geophysical Abstracts by Vashilov, Yu., Ya., (1964), and Pavlovskiy, V.I. and Serebryakov, Ye.B. (1965), have titles indicating that they may describe interpretation techniques similar to those developed in this thesis for the outcropping right rectangular prism, and the gradational density contrast. The above two papers are in the Russian language and as of this writing, have not yet been received for inspection.

The following pages present the derivations and characteristic curves for the three new interpretation methods.

7.1 The right rectangular prism

The gravity effect of a right rectangular prism has been derived and programmed in Fortran IV by Nagy (1966). This program has been used in this thesis for computing gravity effects of postulated geological models. In addition, the program can be used to generate characteristic curves to solve for certain parameters of a gravitating prism. In order to do this, however, it is necessary to show that the gravity effect is linear in some parameter, such as width, of the prism.

The gravity effect of a prism is given by Nagy (1966):

$$\Delta g/G\rho = \left[\left[\left[x \ln (y+r) + y \ln (x+r) - z \sin^{-1} \frac{z^2+y^2+yr}{(y+r)\sqrt{y^2+z^2}}\right]\right]\right]_{x_1 y_1 z_1}^{x_2 y_2 z_2} \qquad (1)$$

where Δg is the gravity effect

G is the gravity constant

ρ is the density contrast

$r = \sqrt{x^2 + y^2 + z^2}$

x_1, x_2 are the x co-ordinates of the prism

y_1, y_2 are the y co-ordinates of the prism

z_1, z_2 are the z co-ordinates of the prism. (Figure 7.1)

With equation (1) as a starting point, we proceed with the following derivation.

Now let w = half the width of the prism

$y_1 = z_1 = 0$ $\qquad$ $x_1 = x - w$

$y_2 = kw$ $\qquad$ $x_2 = x + w$

$z_2 = lw$ $\qquad$ x is the distance to the center of the prism along the x axis (Figure 7.1)

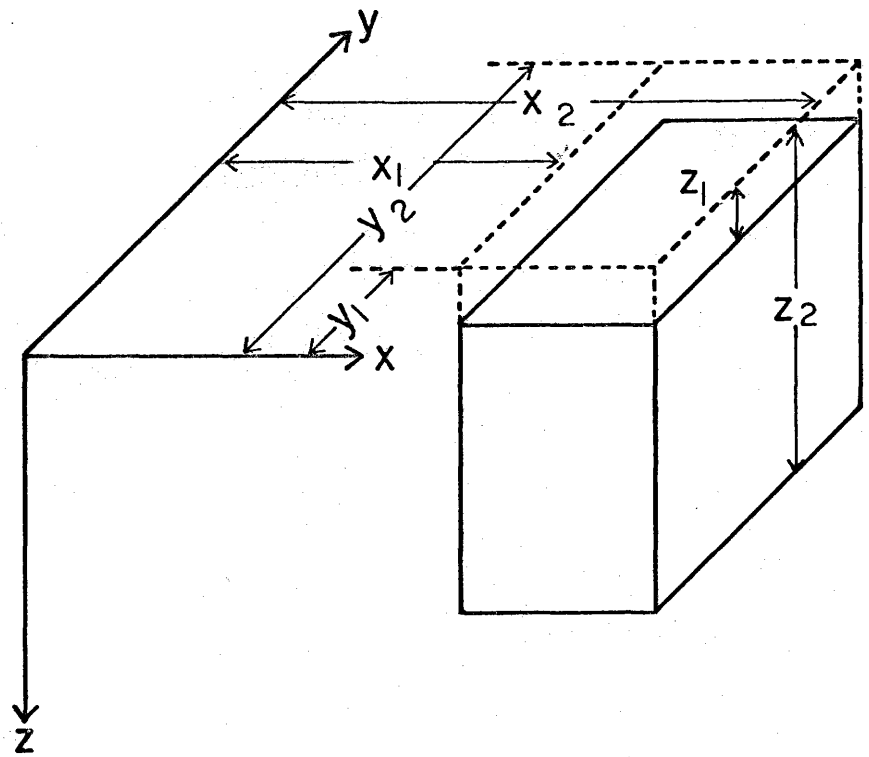

CARTESIAN CO-ORDINATES FOR A PRISM

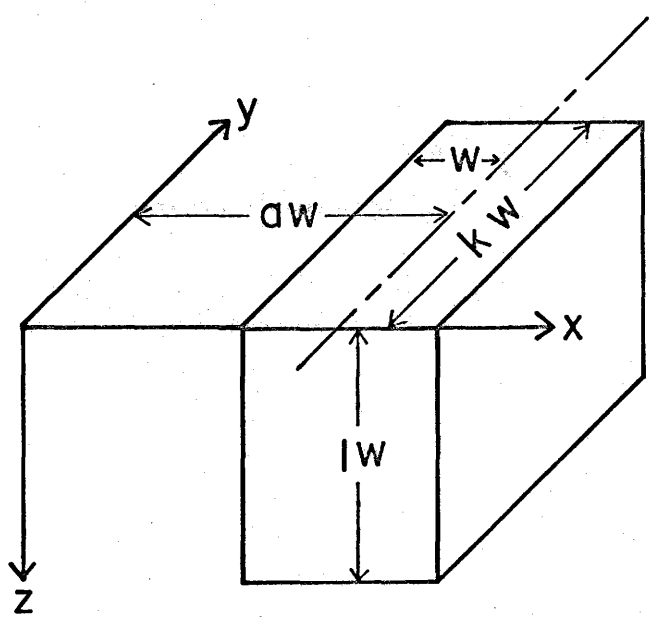

NORMALIZED CO-ORDINATES FOR AN OUTCROPPING PRISM

Drawn by C.S.

Figure 7.1

$$\Delta g/G\rho = \left[\left[\left[x\ln(y+r)+y\ln(x+r)-z\sin^{-1}\frac{z^2+y^2+yr}{(y+r)\sqrt{y^2+z^2}}\right]_{x-w}^{x+w}\right]_0^{kw}\right]_0^{lw}$$

$$= (x+w)\ln\left(kw+\sqrt{(x+w)^2+k^2w^2}\right)-(x-w)\ln\left(kw+\sqrt{(x-w)^2+k^2w^2}\right)$$

$$+kw\ln\left(x+w+\sqrt{(x+w)^2+k^2w^2}\right)-kw\ln\left(x-w+\sqrt{(x-w)^2+k^2w^2}\right)$$

$$-(x+w)\ln\left(kw+\sqrt{(x+w)^2+k^2w^2+l^2w^2}\right)+(x-w)\ln\left(kw+\sqrt{(x-w)^2+k^2w^2+l^2w^2}\right)$$

$$-kw\ln\left(x+w+\sqrt{(x+w)^2+k^2w^2+l^2w^2}\right)+kw\ln\left(x-w+\sqrt{(x-w)^2+k^2w^2+l^2w^2}\right)$$

$$+(x+w)\ln\sqrt{(x+w)^2+l^2w^2}-(x-w)\ln\sqrt{(x-w)^2+l^2w^2}$$

$$-(x+w)\ln(x+w)+(x-w)\ln(x-w)$$

$$-lw\sin^{-1}\frac{l^2w^2+k^2w^2+kw\sqrt{(x+w)^2+k^2w^2+l^2w^2}}{\left(kw+\sqrt{(x+w)^2+k^2w^2+l^2w^2}\right)\sqrt{k^2w^2+l^2w^2}}+lw\sin^{-1}\frac{l^2w^2+kw+kw\sqrt{(x-w)^2+k^2w^2+l^2w^2}}{\left(kw+\sqrt{(x-w)^2+k^2w^2+l^2w^2}\right)\sqrt{k^2w^2+l^2w^2}}$$

$$+lw\sin^{-1}\frac{l^2w^2}{\sqrt{(x+w)^2+l^2w^2}\,lw}-lw\sin^{-1}\frac{l^2w^2}{\sqrt{(x-w)^2+l^2w^2}\,lw} \qquad (2)$$

Now we let x = aw, and remembering that ln(w(a+1)) = ln(w) + ln(a+1), (2) may be simplified and w factored out yielding

$$\begin{aligned}
\Delta g/G\rho W = {} & (a+1)\ln\left(k+\sqrt{(a+1)^2+k^2}\right) - (a-1)\ln\left(k+\sqrt{(a-1)^2+k^2}\right) \\
& + k\ln\left(a+1+\sqrt{(a+1)^2+k^2}\right) - k\ln\left(a-1+\sqrt{(a-1)^2+k^2}\right) \\
& -(a+1)\ln\left(k+\sqrt{(a+1)^2+k^2+l^2}\right) + (a-1)\ln\left(k+\sqrt{(a-1)^2+k^2+l^2}\right) \\
& - k\ln\left(a+1+\sqrt{(a+1)^2+k^2+l^2}\right) + k\ln\left(a-1+\sqrt{(a-1)^2+k^2+l^2}\right) \\
& + (a+1)\ln\sqrt{(a+1)^2+l^2} - (a-1)\ln\sqrt{(a-1)^2+l^2} \\
& - (a+1)\ln(a+1) + (a-1)\ln(a-1) \\
& - l\sin^{-1}\frac{l^2+k^2+k\sqrt{(a+1)^2+k^2+l^2}}{\left(k+\sqrt{(a+1)^2+k^2+l^2}\right)\sqrt{k^2+l^2}} + l\sin^{-1}\frac{l^2+k^2+k\sqrt{(a-1)^2+k^2+l^2}}{\left(k+\sqrt{(a-1)^2+k^2+l^2}\right)\sqrt{k^2+l^2}} \\
& + l\sin^{-1}\frac{l}{\sqrt{(a+1)^2+l^2}} - l\sin^{-1}\frac{l}{\sqrt{(a-1)^2+l^2}} \qquad (3)
\end{aligned}$$

This can be expressed as

$$\Delta g = G\rho W\, F(a-1, a+1, o, k, o, l)$$

Similarly Nagy's expression may be written

$$\Delta g = G\rho F(x_1, x_2, o, y, o, z_2)$$

Combining the two expressions yields

$$WF(a-1, a+1, o, k, o, l) = F(x_1, x_2, o, y_2, o, z_2) \qquad (4)$$

This can be easily extended to include the case where y_1, or z_1, are not zero.

Where its argument is zero, the ln function has a discontinuity and the integration of the function across such points is not permitted.

The point of computation of Δg defines the x, y, and z axes. Therefore, when a point of computation lies on the surface of the prism, the argument of the ln function, $y + r$, or $x + r$, is zero and it is necessary to integrate from the lower limit to the axis and then from the axis to the upper limit. Nagy's computer program does this calculation in parts automatically. The interpreter then has complete freedom to select computation points with the exception that a point may not be inside a prism.

An interpretation chart has been derived for the gravity effect of an outcropping rectangular prism using relationship (4) derived above. This chart may be used if the surface dimensions are known from geological maps, or if they can be estimated accurately from the gravity anomaly. Figure 7.2 permits interpretation of the depth extent of an outcropping prism if the maximum anomaly and the density contrast are known.

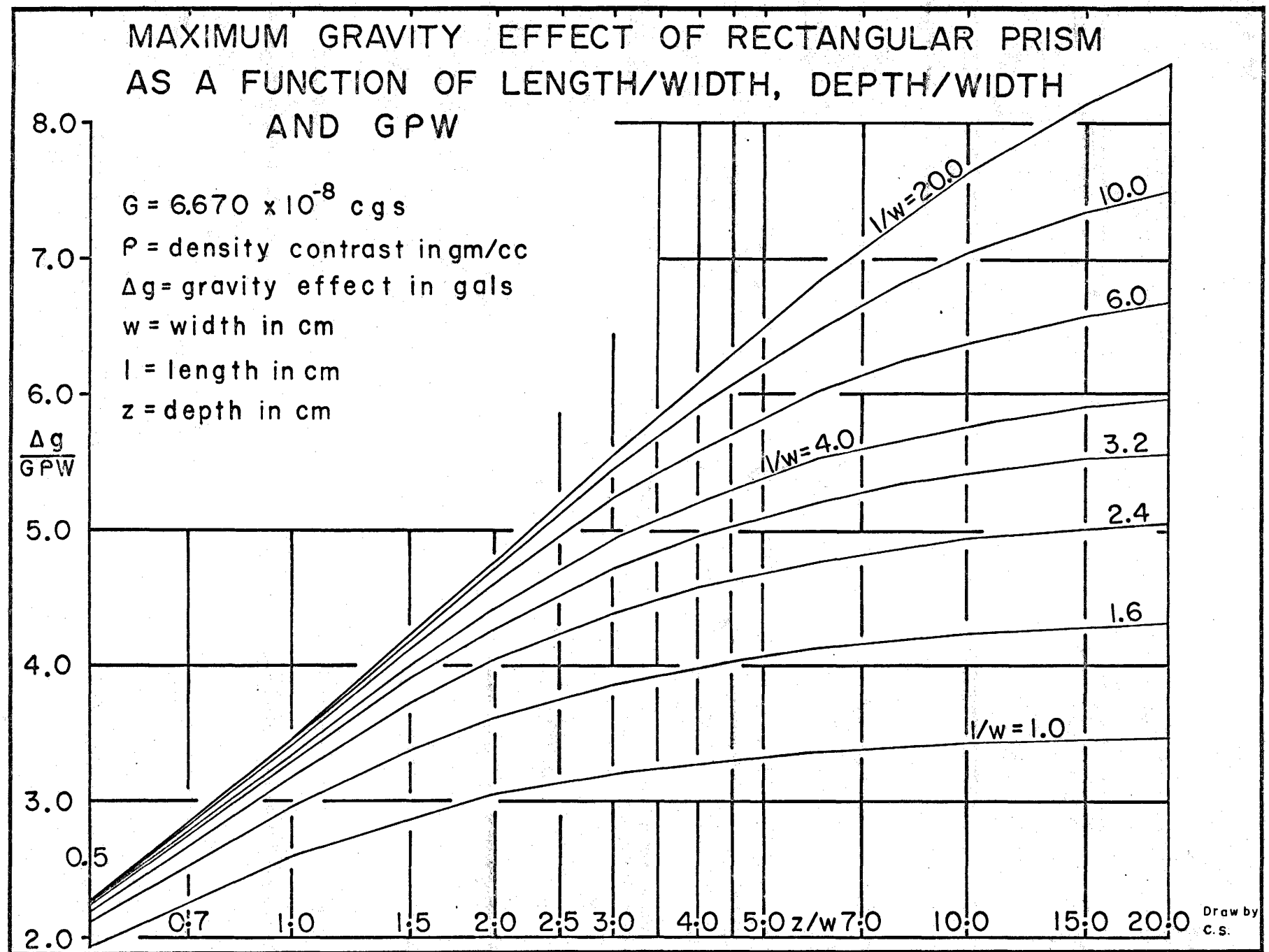
MAXIMUM GRAVITY EFFECT OF RECTANGULAR PRISM
AS A FUNCTION OF LENGTH/WIDTH, DEPTH/WIDTH
AND GPW
G = 6.670 x 10^-8 cgs
P = density contrast in gm/cc
Δg = gravity effect in gals
w = width in cm
l = length in cm
z = depth in cm
Δg / GPW
8.0
7.0
6.0
5.0
4.0
3.0
2.0
0.5
l/w=20.0
10.0
6.0
l/w=4.0
3.2
2.4
1.6
l/w=1.0
0.7
1.0
1.5
2.0
2.5
3.0
4.0
5.0
z/w
7.0
10.0
15.0
20.0
Draw by C.S.

Figure 7.2

7.2 The gradational density contrast

The gravity effect of a uniform horizontal slab with density variable in one horizontal direction is, according to Novosolitskii (1965)

$$\Delta g(x) = G \int_{-\infty}^{\infty} \rho(\xi) \ln \frac{H_2^2 + (x-\xi)^2}{H_1^2 + (x-\xi)^2} d\xi \qquad (5)$$

where $\Delta g(x)$ is the vertical gravity effect at a point x

G is the gravity constant

$\rho(\xi)$ is the density as a function of the position variable

H_2 is the depth to the bottom of the slab

H_1 is the depth to the top of the slab

ξ is the variable distance

x is the point of integration.

Proceeding from equation (5), we make the following derivation.

Simplifying the expression of $\rho(\xi)$ to a linear function, we impose the limits as follows:

$$\rho(\xi) = 0 \qquad -\infty < \xi < J$$
$$\rho(\xi) = k(\xi - J) \qquad J < \xi < L$$
$$\rho(\xi) = K(L - J) \qquad L < \xi < \infty$$

where k is a linear density gradient in gm/cc/km, Fig. 7.3.

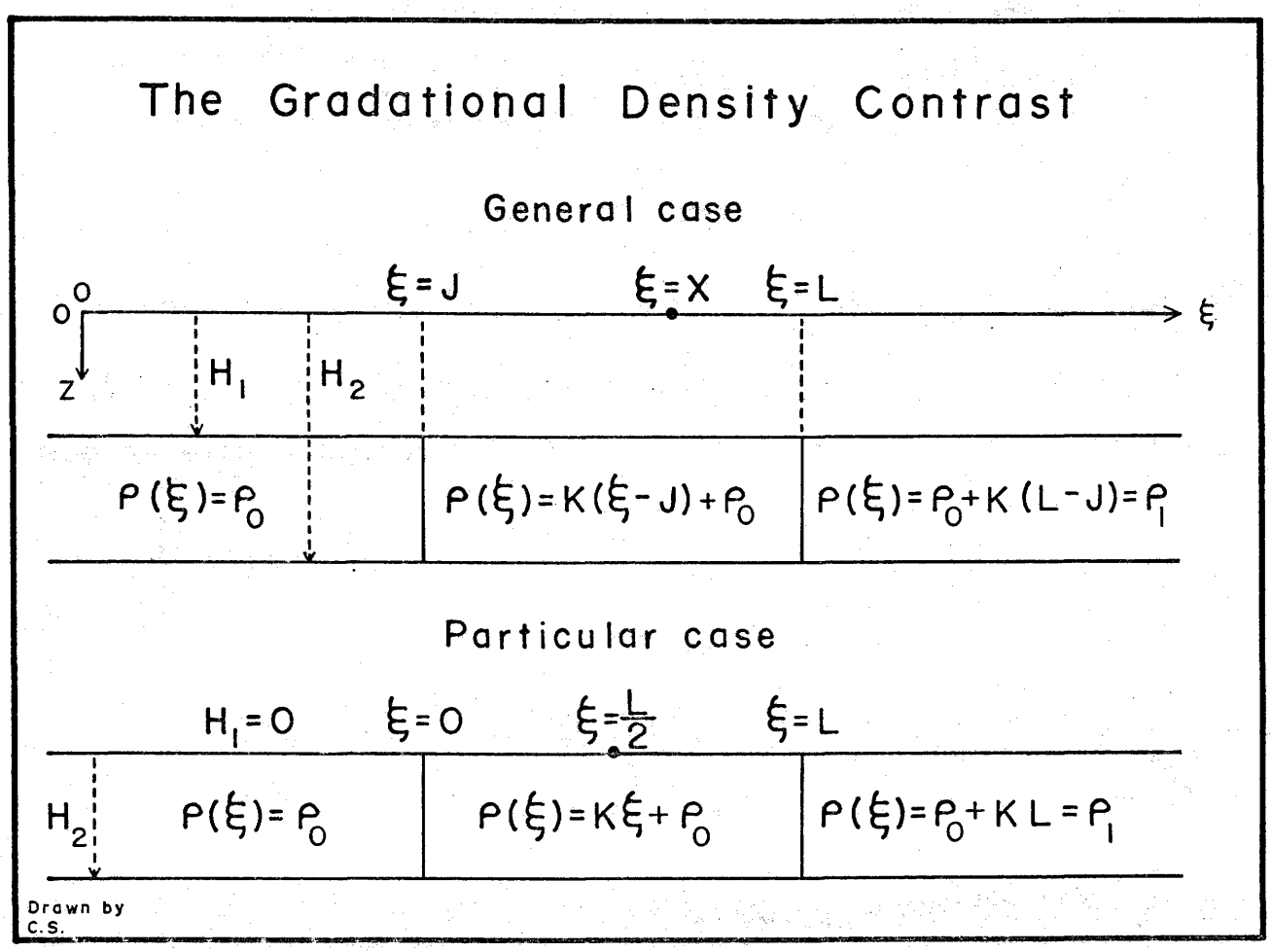
The Gradational Density Contrast
General case
0
ξ=J
ξ=X
ξ=L
ξ
z
H1
H2
ρ(ξ)=ρ0
ρ(ξ)=K(ξ-J)+ρ0
ρ(ξ)=ρ0+K(L-J)=ρ1
Particular case
H1=0
ξ=0
ξ=L/2
ξ=L
H2
ρ(ξ)=ρ0
ρ(ξ)=Kξ+ρ0
ρ(ξ)=ρ0+KL=ρ1
Drawn by C.S.

Figure 7.3

With the new limits,

$$\Delta g(x) = 0 + G\int_{J}^{L} k(\xi - J) \ln \frac{H_2^2+(x-\xi)^2}{H_1^2+(x-\xi)^2}\, d\xi + G\int_{L}^{\infty} k(L-J) \ln \frac{H_2^2+(x-\xi)^2}{H_1^2+(x-\xi)^2}\, d\xi$$

Let J = 0, then L = the width of the variable strip.

$$\Delta g(x) = Gk\int_{o}^{L} \xi \ln \frac{H_2^2+(x-\xi)^2}{H_1^2+(x-\xi)^2} d\xi + GkL\int_{L}^{\infty} \ln \frac{H_2^2+(x-\xi)^2}{H_1^2+(x-\xi)^2}\, d\xi \qquad (6)$$

The second integral of (6) may be simplified as follows:

$$GkL\int_{L}^{\infty} \ln \frac{H_2^2+(x-\xi)^2}{H_1^2+(x-\xi)^2}\, d\xi = GkL\int_{L}^{\infty} \left[\ln\left(H_2^2+(x-\xi)^2\right) - \ln\left(H_1^2+(x-\xi)^2\right)\right] d\xi$$

and using Formula 452, Peirce and Foster (1956),

$$\int_{L}^{\infty} \ln\left(H_1^2+(x-\xi)^2\right)(-d\xi) = \left[(x-\xi)\ln\left(H_1^2+(x-\xi)^2\right) - 2(x-\xi) + 2H_1 \tan^{-1}\frac{x-\xi}{H_1}\right]_{L}^{\infty}$$

Solving similarly for the part involving H_2, combining and inserting the limits,

$$GkL\int_{L}^{\infty} \ln \frac{H_2^2+(x-\xi)^2}{H_1^2+(x-\xi)^2}\, d\xi = GkL\left[(x-L)\ln\left(H_2^2+(x-L)^2\right) + 2H_2 \tan^{-1}\frac{x-L}{H_2}\right.$$

$$\left. - (x-L)\ln\left(H_1^2+(x-L)^2\right) - 2H_1 \tan^{-1}\frac{x-L}{H_1} + \pi(H_2-H_1)\right] \qquad (7)$$

This is the expression for the gravity effect of a vertical step block with its origin at x = L.

The first integral of (6) is more complicated. Separating the ln terms as before we write:

$$Gk\int_0^L \xi \ln \frac{H_2^2 + (x-\xi)^2}{H_1^2 + (x-\xi)^2}\, d\xi = Gk\int_0^L \xi \ln\left(H_2^2 + (x-\xi)^2\right) d\xi - Gk\int_0^L \xi \ln\left(H_1^2 + (x-\xi)^2\right) d\xi \quad (8)$$

Taking the term with H_2 and integrating by parts,

Let $\xi\, d\xi = dU,\ \frac{\xi^2}{2} = U,\ \ln\left(H_2^2 + (x-\xi)^2\right) = V,\ \frac{2(x-\xi)}{H_2^2 + (x-\xi)^2}\ (-d\xi) = dV,$

$$H_2^2 + (x-\xi)^2 = X$$

Then $$\int_0^L \xi \ln X\, d\xi = \frac{\xi^2}{2}\ln X + \int_0^L \frac{\xi^2(x-\xi)}{X}\, d\xi$$

$$= \frac{\xi^2}{2}\ln X + x\int_0^L \frac{\xi^2}{X}\, d\xi - \int_0^L \frac{\xi^3}{X}\, d\xi \quad (9)$$

Using Formulas 70, 75, 78, and 80, (Peirce and Foster, 1956), we write

$$\int_0^L \frac{d\xi}{X} = \left[\frac{1}{H_2}\tan^{-1}\frac{\xi - x}{H_2}\right]_0^L \quad (10)$$

$$\int_0^L \frac{\xi\, d\xi}{X} = \left[\frac{1}{2}\ln X + x\int \frac{d\xi}{X}\right]_0^L \quad (11)$$

$$\int_0^L \frac{\xi^2 d\xi}{X} = \left[\xi + x\ln X + (x^2 - H_2^2)\int \frac{d\xi}{X}\right]_0^L \quad (12)$$

$$\int_0^L \frac{\xi^3 d\xi}{X} = \left[-\frac{\xi^2}{2} + 2x \int \frac{\xi^2}{X} d\xi - (H_2^2 + x^2) \int \frac{\xi}{X} d\xi \right]_0^L \tag{13}$$

Substituting (10, (11), (12), and (13) into (9) we obtain

$$\int_0^L \xi \ln X \, d\xi = \left[\frac{\xi^2}{2} + \frac{H_2^2 - x^2 + \xi^2}{2} \ln X + 2x H_2 \left(\frac{1}{H_2} \tan^{-1} \frac{\xi - x}{H_2} \right) \right]_0^L \tag{14}$$

Solving (8) similarly for the part involving H_1, combining and inserting the limits, we obtain:

$$Gk \int_0^L \xi \ln \frac{H_2^2 + (x-\xi)^2}{H_1^2 + (x-\xi)^2} d\xi =$$

$$Gk \left[\frac{H_2^2 - x^2 + L^2}{2} \ln \left(H_2^2 + (x-L)^2 \right) - 2x H_2 \tan^{-1} \frac{x-L}{H_2} \right.$$

$$- \frac{H_1^2 - x^2 + L^2}{2} \ln \left(H_1^2 + (x-L)^2 \right) + 2x H_1 \tan^{-1} \frac{x-L}{H_1}$$

$$- \frac{H_2^2 - x^2}{2} \ln \left(H_2^2 + x^2 \right) + 2x H_2 \tan^{-1} \frac{x}{H_2}$$

$$\left. + \frac{H_1^2 - x^2}{2} \ln \left(H_1^2 + x^2 \right) - 2x H_1 \tan^{-1} \frac{x}{H_1} \right] \tag{15}$$

This is the expression for the gravity effect of a two dimensional slab with density varying uniformly across its width (L).

Combining (7) and (15) and collecting terms, we write:

$$\Delta g(x) = Gk\left[\frac{H_2^2-(x-L)^2}{2}\ln\left(H_2^2+(x-L)^2\right) - 2H_2(x-L)\tan^{-1}\frac{x-L}{H_2}\right.$$

$$-\frac{H_1^2-(x-L)^2}{2}\ln\left(H_1^2+(x-L)^2\right)+2H_1(x-L)\tan^{-1}\frac{x-L}{H_1}$$

$$-\frac{H_2^2-x^2}{2}\ln\left(H_2^2+x^2\right)+2H_2\,x\tan^{-1}\frac{x}{H_2}$$

$$\left.+\frac{H_1^2-x^2}{2}\ln\left(H_1^2+x^2\right)-2H_1\,x\tan^{-1}\frac{x}{H_1}+\pi L\left(H_2-H_1\right)\right] \qquad (16)$$

This is the expression for the gravity effect of a slab with density varying in one direction as follows:

$$-\infty < \xi < 0 \qquad \rho_o = 0$$

$$0 < \xi < L \qquad \rho = k\xi + \rho_o$$

$$L < \xi < +\infty \qquad \rho_1 = kL + \rho_o$$

If ρ_0 is chosen not equal to zero, the constant term $2\pi G\rho_o(H_2-H_1)$ may be added to the expression and if H_1 is set to zero, then subscripts are unnecessary and (16) becomes

$$\Delta g(x) = 2\pi G\rho_o H + Gk\left[\frac{(H^2-(x-L)^2)}{2}\ln(H^2+(x-L)^2) + \frac{(x-L)^2}{2}\ln(x-L)^2\right. \tag{17}$$

$$\left. - \frac{H^2-x^2}{2}\ln(H^2+x^2) - \frac{x^2}{2}\ln x^2 - 2H(x-L)\tan^{-1}\frac{x-L}{H} + 2Hx\tan^{-1}\frac{x}{H} + \pi LH\right]$$

This equation has been programmed in Fortran IV to obtain the model curves in figure 7.4.

Differentiating (16) with respect to x and simplifying yields:

$$\frac{d\Delta g(x)}{dx} = Gk\left[x\ln\frac{H_2^2+x^2}{H_1^2+x^2} - (x-L)\ln\frac{H_2^2+(x-L)^2}{H_1^2+(x-L)^2} + 2H_1\tan^{-1}\frac{x-L}{H_1}\right.$$

$$\left. - 2H_1\tan^{-1}\frac{x}{H_1} - 2H_2\tan^{-1}\frac{x-L}{H_2} + 2H_2\tan^{-1}\frac{x}{H_2}\right] \tag{18}$$

This is the equation expressing the horizontal derivative of gravity for a strip with variable density.

The second derivative of (16) yields

$$\frac{d^2\Delta g(x)}{dx^2} = \left[\ln\frac{H_2^2+x^2}{H_1^2+x^2} - \ln\frac{H_2^2+(x-L)^2}{H_1^2+(x-L)^2}\right]Gk$$

This expression equals zero if $x = L/2$.

Therefore an inflection point exists at $x = L/2$, or half way across the variable strip. In (18), let $x = L/2$, $H_1 = 0$, $H_2 = H$. Then

$$\frac{d\Delta g(L/2)}{dx} = GkL\left[\ln\left[\left(\frac{2H}{L}\right)^2+1\right] + \frac{4H}{L}\tan^{-1}\frac{L}{2H}\right] \tag{19}$$

This equation has been programmed in Fortran IV and used to obtain figure 7.5.

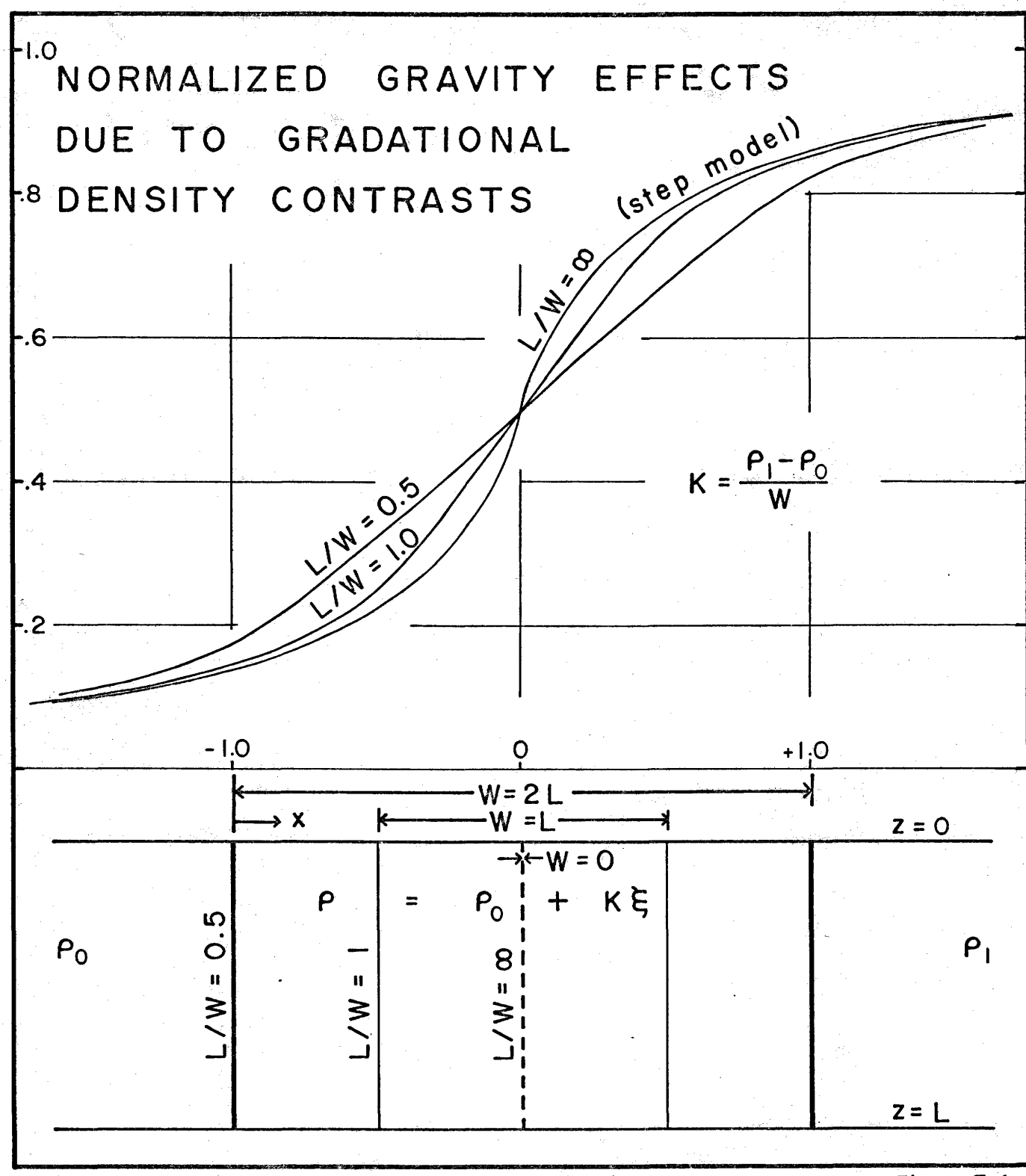
NORMALIZED GRAVITY EFFECTS
DUE TO GRADATIONAL
DENSITY CONTRASTS
1.0
.8
.6
.4
.2
(step model)
L/W = ∞
L/W = 0.5
L/W = 1.0
K = (ρ1 − ρ0) / W
-1.0
0
+1.0
W = 2L
x
W = L
z = 0
W = 0
ρ = ρ0 + Kξ
ρ0
ρ1
L/W = 0.5
L/W = 1
L/W = 8
z = L

Figure 7.4

NOMOGRAM FOR HORIZONTAL GRAVITY GRADIENT DUE TO A STRIP OF VARYING DENSITY

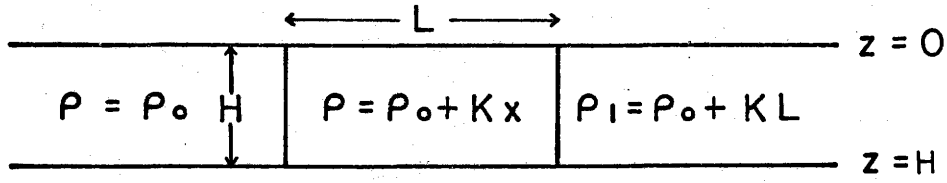

$K = \frac{d\rho}{dx}$ $\frac{gr/cc}{km}$ $\frac{dg}{dx}$ in $\frac{milligals}{km}$

L and H in km

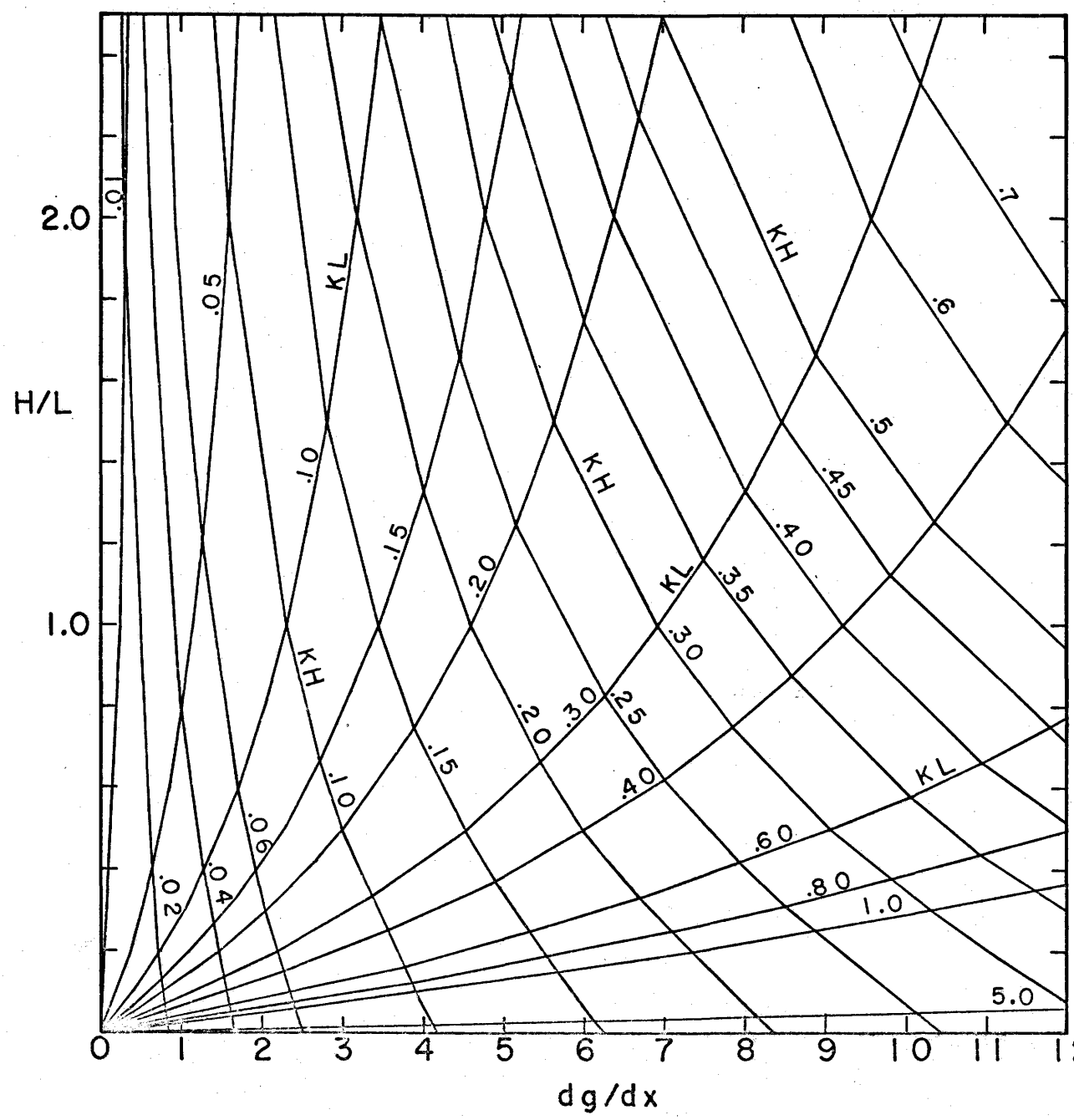

Figure 7.5

In (19), kL represents the total density contrast. If L is very large, densities expressed in grams/cubic centimeter, and distances in kilometers, then (19) may be simplified to:

$$\frac{d\Delta g}{dx} = 41.9 \text{ kH milligals/kilometer} \qquad (20)$$

which is the expression for the gravity gradient due to a slab with density varying uniformly in one direction. Gravity gradients computed from this simplified formula will be too large because, in practice, L is always finite.

7.3 The outcropping sloping step model

The gravity effect of a fault or sloping step is given by Grant and West (1965, p. 283).

$$\Delta g(x) = 2G\rho\left\{\pi/2 + (h+1)\tan^{-1}\frac{x-\cot d}{h+1} - h\tan^{-1}\frac{x}{h}\right.$$

$$+ (x\sin^2 d + h\sin d\cos d)\ln\left[\frac{(x-\cot d)^2+(h+1)^2}{x^2+h^2}\right]^{\frac{1}{2}}$$

$$\left.- (x\sin d\cos d + h\cos^2 d)\left(\tan^{-1}\frac{x\cot d}{h+1} - \tan^{-1}\frac{x}{h}\right)\right\} \qquad (21)$$

where G is the gravity constant

ρ is the density contrast

h is the normalized depth to the top of the step

d is the dip of the face of the step

x is the normalized horizontal distance

l is the thickness of the slab taken as unity, hence h = h/l, x = x/l.

The first derivative of (21) is

$$\frac{d\Delta g(x)}{dx} = 2G\rho\left\{\frac{(h+1)^2}{(x-\cot d)^2+(h+1)^2} + \sin^2 d\left[\frac{(x-1)(x-\cot d)^2-(h+1)^2}{(x-\cot d)^2+(h+1)^2}\right.\right.$$

$$\left. + \ln\left(\frac{(x-\cot d)^2+(h+1)^2}{x^2+h^2}\right)^{\frac{1}{2}}\right] + \sin d\cos d\left[\frac{-h\cot d - x}{(x-\cot d)^2+(h+1)^2}\right.$$

$$\left.\left. - \tan^{-1}\frac{x-\cot d}{h+1} + \tan^{-1}\frac{x}{h}\right] - h\cos^2 d\left[\frac{h+1}{(x-\cot d)^2+(h+1)^2}\right]\right\} \qquad (22)$$

Grant and West (1965, Figures 10-14, 10-15, 10-16) present three sets of characteristic curves for a step model. However, these curves do not take into account the case where h = 0, which is a good approximation to rocks of contrasting density cropping out at the surface. This is because the method of Grant and West requires an estimate of the maximum slope of the anomaly, whereas the maximum slope is infinite in all cases of outcropping contacts.

Equations (21) and (22) were programmed in Fortran IV and used to derive two new sets of characteristic curves, Figures 7.7 and 7.8, for a step model with h = 0. To use the charts, the gravity profile is drawn and the slopes of the curve at a point near a "knee" of the curve estimated. The point of tangency to the same slope at the other "knee" is then determined. The horizontal separation $(x_2 - x_1)$ is measured and also the gravity difference Δg between the points of tangency. The ratio $\Delta g/s(x_2-x_1)$ is formed. Using a geological outcrop map or the maximum slope of the curve, the edge of the step, fault or contact must be located and the ratio x_1/x_2 obtained where x_1 and x_2 are the distances of the points of tangency respectively from that edge. Using these parameters, charts 1 and 2 are then entered to determine $(x_2-x_1)/1$, dip, and $\rho x\ 1/\Delta g$.

Equation 21 describes a family of curves which may be called the step model family. The gravity anomaly arising from certain geological situations is often approximated by a step model. However, the mathematical precision of the step model is never matched by any geological configuration and if a gravity anomaly curve does closely fit a curve of the step model family, the coincidence is remarkable. Figure 7.6 shows two step models and the resulting step model gravity curves. The interpretation procedure outlined above results in correct

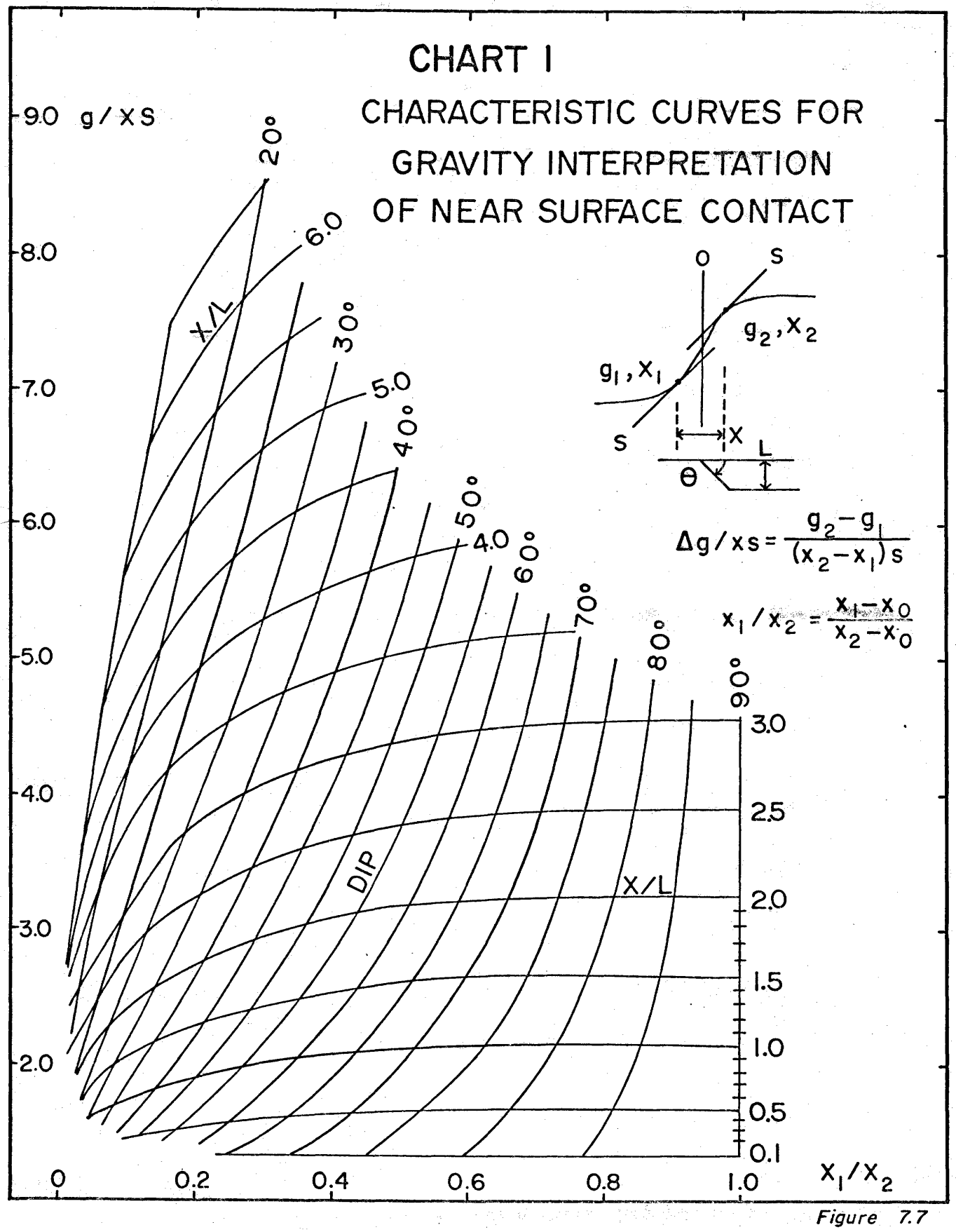
CHART I
CHARACTERISTIC CURVES FOR
GRAVITY INTERPRETATION
OF NEAR SURFACE CONTACT
9.0 g/xs
8.0
7.0
6.0
5.0
4.0
3.0
2.0
0
0.2
0.4
0.6
0.8
1.0
x_1/x_2
X/L
DIP
20°
30°
40°
50°
60°
70°
80°
90°
6.0
5.0
4.0
3.0
2.5
2.0
1.5
1.0
0.5
0.1
O
S
g_2, x_2
g_1, x_1
X
L
θ
$\Delta g/xs = \frac{g_2 - g_1}{(x_2 - x_1)s}$
$x_1/x_2 = \frac{x_1 - x_0}{x_2 - x_0}$

Figure 7.7

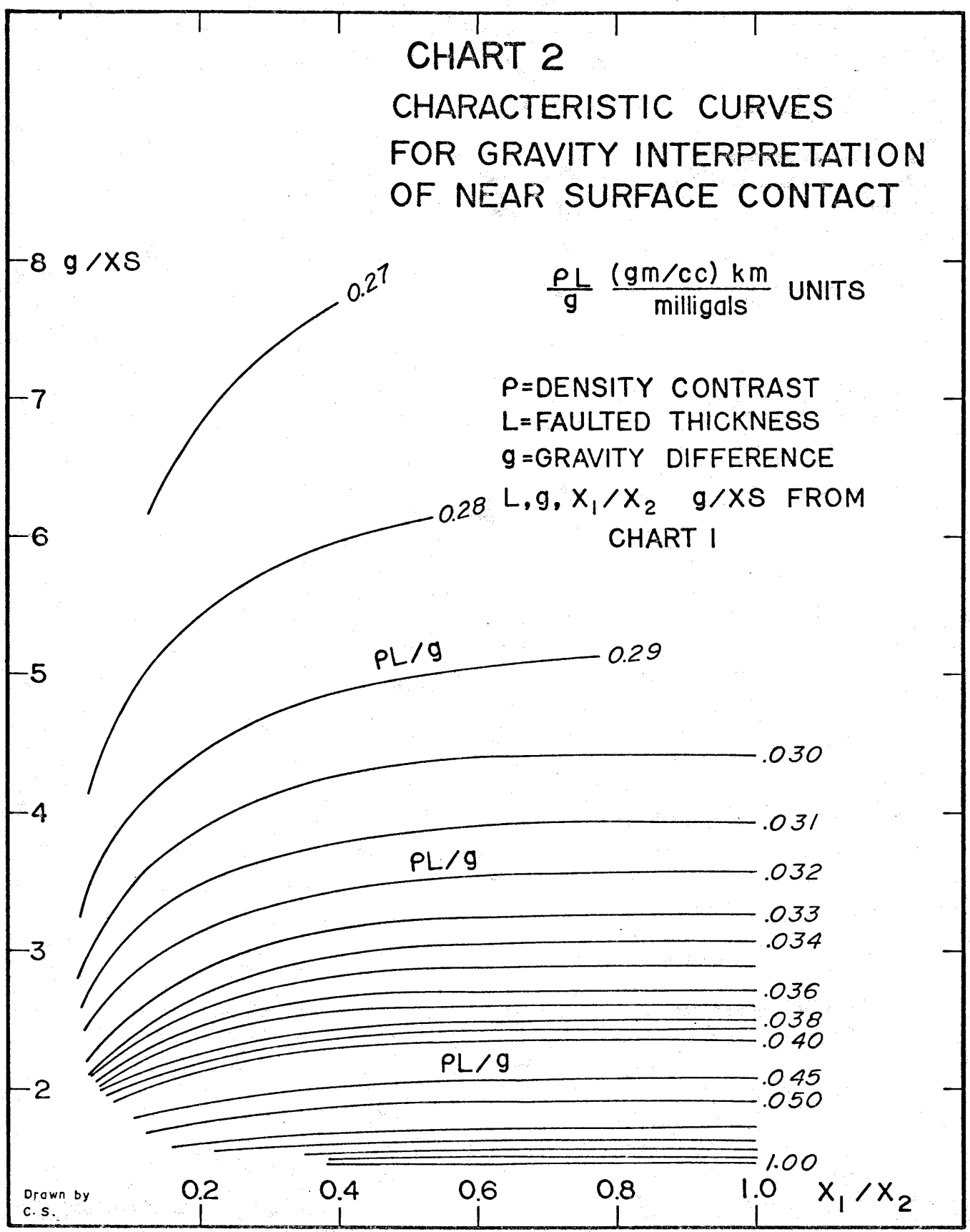
CHART 2
CHARACTERISTIC CURVES
FOR GRAVITY INTERPRETATION
OF NEAR SURFACE CONTACT
8 g/XS
7
6
5
4
3
2
ρL/g (gm/cc) km / milligals UNITS
ρ=DENSITY CONTRAST
L=FAULTED THICKNESS
g=GRAVITY DIFFERENCE
L, g, X1/X2 g/XS FROM
CHART I
0.27
0.28
PL/g
0.29
.030
.031
PL/g
.032
.033
.034
.036
.038
.040
PL/g
.045
.050
1.00
Drawn by
C. S.
0.2
0.4
0.6
0.8
1.0
X1/X2

Figure 7.8

answers when applied to the curves of Figure 7.6. On Figure 7.6 the interpretation parameters are indicated for the 60° step model. Two lines with slopes of 14.5% gravity effect/distance unit are drawn tangent to the gravity curve. The points of tangency are 0.51 and 1.14 distance units from the edge of the step and the gravity difference Δg between tangency points is 67.5% of the total gravity effect. Forming the ratios:

$$\frac{x_1}{x_2} = \frac{-0.51}{1.14} = -0.4475$$

$$\frac{\Delta g}{xs} = \frac{.675}{(1.14-(-.51) \times 0.145/1.0} = 2.82$$

Substituting these values in Figure 7.7 the values $\theta = 58.5°$ and $x/L = 1.7$ are obtained. $x = 1.14 - (-0.51) = 1.65$, therefore $L = 1.65/1.7 = 0.97$ From Figure 7.8, $\rho L/g = 0.0352$ from which is obtained

$$\rho = \frac{0.0352 \times 0.675}{0.97} = 0.0245 \frac{gm}{cc} \frac{km}{mg}$$

Comparing the interpreted values with the correct values we obtain:

	Depth	Dip	Density
Interpreted	0.97	58.5	0.0245
Correct	1.00	60.0	0.0239

The interpreted values are within 3% of the correct values. Other interpretations could be made starting with slopes different from 14.5%, thus obtaining several

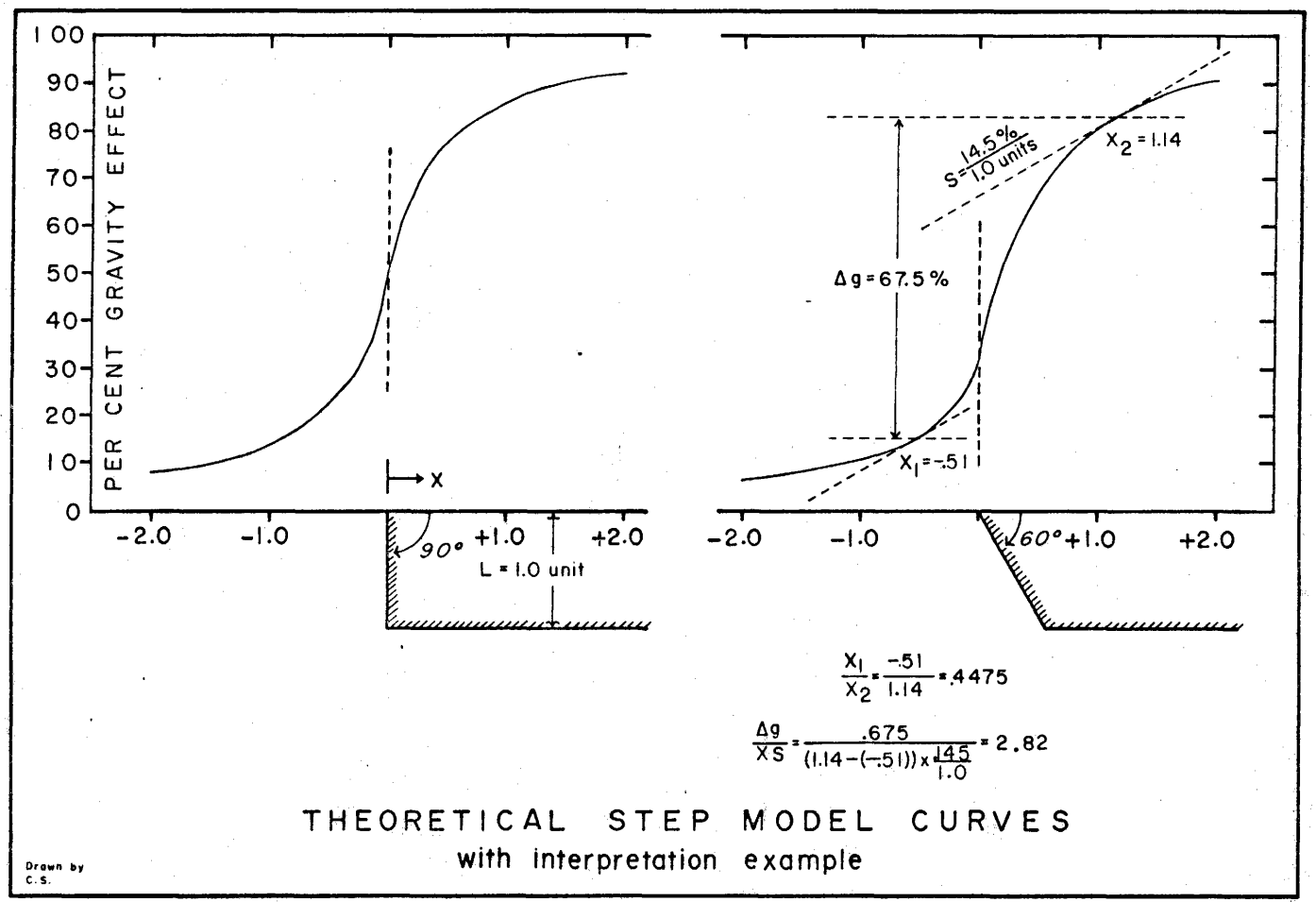
100
90
80
70
60
50
40
30
20
10
0
PER CENT GRAVITY EFFECT
-2.0
-1.0
+1.0
+2.0
X
90°
L = 1.0 unit
Δg = 67.5 %
S = 14.5 % / 1.0 units
X2 = 1.14
X1 = -.51
60°
X1/X2 = -.51/1.14 = .4475
Δg/XS = .675/((1.14-(-.51)) x 14.5/1.0) = 2.82
THEORETICAL STEP MODEL CURVES
with interpretation example
Drawn by C.S.

Figure 7.6

interpretations of the same anomaly. The method of Grant and West allows only one interpretation for each gravity curve. If a geological situation resembles the mathematical step model, all interpretations by Figures 7.7 and 7.8 will be nearly the same, otherwise they will be very different and some other interpretation method should be applied.

8. RESULTS OF INTERPRETATION

The gravity anomalies have been interpreted in terms of the size, shape and structure of the rock units. The anomalies are all associated with outcropping rock units. The only interpretable aspect therefore is the shape and depth extent of the rock units.

Three types of interpretation are presented here. Individual anomalies which have distinctive characteristics are interpreted with the use of methods such as the characteristic curves that have been developed in this thesis, or published elsewhere. Another technique is model curve matching which requires the computation of the gravity effect of some postulated geological model. If the model is reasonable in geological terms, and the computed curve matches the observed data, then the interpretation is accepted. Two such model interpretations are presented here. A qualitative discussion of all the anomalies and their relation to the outcropping rocks is also presented.

8.1 Qualitative Interpretation

The major feature of the gravity field in the Amisk Lake area is a large anomaly, positive with respect to its surroundings (c.f. fig. 3.2, 6.7). The maximum recorded relief is about 28 milligals. The anomaly extends parallel to the shore of Amisk Lake as far as Wolverine Lake, for a distance of at least 13 miles. Its extension south of the map area is unknown but since the amplitude is increasing to the south, it is believed that it becomes even larger, possibly attaining its maximum value in the area of the Meridian Creek

norite described by Byers and Dahlstrom (1954), southwest of Table Lake (fig. 3.1). The gravity maximum is correlated almost everywhere with outcrops of basic intrusive rock. An exception is found west of Mosher Lake where no large basic intrusion is indicated. However, a zone of high density rock (c.f. fig. 5.5) is found in this region, suggesting the possibility of an unrecognized basic intrusive rock in the area.

The anomaly is caused by a combination of the presence of the high density basic intrusions, an increase in the density of the volcanic rocks, and a thickening of the pile of high density rocks. The maximum thickness is indicated by the trend of the gravity "high", the greatest depth being reached south of Table Lake. A model interpretation profile for this anomaly has been calculated and is presented in section 8.3. Somewhat smaller gravity highs are found near Wekach Lake, the west arm of Schist Lake, and the north end of Phantom Lake, all correlating with known outcrops of basic intrusive rock.

On the west shore of Amisk Lake, the Bouguer anomaly is low, -38 to -41 milligals, values characteristic of the mean Bouguer anomaly for the region (c.f. sec. 4.1). The anomaly increases to the east across Amisk Lake, reaching the maximum along the axis of the high referred to above. Although no readings were taken in the center of Missi Island, the gravity anomalies around the island suggest a negative anomaly in the center, probably associated with the acidic intrusions that are mapped there. The deflection in the contours near the east end of North Channel of Amisk Lake is due to the

presence of basic lavas and basic intrusive rocks in that area, flanked on the north by Missi sediments and on the south by the acidic intrusions of Missi Island. Similarly, the deflection of the contours near Crater Island coincides with basic intrusive rocks mapped on that island. Aeromagnetic evidence indicates that the basic rocks extend southward under the water of Amisk Lake. Therefore, a positive gravity anomaly, not yet mapped, may also exist southward from Crater Island.

Along the eastern shore of Amisk Lake, several small anomalies are found. The southernmost is a prominent indentation, almost a closure, of the gravity contours near Sandy Bay, correlating with an intrusion of low density"quartz-eye" diorite. The contours curve out to include several other small "quartz-eye" diorite bodies near Table Lake and Cable Lake. The anomaly over the largest body near Table Lake is very small suggesting that the intrusion is very shallow or flat-dipping.

Near the village of Denare Beach, a reversal in the gravity contours indicates that the bay, facing the village, is underlain by low density, possibly acidic intrusive, rocks. Only basic Amisk Lavas have been mapped on the shore and islands of this area, therefore the low density rocks must lie only under the water of the bay or drift covered areas on shore.

In Comeback Bay, in the northeastern part of Amisk Lake, a positive and a negative gravity anomaly are found. The negative anomaly, a deflection in the -30 milligal contour, reflects a "quartz-eye" diorite intrusion which has been mapped on parts of two islands. The positive anomaly is found

in the widest and deepest part of Comeback Bay, parallel to the east shore. It may indicate a northerly extension of a basic intrusion found on that shore.

In the northern bay of Table Lake and on the east shore of Ruth Lake is a negative trend in the gravity. This local negative anomaly is near the crest of the regional positive anomaly and coincides with ultrabasic pyroxenite and peridotite rocks. The low density indicated by the anomaly is due to extensive serpentinization of these rocks, a fact which has been verified by laboratory measurements of density.

North of Stitt Lake, a small boss-like intrusion of albite granodiorite is marked with a 3 milligal negative anomaly. The anomaly extends southward to the south end of Stitt Lake. A smaller anomaly, which may be connected, is found further south on Meridian Creek. Several intrusive bodies of quartz-feldspar porphyry have been mapped in this region and are probably the cause of some of the gravity anomaly.

Northeastward from Echo Lake, is a mafic rich body within the Reynard Lake granodiorite. Byers et al. (1965)have termed this a meta-gabbro, but Smith (1964) has called it a quartz diorite. Samples of this unit have a high density. A gravity anomaly of about + 3.5 milligals is associated with this body.

The Reynard Lake granodiorite pluton occupies much of the northern part of the map area and is characterized by a negative gravity anomaly compared to that of the basic volcanic and intrusive rocks. The most

negative anomaly is found over the microcline porphyry core zone centered between Mosher and Meridian Lakes. A steep gravity gradient is found along some of the southwestern flank where the pluton is in vertical contact with the heavier basic rocks. South of highway 35, the steep gravity gradient swings eastward and then northeast across the pluton, nearly coinciding with the edge of the core zone. The known density contrast between the low density core and the heavier "contaminated border zone" of the pluton is not sufficient in itself to account for the gravity difference. The granodiorite must be thin at the southern extremity of the body, increasing in depth and thickness to the north.

Byers et al. (1965) consider that the Reynard Lake pluton occupies the core of a major anticline whose axial plane dips steeply southwest. The southern end of the structure is said to plunge approximately 50 degrees in a direction 35 degrees east of south.

Froese (1963, p.23) has interpreted the contact of the pluton to dip 75° to 85° north at the southern extremity and 75° to 85° inward along the flank. All these interpretations seem conflicting at first sight. However, the gravity anomaly reflects the density distribution at depth, the geological interpretations rely on lineations and foliations observed at specific places on the surface. Therefore the two methods are indicating different phenomena and the example serves to illustrate the dangers of attempting to predict details of the geology from a geophysical anomaly or of attempting to extrapolate geological observations over too great distances. The structure may indeed plunge in the indicated directions where observed on the surface,

but the gravity evidence shows that the directions change at depth. A detailed model study of this body is presented in section 8.4.

A flexure in the gravity contours exists near Meridian Lake. This is a combination of several effects. Pyroclastic rocks, basic Amisk lavas, and basic intrusions underlie the shores and bottom of Meridian Lake. Southeast of the lake is the contaminated border zone and granodiorite core of the Reynard Lake pluton. Northwest of the lake is the hornblende granodiorite border and the biotite granodiorite core of the Annabel Lake pluton. Thus, the densities are highest at Meridian Lake, lower in the flanking granodiorite border zones, and lowest in the granodiorite cores.

The Annabel Lake pluton, although not within the survey area, has a significant effect on the gravity contours in the northeast part of the survey area. The gravity field in this vicinity is lower than might be expected from a consideration of the densities alone. In fact, the basic rocks of the area from Wekach Lake to Flin Flon have gravity anomaly values the same as found well within the Reynard Lake pluton. A southern or southeastern plunge of the Annabel Lake granodiorite could explain the situation. This interpretation is nearly in accord with the geological interpretation. Byers et al. (1965, p.44) suggest that the Annabel Lake body occupies a single assymetric anticline plunging about 18 degrees in a direction 33 degrees east of south. Such an attitude would place the low density body at depth under the Amisk rocks and produce the observed gravity effect. A model calculation is presented in section 8.4.

A two milligal positive anomaly exists at the north end of Phantom Lake. This coincides with the largest of the Boundary Intrusions described by Stockwell (1960). Magnetic evidence suggests (c.f. sec. 4.2) that the Boundary Intrusion extends almost to the south end of Phantom Lake. The lack of a gravity anomaly in the south end may be explained by the strong disturbing effect of the Phantom Lake granite.

The Phantom Lake granite causes a pronounced 6 milligal negative anomaly. The anomaly center does not coincide with the apparent center of the granite, probably because the gravity station spacing is not uniform.

The Mystic Lake pluton, where investigated, has little gravity effect. Because the samples taken from this body have densities that are relatively uniform and significantly lower than the densities of surrounding basic rocks, the lack of a pronounced gravity effect is significant. This is most pronounced in the vicinity of Boot Lake where the Bouguer anomaly is actually larger than that observed over the adjacent basic volcanic rocks.

The gravity anomaly suggests that the north end of the Mystic Lake pluton is relatively shallow, and underlain by basic volcanic or intrusive rocks. South of Boot Lake, the tongue of Amisk volcanic rocks which divides the granodiorite nearly in two, also suggests the presence of basic rocks at shallow depths below the granodiorite. This interpretation suggests that the exposed north end of the Mystic Lake pluton is near to the floor of the intrusion, contrary to the interpretation of Byers et al.(1965, p. 35) and Smith (1964, p. 14) who suggest that the exposed surface is close to the top of the original pluton. If it is near the top, and especially if the Mystic

Lake pluton had a central, low density, core as do the other large plutonic granodiorites, a strong negative gravity anomaly should have been recorded, but this is not the case. The gravity anomaly is, in fact, positive in places, so the low density mass of the granodiorite must be small, at least in the northern end. There is, as yet, insufficient gravity data to make a reasonable interpretation for the southern end.

8.2 Deep seated sources

The regional gravity anomaly, (Fig. 4.1) is about 15 miles across. Although the anomaly appears to be associated with the outcropping rock types, the possibility remains that the major portion of the anomaly is due to some density distribution at great depth and that the surficial geology contributes only some local detail to the gravity field.

An interpretation of the large anomaly was made using the regional gravity data supplied by the Dominion Observatory (fig. 4.1), the depths and densities listed by Hall and Brisbin (1965), and the method published by Smith (1960).

A gravity station with the value -20.6 on the east shore of Amisk Lake was chosen for a center value. The gravity values were averaged around a circle with radius 9 kilometers for use in Smith's (1960) formula 2.3.

With these values, the following estimates were made:

1. The minimum permissible density contrast capable of producing the anomaly is 0.0425 gm/cc provided that the contrast extends from surface to unlimited depth.
2. If the anomaly were due to relief on the basaltic layer (Conrad discontinuity), and the maximum density contrast were taken as 0.13 gm/cc, the basaltic layer would have to rise from a depth of 15.5 km to a depth of 4.0 km to explain the anomaly.
3. If the anomaly were due to relief on the upper mantle surface (Mohorovicic discontinuity) and the maximum density contrast were taken as 0.39 gm/cc, the upper mantle surface would have to rise from a depth of 34 km to a depth of 12.9 km to explain the anomaly.

These estimates show that if the anomaly were due, in any substantial part, to relief on the Conrad or Mohorovicic discontinuities, extreme amounts of upward relief would be required, respectively 11.5 km and 21.1 km. However, the fault pattern discussed earlier suggests downward movement rather than upward. Furthermore, if most of the field were due to deep sources, the residual field would be inadequate for any reasonable depth of the surficial rocks.

Therefore it may be concluded that little or none of the Bouguer positive anomaly is due to deep seated sources.

8.3 Individual anomalies

Five anomalies with distinguishing characteristics were chosen to be

interpreted with charts presented in this thesis and elsewhere. Figure 8.1 is an index map showing the locations of the various profiles.

8.3.1 Amisk Lake anomaly

The Bouguer gravity over Amisk Lake, south of Missi Island, shows a steady decrease to the west. The rocks on the west shore of Amisk Lake are acidic in composition and on the east shore they are basic. These facts suggest that the gravity slope is caused by a change in the density of the rocks. Figure 8.2 shows the profile with the necessary interpretation parameters. Using these parameters (dg/dx = 1.1 mg/km, K = 0.00892 gr/cc/km, KL = 0.1 gr/cc. L = 11.2 km) and the interpretation chart for a horizontal gravity gradient due to a strip of varying density, we obtain the following results. Entering the chart on the abscissa at dg/dx = 1.1, we read up to the intersection of the line KL = 0.1, then read across to the ordinate where we find H/L = 0.32. The length used to determine the KL product is 11.2 km. Therefore H = 0.32 x 11.2 = 3.58 km.

A thickness of 3.58 kilometers (11,800 feet) of rock with density varying from 2.79 to 2.89 gms/cc is sufficient to explain the gravity slope on the west side of Amisk Lake.

8.3.2 Mystic Lake anomaly

A gravity anomaly that approximates the step model type is found along the southern part of Mystic Lake. This anomaly is caused by density contrasts due to contacts between a basic intrusive sill, basic Amisk lavas,

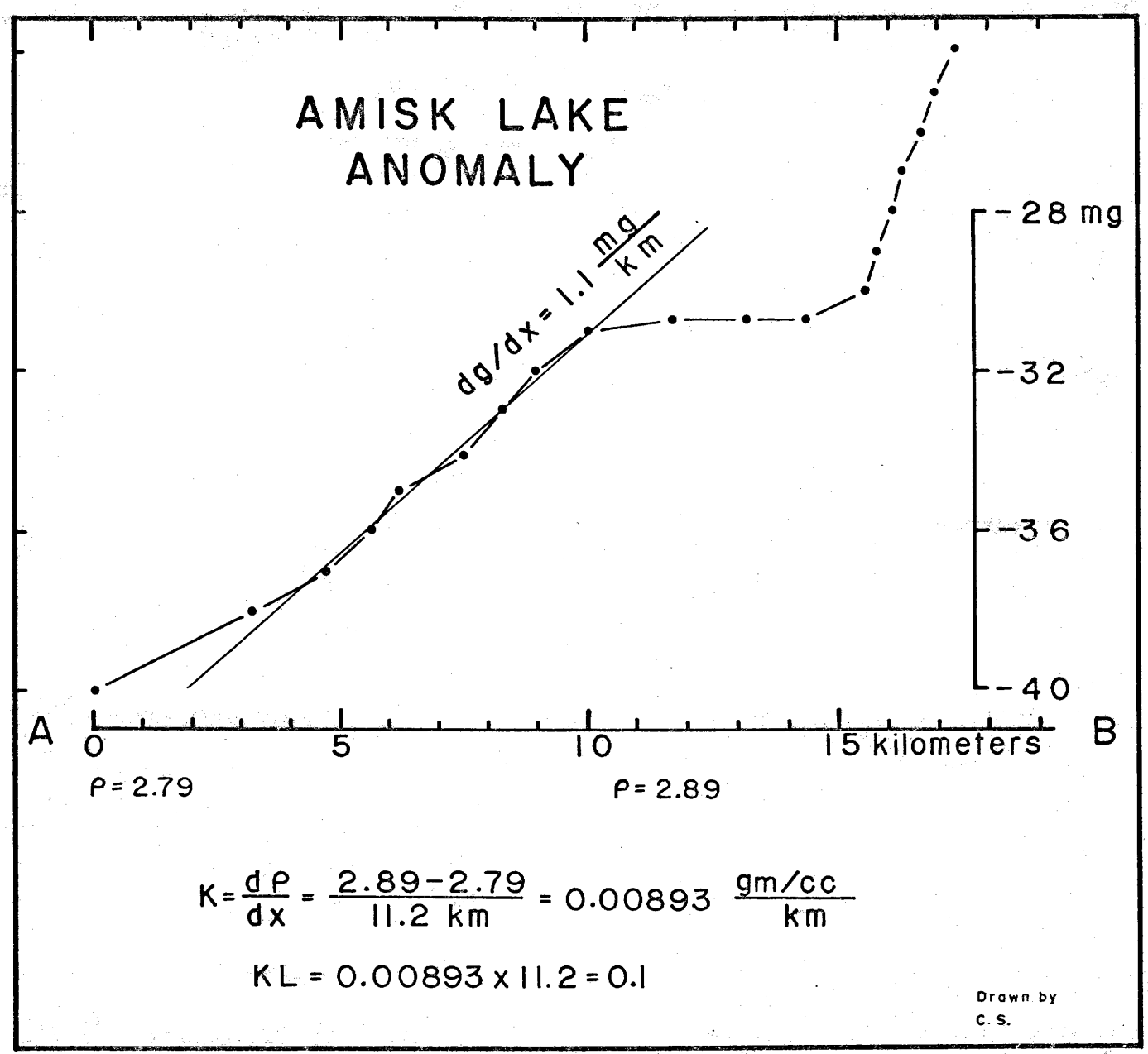
AMISK LAKE
ANOMALY
dg/dx = 1.1 mg/km
-28 mg
-32
-36
-40
A
0
5
10
15 kilometers
B
P = 2.79
P = 2.89
K = dP/dx = 2.89 − 2.79 / 11.2 km = 0.00893 gm/cc/km
KL = 0.00893 x 11.2 = 0.1
Drawn by
C. S.

Figure 8.2

acidic lavas and pyroclastic rocks, and the Mystic Lake pluton.

Two profiles of this gravity slope are shown in figure 8.3. Profile A is taken near the center of Mystic Lake, profile B is taken near the south end of the lake. Two interpretations are shown for each profile and the results are tabulated below. Charts 1 and 2, "Characteristic Curves for Gravity Interpretation of Near Surface Contact" were used for these interpretations.

	Slope mg/km	Δg milligals	Δx kilometer	g/xs	x_1/x_2	Dip	X/L	L Kilometers	ρL/G	ρ gm/cc
B-1	2.29	6.60	1.52	1.90	.61	76°E	.85	1.8	.050	.18
B-2	3.27	4.82	0.85	1.74	.77	83°E	.58	1.47	.059	.19
A-1	.769	6.87	2.45	3.65	1.0	90°	2.3	1.07	.032	.21
A-2	1.63	5.82	1.54	2.32	1.0	90°	1.18	1.30	.04	.18

These results show about 10% variation in the density estimates. Sample densities of the rock units involved are:

Mystic Lake Pluton	2.789 gm/cc
Acidic tuff, west and south of Wekach Lake	2.738 gm/cc
Acidic lava, west and south of Wekach Lake	2.707 gm/cc
Basic Intrusive, Mystic Lake	2.974 gm/cc
Basic Lava, south of Wekach Lake	2.979 gm/cc

From the sample densities, a possible range in density contrast might be taken as 0.185 to 0.272 gm/cc. The four density contrast estimates from the

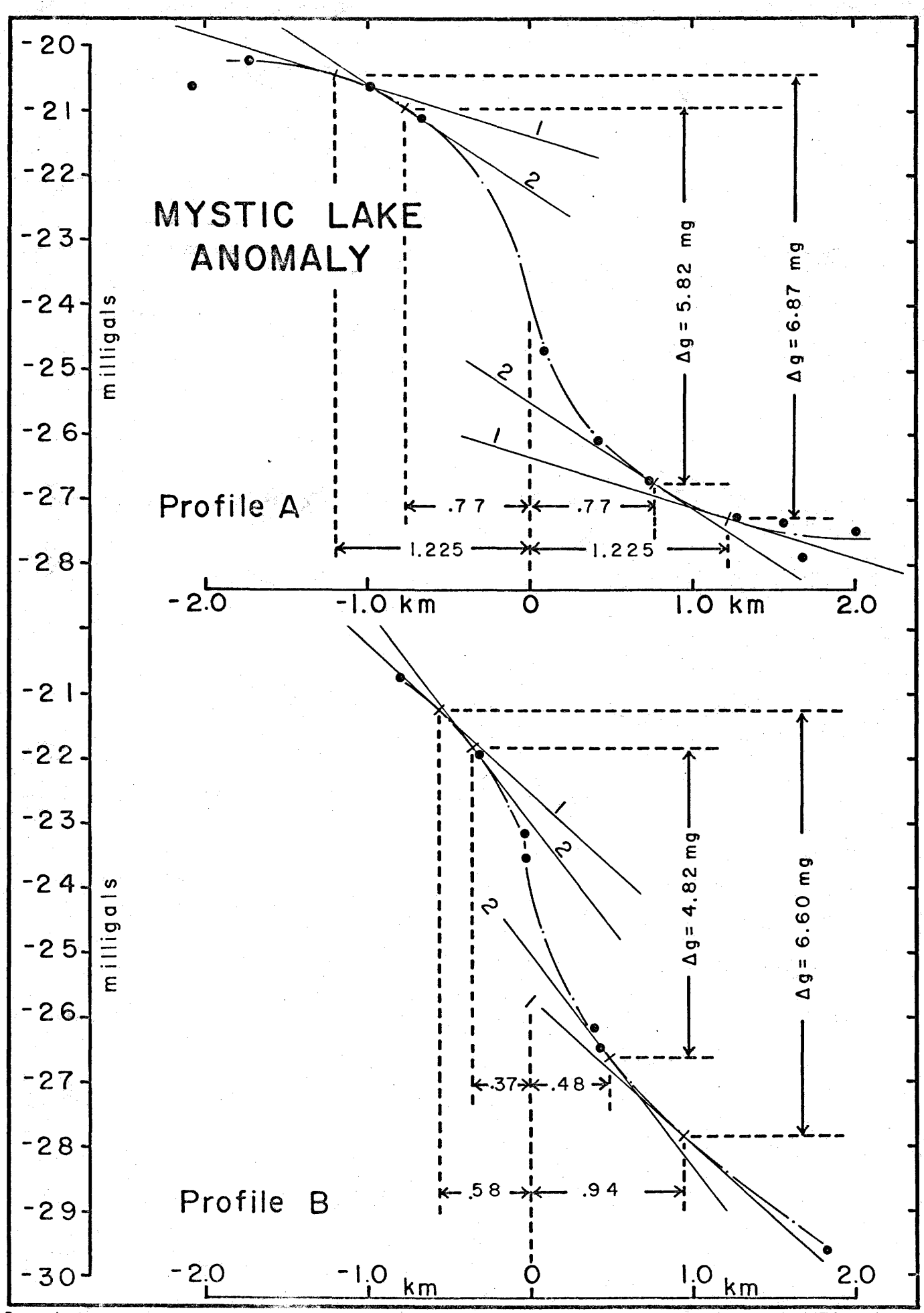

Drawn by C.S.

Figure 8.3

profile interpretations have an average of 0.19 gm/cc.

The two depth estimates on each profile differ by 20% from each other and the means of the estimates for each profile differ by 25%. The density contrast extends to a greater depth near the south end of Mystic Lake than near the center. The respective depths are 1.6 kilometers and 1.2 kilometers $\pm$ 20%.

8.3.3 Phantom Lake anomaly

The negative anomaly at Phantom Lake is due to a granite boss which outcrops on the south west shore of the lake. Sample densities for the rocks in the area are:

Phantom Lake Granite	2.656 gm/cc
Mystic Lake Pluton	2.789 gm/cc
Basic lava, Schist, Phantom & Douglas Lakes	2.936 gm/cc

From the sample densities, a possible range in density contrast is from 0.13 to 0.28 gm/cc. The density for the lavas may be too high in this area (see page 71), therefore a density contrast of 0.18 gm/cc is chosen.

The outcrop dimensions of the Phantom Lake granite are about 2.0 miles by 0.7 miles. Therefore $l/w = 2.0/0.7 = 2.9$. The width = 0.7 miles = 112000 cm.

$$\Delta g/GpW = .006/6.670 \times 10^{-8} \times 0.18 \times 1.12 \times 10^{5}$$

$$= 4.5$$

Using figure 7.2 "Maximum Gravity Effect of Rectangular Prism" and the values for l/w and $\Delta g/GpW$ above, we find that $Z/W = 2.95$. Therefore $Z = 2.95 \times W = 3.3$ km.

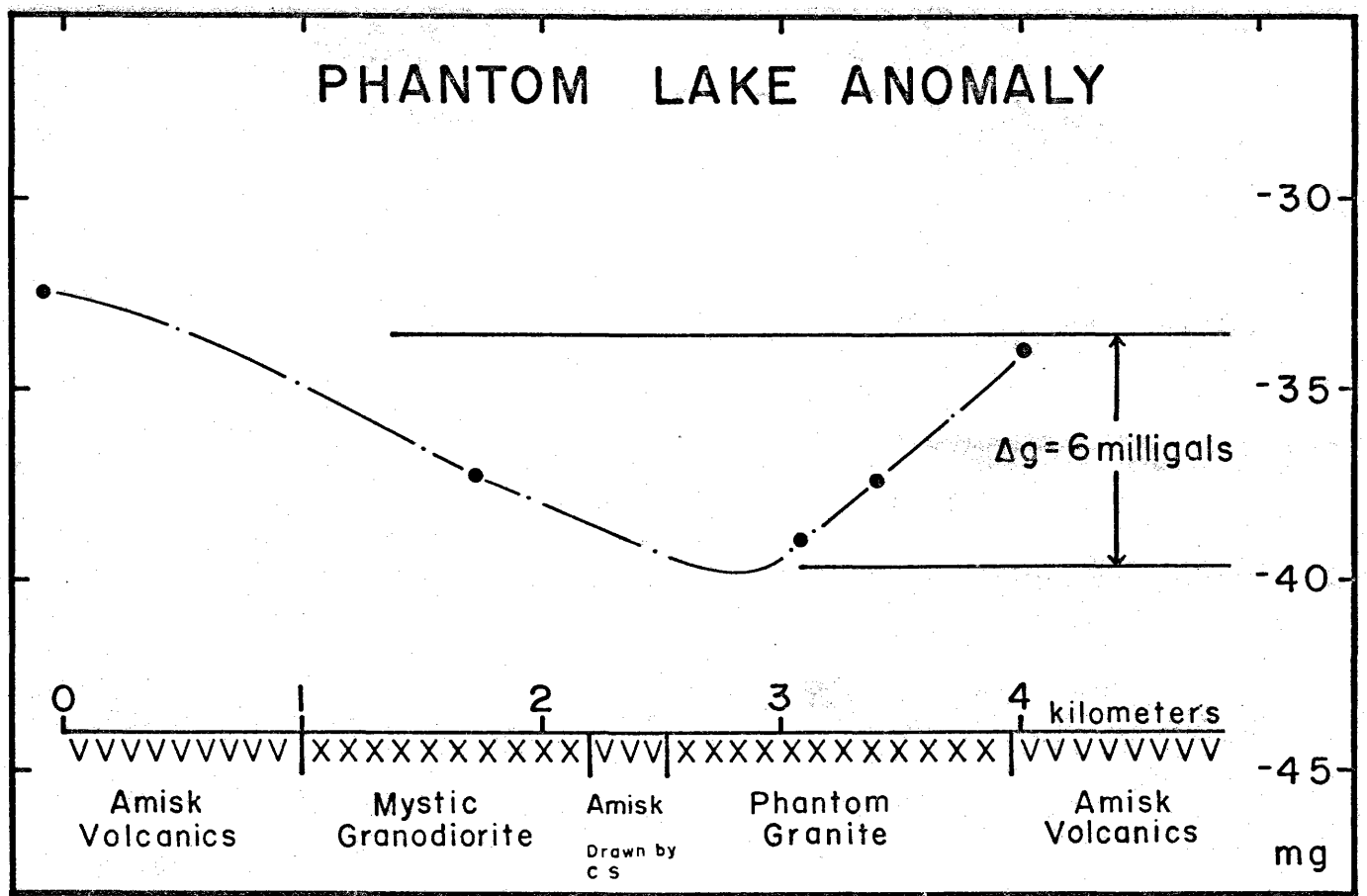
PHANTOM LAKE ANOMALY
-30
-35
-40
-45
mg
Δg = 6 milligals
0
1
2
3
4
kilometers
Amisk Volcanics
Mystic Granodiorite
Amisk
Phantom Granite
Amisk Volcanics
Drawn by C S

Figure 8.4

This depth is close to the interpreted thickness (3.58 km) for Amisk rocks in the west half of Amisk Lake.

8.3.4 Echo Lake anomaly

A basic rock unit is found within the southern part of the Reynard Lake granodiorite. Since its western end reaches Echo Lake it will be called the Echo Lake body in this thesis.

Well defined gravity and aeromagnetic anomalies exist over the Echo Lake body. A gravity high with a maximum of 3.5 milligals is present in the gravity map.

Sample densities indicate a contrast of about 0.22 gm/cc. Samples taken from the narrow southwest end of the body are less dense than those of the wider center section. The surface dimensions are taken as 193,000 cm. by 96,500 cm.

The depth of the base of the Echo Lake body can be determined from:

$\Delta g/G\rho W = .0035/(6.67 \times 10^{-8} \times .22 \times 96{,}500) = 2.47$

$l/w = 193{,}000/96{,}500 = 2.0$

Accepting these values and using fig. 7.2 we find that

$Z/W = 0.65$ and

$Z = 0.65 \times 96{,}500$ cm $= 0.627$ km

$= 2060$ ft.

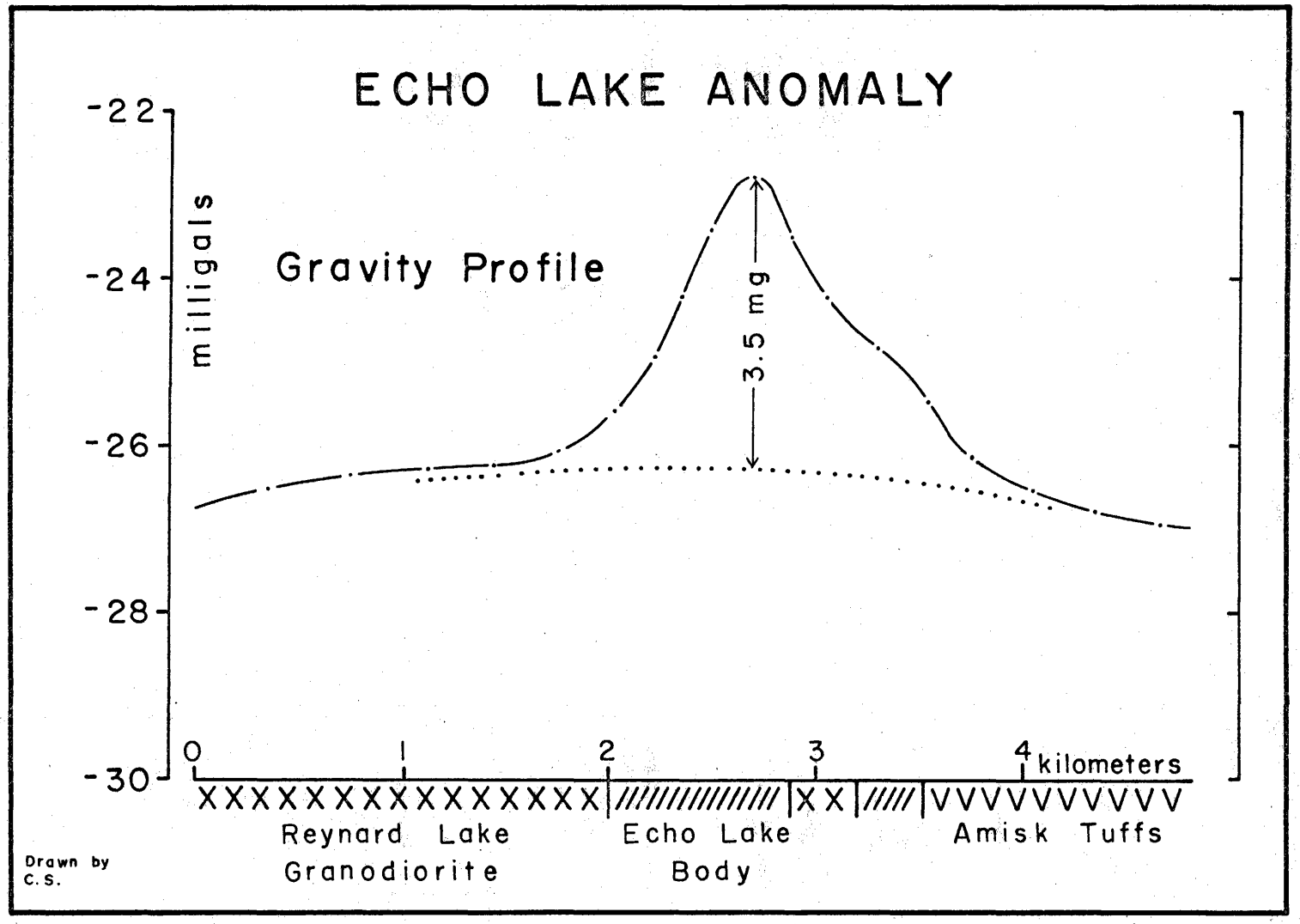
ECHO LAKE ANOMALY
Gravity Profile
milligals
-22
-24
-26
-28
-30
3.5 mg
0
1
2
3
4
kilometers
Reynard Lake Granodiorite
Echo Lake Body
Amisk Tuffs
Drawn by C.S.

Figure 8.5

8.3.5 Reynard Lake anomaly

The Reynard Lake granodiorite is marked by a prominent gravity anomaly along its west side. This anomaly is due to the density contrast between the low density granodiorite and high density lavas and basic intrusions. The gravity profile, figure 8.6, is drawn more or less along the highway where gravity measurements are plentiful. The steepest slope is fairly long and straight and is found over the contaminated border zone of the Reynard Lake pluton. The anomaly therefore appears to be of the gradational density contrast type. The total density contrast is about 0.26 gm/cc, which is the difference between Amisk Lavas (2.93) and microcline granodiorite (2.67). The slope of the "straight" portion of the gravity anomaly is 5.44 milligals/kilometer. Interpolating these values into figure 7.5, we find that H/L = 0.84. The width "L" of the contaminated border zone along this profile is 2.64 kilometers.

H = 2.64 x 0.84 = 2.2 kilometers.

This estimate of the depth of density contrast in this area must be taken as a minimum because the profile was taken near the "nose" of the anomaly. If the anomaly had not been limited in one direction, a sharper, stronger variation from a similar density contrast would have been expected.

8.4 Model interpretation

Since deep crustal sources are ruled out, and since the density of rocks in this area varies almost directly with the basicity of the rock, except for serpentinites, it may be said that the gravity field is largely

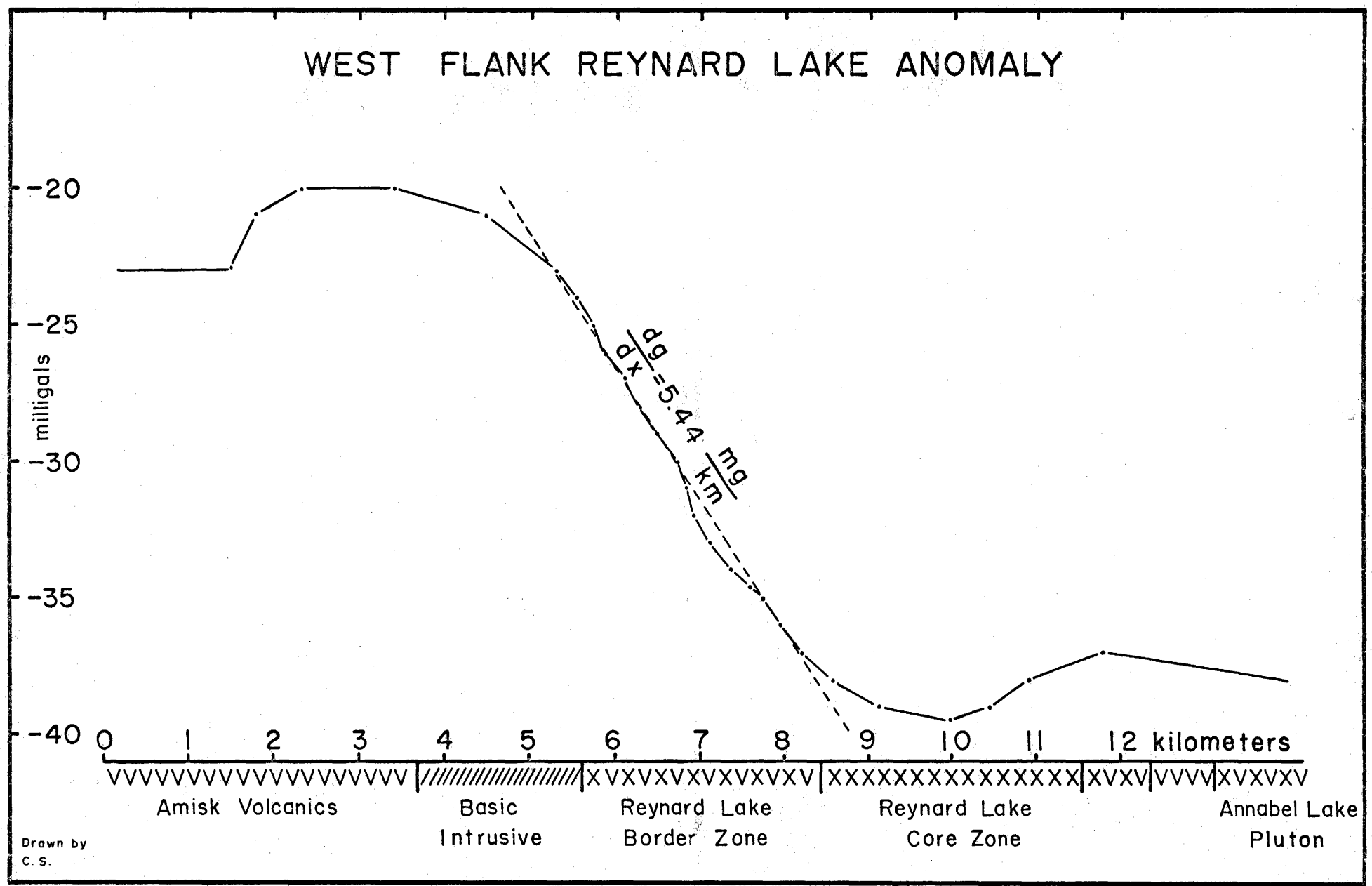
WEST FLANK REYNARD LAKE ANOMALY
-20
-25
-30
-35
-40
milligals
dg/dx = 5.44 mg/km
0 1 2 3 4 5 6 7 8 9 10 11 12 kilometers
Amisk Volcanics
Basic Intrusive
Reynard Lake Border Zone
Reynard Lake Core Zone
Annabel Lake Pluton
Drawn by C. S.

Figure 8.6

explained in terms of the outcropping geology. The amplitude of the anomalies, however, depends on the depth extent of the rock formations. Three factors are important here, the density assigned to the rock units, the thickness of the units, and the dip of the beds. Measured densities of 1585 rock samples from the Amisk Lake area are tabulated earlier in this thesis. Thicknesses of the various volcanic and intrusive units and their dips are given by Byers et al. (1954 and 1965). All dips are steep to vertical.

For this thesis, two model interpretations have been made. The first is an east west profile situated about 4 miles north of the Coronation Mine. The second is a study of the Reynard Lake granodiorite in three dimensions.

In gravity studies of this nature, it is common practice to remove a "regional gravity" effect from the Bouguer map before proceeding to interpret the "residual". This was not done in the Amisk Lake study because the gravity variations seemed to be almost totally controlled by the outcropping rock units. In a sense, this study is interpreting the "regional effect" as it might be considered in a more localized survey.

The interpretation method is by curve matching and the calculations were carried out on the University of Saskatchewan IBM 7040 computer. The equation for the gravity effect of a three dimensional rectangular prism was derived and programmed in Fortan IV by D. Nagy of the Dominion Observatory.

Prisms comprising the model were chosen on the basis of the shape of the outcropping rock units and extended to depths sufficient to obtain the

required gravity anomalies. The model was chosen to fit conditions most closely along the area of interest and only approximately at distant points. The reader should bear in mind that the blocky appearance of the model is a limitation of the computing method and that equally good interpretation could be achieved with curved and slanting contacts. Such an interpretation would be much more costly and no less ambiguous. Densities were assigned on the basis of measured densities in-so-far as possible.

The density for the material lying immediately under the Amisk volcanic rocks was taken as 2.82 for two reasons; the rock at 3 km depth in a hole drilled in the center of the Reynard Lake pluton is similar to the Reynard Lake contaminated border zone whose density is 2.81; the average density of all samples taken from the East Amisk area is 2.86. The mean value 2.86 may be considered unbiased or properly weighted in so far as Smith's (1964) sampling is representative. The sampling was intended to be as representative as possible but was subject to uncontrollable factors such as topography. Probably the value 2.86 is somewhat too high.

Although the density immediately under the Amisk rocks may be 2.82 as assumed, seismic data (sec. 4.3, 4.4) indicates a lower density at greater depth. There is no contradiction in this. The gravity anomaly is insensitive to vertical changes in density where there is no horizontal change.

8.4.1 East west profile

Two hypotheses were tested in computing the model profile, figures 8.7 and 8.8.

The first was that the basic and ultrabasic dikes and sills are deep seated with their roots extending to the basaltic layer. The second hypothesis was that the dikes and sills are limited in depth and the required anomaly amplitude is explained by a thickening of the basic Amisk volcanics. Both models produced satisfactory fits to the observed data but the second was chosen for two reasons. The basic dikes and sills were intruded before the regional folding had ended (Wohlberg, 1964) and therefore may be far removed from any root or feeder dike that exists or might have existed. Secondly, the regional faulting discussed earlier is compatible with a thickening of the Amisk volcanics in the area east of Amisk Lake.

Basic Dikes and Sills

The maximum gravity anomaly is found over the basic intrusions (blocks 10, 12, 21, 30, 32, 40, 50, 60, 70, and 80), but in the Amisk - Mystic Lakes area, the intrusion with the highest density, 3.042, (block 80, east of Ruth and Table Lakes) is not under the peak of the anomaly. To obtain the shape of the observed curve, and still use the measured densities, it was necessary to assume the Ruth Lake sill to be limited in depth (1 km) and extra mass (block 21, Figure 8.8), added at depth below the Konuto Lake (block 2) greenstone belt, implying that basic intrusive material is there also. The small negative anomaly observed on the west side of the Mystic Lake sill (block 30) is due to a small acidic intrusion. No attempt was made to fit this anomaly.

The mass of the basic intrusive rocks is insufficient to explain the amplitude of the gravity anomaly unless the intrusions extend to great depth. Since this is unlikely from structural considerations, a downward bulge of basic volcanic rock was added instead to make up the difference. A total of 4.7 kilometers of basic volcanic and intrusive rocks is inferred in the Amisk - Mystic Lakes area with lighter material below.

Acidic Lavas

Three kilometers of vertical thickness of rock are required to match the observed gravity field over the west half of Amisk Lake if the assumed densities are correct. If the acidic lavas on the west shore of Amisk Lake (block 102) are assigned the density of acidic lavas on the east shore (2.707) instead of the value used (2.82), the vertical thickness required would be reduced to $1\frac{1}{2}$ or 2 km. The larger value was used because some basic rock has been included with the acidic volcanics in the geological map. The geophysical model therefore indicates that the density contrasts observed at the surface disappear within a few kilometers of depth and are replaced by, or change into, material with a density so homogeneous that it does not substantially affect the gravity field. A density of 2.82 has been assumed for this underlying material for reasons listed earlier. If the material were heavier or lighter, the only alteration required to the gravity interpretation would be an increase or decrease in the amount of downwarping required in the Amisk - Mystic Lakes area. The density of the rock may very well decrease uniformly with depth but such a horizontal stratification is not detectable

from considerations of the local Bouguer anomaly.

Pyroclastic and Granodioritic Rocks

East of Mystic Lake, there are relatively few gravity points to interpret. Therefore, the interpretation of the form of the Mystic Lake pluton is not very satisfactory. The entire block 90 has been assigned a density of 2.87, which is appropriate for basic pyroclastics. The Mystic Lake granodiorite samples have an average density of 2.79. If the interpolated Bouguer gravity across the Mystic Lake pluton is fairly realistic, then only 700 meters of granodiorite (block 90C) would be adequate to explain the anomaly. This is less than the thickness determined from the Mystic Lake profile interpretation, page 148 . The postulated density distribution is shown as an alternate interpretation on the profile. Qualitative support for this contention is shown in the Boot Lake area, where the gravity anomaly is seen to increase southward towards the center of the pluton, and reaches values larger than are found over nearby Amisk volcanic rocks. Hence, at least in the area north from the interpretation profile, the Mystic Lake pluton is thin and lacks any low density core as found in the Reynard Lake body. This interpretation is contrary to Smith (1964, p. 14) who suggests that the exposed surface is near the original roof of the pluton, and Byers et al. (1965, p. 35) who suggest that the body is structurally lower than other large intrusions, its central core not yet exposed.

The lavas and basic intrusions outcropping along the west arm of

Schist Lake do not require any excess material at depth to explain their gravity effect. The basic intrusions (block 60 in particular) seem to be quite limited in size in comparison to the Table Lake, and Ruth Lake bodies.

Block 150, east of the West Arm of Schist Lake was included because rocks east of the map area are more acidic in composition.

8.4.2 Reynard Lake pluton

The Reynard Lake Pluton is associated with a distinctive negative gravity anomaly. A three dimensional interpretation of this anomaly was made using preliminary interpretations, sample densities, the various publications on the geology, and the logs from the deep bore hole (Findlay, 1966). Calculations were made using Nagy's (1966) computer program.

Four aspects of the geology had to be considered in the interpretation;

(1) The microcline granodiorite core zone and the biotite granodiorite zone of the pluton.

(2) The basic lavas and intrusive rocks south and west of the pluton.

(3) The Amisk rocks and intrusive rocks east of the pluton.

(4) The biotite granodiorite zone of the Annabel Lake pluton.

The density of the Reynard Lake border zone is 2.82 gm/cc (c.f. page 73). The rocks at depth were taken as 2.82 gm/cc because this is the density of the material found at 3 kilometers depth in the JXWS deep bore hole. Furthermore, the mean density of all the rock samples from the area is 2.86 gm/cc, a value which may be biased. The actual mean should probably be slightly less.

Figures 8.9 and 8.10 show the plan of the calculation model and the computed gravity field.

Reynard Lake core zone

The microcline granodiorite and the biotite granodiorite of the Reynard Lake pluton have densities of 2.66 gm/cc and 2.68 gm/cc respectively. In this interpretation they are treated as a single unit. The deep bore hole JXWS described by Findlay (1966) was drilled through these rocks to a depth of 7,570 feet. To match the observed gravity field, it was necessary to assume that the core zone of the granodiorite plunges north - northwest at about 30°. There should also be a westward dip of the west flank. However, the amount of dip is not well established because gravity measurements are lacking in the area east of Mosher and Wolverine Lakes. A maximum depth of the core zone, from the gravity interpretation, is three kilometers, some distance north of JXWS borehole.

Basic lavas and intrusive rocks

South of the Reynard Lake pluton, the basic rocks extend to a depth of 4.7 kilometers (c.f. page 152). Similar high density rocks are found east and west of the granodiorite, but the associated gravity anomalies are much smaller. The depth of these units becomes progressively less in the more northern areas. In the vicinity of Wolverine Lake, the heavy basic rocks need only extend to depths of 2 kilometers to satisfy the gravity anomaly.

A particularly interesting situation is found near the nose of the granodiorite. The density of the granodiorite border zone is 2.82 gm/cc and it is in contact with basic intrusive rocks, density 2.97 gm/cc. The gravity anomaly throughout the area is higher than might be expected if the granodiorite contact were vertical, and much higher than if the granodiorite plunged 50 degrees southeast, as suggested by Byers et al. (1965, p. 45).

A satisfactory agreement can be made with the observed gravity field if the granodiorite is assumed to plunge at about 30 degrees to the north - northwest. Froese (1963) has interpreted a steep (80°) northerly plunge for the southern end of the granodiorite. If Froese is correct, the contact between granodiorite and basic rock is almost vertical at the surface and flattens to about 30 degrees northwest at depth.

The Echo Lake body complicates the situation but its presence tends to support the hypothesis that basic rocks underlie the nose of the Reynard Lake pluton. Figure 8.11 shows the relationship of these features in profile.

Amisk rocks east of the Reynard Lake Pluton

The unweighted mean density of 170 samples in the northeast corner of the map area (excluding granodiorite samples) is 2.90 gm/cc. A certain bias was used in collecting these samples. The unweighted mean density is therefore, too large (c.f. page 67), and ought to be reduced to perhaps as low as 2.82 gm/cc. The gravity anomaly supports this since the anomaly amplitude in the area (-35 to -32 milligals) is the same as found over parts of the Reynard Lake body.

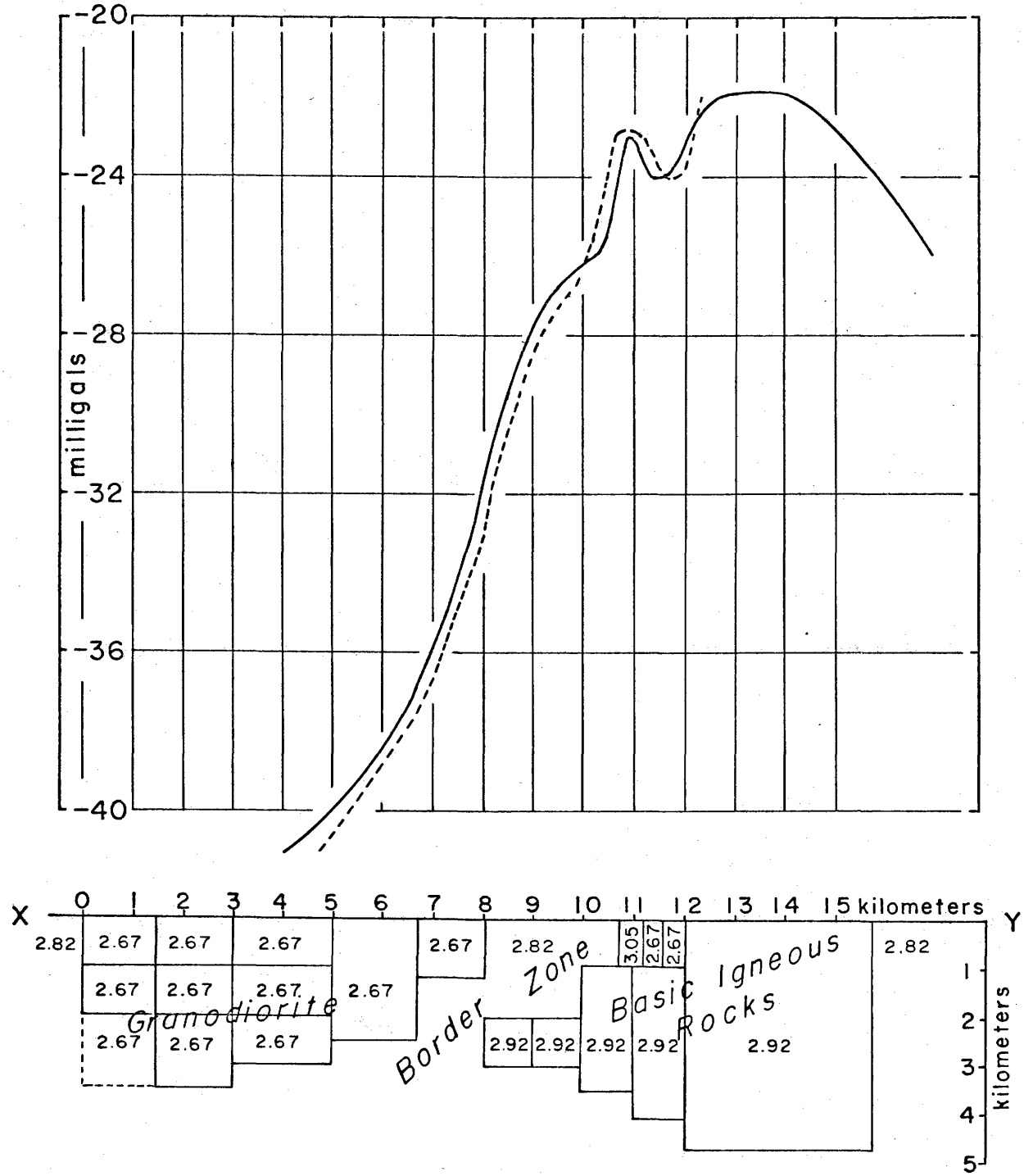

GRAVITY INTERPRETATION PROFILE
REYNARD LAKE PLUTON

2.67 Model prism with density

Observed gravity

Computed gravity

See plan map
Gravity Calculation Model
for profile location.

Drawn by
C.S.

Figure 8.11

The density contrast is non-existent, or so small, that gravity methods are not effective in estimating the relation of these rocks to the Reynard Lake border zone. The effect of the Annabel Lake Pluton further complicates the gravity interpretation of these Amisk rocks.

Annabel Lake Pluton

A portion of the Annabel Lake granodiorite extends into the map area northeast of Meridian Lake. This body has a central core of biotite granodiorite surrounded by hornblende granodiorite. No samples are available for the biotite granodiorite and only 21 for the hornblende rock. Densities for these rocks were assumed to be the same as for similar rocks in the sampled area.

On the regional gravity map, (Figure 4.1), an intense negative anomaly (-53 milligals) is found in the area of the Annabel Lake pluton core. This is more intense than the anomaly associated with the Reynard Lake pluton and indicates that the Annabel Lake core is wider, deeper, and/or lower density than the Reynard Lake core zone.

The gravity effect of the Annabel Lake body is important for several miles south of the outcrop and it is necessary to assume that the core zone plunges 45 degrees south - southeast. The plunge indicated from the gravity interpretation is in the same general direction as that suggested by Byers et al. (1965, page 44). They give a plunge 18 degrees in the direction 33 degrees east of south.

The maximum depth of the Annabel Lake body given here is four kilometers. This is somewhat ambigous with the density assumed for the Amisk rocks in the area. If the mean density of the Amisk rocks is, in fact, larger than 2.82 gm/cc, the same gravity effect could be computed by adjusting the depth and plunge of the granodiorite. The simplest interpretation which involves the fewest assumptions is that the Amisk rocks have a density of 2.82.

8.5 Discussion

The major conclusions drawn from the gravity study are

1. The density differences associated with the steeply dipping basic to acidic rocks of the Amisk group are limited in depth. In western Amisk Lake the depth is about 3 km, in the vicinity of Ruth Lake it is 4.7 km, in the vicinity of Wolverine Lake it is 2 km, in the vicinity of Phantom Lake it is 3 km.

2. Lateral variations in rock density may exist below the depths indicated above, but only on a scale so small that they do not appreciably affect the gravity field at surface. The density of the rocks immediately below the Amisk group has been assumed to be 2.82 gm/cc but at greater depths to 10 km the density must be even lower (2.7 - 2.6 gm/cc) to account for the 6.0 km/sec seismic velocity.

3. The Reynard Lake pluton is relatively shallow at its southern end and is underlain by basic lavas or intrusive rocks. The base of the granodiorite plunges to the north-northwest at about 30°. At a depth of about three to four kilometers the density contrast disappears and all rocks below that depth have a grossly uniform, low density.

4. The Annabel Lake pluton plunges southward under the Amisk volcanic rocks in the northeast corner of the area. Density contrasts associated with the Annabel Lake body extend to about four kilometers depth.

5. The Phantom Lake granite extends in depth to a little more than three kilometers. Below this depth the density contrast disappears.

6. The Amisk rocks and basic intrusions in and north of Mystic Lake extend to 3 km depth. They are not in a roof pendant type of structure as related to the granodiorite masses.

7. The Mystic Lake granodiorite pluton is probably less than one kilometer in thickness in its northern part. It may have a sill-like shape. There are insufficient gravity data in the southern part to make an interpretation.

The gravity data indicate that the dense Amisk rocks lie in a depression of the underlying lighter rocks, probably having been lowered by a combination of faulting and folding. The basic rocks reach their greatest thickness in the area south of Table Lake, over 4.7 km., and diminish in thickness to the north, west, east, and probably also to the south. Basic intrusive sills and dikes found in the areas of greatest depression have increased the overall density and gravity anomalies. Syntectonic and post-tectonic acidic intrusions penetrate the basic Amisk strata, having risen 3 to 4 km from the depths of the low-density substrata. These intrusions exhibit nearly vertical contacts with the country rock in most places, but in some areas they are more flat and shallow, underlain by denser, basic rock. The south end of the Reynard Lake pluton and the north end of the Mystic Lake pluton are both relatively thin

and separated by a short distance on the surface. Thus, there is an unsupported suggestion that the north end of the Mystic Lake pluton is a sill-like extension of the Reynard Lake body, the connecting link now removed by erosion.

Two problems present themselves as a result of the above interpretation. The first problem is the nature of the substrata under the Amisk, the second is a "room" problem for the known structures of the Amisk group.

North of Amisk Lake, the Amisk and Missi strata have been observed to grade laterally into Kisseynew rocks, (Byers et al., 1965, p. 31). Although the Kisseynew is considered to be derived mainly from sedimentary rocks, (op. cit., p. 27) Amisk lavas have also been observed to grade into hornblende gneisses in some areas. Thus, at a depth of several kilometers beneath Amisk Lake, the pressure and temperature are and were undoubtedly greater than at the present erosion level of the Kisseynew rocks, and the Amisk lavas at that depth may be extensively metamorphosed in addition to being intruded by many large and small granitic plutons. In its metamorphic state and degree of intrusion, the material immediately below the Amisk may resemble Kisseynew rocks. At greater depths, the proportion of acidic material must increase until the bulk of the rock has the density of granite.

The increase in the content of acidic material in the rock might also be explained as the result of metasomatic granitization increasing in intensity with depth. However, there is no geological evidence to indicate that granitization of basic Amisk rock has occurred. All of the large acidic intrusions have been interpreted by Byers et al. (1954 and 1965) to be the result of magmatic intrusion. Therefore, granitization of Amisk lavas is not likely as a cause of the lower density at depth.

The change of density with depth could also represent a pre-Amisk surface upon which the lavas were deposited. If this were the case, one might expect that surface to be exposed in the center of some of the larger anticlines. This has not been observed in the Amisk Lake area although Bateman and Harrison (1945) found such a unit surrounding the Wabishkok Lake dome of granodiorite gneiss in Manitoba, about 15 miles northeast of Flin Flon. This assemblage of quartz-oligoclase gneiss and hornblende gneiss and schist has an apparent thickness of 1,500 feet computed perpendicular to the schistosity. The gneiss and schist assemblage underlies altered pillow lavas of the Amisk group and is itself intruded by the granodiorite gneiss. Since this pre-Amisk rock is relatively thin and underlain by intrusive granodiorite gneiss, it seems unlikely to represent any extensive pre-Amisk basement.

The thickness of the Amisk group has been stated by Byers and Dahlstrom (1954, p. 25) to be in the order of 21,000 feet (6.4 km) and these rocks are now vertically dipping and isoclinally folded. However, it is also pointed out, (ibid.) that the entire stratigraphic sequence is not present everywhere in the area. Basic volcanics predominate in the area of eastern Amisk Lake, acidic volcanics are found in quantity west of and to the northeast of the lake, and sediments predominate west and northwest of the Lake. Moreover, large quantities of Amisk rock were removed by erosion before and after deposition of the Missi sediments and the present surface, of course, represents a profound unconformity. Therefore the full 21,000 feet of Amisk rocks is certainly not involved in each of the isoclinal folds. In eastern Amisk Lake, basic volcanics

predominate and their thickness is estimated as 10,000 feet (3.05 km), (ibid.). Allowing for some variability in the thickness from place to place, and plastic flow which tends to thicken the crests and troughs of isoclinal folds, the gravity estimates of depth, 2 km to 4.7+ km, seem quite reasonable.

The present erosion surface, at least near the Coronation Mine, is near the bottom of a once gigantic volcanic pile. Froese (1963), from studies of the metamorphic minerals, concludes that rocks in the Coronation Mine area were metamorphosed at temperatures of 500° to 550°C and at 4 kilobars pressure, equivalent to about 13 kilometers depth. Part of this pressure may have been due to tectonic forces but most of it came from depth of burial since rocks at high temperature cannot sustain directed high pressure for long periods and will flow, tending to restore a lithostatic equilibrium. Jeffreys, (1962, p. 210) concludes that stress differences of at least 1.5 kilobar exist in the outer 50 km of the earth and 150 bars below 50 km. The Coronation Mine area then could have had a lithostatic load of slightly less than 2.5 kilobars to as much as 4 kilobars corresponding to depths of 7.7 and 13 km. This figure gives a clue to a possible reason for the downward thickening of the Amisk rocks. If the 7.7 to 13 km of the now-vanished overlying rock were composed wholly, or even partly, of basic volcanic rock, a large isostatic anomaly would result, in the order of 100 milligals, and because the basic rock covers a large area, isostatic adjustment would result. The width of the area of basic volcanic rock and its derivatives is about 50 km which, according to

Jeffreys (1962, p. 208), is a critical distance at which the strength of the crust begins to be unable to support large gravity anomalies. Therefore the downwarping of the Amisk rocks may be the result of isostatic adjustment to a previous load. The existing gravity anomaly is well within the load bearing capacity of the crust.

9. CONCLUSIONS

The contribution of this thesis in gravity interpretation is three-fold. A detailed study of the densities of outcropping rocks and their relation to the Bouguer gravity anomaly in the Amisk Lake area is presented. Three new interpretation methods are given that are intended for interpretation of gravity anomalies due to very shallow or outcropping density anomalies. An interpretation of the structure of some of the major rock units in the Amisk Lake area is presented.

Densities of rocks in the Amisk Lake area are variable and range from about 2.6 gm/cc to 3.1 gm/cc. Rock densities depend on many variables, but in the Amisk Lake area for rocks of known mineral composition the most important single criterion is the mineral composition of the rock. The porosity of these igneous and metamorphic rocks is very low and therefore has little effect on the densities.

A collection of samples from any particular rock unit always has a range of densities because the composition of the rocks varies from place to place. The range of densities of different rock units overlaps. Geological contacts are usually very complex in the Amisk Lake area. Contacts are frequently not sharp but gradational and complex in overall form. Because of these factors, the contrast in density between different rock units is not sharp and distinct.

Because rocks with contrasting densities crop out at the surface in the

Amisk Lake area, and because density contrasts are not usually sharp and distinct, it was found necessary to develop new interpretation methods. Published interpretation methods are designed mostly for gravity anomalies due to deeply buried sources and when this work was begun, there was no published technique for anomalies due to gradational density contrasts. The method of Grant and West (1965) for step model anomalies was modified to adapt it to outcropping or zero depth step model anomalies. The equation for the gravity effect of a right rectangular prism given by Nagy (1966), was shown to be linear with the width of the prism. On this basis, an interpretation chart was computed and drawn to facilitate the interpretation of the gravity effect of prisms with their upper surface in the plane of observation. The gravity effect of a straight, vertical contact, with density changing gradually rather than abruptly across the contact, has been considered and the equations developed to describe it. The equations were programmed in Fortran IV and used to generate several model anomaly curves and a set of characteristic curves for interpretation of gradational density contrasts. These methods have proven useful in the Amisk Lake gravity study.

A velocity log in a 10,000 foot borehole in the Reynard Lake granodiorite shows that the seismic velocity increases with depth to a maximum recorded 6.7 km/sec near the bottom of the hole. Surface seismic measurements indicate a mean velocity of only 6.0 km/sec to a depth of 10 km. Laboratory measurements show empirically a direct relationship between rock density and velocity. Therefore, a low density, low velocity material must underlie the rocks of the

Amisk Lake area in order to explain the low seismic velocity at depth. This interpretation is consistent with the gravity interpretation.

The geological interpretation of the gravity data has several interesting results. Variations in the Bouguer gravity field in the Amisk Lake area are controlled entirely by the densities of the outcropping rock units and their shape and depth. All the gravity anomalies in the area can be explained as the effect of outcropping bodies which extend to depths ranging from 2 to over 4.7 kilometers. Basic intrusive dikes and sills east of Amisk Lake are shown to be within a downbuckling of Amisk rocks although it is not clear from the gravity data whether the intrusions were emplaced before or after the downward movement. Large granite and granodiorite intrusions are shown to have densities distinctive from the surrounding rocks to depths as great as 3 to 4 kilometers. Below that depth, all rocks must have a grossly uniform, low density, and may approach granite in composition.

The gravity and aeromagnetic anomalies indicate the possible existence of some rocks which have not been recognized in the regional geological mapping. Among these are a basic intrusion under the water of Comeback Bay, an acidic intrusion under water and overburden near Denare Beach, and a zone of basic intrusions in central Amisk Lake extending more than ten miles south from Missi Island. Between Mosher Lake and Amisk Lake, gravity and density anomalies suggest the existence of an unrecognized fine-grained basic intrusion.

Large sections of the Reynard Lake and Mystic Lake syntectonic granodiorite intrusions are shown to be sill-like in shape and underlain by

denser, probably basic, rock which is in turn underlain by the low density acidic rock at depth. This interpretation may have some economic significance because Byers and Dahlstrom (1954, p. 89) and Smith (1964, p. 28) have observed an areal relationship between copper and zinc bearing sulfides, the copper concentrations in basic lavas, and the large granodiorite intrusions. The bottoms of some of the granodiorite bodies are relatively shallow, so they may be accessible for exploration of the potentially mineralized lavas below.

Similarly, basic intrusive rocks are considered by Byers et al. (1965, p. 83) and Stockwell (1960) to be related to mineral occurrences. The geophysical indication of possible unrecognized basic intrusions west of Mosher Lake and in the center of Amisk Lake is significant to this theory.

10. LIST OF REFERENCES

Army Survey Establishment, R.C.E., 1965, Amisk Lake, Saskatchewan: Map scale 1:250,000, Dept. of Mines and Tech. Surv., Ottawa.

Army Survey Establishment, R.C.E., 1965, Cormorant Lake, Manitoba-Saskatchewan: Map scale 1:250,000, Dept. of Mines and Tech. Surv., Ottawa.

Bateman, J.D. and Harrison, J.M., 1945, Mikanagan Lake, Manitoba: Geol. Surv. Canada, Map 832A.

Birch,F. and Simmons, G. 1966, Compressional Wave Velocities in Rocks as a Function of Pressure: In Handbook of Physical Constants, Geol. Soc. Amer., Memoir 97, Table 9-2, p. 198.

Birch, F., 1964, Longitudinal Wave Velocity in Rocks at Pressures of up to 10 Kbar: In Ultrasonics in Geophysics, "Mir" press.

Buckham, A.F., 1944, Athapapuskow Lake, Manitoba: Geo. Surv. Canada, Map 807A, with descriptive notes.

Burke, K.B., 1968, Personal written communication, University of Saskatchewan.

Byers, A.R., Editor, in press, Coronation Mine Study Volume: Geol. Surv. Canada.

Byers, A.R., 1957, Geology and Mineral Deposits of the Hanson Lake Area, Saskatchewan: Sask. Dept. Mineral Res., Rept. 30.

Byers, A.R. and Dahlstrom, C.D.A., 1954, Geology and Mineral Deposits of the Amisk-Wildnest Lakes Area, Saskatchewan: Sask. Dept. Mineral Res., Rept. 14.

Byers, A.R., Kirkland, S.J.T., and Pearson, W.J., 1965, Geology and Mineral Deposits of the Flin Flon Area, Saskatchewan: Sask. Dept. Mineral Res., Rept. 62.

Christensen, N.I., 1965, Compressional Wave Velocities in Metamorphic Rocks at Pressures to 10 Kilobars: Jour. Geophys. Res., v. 70, no. 24, p. 6147.

Clairaut, A.C., 1743, Theorie de la Figure de la Terre: Paris.

Clark, S.P. Jr., Editor, 1966, Handbook of Physical Constants, Revised Edition: Geol. Soc. Amer., Mem. 97.

Daly, R.A., 1933, Igneous Rocks and the Depths of the Earth: McGraw-Hill Book Co. Inc., New York and London.

Dana, E.S., 1953, A Textbook of Mineralogy (Fifteenth Printing): John Wiley & Sons Inc., New York.

Danes, Z.F., 1960, A Chemical Correction Factor in Gamma-Gamma Density Logging: Jour. Geophys. Res., v. 65, no. 7, p. 2149.

Dobrin, M.B., 1952, Introduction to Geophysical Prospecting: McGraw-Hill Book Company Inc., New York.

Eastwood, G.E.P., 1951, Snake Rapids, Saskatchewan: Geol. Surv. Canada, Map 1009A, with descriptive notes.

Eckstrand, N.L., 1962, Some Intrusive Rocks of the Mystic Lake Area, Sask: University of Saskatchewan, Unpublished B.Sc. Thesis.

Findlay, D.C., 1966, The JXWS Drilling Project: Geol. Surv. Canada, Unpublished Manuscript.

Froese, E., 1963, Structural Geology and Metamorphic Petrology of the Coronation Mine Area, Saskatchewan: Queen's University, Unpublished Ph.D. Thesis.

Garland, G.D., 1965, The Earth's Shape and Gravity: Pergammon Press Ltd.

Gendzwill, D.J., in press, A Gravity Investigation of the Amisk Lake Area, Saskatchewan: In The Coronation Mine Study, Geol. Surv. Canada, Ottawa.

Gendzwill, D.J., 1967, Subsurface and Surface Gravity Measurements Yarbo Area, Saskatchewan: Saskatchewan Research Council, Physics Division, Rept. P67-1.

Geological Survey of Canada, 1961, Aeromagnetic Series, Geophysics Paper 1028, Coronation Mine Area, Saskatchewan and Manitoba.

Geological Survey of Canada, 1963, Aeromagnetic Series, Geophysics Paper 2453, Athapapuskow Lake, Manitoba.

Geological Survey of Canada, 1963, Aeromagnetic Series, Geophysics Paper 2454G, Flin Flon, Manitoba.

Geological Survey of Canada, 1967, Aeromagnetic Series, Geophysics Paper 4596, Annabel Lake, Saskatchewan.

Geological Survey of Canada, 1967, Aeromagnetic Series, Geophysics Paper 4606G, Denare Beach, Saskatchewan.

Gibson, M.O., 1941, Network Adjustment by Least Squares - Alternative Formulation and Solution by Iteration: Geophysics, v. 6, no. 2, p. 168-179.

Grant, F.S. and Elsaharty, A.E., 1962, Bouguer Gravity Corrections Using a Variable Density: Geophysics, v. 27, no. 5, p. 616-626.

Grant, F.S. and West, G.F., 1965, Interpretation Theory in Applied Geophysics: McGraw-Hill Book Co., New York.

Haalk, H., 1932, A Statical Apparatus for Gravity Measurements: Zeitschrift fur Geophysik, Braunschweig, v. 8, no. 1/2, p. 17-30.

Hall, D.H. and Brisbin, W.C., 1965, Crustal Structure From Converted Head Waves in Central Western Manitoba: Geophysics, v. 30, no. 6, p. 1053.

Hamilton, A.C. and Winter, P.J., 1962, Primary Gravity Stations and Excentre Connections: Dominion Observatory, Gravity Division, Unpublished Manuscript.

Hammer, Sigmund, 1950, Density Determinations by Underground Gravity Measurements: Geophysics, 1950, v. 15, no. 4, p. 637-652.

Heywood, W.W., 1958, Ledge Lake Area, Manitoba and Saskatchewan: Geol. Surv. Canada, Map 24, 1957.

Hodgman, M.S., Editor-in-Chief, 1955-1956, Handbook of Chemistry and Physics, 37th Ed: Chemical Rubber Publishing Co., Cleveland.

Hubbert, M.K., 1948, Gravitational Terrain Effects of Two Dimensional Topographic Features: Geophysics, v. 13, no. 2, p. 226.

Hughes, D. and Morett, T.K., 1964, Elastic Wave Velocity in Granite When Pressure and Temperature Alter: In "Ultrasonics in Geophysics", "Mir" Press.

Innes, M.J.S., 1960, Gravity and Isostasy in Northern Ontario and Manitoba: Dominion Observatory, Ottawa, Pubs., v. 21, no. 6.

Jakosky, J.J., 1950, Exploration Geophysics, 2nd Ed: Trija Publishing Co., Los Angeles.

Jeffreys, H., 1962, The Earth, It's Origin, History, and Physical Constitution, Fourth Edition: University Press, Cambridge.

Jung, K., 1959, On the Gravimetric Determination of the Density of the Ground: Gerlands Beitr. Geophy., v. 68, no. 5, p. 268.

Kalliokoski, J., 1953, Weldon Bay, Manitoba: Geol. Surv. Canada, Map 1020A with descriptive notes.

Lacoste, L.J.B., 1934, A New Type of Long Period Vertical Seismograph: Physics, v. 5, p. 178.

Lacoste and Romberg, no date, Instruction Manual for Lacoste and Romberg Model G Geodetic Gravity Meter no. 52: Lacoste and Romberg, 6605 North Lamar, Austin 5, Texas.

Lowden, J.A., Stockwell, C.H., Tripper, H.W., Wanless, R.K., 1963, Age Determination and Geological Studies Including Isotopic Ages - Report 3: Geol. Surv. Canada, Paper 62-17, 140 p.

McConnell, K., 1966, Personal written communication, Dominion Observatory.

McCulloh, T.H., 1965, A Confirmation by Gravity Measurements of an Underground Density Profile Based on Core Densities: Geophysics, v. 30, no. 6, p. 1108.

McGlynn, J.C., 1959, Heming Lake, Manitoba: Geol. Surv. Canada, Map 1071A, with descriptive notes.

Nagy, D., 1966, The Gravitational Attraction of a Right Rectangular Prism: Geophysics, v. 31, no. 2, p. 362.

Nagy, D., 1965, Personal written communication, Dominion Observatory.

Nettleton, L.L., 1942, Gravity and Magnetic Calculations: Geophysics, v. 7, no. 3, p. 293.

Nettleton, L.L., 1940, Geophysical Prospecting for Oil: McGraw-Hill Book Co. Inc., New York.

Nettleton, L.L., 1939, Determination of Density for Reduction of Gravimeter Observations: Geophysics, v. 4, no. 3, p. 176.

Novoselitskii, V.M., 1965, The Theory of the Determination of Density Changes in a Horizontal Layer from Anomalies in the Force of Gravity: Izvestia, Physics of the Solid Earth, Trans. by Amer. Geophys. Union, no. 5, p. 300.

Parasnis, D.S., 1952, A Study of Rock Densities in the English Midlands: Royal Astron. Soc. Monthly Notices, Geophys. Supp., v. 6, no. 5, p. 252-271.

Pavlovskiy, V.I. and Serebryakov, Ye.B., 1965, On the Nature of the Gravity Field Over a Vertical Step in the Case of Gradual Change in Density in the Transition Zone: Razved. Geofizika, no. 5, p. 47-55.

Peirce, B.O. and Foster, R.M., 1956, A Short Table of Integrals, Fourth Edition: Ginn and Company, Boston.

Podolsky, T., 1958, Cranberry Portage (East Half), Manitoba: Geol. Surv. Canada, Map with descriptive notes.

Podolsky, T., 1951, Cranberry Portage (West Half), Manitoba: Geol. Surv. Canada, Map 26-1957, with descriptive notes.

Pyke, M.W., 1966, The Geology of the Pelican Narrows and Birch Portage Areas, Saskatchewan: Sask. Dept. Mineral Res., Rept. 93.

Saskatchewan Department of Natural Resources, no date, Depth Sounding Map, Amisk Lake.

Smith, J.R., 1964, Distribution of Nickel, Copper and Zinc in Bedrock of the East Amisk Area, Saskatchewan: Saskatchewan Research Council, Geology Division, Rept. 6.

Smith, R.A., 1960, Some Formulae for Interpreting Local Gravity Anomalies: Geophysical Prospecting, v. 8, no. 4, p. 576.

Stockwell, C.H., 1961, Structural Provinces, Orogenies and Time Classification of Rocks of the Canadian Precambrian Shield: Geol. Surv. Canada, Paper 61-17, p. 108-118.

Stockwell, C.H., 1960, Flin Flon Mandy Area, Manitoba and Saskatchewan: Geol. Surv. Canada, Map 1078A.

Sullivan, C.J., 1965, Geophysics and the Ore Environment: Program of Soc. Expl. Geophys. 35th Ann. Internat. Meet., Dallas, Texas, p. 30.

Tanner, J.G., 1967, Gravity Measurements in Canada: Dominion Observatory, Ottawa, Pubs., v. 36, no. 2.

Tanton, T.L., 1941a, Flin Flon, Saskatchewan and Manitoba: Geol. Surv. Canada, Map 632A with descriptive notes.

Tanton, T.L., 1941b, Schist Lake, Saskatchewan and Manitoba: Geol. Surv. Canada, Map 633A with descriptive notes.

Tittman, J. and Wahl, J.S., 1965, The Physical Foundations of Formation Density Logging (Gamma-Gamma): Geophysics, v. 30, no. 2, p. 284.

Turner, F.J. and Verhoogen, J., 1951, Igneous and Metamorphic Petrology: McGraw-Hill Book Co. Inc., New York.

Vashchilov, Yu. Ya., 1964, Bilogarithmic Master Chart for Interpreting Anomalies from Disturbing Bodies in the Form of a Rectangular Parallelopiped with the Upper Boundary in the Plane of Observation: Moskov. Univ. Geofiz. Issled, Sbornik, no. 11, p. 223-227.

Volarovich, M.P., Kurskeev, A.K., Tomoshevskaya, I.S., Tuzova, I.L. and Urazaev, B.M 1967, The Correlation Between the Longitudinal Wave Propagation Velocity and Rock Density at High Confining Pressures: Izvestia, Physics of the Solid Earth, Trans. by Amer. Geophys. Union, no. 5, p. 276.

Wanless, R.K., Stevens, R.D., Lachance, G.R. and Rimsaite, R.Y.H., 1965, Age Determinations and Geological Studies, Part 1 - Isotopic Ages, Report 5: Geo. Surv. Canada, Paper 64-17.

Whitham, K., 1967, National Report for Canada, Seismology and Physics of the Earth's Interior 1963-1966: Contributions from the Dominion Observatory, Ottawa, v. 7, no. 26.

Wohlberg, E.G., 1964, Genesis of a Meta-Gabbroic Sill in the Amisk Lake Area, Northern Saskatchewan: University of Saskatchewan, Unpublished M.A. Thesis.

Woolard, G.P., 1963, International Gravity Measurements: University of Wisconsin, Madison.

Yungul, S.H., 1961, Gravity Prospecting for Reefs: Effects of Sedimentation and Differential Compaction: Geophysics, v. 26, no. 1, p. 45-56.

SAMPLE DENSITIES CLASSIFIED ACCORDING TO ROCK TYPE

UNIT NUMBERS REFER TO LEGEND OF PLATE 1 , SMITH (1964)

EAST AND NORTH COORDINATES ARE IN UNITS OF 1/2 MILE FROM ORIGIN

MISSI SERIES , ARKOSE AND GREYWACKE , UNIT 7

NUMBER	EAST	NORTH	DENSITY	NUMBER	EAST	NORTH	DENSITY
1599	24.0	24.2	2.669 *	1598	24.3	24.2	2.658 *
1597	24.6	24.2	2.703 *	1595	24.1	23.3	2.745 *
1600	23.7	24.1	2.635 *				

**********SAMPLES 5 SAMPLES**********

META-BASALT AND MET-ANDESITE LAVAS
GREENSCHIST FACIES , UNIT 1-1

NUMBER	EAST	NORTH	DENSITY	NUMBER	EAST	NORTH	DENSITY
93	3.0	17.5	2.863 *	637	6.2	1.4	2.940 *
112	4.2	17.6	2.879 *	136	5.9	12.8	2.801 *
281	6.2	12.8	2.795 *	58	1.9	20.7	2.814 *
280	6.9	12.1	2.937 *	168	4.1	7.9	2.826 *
638	5.8	1.5	3.053 *	182	1.8	2.7	2.827 *
644	3.4	1.3	2.828 *	159	4.7	5.9	3.058 *
184	1.2	2.0	2.757 *	141	4.5	10.6	3.035 *
629	4.2	2.1	3.100 *	197	7.2	7.9	2.939 *
599	5.2	4.9	2.957 *	1299	6.9	15.8	3.058 *
187	1.1	0.5	2.805 *	59	2.5	20.0	2.910 *
63	3.9	19.0	2.840 *	3	6.8	11.8	2.981 *
1018	4.9	19.0	2.948 *	50	3.1	-0.3	2.898 *
43	3.4	0.5	2.908 *	96	2.6	18.3	2.874 *
171	4.4	5.1	2.940 *	613	5.7	3.5	3.068 *
169	3.6	7.3	2.998 *	646	5.8	3.6	3.011 *
51	2.8	-0.3	2.941 *	165	4.7	6.6	2.785 *
60	2.8	19.6	2.968 *	1297	6.9	13.9	3.045 *
41	2.8	0.5	2.937 *	45	5.2	0.5	3.079 *
82	4.6	11.9	2.962 *	64	4.0	19.4	2.967 *
104	5.9	18.4	2.840 *	277	7.1	13.4	3.050 *
146	4.2	8.5	2.975 *	151	5.0	9.2	2.939 *
189	1.3	-0.4	2.909 *	276	6.8	13.4	2.989 *
584	4.9	4.2	3.053 *	643	4.2	1.6	2.295 *
65	4.0	19.7	2.956 *	81	4.9	11.9	2.896 *
154	5.4	7.3	2.872 *	172	4.9	4.9	2.920 *
175	3.8	3.5	2.749 *	627	3.2	2.0	3.045 *
634	5.9	2.3	3.015 *	84	4.1	12.8	2.866 *
85	3.7	13.6	2.822 *	127	6.4	15.3	3.072 *
129	7.0	15.3	3.013 *	181	2.1	2.2	2.771 *
275	6.4	13.4	2.964 *	585	5.3	4.2	3.077 *
102	5.2	18.3	3.043 *	190	1.9	3.5	2.861 *
191	2.3	3.5	2.806 *	628	3.8	2.1	2.999 *
79	2.6	18.1	2.841 *	140	4.4	11.2	2.970 *

NUMBER	EAST	NORTH	DENSITY		NUMBER	EAST	NORTH	DENSITY	
278	7.1	13.0	2.922	*	14	6.0	8.6	2.984	*
126	6.0	15.3	3.043	*	130	6.5	14.4	3.077	*
144	3.9	10.0	2.994	*	163	4.5	7.3	2.969	*
624	4.4	2.7	3.064	*	775	4.6	19.8	2.957	*
53	3.4	19.4	2.785	*	1305	6.9	17.2	3.057	*
83	4.2	11.8	3.030	*	101	4.6	17.3	3.014	*
1301	6.3	16.6	3.035	*	1307	6.8	16.2	3.038	*
132	5.7	14.4	3.005	*	279	7.1	12.6	2.979	*
1298	7.1	14.9	3.000	*	157	5.0	6.6	2.833	*
57	2.2	20.7	2.967	*	103	5.5	18.4	2.916	*
149	4.5	10.0	2.820	*	185	1.1	1.3	2.953	*
94	3.0	17.9	2.907	*	116	4.5	12.8	2.802	*
120	5.7	16.9	2.886	*	639	5.4	1.5	3.174	*
70	3.5	15.1	2.864	*	86	3.7	14.5	2.993	*
143	4.2	10.0	2.803	*	162	4.1	7.3	2.947	*
1304	6.9	17.6	3.012	*	71	3.2	15.1	2.973	*
89	3.3	16.2	2.819	*	142	4.2	10.6	2.870	*
145	4.1	9.3	2.968	*	1260	6.8	17.9	2.998	*
97	4.3	16.0	2.822	*	117	4.4	16.9	2.799	*
148	4.6	9.3	3.054	*	178	2.3	2.8	2.762	*
1302	6.4	17.1	3.039	*	88	4.2	15.7	2.835	*
108	6.1	17.8	3.003	*	113	4.4	14.5	2.820	*
118	4.7	16.9	2.745	*	121	6.1	16.9	3.032	*
123	5.4	16.0	2.807	*	180	2.4	1.6	2.981	*
56	2.6	20.7	2.768	*	1282	7.2	16.8	2.933	*
80	5.2	11.9	2.914	*	128	6.7	15.3	3.014	*
131	6.1	14.4	2.976	*	282	6.5	12.5	3.047	*
642	4.6	1.6	2.901	*	776	5.2	20.0	2.997	*
105	6.3	18.5	3.082	*	133	5.1	13.7	2.817	*
158	5.4	5.8	2.853	*	183	1.5	2.8	3.018	*
115	4.4	13.7	2.840	*	177	2.7	2.8	2.888	*
612	5.3	3.5	3.112	*	135	5.6	12.8	2.738	*
139	4.8	11.1	3.042	*	1306	6.9	16.6	2.971	*
106	6.5	18.5	3.026	*	1016	5.7	19.3	2.992	*
40	2.2	0.5	2.824	*	55	2.8	20.3	3.018	*
67	3.4	20.4	2.889	*	167	4.9	7.8	2.821	*
1300	6.2	15.8	2.941	*	153	5.3	7.9	2.969	*
161	4.1	6.6	2.959	*	68	3.7	20.3	2.804	*
137	5.2	10.6	2.790	*	42	3.0	0.5	3.068	*
99	4.5	15.2	2.718	*	138	5.4	11.2	2.867	*
166	4.9	7.3	2.901	*	1017	5.4	19.2	2.883	*
4	6.9	9.3	3.133	*	48	4.1	-0.2	2.988	*
160	3.9	6.0	2.560	*	54	3.2	19.7	2.867	*
49	3.5	-0.2	2.924	*	122	6.1	16.3	3.012	*
150	4.9	9.9	2.893	*	95	2.8	18.0	2.930	*
1303	6.3	17.6	3.011	*	109	5.7	17.7	2.900	*
91	3.7	16.9	2.797	*	98	4.7	15.3	2.868	*
147	5.1	8.5	2.826	*	125	5.5	15.1	2.900	*
164	4.3	6.6	2.739	*	170	3.5	7.8	2.795	*
62	3.5	18.9	2.790	*	66	3.7	20.0	2.810	*
72	2.2	16.2	2.697	*	77	2.5	17.5	2.832	*
188	1.7	0.2	2.888	*	78	2.8	17.5	2.787	*
114	4.5	14.3	2.907	*	124	5.0	16.0	2.780	*
176	3.0	3.5	2.820	*	90	3.7	16.2	2.814	*

NUMBER	EAST	NORTH	DENSITY		NUMBER	EAST	NORTH	DENSITY	
100	4.3	18.1	2.805	*	52	1.9	-0.3	2.813	*
626	2.9	2.0	2.984	*	645	2.8	1.3	3.000	*
44	4.5	0.5	2.996	*	69	3.7	20.8	2.848	*
174	4.2	3.5	3.096	*	92	3.5	16.9	2.885	*
61	3.1	19.0	2.722	*	87	4.2	15.2	2.844	*
134	5.8	13.6	2.816	*					

**********SAMPLES 185 SAMPLES**********

META-BASALT AND MET-ANDESITE LAVAS
EPIDOTE - AMPHIBOLITE FACIES , UNIT 1-2

NUMBER	EAST	NORTH	DENSITY		NUMBER	EAST	NORTH	DENSITY	
969	8.5	15.9	2.911	*	1271	8.0	17.6	2.822	*
970	8.3	16.0	2.876	*	1006	7.6	19.3	2.957	*
570	7.5	14.2	2.963	*	556	7.5	12.3	3.014	*
781	7.3	20.9	2.885	*	568	7.8	13.3	2.970	*
761	5.9	21.0	3.159	*	1269	7.8	17.4	2.767	*
1268	7.5	17.6	2.872	*	762	6.4	21.5	2.989	*
569	7.5	13.4	3.041	*	779	6.4	20.6	2.948	*
1258	7.3	18.6	2.911	*	1013	6.9	20.1	2.991	*
1252	6.6	18.9	3.061	*	1254	6.6	19.8	3.074	*
1272	7.6	18.0	2.916	*	575	7.8	15.0	3.077	*
1001	6.2	22.3	2.965	*	1259	7.2	18.3	2.900	*
972	8.5	16.5	3.047	*	1002	5.9	22.1	2.966	*
790	7.9	19.4	2.889	*	988	4.8	22.8	3.057	*
1279	7.3	17.5	2.850	*	1294	7.5	13.8	2.974	*
973	8.9	16.4	2.993	*	1286	8.0	16.8	2.875	*
980	4.1	23.4	3.117	*	574	7.4	15.0	2.914	*
778	6.1	20.7	2.982	*	987	5.1	23.2	3.101	*
1253	6.5	19.3	3.073	*	577	8.6	14.9	2.978	*
780	6.8	20.7	3.058	*	1255	6.7	19.4	2.978	*
1257	7.2	18.8	3.078	*	1014	6.7	20.0	2.938	*
573	7.9	14.2	3.015	*	994	5.5	22.4	3.029	*
1291	7.5	15.5	3.013	*	576	8.2	15.0	2.893	*
1261	7.1	17.9	2.955	*	1285	7.8	16.4	2.953	*
993	5.2	22.2	2.979	*	1256	6.9	19.1	2.966	*
763	6.7	21.6	3.038	*	1296	7.5	12.7	2.836	*
1270	7.9	17.2	2.923	*	1287	8.0	15.9	2.784	*
1288	7.6	16.1	3.013	*	1283	7.5	17.1	2.847	*
971	8.2	16.5	2.884	*	1278	8.3	16.9	2.831	*
1267	6.7	18.5	2.925	*	1265	6.8	18.6	2.919	*

**********SAMPLES 58 SAMPLES**********

META-BASALT AND MET-ANDESITE LAVAS
EPIDOTE - AMPHIBOLITE FACIES , UNIT 1-3

NUMBER	EAST	NORTH	DENSITY		NUMBER	EAST	NORTH	DENSITY	
11	7.5	8.5	2.879	*	660	7.6	6.6	2.863	*
368	8.2	-0.9	3.036	*	371	8.2	-1.2	3.005	*
1340	7.7	7.4	2.912	*	8	8.1	9.3	2.978	*
6	7.6	9.3	2.938	*	1343	8.2	8.0	2.835	*
9	7.8	9.1	2.924	*	581	9.2	14.0	2.799	*
334	7.6	1.3	2.953	*	617	7.6	3.5	2.995	*
636	7.1	1.4	2.928	*	7	7.9	9.3	2.989	*
597	7.7	5.1	2.909	*	603	8.8	11.9	2.797	*
12	7.1	8.6	2.844	*	590	7.8	4.3	2.947	*
652	8.4	5.9	2.958	*	1339	8.2	7.5	2.972	*
1330	8.4	8.9	2.985	*	650	7.6	5.9	2.943	*
651	8.0	5.9	2.866	*	1067	8.0	2.6	2.941	*
602	8.5	11.9	2.929	*	1329	8.1	8.8	2.921	*
1337	8.4	7.5	2.871	*	1338	8.4	7.6	3.097	*
1066	8.1	3.2	2.946	*	659	8.1	6.6	2.953	*
618	7.7	2.8	2.922	*	332	7.8	2.1	2.974	*
1332	8.3	8.4	2.941	*	1342	8.0	8.0	2.909	*
596	8.0	5.1	2.953	*					

**********SAMPLES 35 SAMPLES**********

META-BASALT AND MET-ANDESITE LAVAS
EPIDOTE - AMPHIBOLITE FACIES , UNIT 1-4

NUMBER	EAST	NORTH	DENSITY		NUMBER	EAST	NORTH	DENSITY	
408	9.3	9.5	2.797	*	1322	9.7	7.1	2.922	*
1324	9.6	6.4	2.992	*	405	9.3	9.1	2.766	*
1323	9.7	6.7	2.945	*	655	9.5	5.9	2.992	*
420	11.1	7.8	2.948	*	415	10.9	8.4	2.863	*
409	9.8	9.7	2.921	*	314	11.4	4.0	2.970	*
1315	9.8	9.0	2.964	*	1047	11.3	1.9	2.994	*
801	12.2	7.7	2.816	*	1044	11.4	1.4	2.885	*
1098	12.7	0.7	2.952	*	1357	12.2	2.4	2.912	*
1354	11.9	1.7	2.904	*	346	11.7	5.7	2.809	*
1042	12.6	2.3	3.033	*	1041	12.7	2.5	2.946	*
1040	13.5	2.9	3.019	*	1145	12.5	5.2	3.000	*
1314	9.2	8.6	2.878	*	1019	9.8	14.3	2.971	*
1313	9.9	8.5	2.876	*	1104	12.7	1.5	3.173	*
1033	13.4	2.0	2.849	*	310	11.5	8.4	3.127	*
324	11.2	2.5	2.877	*	349	11.6	3.6	3.010	*
1043	11.6	2.2	2.920	*	316	11.8	3.0	2.802	*
1081	11.5	4.1	2.947	*	1157	12.2	5.5	2.919	*
1350	12.0	0.8	2.826	*	315	11.8	3.4	3.004	*
1325	9.8	6.3	2.991	*	1030	10.1	13.5	2.939	*
1346	12.2	0.7	2.865	*	325	11.6	2.6	2.848	*
347	11.4	5.4	2.861	*	1319	9.8	7.8	3.003	*
1347	11.2	1.2	2.979	*	1082	11.6	7.1	3.047	*
1356	11.9	2.2	2.889	*	1031	12.6	1.9	3.054	*
1359	12.4	2.6	2.888	*	414	11.2	8.4	2.979	*

NUMBER	EAST	NORTH	DENSITY		NUMBER	EAST	NORTH	DENSITY	
401	10.3	12.0	2.800	*	1353	12.5	1.3	3.039	*
1348	11.2	1.0	3.003	*	350	10.9	3.6	3.035	*
1144	12.1	5.2	2.924	*	356	10.9	4.3	3.071	*
656	9.7	5.9	2.970	*	1083	12.0	7.1	2.895	*
381	10.1	12.8	2.924	*					

**********SAMPLES 57 SAMPLES**********

META-BASALT AND MET-ANDESITE LAVAS
EPIDOTE - AMPHIBOLITE FACIES , UNIT 1-5

NUMBER	EAST	NORTH	DENSITY		NUMBER	EAST	NORTH	DENSITY	
504	15.3	4.2	2.993	*	483	18.6	10.8	3.008	*
462	18.7	13.2	3.036	*	868	17.3	8.9	2.914	*
508	14.3	7.5	3.035	*	451	18.0	11.9	2.946	*
1074	14.7	4.1	2.996	*	1136	14.4	9.3	3.015	*
1075	14.9	4.7	3.012	*	855	18.8	11.3	2.918	*
430	18.5	14.2	2.999	*	1150	14.9	5.3	2.951	*
463	18.5	12.9	2.829	*	841	18.2	11.8	2.957	*
1151	14.6	5.8	2.999	*	520	16.1	11.2	3.035	*
842	18.4	11.9	2.954	*	796	14.0	8.4	3.032	*
465	18.0	12.1	2.862	*	503	14.7	3.9	3.026	*
453	18.6	12.3	2.974	*	1089	14.4	7.3	3.037	*

**********SAMPLES 22 SAMPLES**********

META-BASALT AND MET-ANDESITE LAVAS
GREENSCHIST FACIES , UNIT 1-6

NUMBER	EAST	NORTH	DENSITY		NUMBER	EAST	NORTH	DENSITY	
1175	19.4	17.7	2.965	*	931	22.7	8.5	2.930	*
541	22.8	7.7	2.969	*	1167	19.9	18.5	3.054	*
928	23.7	9.2	3.172	*	554	24.3	7.7	2.943	*
917	22.0	12.2	2.836	*	1168	19.7	18.7	2.876	*
475	21.5	10.0	3.039	*	540	23.2	7.9	3.105	*
947	22.7	9.3	3.071	*	477	21.6	10.5	2.991	*
551	23.1	6.7	2.997	*	945	21.7	8.8	2.971	*
930	23.0	8.7	3.049	*	1177	18.5	17.7	2.931	*
553	23.7	7.3	3.091	*	929	23.3	9.0	3.085	*
1182	21.2	17.0	2.960	*	539	23.6	8.2	3.106	*
538	24.2	8.2	3.105	*	807	21.1	16.4	2.926	*
1159	20.0	18.8	2.991	*	1176	18.9	17.7	2.838	*
1158	19.5	18.8	2.912	*	1171	21.5	17.8	2.979	*
1518	24.0	17.6	2.950	*	1519	23.6	17.6	3.154	*
1602	22.9	23.8	3.015	*	1593	23.5	23.3	2.986	*
1431	20.5	22.5	3.166	*	1516	24.4	18.6	2.968	*
1491	22.7	20.2	2.902	*	1435	21.7	23.4	2.824	*
1458	21.2	20.9	3.046	*	1552	21.6	19.1	3.209	*

NUMBER	EAST	NORTH	DENSITY		NUMBER	EAST	NORTH	DENSITY	
1587	23.0	22.5	2.765	*	1584	24.1	22.5	2.904	*
1546	23.4	15.4	2.999	*	1554	21.9	14.0	2.921	*
1514	23.7	18.6	2.899	*	1592	23.0	23.3	2.798	*
1515	24.1	18.5	2.818	*	1581	24.1	21.7	2.963	*
1522	24.3	17.0	2.943	*	1564	23.4	13.2	2.834	*
1507	22.4	18.5	3.070	*	1560	24.2	14.0	2.953	*
1585	23.7	22.6	2.891	*	1432	20.8	22.7	3.093	*
1362	18.5	17.0	3.059	*	1463	21.7	22.2	2.899	*
1368	17.7	17.1	3.051	*	1545	23.7	15.5	2.923	*
1556	22.7	14.0	2.959	*	1601	23.2	24.0	2.886	*
1441	18.5	20.5	2.815	*	1455	22.2	21.6	2.923	*
1525	24.6	16.2	2.967	*	1490	22.3	20.0	3.074	*
1408	20.5	20.5	3.061	*	1434	21.4	23.2	3.068	*
1529	23.4	16.2	2.962	*	1521	23.9	17.0	2.929	*
1524	24.6	16.5	2.979	*	1582	24.5	21.7	2.925	*
1594	23.7	23.3	2.850	*	1456	21.8	21.3	2.922	*
1573	21.9	11.6	3.073	*	1445	17.2	19.6	2.801	*
1578	23.0	21.7	3.063	*	1591	22.7	23.3	2.805	*
1454	22.4	21.8	2.807	*	1440	17.1	20.5	2.870	*
1563	23.8	13.1	2.873	*	1381	17.1	21.4	2.902	*
1415	19.6	21.0	2.871	*	1423	20.2	23.1	2.877	*
1459	20.4	21.4	2.918	*	1549	21.6	18.5	2.791	*
1586	23.4	22.5	2.967	*	1480	20.9	23.6	2.966	*
1501	24.1	19.3	2.899	*	1502	23.7	19.4	2.893	*
1538	23.2	14.7	2.902	*	1537	22.8	14.6	2.932	*
1411	19.4	20.0	2.960	*	1428	19.7	21.8	2.836	*
1558	23.5	14.0	3.022	*	1427	19.4	21.5	2.954	*
1433	21.1	22.9	2.991	*	1481	21.2	23.6	3.072	*
1596	24.5	23.4	2.752	*	1555	22.3	14.0	2.849	*
1588	22.7	22.5	2.834	*	1562	24.2	13.1	2.789	*
1577	22.6	21.8	2.893	*	1603	22.6	23.8	2.776	*
1469	17.3	22.0	2.855	*	1471	18.0	22.4	2.929	*
1539	23.6	14.7	2.966	*	1474	18.4	23.2	2.945	*
1174	19.8	17.8	2.944	*	1464	22.1	22.6	2.855	*
1506	22.0	19.1	2.930	*	1447	17.9	19.5	2.916	*
1484	22.5	20.8	2.866	*	1583	24.6	22.8	2.925	*
1617	17.0	22.5	2.865	*	1429	20.1	22.0	3.018	*
1476	19.1	23.4	3.016	*	1548	22.1	18.5	2.951	*
1503	23.3	19.2	2.837	*	1614	17.1	23.0	2.941	*
1410	19.7	20.1	2.955	*	1543	24.5	15.6	2.976	*
1422	19.9	22.9	3.011	*	1418	18.6	22.0	2.893	*
1439	17.5	20.5	2.830	*	1436	22.0	23.6	2.958	*
1482	21.4	23.7	2.932	*	1485	22.2	20.6	2.934	*
1550	21.2	18.5	2.971	*	1483	22.3	23.9	2.879	*
1496	24.6	21.0	2.763	*	1589	22.4	22.5	2.791	*
1437	18.2	20.9	2.789	*	1473	18.0	23.2	3.052	*
1541	24.4	14.8	2.929	*	1407	20.8	20.6	2.803	*
1409	20.1	20.2	2.826	*	1425	18.8	21.2	2.970	*
1565	23.0	13.2	2.866	*	1414	19.3	20.8	2.956	*
1421	19.5	22.7	2.986	*	1551	21.2	19.1	2.881	*
1470	17.7	22.2	2.886	*	1424	18.5	21.1	2.797	*
1426	19.1	21.3	3.009	*	1477	19.7	23.5	2.773	*
1393	17.4	18.1	3.068	*	1475	18.8	23.3	3.008	*
1430	20.3	22.3	2.794	*	1542	24.8	14.9	2.836	*

NUMBER	EAST	NORTH	DENSITY		NUMBER	EAST	NORTH	DENSITY	
1453	19.3	19.3	2.784	*	1446	17.6	19.2	2.879	*
1615	17.4	23.0	3.045	*	1536	22.3	14.7	3.046	*
1509	22.5	17.8	3.003	*	1472	18.3	22.7	2.857	*
1559	23.9	14.0	2.863	*	1413	18.9	20.6	3.041	*
1412	19.1	19.9	2.779	*	1616	17.4	22.7	2.854	*
1405	21.3	19.8	2.917	*	1417	18.2	21.7	3.052	*
1590	22.2	23.2	2.898	*	1450	18.8	19.7	2.834	*
1449	18.5	20.0	2.798	*	1402	20.1	19.4	2.906	*
1401	19.7	19.4	3.038	*					

**********SAMPLES 161 SAMPLES**********

GREY DIORITE , UNIT 11-6 SOUTHWEST OF DOUGLAS LAKE

NUMBER	EAST	NORTH	DENSITY		NUMBER	EAST	NORTH	DENSITY	
1374	16.6	20.2	2.940	*	1390	18.8	16.9	2.912	*
1386	18.7	18.5	2.870	*	1517	24.4	17.8	2.948	*
1377	15.8	20.5	3.070	*	1520	23.3	17.7	3.037	*
1416	20.0	21.2	2.999	*	1499	23.3	20.9	3.033	*
1395	16.9	17.5	2.755	*	1493	23.8	20.1	2.909	*
1497	24.2	21.0	2.894	*	1444	17.5	19.9	2.853	*
1561	24.7	14.0	2.790	*	1451	18.7	19.2	2.927	*
1379	16.6	21.0	2.962	*	1478	20.1	23.4	2.998	*
1383	17.9	21.6	2.793	*	1387	19.1	18.3	2.929	*
1388	19.4	18.2	2.950	*	1419	18.8	22.2	2.968	*
1540	24.0	14.7	2.958	*	1479	20.3	23.6	2.983	*
1557	23.1	14.0	2.969	*	1498	23.8	20.9	2.917	*
1492	23.5	20.1	2.973	*	1420	19.2	22.4	2.942	*
1494	24.3	20.1	2.845	*	1495	24.7	20.1	2.729	*
1382	17.5	21.4	2.887	*	1526	24.2	16.2	2.975	*
1528	23.6	16.2	2.958	*	1580	23.7	21.7	2.890	*
1378	16.3	20.7	2.962	*					

**********SAMPLES 33 SAMPLES**********

META-DACITE AND META-RHYOLITE LAVAS
SOUTH AND WEST OF WEKACH LAKE , UNIT 2

NUMBER	EAST	NORTH	DENSITY		NUMBER	EAST	NORTH	DENSITY	
1156	12.4	5.9	2.716	*	506	15.1	7.0	2.676	*
802	11.7	7.7	2.687	*	1080	12.9	4.4	2.780	*
510	14.9	8.5	2.748	*	1096	11.7	6.4	2.766	*
856	18.2	11.3	2.722	*	1069	12.6	3.8	2.713	*
517	15.8	9.4	2.652	*	119	5.4	16.9	2.675	*
1032	13.1	2.0	2.736	*	298	7.8	18.4	2.748	*
1277	8.2	17.3	2.773	*	317	10.8	2.9	2.674	*

**********SAMPLES 14 SAMPLES**********

META-DACITE AND META-RHYOLITE LAVAS
NORTH AND EAST OF WEKACH LAKE , UNIT 2

NUMBER	EAST	NORTH	DENSITY		NUMBER	EAST	NORTH	DENSITY	
1460	20.7	21.7	2.669	*	1527	23.8	16.2	2.648	*
1169	22.4	17.8	2.743	*	1404	20.8	19.7	2.678	*
1403	20.3	19.4	2.723	*	1170	22.0	17.8	2.733	*
1547	22.9	15.4	2.712	*	1406	21.2	20.4	2.677	*
1452	19.0	19.3	2.728	*	1389	18.3	19.0	2.766	*
1544	24.1	15.5	2.699	*					

**********SAMPLES 11 SAMPLES**********

BASIC TUFF AND AGGLOMERATE
SOUTH AND WEST OF WEKACH LAKE , UNIT 4

NUMBER	EAST	NORTH	DENSITY		NUMBER	EAST	NORTH	DENSITY	
728	5.9	27.2	2.977	*	564	9.2	13.3	2.690	*
516	15.6	9.9	2.868	*	467	17.9	9.9	2.778	*
505	15.0	6.3	3.038	*	522	17.1	11.4	2.740	*
1135	14.5	9.9	2.963	*	519	17.1	10.0	2.898	*
514	16.0	10.5	2.890	*	509	14.7	7.9	2.840	*

**********SAMPLES 10 SAMPLES**********

ACIDIC TUFF AND AGGLOMERATE
SOUTH AND WEST OF WEKACH LAKE , UNIT 4

NUMBER	EAST	NORTH	DENSITY		NUMBER	EAST	NORTH	DENSITY	
524	15.4	9.2	2.704	*	511	15.1	9.3	2.765	*
525	15.2	9.8	2.729	*	507	15.2	8.3	2.738	*
679	5.5	27.4	2.749	*	518	16.7	10.0	2.713	*
521	16.7	11.9	2.771	*					

**********SAMPLES 7 SAMPLES**********

BASIC TUFF AND AGGLOMERATE
NORTH AND EAST OF WEKACH LAKE , UNIT 4

NUMBER	EAST	NORTH	DENSITY		NUMBER	EAST	NORTH	DENSITY	
1376	15.5	20.4	2.799	*	1398	16.8	18.5	3.100	*
1574	22.3	11.7	2.800	*	1367	17.3	16.9	2.915	*
1627	15.0	20.8	3.029	*	1438	17.8	20.6	2.972	*
1448	18.2	19.8	2.854	*	1443	17.8	20.1	2.866	*
1575	22.8	11.7	2.850	*	1399	17.1	18.7	3.016	*
1373	16.3	19.8	2.850	*	1365	17.4	16.3	2.940	*
1371	16.7	19.3	2.697	*	946	22.2	9.0	2.895	*

NUMBER	EAST	NORTH	DENSITY		NUMBER	EAST	NORTH	DENSITY	
1500	24.5	19.4	2.990	*	1442	18.0	20.4	2.950	*
1397	16.6	18.1	2.869	*	1217	16.2	17.7	2.819	*
1369	18.2	17.4	2.853	*	1366	17.0	16.6	2.858	*
693	16.1	19.9	3.083	*	1385	18.4	18.6	2.922	*
1391	18.1	17.8	2.840	*	1628	15.4	20.9	2.997	*
1400	17.2	18.9	2.785	*					

**********SAMPLES 25 SAMPLES**********

ACIDIC TUFF AND AGGLOMERATE
NORTH AND EAST OF WEKACH LAKE , UNIT 4

NUMBER	EAST	NORTH	DENSITY		NUMBER	EAST	NORTH	DENSITY	
1372	16.1	19.5	2.759	*	1370	16.4	19.0	2.752	*
1576	23.2	11.7	2.759	*	1375	15.8	20.0	2.696	*
1178	19.3	16.9	2.797	*	1626	14.0	21.8	2.781	*
1384	18.0	18.6	2.747	*					

**********SAMPLES 7 SAMPLES**********

META-GABBROIC ROCKS UNIT 11-1

NUMBER	EAST	NORTH	DENSITY		NUMBER	EAST	NORTH	DENSITY	
588	6.9	4.2	3.033	*	663	6.2	6.6	2.990	*
10	7.4	8.8	3.015	*	589	7.5	4.2	2.967	*
615	6.9	3.5	3.066	*	196	7.4	7.9	3.014	*
647	6.5	5.9	3.090	*	662	6.6	6.6	3.007	*
194	7.3	7.3	3.068	*	195	7.4	7.3	2.990	*
192	6.4	7.3	2.937	*	635	6.5	2.3	2.999	*
193	6.8	7.3	3.008	*	198	7.0	7.8	3.044	*
1341	7.4	6.9	3.034	*	587	6.4	4.2	3.082	*
5	7.3	9.3	3.079	*	648	6.8	5.9	2.935	*
640	5.0	1.5	3.052	*	649	7.2	5.9	3.080	*
619	7.1	2.8	3.077	*	598	6.9	5.0	3.010	*
661	7.0	6.6	3.085	*	186	0.7	0.5	2.762	*
616	7.3	3.5	3.079	*	156	6.0	6.8	2.970	*
13	6.5	8.6	2.995	*	155	6.1	7.3	2.891	*
586	5.6	4.2	3.027	*	199	6.5	7.9	2.983	*
179	3.4	2.8	2.933	*	152	6.1	7.9	2.824	*
614	5.9	3.5	3.016	*					

**********SAMPLES 33 SAMPLES**********

META-GABBROIC ROCKS UNIT 11-2

NUMBER	EAST	NORTH	DENSITY		NUMBER	EAST	NORTH	DENSITY	
777	5.7	20.5	2.992	*	760	5.6	21.0	3.024	*
992	4.9	22.0	3.064	*	990	4.4	22.2	3.079	*
991	4.5	21.7	3.076	*	1005	4.8	21.5	3.037	*
1003	5.5	21.8	2.948	*	1004	5.1	21.7	3.064	*
1012	7.2	20.3	3.061	*	989	4.7	22.5	3.037	*
111	4.6	17.6	2.949	*	979	3.7	22.9	3.004	*
1015	6.1	19.5	3.047	*	107	6.3	18.2	3.081	*
110	4.8	17.6	3.039	*					

**********SAMPLES 15 SAMPLES**********

META-GABBROIC ROCKS UNIT 11-3

NUMBER	EAST	NORTH	DENSITY		NUMBER	EAST	NORTH	DENSITY	
327	9.0	1.3	2.897	*	1057	9.0	4.5	2.960	*
1336	8.7	7.4	2.912	*	604	8.9	12.0	3.038	*
658	8.6	6.7	3.027	*	563	9.4	13.3	3.073	*
1061	8.9	3.6	2.931	*	654	9.3	5.9	2.816	*
372	8.7	-1.9	2.999	*	601	9.2	11.9	2.841	*
373	9.4	-1.7	3.060	*	593	9.2	4.6	2.929	*
369	9.0	-1.1	3.104	*	562	9.6	13.2	2.943	*
657	8.9	6.7	3.009	*	377	9.2	-0.5	3.051	*
1056	9.1	5.0	3.005	*	1333	8.5	8.4	3.050	*
1316	8.8	8.7	3.012	*	1320	9.3	7.9	2.722	*
1328	8.4	9.1	3.029	*	331	8.3	2.1	2.982	*
362	8.3	0.6	2.944	*	606	9.5	12.3	2.985	*
1064	9.0	2.9	2.922	*	1321	9.1	7.1	2.998	*
592	8.4	4.5	3.015	*	1292	7.5	14.7	2.967	*
364	7.9	-0.1	3.040	*	578	9.0	14.9	2.938	*
609	9.6	12.7	2.852	*	1334	8.8	8.4	3.009	*
653	8.9	5.9	2.930	*	370	8.5	-1.5	2.915	*
407	8.7	9.4	3.002	*	406	8.9	9.1	2.911	*
594	9.1	5.1	2.982	*	1065	8.5	2.8	2.978	*
1345	9.0	8.1	2.999	*	600	9.6	11.9	2.944	*
329	8.7	2.0	2.973	*	558	8.0	12.5	2.878	*
1344	8.4	7.9	3.046	*	39	9.2	9.9	2.912	*
595	8.7	5.0	3.031	*	1331	8.6	8.7	3.041	*
1060	9.5	3.5	2.862	*	1327	8.4	9.5	2.962	*
1335	8.7	7.9	2.873	*	555	7.4	11.8	2.935	*
365	8.5	0.0	2.978	*	968	9.2	15.4	2.898	*
366	8.3	-0.6	3.020	*	1	7.7	11.9	2.966	*
605	9.2	12.2	2.839	*	367	8.0	-0.5	3.021	*
608	8.9	12.5	3.005	*	1063	9.2	2.9	3.011	*
341	9.5	4.9	2.887	*	607	8.4	12.2	2.783	*
2	8.1	11.9	2.824	*	557	7.6	12.5	2.945	*
567	8.2	13.4	2.847	*	336	8.0	0.6	2.987	*
571	8.6	14.1	2.896	*	328	8.5	1.2	2.966	*
335	7.5	0.6	3.070	*	560	8.5	12.5	2.913	*

NUMBER	EAST	NORTH	DENSITY		NUMBER	EAST	NORTH	DENSITY	
591	8.2	4.3	2.936	*	566	8.7	13.4	2.989	*
559	8.1	12.5	2.938	*	572	8.2	14.2	2.875	*
326	9.1	1.9	3.082	*	561	9.0	13.1	2.824	*
337	8.1	1.2	3.005	*	565	9.0	13.3	2.909	*

**********SAMPLES 76 SAMPLES**********

META-GABBROIC ROCKS UNIT 11-4

NUMBER	EAST	NORTH	DENSITY		NUMBER	EAST	NORTH	DENSITY	
1048	11.0	1.5	3.117	*	319	10.0	2.9	3.073	*
358	10.2	6.3	3.083	*	1308	10.9	1.2	3.133	*
1311	10.0	1.2	3.071	*	1055	9.7	1.2	3.081	*
339	10.0	4.9	3.060	*	343	10.5	5.6	3.028	*
1045	11.0	1.0	3.069	*	321	9.9	2.4	3.050	*
379	9.5	0.2	3.075	*	359	10.4	7.0	2.952	*
1097	11.3	6.4	3.072	*	1310	10.2	1.2	3.108	*
1051	9.8	1.7	3.057	*	1052	9.9	1.8	3.102	*
312	11.0	6.5	2.961	*	313	10.9	4.9	2.931	*
416	10.6	8.4	3.088	*	322	10.1	2.1	3.034	*
417	10.4	7.9	3.116	*	352	9.9	3.6	3.029	*
323	10.4	2.2	3.021	*	1317	10.7	8.7	3.067	*
351	10.6	3.6	2.995	*	338	10.5	4.9	2.889	*
1050	10.4	1.5	3.046	*	1352	10.9	0.8	3.067	*
419	10.8	7.8	3.030	*	1351	10.2	0.7	3.092	*
344	10.9	5.6	3.081	*	361	11.2	7.0	2.952	*
348	11.2	5.2	3.044	*	1046	11.0	2.2	3.107	*
360	10.8	7.1	2.861	*	354	10.1	4.3	3.048	*
355	10.6	4.2	2.984	*	1309	10.6	1.2	3.045	*
1049	10.3	1.7	3.052	*	357	10.6	6.3	3.135	*
418	10.4	7.7	2.906	*					

**********SAMPLES 41 SAMPLES**********

META-GABBROIC ROCKS UNIT 11-5

NUMBER	EAST	NORTH	DENSITY		NUMBER	EAST	NORTH	DENSITY	
1142	11.9	9.2	2.895	*	1137	14.0	9.3	3.073	*
403	10.8	9.1	3.072	*	1139	13.1	9.3	2.905	*
798	13.6	7.8	2.955	*	1138	13.6	9.3	2.907	*
791	11.7	8.4	2.885	*	792	12.2	8.4	2.835	*
839	14.8	11.9	2.950	*	794	13.3	8.5	3.010	*
1078	13.7	4.5	2.849	*	1148	13.8	5.2	2.874	*
1106	11.1	10.5	2.942	*	1087	13.5	7.2	3.002	*
1077	14.0	4.6	2.890	*	1122	10.8	11.3	2.949	*
1154	13.1	5.9	2.926	*	466	17.4	9.9	2.798	*

NUMBER	EAST	NORTH	DENSITY		NUMBER	EAST	NORTH	DENSITY	
840	15.9	11.7	3.019	*	1086	13.1	7.2	3.006	*
404	10.2	9.0	3.074	*	1072	13.9	4.0	2.854	*
1073	14.3	4.0	2.923	*	1198	17.2	13.9	2.961	*
858	17.3	12.4	2.964	*	1124	10.2	10.7	3.083	*
1079	13.3	4.5	2.910	*	1155	12.7	5.9	3.025	*
1229	16.6	16.2	2.920	*	1189	17.4	14.6	2.977	*
413	10.9	9.4	2.887	*	795	13.7	8.5	3.027	*
797	14.0	7.8	3.015	*	862	17.1	13.6	2.902	*
1092	13.4	6.5	2.979	*	1105	10.8	10.3	2.883	*
1147	13.4	5.2	2.947	*	1200	17.9	13.8	2.860	*
1153	13.6	5.9	3.027	*	1152	14.0	5.9	2.988	*
513	16.0	11.3	2.885	*	1141	12.3	9.3	3.006	*
1093	12.9	6.5	2.926	*	1190	17.0	14.6	2.784	*
429	18.7	14.3	2.931	*	495	15.0	11.1	2.906	*
1140	12.8	9.3	2.960	*	1228	16.1	16.2	2.951	*
1070	13.1	3.9	2.940	*	1149	14.5	5.2	2.949	*
1231	16.7	15.4	2.875	*	512	15.5	11.1	2.971	*
1126	11.3	10.2	3.038	*	1146	13.1	5.2	2.975	*
1134	14.7	10.4	3.020	*	1199	17.7	14.0	2.901	*
1197	16.8	13.9	3.202	*	1076	14.6	4.7	3.027	*
1123	10.4	10.9	2.788	*	857	17.2	12.1	3.004	*
1125	10.9	10.2	3.005	*	793	12.9	8.5	2.923	*
1090	14.5	6.4	3.033	*	800	12.7	7.8	3.002	*
860	17.8	13.3	3.049	*	400	10.6	12.1	2.847	*
492	14.3	11.4	3.017	*	1129	12.5	10.3	2.867	*
399	10.9	12.2	2.944	*	859	17.6	12.9	3.119	*
1188	17.7	14.6	2.888	*	412	10.8	9.9	2.948	*
1113	13.9	11.6	2.959	*	515	15.5	10.5	2.914	*
1029	10.6	13.8	3.061	*	1111	13.4	11.3	3.098	*
1112	13.7	11.4	2.990	*	491	13.9	11.0	3.120	*
493	14.7	11.8	3.045	*	861	17.7	13.6	3.002	*
1039	13.9	3.0	3.040	*	402	11.2	9.1	3.046	*
1143	11.4	9.1	2.993	*	1071	13.5	3.9	2.948	*
490	13.7	10.7	3.211	*	1088	14.0	7.2	2.984	*
1110	13.0	11.1	3.039	*	450	15.1	12.6	2.972	*
440	15.0	12.3	2.967	*	1191	16.5	14.6	2.985	*
1091	14.2	6.5	3.042	*	1364	17.9	16.5	3.167	*
486	15.0	10.6	3.082	*	431	18.3	14.0	2.967	*
494	14.9	11.5	2.963	*	1363	18.1	16.7	3.136	*
1187	18.1	14.6	3.104	*	1230	17.0	16.1	3.003	*

**********SAMPLES 98 SAMPLES**********

META-GABBROIC ROCKS UNIT 11-6

NUMBER	EAST	NORTH	DENSITY		NUMBER	EAST	NORTH	DENSITY	
949	23.5	9.8	3.017	*	1523	24.6	17.1	2.994	*
476	22.0	10.4	3.029	*	916	22.8	12.4	3.027	*
1513	23.3	18.6	2.962	*	552	23.3	7.1	3.016	*
948	23.1	9.5	3.079	*	1394	17.2	17.8	3.029	*
1380	16.8	21.2	2.857	*					

**********SAMPLES 9 SAMPLES**********

PYROXENITE , PERIDOTITE
DERIVED SERPENTINE AND TALC-MAGNESITE ROCKS , UNIT 12

NUMBER	EAST	NORTH	DENSITY		NUMBER	EAST	NORTH	DENSITY	
1295	7.3	13.3	2.953	*	774	4.1	21.8	2.844	*
411	10.4	10.0	2.865	*	1276	8.5	17.2	2.671	*

**********SAMPLES 4 SAMPLES**********

SERPENTINITE , UNIT 12

NUMBER	EAST	NORTH	DENSITY		NUMBER	EAST	NORTH	DENSITY	
1053	9.6	1.9	2.673	*	1326	10.0	6.6	2.632	*
1280	7.3	17.3	2.657	*	1290	7.2	15.5	2.615	*
1062	9.6	2.9	2.660	*	1264	6.8	18.5	2.635	*
1266	6.7	18.6	2.729	*	1281	7.3	16.9	2.655	*
380	9.4	0.6	2.645	*	363	8.8	0.5	2.912	*
1293	7.2	14.3	2.663	*	376	9.6	-0.5	2.700	*
1284	7.5	16.7	2.749	*	1289	7.2	15.6	2.843	*
375	9.6	-1.0	2.671	*	1262	6.9	18.3	2.699	*
1058	9.7	4.4	2.677	*	378	9.3	0.1	2.683	*
1263	6.9	18.4	2.912	*	345	11.2	5.7	2.790	*
1059	9.8	3.5	2.735	*	410	10.1	9.9	3.007	*
374	9.6	-1.8	2.668	*	1054	9.6	1.2	2.805	*
320	9.8	2.9	2.786	*					

**********SAMPLES 25 SAMPLES**********

META-PEROXENITES AND PERIDOTITES , UNIT 12

NUMBER	EAST	NORTH	DENSITY		NUMBER	EAST	NORTH	DENSITY	
342	9.7	5.3	3.003	*	340	9.7	4.9	2.900	*
1312	10.1	8.5	3.038	*	353	9.7	4.3	2.976	*
1318	10.2	8.2	3.022	*					

**********SAMPLES 5 SAMPLES**********

'QUARTZ-EYE' DIORITE , UNIT 13

NUMBER	EAST	NORTH	DENSITY		NUMBER	EAST	NORTH	DENSITY	
76	2.2	16.7	2.682	*	74	2.9	16.8	2.712	*
632	5.4	2.2	2.685	*	75	2.7	16.9	2.671	*
333	7.3	1.2	2.673	*	625	4.4	2.8	3.233	*
582	4.5	4.2	2.721	*	630	4.6	2.1	2.712	*

NUMBER	EAST	NORTH	DENSITY		NUMBER	EAST	NORTH	DENSITY	
610	4.5	3.5	2.692	*	1068	7.1	2.0	2.700	*
633	5.7	2.2	2.726	*	620	5.9	2.7	2.745	*
173	4.3	3.5	2.659	*	621	5.4	2.7	2.691	*
623	4.8	2.7	2.684	*	47	5.1	-0.1	2.737	*
641	4.9	1.5	2.728	*	631	5.0	2.2	2.696	*
73	2.4	16.2	2.693	*	330	9.2	2.6	2.785	*
611	4.8	3.5	2.672	*	583	4.8	4.2	2.730	*
46	5.7	0.5	2.696	*	622	5.1	2.7	2.718	*

**********SAMPLES 24 SAMPLES**********

BIOTITE GRANODIORITE , UNIT 14-A

NUMBER	EAST	NORTH	DENSITY		NUMBER	EAST	NORTH	DENSITY	
1085	12.7	7.2	2.663	*	234	9.2	24.6	2.642	*
1131	13.3	10.3	2.663	*	304	11.0	16.5	2.671	*
799	13.0	7.8	2.625	*	961	12.1	18.4	2.645	*
286	9.9	19.2	2.686	*	786	9.0	20.4	2.688	*
714	4.5	25.7	2.674	*	753	12.0	19.6	2.675	*
206	8.3	24.4	2.638	*	952	9.5	17.7	2.723	*
1023	11.5	15.3	2.662	*	977	10.5	16.2	2.664	*
1026	11.9	14.6	2.663	*	668	13.3	19.7	2.686	*
712	4.9	26.3	2.679	*	254	11.0	22.8	2.669	*
255	10.8	22.3	2.670	*	1223	14.8	16.6	2.682	*
978	3.4	22.7	2.671	*	984	5.0	24.2	2.685	*
1024	11.9	15.4	2.667	*	695	15.3	19.3	2.688	*
716	4.0	25.0	2.700	*	221	10.8	20.9	2.661	*
264	9.1	21.3	2.682	*	218	11.4	22.3	2.668	*
228	12.1	21.5	2.685	*	1025	11.9	15.0	2.660	*
757	12.8	21.3	2.663	*	715	4.3	25.3	2.673	*
245	9.3	23.3	2.679	*	237	8.4	23.6	2.665	*
953	9.9	17.9	2.673	*	955	10.4	18.4	2.653	*
1022	11.0	15.0	2.678	*	1130	12.9	10.3	2.668	*
713	4.7	26.0	2.781	*	737	5.6	24.0	2.693	*
305	10.8	16.3	2.672	*	1274	8.4	18.5	2.704	*
976	10.1	16.2	2.673	*	830	15.6	14.6	2.694	*
685	3.5	26.4	2.659	*	741	6.7	24.9	2.666	*
235	8.9	24.3	2.686	*	263	8.9	21.1	2.689	*
287	10.2	19.4	2.659	*	954	10.0	18.1	2.664	*
669	12.9	19.4	2.687	*	733	6.3	25.5	2.728	*
253	11.2	23.1	2.684	*	750	12.8	20.4	2.676	*
755	12.0	20.6	2.674	*	767	7.9	22.4	2.682	*
213	7.5	24.6	2.680	*	285	9.5	18.8	2.633	*
293	9.9	19.9	2.657	*	1248	13.2	15.0	2.671	*
1027	11.4	14.3	2.669	*	261	6.9	20.3	2.667	*
1246	13.4	14.6	2.682	*	1249	13.5	15.3	2.661	*
448	14.7	13.3	2.670	*	271	10.6	23.7	2.691	*
489	13.9	10.7	2.669	*	684	3.8	26.0	2.662	*
699	14.1	18.2	2.707	*	734	6.2	25.2	2.667	*
1247	12.9	14.6	2.662	*	1251	14.1	15.9	2.682	*

NUMBER	EAST	NORTH	DENSITY		NUMBER	EAST	NORTH	DENSITY	
1116	13.2	12.4	2.685	*	1121	11.1	11.4	2.689	*
756	12.5	21.0	2.661	*	832	15.3	15.1	2.664	*
1115	13.5	12.5	2.684	*	749	13.2	20.6	2.671	*
246	9.5	23.5	2.693	*	247	9.8	23.9	2.694	*
1117	16.8	12.2	2.699	*	1132	13.8	10.4	2.685	*
751	12.6	19.9	2.680	*	686	3.2	26.7	2.680	*
687	3.0	27.0	2.686	*	722	5.3	25.2	2.666	*
723	5.5	25.5	2.677	*	1084	12.3	7.2	2.663	*
236	8.7	23.9	2.657	*	262	9.2	20.7	2.655	*
748	13.4	20.8	2.685	*	528	13.2	16.0	2.670	*
1095	12.1	6.4	2.656	*	295	9.1	19.4	2.725	*
720	4.6	24.6	2.724	*	227	11.8	21.2	2.641	*
752	12.3	19.7	2.660	*	732	6.5	25.7	2.673	*
1094	12.5	6.5	2.674	*	1109	12.4	11.0	2.744	*
229	12.5	21.8	2.748	*	724	5.6	25.9	2.681	*
202	11.8	22.6	2.588	*	1133	14.2	10.4	2.635	*

**********SAMPLES 104 SAMPLES**********

PORPHYRITIC MICROCLINE GRANODIORITE , UNIT 14-E

NUMBER	EAST	NORTH	DENSITY		NUMBER	EAST	NORTH	DENSITY	
265	9.4	21.6	2.679	*	244	8.9	22.6	2.667	*
962	11.8	18.2	2.650	*	220	11.0	21.4	2.672	*
210	7.6	23.2	2.671	*	671	12.4	18.7	2.645	*
291	10.7	20.6	2.631	*	301	12.0	17.2	2.673	*
289	10.9	20.2	2.646	*	672	13.0	18.6	2.677	*
211	7.2	23.8	2.660	*	238	8.3	23.3	2.676	*
239	8.2	23.0	2.666	*	300	12.3	17.4	2.646	*
958	11.5	19.3	2.639	*	537	13.3	16.7	2.665	*
258	10.1	21.3	2.651	*	288	10.5	19.7	2.651	*
299	12.6	17.6	2.640	*	963	11.5	18.0	2.658	*
222	10.7	20.7	2.637	*	957	11.2	19.1	2.663	*
209	7.7	23.3	2.668	*	257	10.4	21.7	2.668	*
259	10.0	21.0	2.646	*	267	9.8	22.3	2.652	*
960	12.2	18.7	2.667	*	266	9.6	22.0	2.653	*
766	7.7	22.3	2.679	*	956	10.9	18.8	2.668	*
959	11.9	19.0	2.651	*	535	12.6	16.6	2.661	*
223	11.0	20.4	2.648	*	224	11.5	20.0	2.648	*
225	11.7	20.4	2.653	*	212	7.3	24.2	2.679	*
303	11.4	16.7	2.667	*	536	12.9	16.6	2.657	*
208	7.9	23.7	2.678	*	226	12.0	20.8	2.671	*
240	8.1	22.8	2.689	*	219	11.2	21.9	2.657	*
242	8.4	22.3	2.683	*	768	8.8	22.1	2.677	*
770	8.1	21.9	2.680	*	534	12.3	16.3	2.687	*
673	13.5	18.6	2.680	*	268	10.0	22.6	2.666	*
290	11.0	20.3	2.653	*	965	10.8	17.5	2.678	*
702	13.7	17.2	2.676	*	256	10.6	22.0	2.666	*
260	9.7	20.5	2.661	*	302	11.7	16.9	2.664	*
674	13.7	19.0	2.681	*	700	13.9	18.0	2.693	*

NUMBER	EAST	NORTH	DENSITY		NUMBER	EAST	NORTH	DENSITY	
670	12.5	19.2	2.660	*	738	6.2	23.8	2.662	*
243	8.7	22.4	2.685	*	292	10.6	20.4	2.651	*
998	6.5	23.4	2.670	*	533	12.1	16.1	2.684	*
207	8.2	24.1	2.672	*	721	5.2	24.8	2.670	*
667	13.6	20.0	2.686	*	739	6.4	24.2	2.668	*
241	8.3	22.5	2.674	*	1250	13.8	15.7	2.673	*
964	11.1	17.8	2.667	*	529	12.8	15.8	2.680	*
527	13.5	16.3	2.683	*	682	4.4	26.5	2.678	*
736	5.8	24.3	2.667	*	769	8.5	22.0	2.824	*
530	12.5	15.6	2.676	*	531	12.3	15.7	2.669	*
701	13.5	17.7	2.687	*	735	5.9	24.7	2.682	*
683	4.1	26.2	2.669	*	740	6.6	24.6	2.679	*
269	10.2	22.9	2.676	*	703	14.2	17.3	2.676	*
532	12.0	15.7	2.673	*					

**********SAMPLES 83 SAMPLES**********

CONTAMINATED BORDER ZONE , REYNARD LAKE PLUTON , UNIT 14-F

NUMBER	EAST	NORTH	DENSITY		NUMBER	EAST	NORTH	DENSITY	
711	5.1	26.8	2.766	*	689	3.7	27.2	2.665	*
681	4.8	26.8	2.797	*	691	4.4	27.3	2.784	*
725	5.7	26.3	2.858	*	727	5.9	26.9	2.682	*
785	8.7	20.7	2.724	*	985	5.5	23.8	2.709	*
201	11.9	22.8	2.714	*	834	15.3	14.1	2.730	*
729	7.1	26.3	2.687	*	308	9.9	15.2	2.727	*
1216	15.7	17.5	2.706	*	678	15.1	20.2	2.698	*
232	9.6	25.3	2.685	*	828	15.8	13.7	2.715	*
488	14.3	10.7	2.687	*	690	4.1	27.3	2.660	*
272	10.8	24.1	2.733	*	745	14.1	21.3	2.699	*
680	5.1	27.0	2.695	*	664	14.4	20.8	2.693	*
831	15.6	14.9	2.673	*	487	14.5	10.6	2.690	*
974	9.4	16.3	2.708	*	1232	16.3	15.5	2.739	*
981	4.3	23.9	2.714	*	708	15.7	18.4	2.716	*
835	15.5	13.7	2.704	*	754	11.9	20.1	2.703	*
782	7.4	20.9	2.685	*	383	11.2	13.3	2.707	*
1227	15.6	16.2	2.849	*	1118	12.4	12.1	2.871	*
250	10.1	25.0	2.709	*	217	8.2	25.8	2.688	*
758	13.1	21.5	2.729	*	445	13.9	13.4	2.675	*
1020	10.1	14.5	2.775	*	983	4.6	24.3	2.531	*
579	9.4	14.9	2.931	*	731	6.7	26.0	2.724	*
393	13.0	13.1	2.742	*	665	14.2	20.5	2.763	*
829	15.7	14.0	2.716	*	385	11.8	13.6	2.779	*
441	14.7	12.4	2.683	*	719	4.1	24.7	2.741	*
1273	7.9	18.8	3.041	*	788	8.4	19.9	2.742	*
395	12.4	12.8	2.879	*	396	12.0	12.9	2.774	*
1107	11.6	10.6	2.805	*	1114	13.7	11.9	2.839	*
1127	11.7	10.2	2.799	*	273	11.0	24.4	2.699	*
692	4.9	27.5	2.811	*	707	15.5	18.2	2.779	*
975	9.7	16.3	2.766	*	726	5.9	26.8	2.754	*

NUMBER	EAST	NORTH	DENSITY		NUMBER	EAST	NORTH	DENSITY	
747	13.5	20.8	2.761	*	1008	7.9	19.9	2.729	*
864	16.6	12.9	2.864	*	1218	16.4	17.1	2.736	*
251	11.7	23.6	2.689	*	866	16.7	12.2	2.877	*
1213	14.6	17.1	2.854	*	1000	6.5	22.5	2.848	*
1011	7.8	20.4	2.701	*	215	7.9	25.3	2.772	*
951	9.3	17.5	2.751	*	675	14.1	19.4	2.785	*
710	5.3	27.1	2.844	*	248	9.9	24.4	2.826	*
787	8.7	20.1	2.832	*	384	11.5	13.5	2.878	*
1215	15.3	17.3	2.856	*	1120	11.6	11.7	2.918	*
1194	16.1	14.0	2.869	*	865	16.7	12.5	2.876	*
982	4.4	24.2	2.867	*	999	6.9	22.6	2.829	*
1108	12.0	10.8	2.985	*	297	8.5	18.9	2.843	*
1195	16.1	13.8	2.819	*	1219	16.0	16.9	2.781	*
743	7.2	25.7	2.870	*	233	9.4	25.0	2.841	*
306	10.5	15.8	2.775	*	205	8.6	24.9	2.860	*
387	12.5	14.1	2.696	*	1192	16.1	14.6	2.926	*
996	6.0	22.9	2.862	*	580	9.4	14.2	2.816	*
789	8.1	19.6	2.731	*	1239	14.4	15.4	2.800	*
1242	15.0	14.4	2.798	*	1245	13.8	14.5	2.801	*
995	5.7	22.7	2.822	*	1010	8.1	20.5	2.850	*
1119	11.9	11.8	2.868	*	742	6.9	25.3	2.934	*
231	12.9	22.2	2.720	*	783	7.8	21.0	2.920	*
1221	15.3	16.8	2.874	*	986	5.3	23.4	2.893	*
706	15.2	18.0	2.945	*	307	10.0	15.5	2.818	*
1226	15.2	16.2	2.855	*	997	6.3	23.2	2.837	*
204	8.7	25.2	2.851	*	284	9.3	18.6	2.894	*
386	12.2	13.8	2.833	*	1021	10.6	14.8	2.853	*
697	14.8	18.8	2.819	*	837	15.6	12.6	2.865	*
827	15.9	13.4	2.807	*	391	13.4	13.6	2.908	*
1233	15.9	15.5	2.872	*	283	8.9	18.3	2.835	*
382	10.8	13.1	3.012	*	773	7.1	21.7	2.762	*
390	13.3	14.0	2.737	*	446	13.9	13.6	2.870	*
1212	14.3	17.0	2.850	*	1396	16.6	17.3	2.864	*
966	9.9	15.2	2.801	*	730	6.9	26.2	2.876	*
443	14.0	12.6	2.769	*	444	13.9	13.0	2.859	*
1241	14.8	14.8	2.819	*	696	15.0	19.0	2.926	*
1009	8.0	20.2	2.859	*	705	14.8	17.7	2.866	*
765	7.3	22.0	2.856	*	398	11.3	12.4	2.844	*
1236	14.7	15.7	2.889	*	1238	14.2	15.8	2.829	*
666	13.8	20.2	2.761	*	394	12.7	12.9	2.748	*
449	15.1	13.2	2.865	*	1193	16.1	14.3	2.814	*
1220	15.7	16.9	2.941	*	1240	14.6	15.1	2.839	*
950	8.7	17.4	2.798	*	704	14.6	17.5	2.849	*
709	16.1	18.7	2.871	*	249	10.0	24.7	2.836	*
392	13.4	13.3	2.900	*	1243	14.6	14.4	2.902	*
1275	8.6	18.6	2.799	*	967	9.6	15.3	2.892	*
688	3.3	27.1	2.815	*	718	3.7	24.5	2.855	*
784	8.2	21.1	2.774	*	694	15.8	19.6	2.847	*
230	12.7	22.0	2.818	*	1237	14.3	15.9	2.816	*
677	14.9	20.0	2.832	*	252	11.4	23.4	2.928	*
1244	14.2	14.5	2.865	*	214	7.7	25.0	2.898	*
309	9.6	14.9	2.856	*	388	12.8	14.2	2.840	*
746	13.8	21.2	2.845	*	1222	14.8	16.7	2.873	*
1235	15.2	15.5	2.828	*	1128	12.1	10.2	2.778	*

NUMBER	EAST	NORTH	DENSITY		NUMBER	EAST	NORTH	DENSITY	
389	13.1	14.4	2.825	*	1234	15.5	15.5	2.890	*
698	14.4	18.5	2.845	*	744	7.4	26.0	2.968	*
824	16.5	12.2	2.876	*	826	16.0	12.9	2.867	*
397	11.5	12.5	2.841	*	442	14.3	12.5	2.942	*
216	8.0	25.5	2.806	*	296	8.8	19.2	2.771	*
759	13.4	21.8	2.855	*	676	14.6	19.7	2.800	*
863	16.6	13.3	2.898	*	771	7.8	21.8	2.862	*
772	7.5	21.7	2.839	*	825	16.2	12.6	2.928	*
833	15.3	14.6	2.892	*	447	14.3	13.5	2.864	*
1196	16.4	13.8	2.830	*	717	3.9	24.8	2.868	*
200	12.3	23.0	2.883	*	836	15.4	13.2	2.872	*
1224	14.3	16.2	2.737	*	203	8.9	25.5	2.657	*
1225	14.8	16.2	2.868	*	764	6.9	21.8	2.875	*
1214	14.9	17.2	2.923	*	838	15.7	12.4	2.865	*
1028	11.0	14.1	2.839	*					

**********SAMPLES 197 SAMPLES**********

HORNBLENDE GRANODIORITE AND MAFIC RICH VARIENT
ANNABEL LAKE PLUTON ONLY , UNIT 14-B-2

NUMBER	EAST	NORTH	DENSITY		NUMBER	EAST	NORTH	DENSITY	
1605	13.7	22.7	2.729	*	1625	14.1	21.9	2.749	*
1606	14.1	22.7	2.778	*	1624	14.5	21.9	2.751	*
1466	16.1	21.4	2.731	*	1613	16.8	22.9	2.752	*
1465	15.7	21.2	2.743	*	1609	15.3	22.7	2.776	*
1619	16.3	22.2	2.732	*	1610	15.6	22.8	2.921	*
1612	16.4	22.9	2.776	*	1611	16.0	22.8	2.805	*
1623	14.9	21.9	2.822	*	1621	15.7	22.0	2.834	*
1618	16.7	22.4	2.760	*	1608	14.9	22.7	2.718	*
1622	15.3	21.9	2.854	*	1607	14.5	22.7	2.864	*
1467	16.4	21.5	2.851	*	1468	16.8	21.6	2.787	*
1620	16.0	22.1	2.881	*					

**********SAMPLES 21 SAMPLES**********

HORNBLENDE GRANODIORITE AND MAFIC RICH VARIENTS , UNIT 14-B-1
QUARTZ DIORITE , UNIT 14-D-1 , MYSTIC LAKE PLUTON ONLY

NUMBER	EAST	NORTH	DENSITY		NUMBER	EAST	NORTH	DENSITY	
852	20.1	11.2	2.705	*	847	19.9	11.8	2.657	*
461	18.8	13.5	2.870	*	457	19.7	13.2	2.704	*
1164	20.7	18.2	2.680	*	1163	20.8	18.4	2.703	*
1172	21.0	17.7	2.736	*	1165	20.6	17.9	2.711	*
1166	20.3	18.2	2.687	*	1173	20.6	17.7	2.715	*
1160	20.3	18.9	2.721	*	853	19.7	11.2	2.696	*
919	21.7	12.2	2.861	*	464	18.3	12.6	3.002	*
908	22.0	4.0	2.704	*	1100	14.4	0.7	2.866	*

NUMBER	EAST	NORTH	DENSITY		NUMBER	EAST	NORTH	DENSITY	
500	16.2	3.6	2.724	*	817	19.6	15.3	2.708	*
456	19.4	13.0	2.723	*	895	17.2	5.1	2.761	*
1101	14.9	1.4	2.737	*	472	20.3	9.8	2.731	*
846	19.8	11.8	2.723	*	907	22.3	4.3	2.707	*
910	21.2	3.6	2.734	*	939	19.7	7.9	2.799	*
909	21.6	3.6	2.725	*	942	20.8	8.4	2.777	*
1206	20.9	5.5	2.768	*	890	20.3	7.1	2.765	*
915	17.0	4.2	2.805	*	936	21.0	7.5	2.770	*
811	19.4	16.3	2.828	*	1183	21.6	17.1	2.686	*
845	19.4	12.0	2.721	*	850	20.7	11.5	2.723	*
899	19.3	4.7	2.755	*	1572	21.5	11.6	2.838	*
545	21.4	6.7	2.724	*	891	20.0	7.3	2.747	*
944	21.4	8.7	2.737	*	1207	20.9	5.2	2.777	*
892	19.6	7.5	2.767	*	937	20.7	7.4	2.713	*
1102	14.4	1.4	2.713	*	848	20.3	11.7	2.747	*
1038	14.7	3.4	2.910	*	1103	14.0	1.5	2.747	*
843	19.0	12.0	2.794	*	844	19.3	12.1	2.883	*
1210	19.4	5.1	2.749	*	550	22.8	6.5	2.786	*
894	19.1	7.5	2.733	*	898	18.9	4.7	2.761	*
914	17.3	4.1	2.753	*	459	19.4	13.8	2.724	*
1203	20.5	6.3	2.741	*	546	21.7	6.1	2.726	*
882	19.1	8.1	2.733	*	896	17.3	4.6	2.759	*
900	19.8	4.7	2.763	*	913	18.6	3.9	2.754	*
1201	19.7	6.0	2.767	*	1566	22.6	13.2	2.742	*
1034	13.9	2.1	2.765	*	452	18.3	12.1	3.005	*
873	19.1	8.9	2.732	*	884	18.3	8.1	2.718	*
912	18.8	3.9	2.761	*	454	18.9	12.6	2.813	*
1099	14.0	0.7	2.720	*	887	19.5	6.8	2.750	*
893	19.3	7.7	2.786	*	814	18.4	15.3	2.863	*
428	19.0	14.6	2.818	*	877	20.8	8.8	2.737	*
889	20.0	7.0	2.738	*	943	21.1	8.5	2.737	*
523	17.8	11.1	2.868	*	904	21.2	4.4	2.744	*
810	20.0	16.3	2.767	*	482	19.0	10.8	2.772	*
1205	20.9	5.9	2.785	*	888	19.8	6.9	2.776	*
923	20.5	13.5	2.738	*	548	22.4	6.0	2.743	*
875	20.0	8.9	2.757	*	901	20.1	4.6	2.756	*
941	20.4	8.2	2.740	*	432	19.0	14.2	2.845	*
881	19.3	8.5	2.743	*	473	20.8	9.8	2.769	*
496	15.2	3.6	2.838	*	869	17.6	9.0	2.790	*
874	19.6	8.9	2.759	*	886	17.0	8.3	2.773	*
460	19.1	13.9	2.771	*	1567	22.1	13.2	2.755	*
876	20.4	8.8	2.763	*	878	20.7	8.6	2.749	*
902	20.5	4.4	2.745	*	809	20.4	16.4	2.812	*
815	18.8	15.3	2.790	*	427	18.9	14.8	2.816	*
1208	20.5	5.2	2.764	*	544	21.8	7.0	2.720	*
1204	21.0	6.2	2.813	*	1209	19.9	5.3	2.770	*
543	22.2	7.2	2.792	*	849	21.1	11.5	2.730	*
867	17.2	9.1	2.804	*	474	21.2	9.8	2.794	*
547	22.1	6.0	2.725	*	549	22.8	6.0	2.740	*
897	17.7	4.6	2.762	*	935	21.4	7.8	2.790	*
458	19.6	13.6	2.721	*	906	22.0	4.3	2.745	*
542	22.4	7.3	2.763	*	934	21.7	8.0	2.783	*
818	19.9	15.5	2.780	*	920	20.6	12.4	2.774	*
938	20.1	7.7	2.732	*	1568	20.9	12.8	2.732	*

NUMBER	EAST	NORTH	DENSITY		NUMBER	EAST	NORTH	DENSITY	
1570	21.6	12.6	2.747	*	502	15.5	3.6	2.880	*
485	18.1	11.2	3.019	*	879	20.2	8.5	2.727	*
808	20.8	16.4	2.870	*	911	19.3	3.9	2.805	*
940	20.1	8.0	2.735	*	870	17.9	9.0	2.857	*
480	20.2	10.6	2.831	*	1180	20.1	17.0	2.841	*
478	21.1	10.5	2.792	*	481	19.6	10.7	2.777	*
1202	20.0	6.2	2.738	*	1035	14.6	2.2	2.838	*
883	18.7	8.1	2.838	*	501	15.8	3.6	2.883	*
903	20.9	4.4	2.766	*	816	19.0	15.3	2.826	*
1181	20.5	17.1	2.847	*	905	21.5	4.3	2.687	*
933	22.1	8.2	2.841	*	812	18.8	16.2	2.907	*
1036	15.3	2.9	2.722	*	851	20.4	11.1	2.985	*
426	19.5	14.7	2.674	*	1179	19.7	17.0	2.868	*
1569	21.3	12.7	2.788	*	872	18.8	8.9	2.886	*
880	19.8	8.4	2.749	*	921	19.9	12.4	2.810	*
471	20.0	9.8	2.791	*	1037	14.9	3.2	3.086	*
854	19.2	11.2	2.890	*	922	20.4	12.9	2.772	*
479	20.7	10.6	2.789	*	497	14.9	3.5	3.016	*
499	15.7	3.3	2.931	*	932	22.4	8.3	2.897	*
871	18.4	9.0	2.885	*	470	19.4	9.8	2.905	*
885	17.2	8.2	2.804	*	813	18.5	16.2	2.843	*
498	14.7	2.8	2.898	*	468	18.3	9.9	2.876	*
484	18.3	10.9	2.903	*	1571	21.2	12.1	2.901	*
455	19.1	12.8	2.947	*	918	21.9	12.1	2.934	*
469	18.9	9.8	3.012	*	1161	20.7	18.9	2.918	*
1211	17.3	5.1	2.813	*	1162	20.9	18.8	2.919	*

**********SAMPLES 176 SAMPLES**********

BOUNDARY INTRUSION
INTERMEDIATE , BASIC , AND ULTRABASIC DIKE ROCKS , UNIT 17

NUMBER	EAST	NORTH	DENSITY		NUMBER	EAST	NORTH	DENSITY	
1489	21.9	20.2	2.957	*	1457	21.5	21.2	2.891	*
1553	22.1	19.5	3.061	*	1461	21.0	21.9	2.860	*
1486	21.9	20.5	3.111	*	1505	22.4	19.2	2.838	*
1508	22.9	17.8	2.868	*	1488	21.6	19.9	2.966	*
1487	21.5	20.5	2.955	*	1462	21.3	22.1	3.058	*

**********SAMPLES 10 SAMPLES**********

PORPHYRITIC MICROCLINE GRANITE , PHANTOM LAKE BODY , UNIT 18

NUMBER	EAST	NORTH	DENSITY		NUMBER	EAST	NORTH	DENSITY	
1511	23.0	17.1	2.671	*	1512	23.5	17.0	2.691	*
1531	22.0	16.0	2.632	*	1533	22.1	15.5	2.646	*
422	20.9	14.8	2.649	*	803	22.7	16.7	2.646	*
1184	21.8	17.1	2.675	*	927	21.8	13.3	2.650	*
1530	22.3	16.1	2.647	*	433	19.9	14.1	2.662	*
926	21.4	13.4	2.611	*	924	20.6	13.5	2.675	*
436	21.1	14.1	2.646	*	1535	21.9	14.6	2.664	*
437	21.6	14.1	2.657	*	1532	21.8	15.5	2.695	*
1534	21.9	15.1	2.663	*	806	21.3	16.4	2.656	*
1185	22.2	17.1	2.689	*	1186	22.6	17.2	2.665	*
820	20.5	15.5	2.656	*	822	21.1	15.7	2.652	*
421	21.4	14.8	2.668	*	821	20.7	15.6	2.645	*
804	22.3	16.5	2.648	*	435	20.6	14.1	2.655	*
1510	22.7	17.2	2.667	*	424	20.1	14.8	2.652	*
425	19.8	14.8	2.383	*	434	20.3	14.1	2.650	*
805	21.6	16.5	2.647	*	819	20.1	15.5	2.655	*
925	21.0	13.5	2.641	*	823	21.3	15.7	2.650	*
423	20.5	14.8	2.642	*					

**********SAMPLES 44 SAMPLES**********

**********SAMPLES 1586 SAMPLES**********

G R A V I T Y D A T A L I S T I N G

100 S T A T I O N S

COORDINATES IN UNITS OF 1/2 MILE EAST AND NORTH OF ORIGIN

STATION	EAST	NORTH	ELEV	BOUG	STATION	EAST	NORTH	ELEV	BOUG
4078	1.44	16.15	970.8	-30.62*	4139	1.48	3.08	969.8	-23.73
4076	1.50	16.71	969.8	-30.51*	4085	1.50	14.72	970.3	-29.65
4690	1.55	10.52	974.2	-31.78*	4080	1.58	15.41	972.8	-30.11
4693	1.68	12.42	973.7	-31.26*	4128	1.73	5.62	970.8	-27.05
4613	1.73	14.30	974.2	-29.43*	4601	1.75	15.10	977.2	-29.55
4086	1.75	14.21	969.8	-29.83*	4064	1.82	20.50	970.8	-32.41
4074	1.83	17.23	969.8	-30.67*	4063	1.88	20.83	971.3	-31.92
4135	1.89	4.58	970.3	-24.80*	4084	1.90	15.00	970.3	-29.83
1209565	1.92	26.40	1094.0	-39.80*	4081	1.93	15.80	969.8	-30.19
4121	1.94	6.96	969.8	-28.84*	4140	2.01	2.53	969.8	-22.40
4071	2.05	18.49	969.8	-31.26*	4065	2.09	20.21	970.3	-31.63
4068	2.14	19.30	970.8	-31.09*	4062	2.15	20.61	969.8	-31.04
4082	2.15	16.10	969.8	-30.47*	4066	2.18	19.97	970.3	-31.23
4075	2.19	16.90	970.8	-30.85*	4087	2.19	14.50	971.8	-29.25
4089	2.25	15.14	970.8	-29.79*	4072	2.27	17.99	970.3	-30.49
4073	2.30	17.49	970.3	-30.44*	4105	2.31	10.90	970.3	-30.30
2030	2.33	1.00	984.8	-19.83*	4119	2.40	8.50	970.8	-27.95
4136	2.40	5.50	971.8	-24.89*	4067	2.41	19.68	970.8	-30.61
4122	2.41	6.50	970.3	-26.35*	4090	2.42	15.47	970.3	-29.69
4069	2.42	18.96	969.8	-30.38*	4061	2.45	20.19	970.8	-30.31
4106	2.45	10.02	970.8	-29.62*	4070	2.48	18.49	970.8	-30.10
4104	2.51	11.85	971.3	-30.02*	4088	2.52	14.78	970.8	-28.34
4138	2.52	4.26	971.3	-23.56*	4120	2.60	7.98	972.8	-27.12
4055	2.64	18.21	970.3	-29.26*	4083	2.65	16.41	971.3	-30.56
4695	2.65	10.88	973.7	-29.32*	2029	2.65	1.38	998.8	-19.22
4054	2.66	17.80	970.8	-29.49*	4097	2.68	13.93	971.3	-28.38
4694	2.72	11.70	974.2	-28.79*	4060	2.78	19.88	969.8	-29.24
4058	2.80	18.95	970.3	-27.87*	4141	2.80	1.99	971.3	-20.34
4123	2.82	5.90	969.8	-24.79*	4124	2.83	7.18	971.8	-25.60
4099	2.85	12.98	971.8	-28.27*	4091	2.87	15.82	969.8	-29.04
4098	2.88	13.40	974.8	-28.42*	4137	2.88	4.70	969.8	-23.70
4142	2.88	2.92	972.8	-21.85*	4093	2.89	15.06	970.8	-28.48
4057	2.92	18.60	970.3	-27.62*	4053	2.94	17.42	970.3	-29.55
4052	2.95	17.00	970.3	-30.24*	2028	2.95	1.72	1010.7	-19.26
4095	2.99	14.67	970.3	-27.67*	4118	2.99	8.62	969.8	-26.75
4107	3.03	9.69	971.8	-27.16*	4059	3.07	19.40	969.8	-28.35
4103	3.10	12.13	970.3	-28.03*	4144	3.10	3.65	969.8	-22.42
4056	3.12	18.02	970.8	-29.04*	5004	3.20	22.60	974.4	-32.22
4092	3.22	15.59	970.3	-28.20*	5003	3.25	21.91	977.4	-31.04
2027	3.27	2.10	1019.9	-19.03*	4042	3.30	18.94	971.8	-28.56
4094	3.31	14.98	970.8	-27.31*	4051	3.37	16.49	969.8	-28.66
4049	3.38	21.10	970.3	-29.69*	4096	3.38	14.22	969.8	-27.25
5005	3.40	22.70	975.4	-31.71*	4125	3.44	7.29	969.8	-24.59
4048	3.49	20.53	970.3	-28.23*	4102	3.51	11.83	970.3	-26.96
4026	3.53	15.37	970.8	-26.96*	905965	3.56	18.60	974.0	-28.30
4108	3.58	10.85	969.8	-26.51*	4041	3.59	18.62	970.8	-28.11
5006	3.59	22.28	974.4	-31.10*	4024	3.60	15.90	969.8	-27.61
4043	3.61	19.24	969.8	-27.54*	4029	3.62	14.26	969.8	-26.72
5002	3.62	21.82	973.9	-30.72*	2026	3.62	2.43	1031.6	-19.17
4032	3.67	13.05	969.8	-26.58*	5001	3.68	21.41	974.9	-30.27

G R A V I T Y D A T A L I S T I N G

100 S T A T I C N S

COORDINATES IN UNITS OF 1/2 MILE EAST AND NORTH OF ORIGIN

STATION	EAST	NORTH	ELEV BOUG	STATION	EAST	NORTH	ELEV BOUG
4028	3.71	14.56	969.8-26.47*	4050	3.71	17.00	969.8-28.36
4115	3.71	8.75	971.3-25.17*	4030	3.74	13.78	971.8-26.42
4143	3.78	3.47	970.8-21.66*	4023	3.79	16.30	970.8-27.80
4045	3.79	19.52	970.3-27.69*	4116	3.79	9.61	970.8-25.41
4040	3.81	18.50	970.3-27.68*	4147	3.82	4.82	972.8-22.59
4047	3.87	20.18	970.3-27.50*	4127	3.89	6.05	969.7-22.62
4027	3.90	14.93	971.3-26.36*	4031	3.90	13.44	969.8-26.27
5007	3.90	22.02	973.9-29.48*	2025	3.94	2.79	979.2-20.48
4044	3.96	19.12	972.3-27.36*	5020	3.98	21.21	975.4-29.31
4126	4.11	6.92	971.8-22.71*	4113	4.12	7.97	970.8-23.58
4033	4.14	12.78	969.8-25.81*	4038	4.15	17.77	969.8-27.51
4046	4.17	19.81	970.3-27.02*	4101	4.18	11.92	970.8-25.14
4037	4.20	17.40	970.3-27.67*	4114	4.20	8.74	970.3-23.41
5019	4.20	20.71	975.9-27.99*	4025	4.21	15.80	969.8-26.87
5008	4.21	21.78	978.9-28.61*	4039	4.28	18.18	969.8-27.13
4117	4.28	10.70	970.8-24.38*	4014	4.30	14.96	970.3-26.14
5018	4.30	20.12	974.9-27.19*	4013	4.32	14.31	969.8-25.63
2024	4.35	3.01	988.0-22.02*	4022	4.38	16.11	970.3-27.08
5009	4.41	21.50	974.4-28.22*	4036	4.43	16.93	972.8-27.19
4148	4.44	5.19	969.8-21.43*	4146	4.47	4.26	969.8-21.76
4035	4.48	12.97	970.8-24.70*	4021	4.54	16.58	970.3-27.86
5016	4.56	19.77	974.9-26.67*	4012	4.60	13.82	970.8-25.02
4100	4.61	11.88	971.3-23.42*	4145	4.61	3.79	969.8-22.17
4034	4.62	12.48	969.8-24.27*	5010	4.62	21.09	975.9-27.63
5015	4.62	20.35	974.4-27.23*	4015	4.63	15.21	970.8-26.07
5017	4.64	19.33	977.4-26.38*	4149	4.69	5.98	971.3-21.59
4110	4.74	9.82	970.3-22.91*	2023	4.74	3.37	1005.9-22.28
5011	4.75	21.53	976.4-27.92*	4109	4.77	10.73	970.3-23.06
4112	4.80	7.95	970.8-22.52*	4008	4.83	13.26	971.8-24.55
4020	4.83	16.28	970.8-26.62*	4111	4.83	8.90	970.8-22.58
2020	4.84	4.73	1046.5-19.70*	4150	4.90	6.74	970.8-21.87
2022	4.91	3.80	1022.9-21.38*	2021	4.92	4.27	1023.0-19.65
4016	4.95	14.86	970.3-25.93*	5014	4.95	20.75	974.9-26.97
4007	4.97	12.53	972.8-23.87*	5012	5.05	21.12	975.9-27.11
2019	5.10	5.10	1045.2-19.28*	4011	5.12	13.97	970.8-24.49
24031	5.15	3.00	1032.0-21.56*	4002	5.20	10.70	975.3-22.45
4006	5.25	12.02	972.8-23.07*	5013	5.34	20.75	973.4-26.55
314360	5.35	0.55	1013.0-16.60*	4153	5.47	7.52	970.8-21.49
2018	5.48	5.39	1049.6-18.57*	4019	5.51	15.41	970.8-25.44
4018	5.56	15.10	970.8-24.47*	4151	5.58	6.05	969.8-20.37
4005	5.59	12.82	970.8-23.23*	24032	5.60	2.82	1029.0-21.18
4000	5.62	11.65	973.2-23.05*	4001	5.66	10.72	969.8-22.90
4010	5.74	14.00	970.3-23.44*	4004	5.75	12.15	969.8-22.57
4017	5.78	14.75	970.3-22.97*	2017	5.81	5.70	1035.1-18.60
4155	5.83	8.95	969.8-21.18*	314460	5.88	12.31	968.0-23.50
4154	5.95	8.06	971.8-20.86*	4009	5.97	13.29	970.3-22.30
2006	5.97	10.69	991.8-20.78*	4152	5.99	6.92	970.8-19.92
2005	5.99	11.10	1000.7-20.73*	2004	6.00	11.59	1027.6-21.12
2007	6.00	10.18	1001.3-20.35*	2003	6.03	12.03	989.9-20.83
905665	6.06	6.53	972.0-20.60*	2016	6.07	6.12	1006.1-19.32

G R A V I T Y D A T A L I S T I N G

100 S T A T I O N S

COORDINATES IN UNITS OF 1/2 MILE EAST AND NORTH OF ORIGIN

STATION	EAST	NORTH	ELEV	BOUG	STATION	EAST	NORTH	ELEV	BOUG
24033	6.08	2.65	1028.0	-18.74*	24041	6.10	5.38	1045.0	-17.85
14102	6.20	17.93	1041.0	-23.90*	2008	6.21	9.70	1063.8	-18.79
2015	6.21	6.58	1014.2	-18.16*	3514	6.25	10.54	993.3	-20.36
14101	6.28	16.71	1030.0	-22.88*	2014	6.30	7.07	1031.4	-18.54
14025	6.34	13.10	984.6	-21.28*	24034	6.42	2.50	1030.0	-18.24
2002	6.45	12.19	996.2	-19.82*	2009	6.48	9.28	1012.6	-19.23
14024	6.50	12.61	982.6	-20.21*	2012	6.50	8.00	1060.1	-18.37
2013	6.51	7.50	1038.7	-18.40*	2011	6.56	8.40	1043.7	-18.85
24040	6.58	5.22	1029.0	-17.10*	14020	6.63	18.70	983.3	-26.59
2010	6.67	8.82	1003.9	-19.03*	3513	6.69	10.60	993.5	-19.81
14026	6.73	12.70	987.1	-19.80*	14021	6.84	18.00	983.3	-26.03
24035	6.87	2.37	1007.0	-18.78*	14006	6.91	14.03	983.8	-20.73
14022	6.91	17.02	986.3	-24.07*	14009	6.93	15.99	984.8	-23.50
3512	6.97	10.89	994.2	-19.82*	14007	7.03	14.73	983.3	-21.35
24039	7.03	5.10	1041.0	-17.05*	2001	7.03	12.13	992.2	-19.60
8017	7.12	0.22	1003.9	-16.93*	8020	7.13	2.15	1005.9	-18.22
14002	7.17	12.66	988.3	-20.11*	3511	7.19	11.30	991.1	-19.96
8019	7.20	1.53	1003.4	-18.19*	14003	7.22	12.60	983.3	-20.27
905765	7.23	12.55	980.0	-20.90*	14001	7.27	12.00	982.8	-19.81
14004	7.31	13.37	983.3	-20.77*	16005	7.33	6.80	1032.1	-17.11
14019	7.40	17.62	983.3	-27.03*	3057	7.41	11.71	1000.6	-19.61
14008	7.44	15.32	985.8	-22.92*	14005	7.46	14.10	986.3	-21.56
14023	7.50	16.90	984.3	-26.50*	16003	7.53	8.33	1030.6	-17.49
8016	7.56	0.70	1003.4	-16.68*	14017	7.56	19.21	984.3	-31.11
16001	7.58	9.10	1029.6	-18.03*	16004	7.59	7.79	1030.6	-17.50
24038	7.59	5.00	1034.0	-16.94*	14010	7.60	16.07	982.8	-25.83
3055	7.62	12.10	1010.9	-20.12*	14018	7.73	18.38	985.8	-29.74
24037	7.74	4.46	1032.0	-17.14*	16006	7.77	7.10	1031.1	-17.24
8018	7.79	1.16	1002.9	-16.21*	14016	7.81	17.95	983.3	-28.55
16002	7.83	8.73	1030.6	-17.83*	3054	7.84	12.28	1037.5	-19.86
16019	7.96	8.10	1031.6	-17.73*	8023	7.98	2.94	1003.4	-16.57
8011	8.00	-1.91	1002.9	-12.71*	16007	8.00	6.82	1031.6	-17.43
8015	8.03	0.32	1003.4	-14.82*	24036	8.03	4.02	1020.0	-16.62
16009	8.08	7.81	1030.6	-17.74*	3053	8.09	12.43	1040.8	-20.12
14012	8.09	16.72	984.8	-27.53*	16016	8.10	9.39	1030.6	-17.94
16017	8.14	8.98	1030.6	-17.73*	14013	8.15	17.52	983.8	-29.03
8012	8.21	-0.76	1002.9	-13.65*	15005	8.21	12.27	1021.3	-20.41
8022	8.25	1.79	1003.4	-16.14*	8024	8.32	3.60	1003.4	-16.92
14015	8.33	18.08	984.3	-31.03*	14011	8.34	15.98	982.8	-26.87
3051	8.38	12.92	1068.0	-20.87*	16008	8.38	6.90	1029.6	-17.53
3049	8.43	13.50	1052.8	-21.73*	14014	8.44	16.84	983.3	-29.02
16018	8.45	8.60	1029.6	-17.68*	8010	8.49	-1.40	1003.4	-13.66
8014	8.51	0.09	1003.4	-15.46*	8027	8.51	1.28	1003.4	-16.39
8025	8.52	2.40	1003.4	-16.80*	16015	8.53	9.98	1030.6	-18.33
16014	8.60	9.49	1030.1	-17.75*	16013	8.65	8.88	1032.1	-17.64
8026	8.68	2.08	1004.4	-17.30*	16010	8.69	7.57	1031.1	-17.43
3047	8.71	14.03	1081.6	-22.61*	15006	8.71	12.08	1018.3	-20.27
8009	8.76	-2.10	1003.4	-13.78*	16011	8.79	8.00	1030.6	-17.36
8013	8.88	-0.16	1003.4	-14.29*	8028	8.88	0.79	1005.4	-15.68
8031	8.89	3.52	1003.9	-17.33*	8033	9.02	4.49	1003.4	-17.92

G R A V I T Y D A T A L I S T I N G

100 S T A T I O N S

COORDINATES IN UNITS OF 1/2 MILE EAST AND NORTH OF ORIGIN

STATION	EAST	NORTH	ELEV	BOUG	STATION	EAST	NORTH	ELEV	BOUG
3045	9.03	14.51	1047.6-	4.63*	16012	9.03	8.25	1030.6	-17.88
15004	9.05	13.16	1017.3-	22.73*	8006	9.09	-1.07	1002.9	-14.31
17005	9.09	6.68	1009.2-	18.66*	17004	9.11	7.23	1009.2	-18.39
8029	9.13	2.00	1003.4-	17.03*	8030	9.17	2.64	1005.9	-17.94
8034	9.19	5.24	1002.9-	18.36*	17003	9.21	7.71	1010.7	-18.51
17006	9.22	6.17	1007.7-	18.35*	21007	9.30	17.59	1015.5	-34.01
1207165	9.30	20.50	1065.0-	40.80*	8032	9.31	3.84	1003.9	-18.26
15007	9.38	12.65	1017.8-	21.95*	15011	9.40	10.60	1017.3	-19.48
905565	9.40	3.98	1003.0-	18.90*	8038	9.42	1.60	1003.4	-16.27
15012	9.44	9.73	1017.8-	19.29*	8008	9.45	-2.18	1004.9	-16.73
15003	9.45	13.00	1018.3-	22.45*	17001	9.50	8.22	1007.7	-19.36
3043	9.53	14.88	1029.0-	26.96*	17007	9.54	6.92	1007.7	-18.79
8004	9.55	0.24	1003.4-	14.10*	8005	9.56	-0.37	1003.4	-14.07
8003	9.61	1.02	1003.4-	15.07*	8007	9.61	-1.16	1004.4	-14.96
15002	9.61	13.65	1018.3-	24.81*	8035	9.63	4.60	1003.4	-18.25
15001	9.63	14.47	1017.3-	26.40*	1034	9.65	14.96	1029.1	-28.44
8037	9.65	3.06	1002.9-	17.82*	15009	9.65	11.94	1017.3	-21.17
21006	9.67	17.72	1014.5-	36.01*	1033	9.69	14.68	1048.6	-26.96
3101	9.70	15.42	1040.1-	29.66*	17002	9.70	7.80	1007.7	-18.94
17008	9.71	6.30	1008.2-	18.38*	8002	9.75	2.33	1003.9	-16.46
8001	9.78	1.77	1003.9-	15.95*	15010	9.80	11.27	1017.8	-20.90
21003	9.82	17.02	1015.0-	35.04*	1032	9.83	14.27	1033.5	-25.89
8036	9.85	3.69	1003.4-	17.16*	15013	9.85	10.48	1018.3	-19.91
17009	9.89	5.77	1009.7-	18.23*	17015	9.90	8.15	1008.2	-19.00
21002	9.90	16.43	1015.0-	33.56*	905865	9.91	12.80	1014.0	-23.00
3102	9.93	15.74	1038.4-	31.65*	21005	9.93	17.48	1015.0	-36.47
15008	10.04	12.40	1017.8-	22.74*	17010	10.05	6.70	1008.2	-19.85
1031	10.12	13.87	1046.3-	25.60*	1025	10.20	10.88	1035.3	-20.35
17014	10.21	8.60	1008.7-	19.72*	3103	10.23	15.88	1060.4	-33.00
21001	10.23	16.30	1016.5-	34.78*	1028	10.24	12.35	1033.9	-22.84
1030	10.25	13.38	1046.5-	25.51*	17011	10.26	7.19	1007.7	-19.34
1029	10.26	12.90	1030.1-	24.51*	1027	10.29	11.90	1044.2	-22.51
1026	10.30	11.38	1052.5-	20.83*	21004	10.38	17.18	1015.0	-36.96
17012	10.39	7.91	1009.2-	19.70*	3200	10.50	16.83	1040.3	-36.77
3041	10.52	16.00	1036.8-	34.01*	3100	10.55	16.43	1019.0	-35.66
17013	10.55	8.74	1008.2-	20.30*	1024	10.55	10.58	1050.2	-20.21
19001	10.65	9.05	1050.6-	19.65*	1023	10.72	10.15	1044.3	-19.98
3300	10.81	17.23	1057.6-	37.87*	19002	10.83	8.62	1051.1	-19.35
7006	10.91	1.66	1003.4-	17.23*	1022	10.91	9.65	1059.3	-19.56
1013	10.93	5.58	1048.9-	19.20*	7007	10.97	2.43	1005.9	-18.22
1012	10.98	5.09	1042.1-	19.22*	1014	10.98	6.03	1044.3	-19.23
1011	11.00	4.67	1015.4-	19.66*	1015	11.02	6.50	1044.2	-19.17
7005	11.05	1.10	1006.4-	17.05*	19003	11.12	8.65	1051.1	-19.49
1021	11.16	9.30	1057.5-	19.55*	24001	11.17	6.90	1047.0	-19.24
1016	11.18	6.94	1047.4-	19.55*	18004	11.19	5.35	1011.2	-20.26
3400	11.22	17.60	1088.2-	38.71*	1010	11.28	4.36	1018.3	-20.26
18001	11.29	4.90	1011.7-	21.13*	24030	11.31	21.80	1078.0	-41.24
1017	11.32	7.41	1051.1-	19.90*	25014	11.34	24.20	1060.9	-39.84
24029	11.35	20.32	1078.0-	41.70*	24212	11.39	13.05	1080.0	-25.33
1018	11.40	7.91	1064.6-	19.53*	1020	11.40	8.94	1058.4	-19.46

G R A V I T Y D A T A L I S T I N G

100 S T A T I C N S

COORDINATES IN UNITS OF 1/2 MILE EAST AND NORTH OF ORIGIN

STATION	EAST	NORTH	ELEV	BOUG	STATION	EAST	NORTH	ELEV	BOUG
7004	11.41	1.83	1005.9	-18.97*	20003	11.42	10.29	1048.0	-22.52
1019	11.47	8.43	1058.9	-19.25*	24002	11.48	6.90	1040.0	-20.52
18005	11.50	5.04	1011.2	-21.43*	906265	11.50	22.90	1060.0	-40.40
20002	11.52	9.72	1046.5	-21.32*	20001	11.53	9.21	1046.5	-20.12
7003	11.57	2.32	1004.9	-19.62*	1009	11.60	4.10	1037.2	-19.70
3500	11.61	17.81	1087.4	-39.45*	24015	11.63	8.21	1069.0	-19.98
18002	11.67	4.40	1011.2	-21.42*	905465	11.75	10.07	1046.0	-23.80
1008	11.80	3.70	1042.1	-19.86*	24003	11.90	6.90	1018.0	-22.91
18003	11.95	4.98	1011.2	-22.26*	20007	11.95	9.59	1046.5	-22.49
1007	11.97	3.28	1019.8	-20.39*	20004	12.00	10.10	1046.5	-22.96
25013	12.00	23.97	1061.9	-40.88*	3600	12.10	17.88	1080.4	-39.83
24014	12.11	8.21	1061.0	-20.49*	25012	12.11	23.35	1060.4	-40.33
1006	12.13	2.85	1007.6	-20.41*	1005	12.32	2.40	1014.2	-20.58
24004	12.36	6.90	1034.0	-23.33*	7002	12.40	3.17	1005.9	-21.42
24211	12.45	12.80	1085.0	-26.05*	20006	12.46	9.90	1046.0	-23.72
20005	12.49	9.47	1046.5	-23.07*	24201	12.49	9.30	1057.0	-22.63
25011	12.52	23.52	1061.4	-41.13*	1004	12.52	1.95	1019.5	-20.92
3700	12.55	18.14	1079.7	-40.20*	24013	12.57	8.28	1068.0	-20.09
1003	12.64	1.46	1026.9	-21.40*	1002	12.69	0.91	1026.8	-21.76
1001	12.70	0.42	1022.5	-22.34*	7001	12.71	2.46	1002.9	-20.92
25009	12.71	22.72	1060.9	-39.90*	22001	12.71	17.69	1051.7	-39.53
24202	12.74	9.75	1074.0	-23.75*	24005	12.78	6.90	1055.0	-20.88
24101	12.83	17.75	1055.0	-39.19*	24106	12.84	14.60	1056.0	-32.54
3030	12.85	18.12	1071.7	-39.65*	24203	12.99	10.20	1062.0	-24.76
22103	13.00	19.72	1059.0	-39.70*	6040	13.05	3.52	1002.9	-20.76
24012	13.05	8.32	1051.0	-21.31*	24105	13.10	14.95	1111.0	-33.54
22004	13.12	17.18	1051.7	-38.43*	22102	13.18	19.50	1060.0	-39.35
24006	13.21	6.90	1056.0	-20.40*	25010	13.21	23.08	1060.9	-40.65
24107	13.23	14.25	1070.0	-30.69*	23019	13.29	1.30	1040.0	-23.27
24210	13.32	13.10	1076.0	-27.60*	22002	13.33	17.92	1051.2	-38.75
22101	13.35	18.97	1062.0	-39.23*	3028	13.35	18.41	1076.4	-38.88
22005	13.41	16.71	1051.7	-37.51*	24104	13.41	15.20	1077.0	-34.23
25007	13.42	22.03	1060.9	-39.34*	24108	13.46	13.90	1101.0	-29.14
24204	13.49	10.65	1079.0	-24.37*	24011	13.50	8.42	1054.0	-20.54
25008	13.52	22.62	1061.9	-39.55*	24209	13.55	12.50	1084.0	-27.19
3027	13.55	18.62	1060.3	-38.44*	24109	13.64	13.60	1092.0	-28.56
24028	13.67	12.05	1082.0	-26.12*	24007	13.69	6.90	1046.0	-20.41
24103	13.71	15.70	1097.0	-34.77*	24110	13.75	14.10	1094.0	-29.43
22003	13.78	17.39	1051.7	-37.31*	23018	13.78	2.20	1041.0	-22.77
24205	13.85	11.10	1081.0	-23.06*	6039	13.87	3.53	1029.6	-20.94
24010	13.88	8.65	1054.0	-21.06*	24111	13.92	14.65	1096.0	-30.28
3026	13.96	19.08	1069.1	-37.63*	24112	13.97	15.20	1098.0	-32.85
24208	14.00	11.60	1081.0	-24.28*	22007	14.01	16.66	1051.7	-36.00
24102	14.01	16.05	1055.0	-34.83*	25006	14.02	22.00	1060.9	-39.39
24009	14.03	7.85	1052.0	-21.27*	24113	14.03	15.65	1063.0	-34.66
22006	14.04	16.09	1051.2	-34.88*	3025	14.09	19.18	1108.5	-37.28
24008	14.12	6.90	1053.0	-20.79*	22008	14.21	17.28	1052.2	-35.79
24206	14.25	11.50	1074.0	-23.62*	23017	14.28	3.05	1045.0	-22.57
25005	14.30	21.42	1061.4	-38.54*	3024	14.31	19.37	1120.4	-36.75
6029	14.33	7.78	1025.9	-22.44*	6038	14.35	4.02	1030.6	-22.11

G R A V I T Y D A T A L I S T I N G

100 S T A T I C N S

COORDINATES IN UNITS OF 1/2 MILE EAST AND NORTH OF ORIGIN

STATION	EAST	NORTH	ELEV	BOUG	STATION	EAST	NORTH	ELEV	BOUG
3023	14.53	19.60	1114.6	-36.40*	6030	14.54	6.68	1025.9	-22.69
24207	14.60	11.85	1092.0	-24.80*	6032	14.67	5.93	1025.9	-22.74
25002	14.70	20.84	1061.4	-37.93*	6037	14.74	3.57	1025.9	-23.97
25004	14.74	21.20	1060.4	-38.05*	6020	14.79	8.70	1026.4	-24.81
6018	14.85	9.79	1025.9	-26.07*	6028	14.89	7.89	1025.9	-25.37
13002	14.89	20.71	1085.1	-35.12*	6034	14.90	4.66	1025.4	-23.73
24026	14.95	13.57	1085.0	-30.11*	3021	15.00	19.90	1094.8	-36.78
6031	15.01	6.43	1025.9	-25.01*	6017	15.02	10.80	1026.4	-26.41
6019	15.08	9.43	1025.4	-26.05*	6033	15.10	5.35	1026.9	-25.45
906365	15.10	20.72	1060.0	-38.00*	6027	15.11	7.28	1026.4	-25.65
24027	15.12	14.88	1083.0	-30.45*	6021	15.23	8.20	1025.4	-26.25
3020	15.27	20.00	1072.0	-37.00*	13001	15.35	21.41	1084.6	-35.96
6036	15.36	3.99	1025.4	-26.38*	6016	15.38	11.18	1027.4	-26.55
6035	15.50	4.60	1028.9	-26.64*	3019	15.50	20.19	1060.4	-36.97
13004	15.51	19.97	1084.6	-34.27*	6022	15.59	8.81	1025.9	-26.84
25003	15.62	21.13	1060.9	-38.54*	13003	15.67	20.66	1085.1	-35.18
1209665	15.70	26.68	1099.0	-53.50*	6026	15.71	6.78	1027.4	-26.78
3018	15.75	20.43	1068.7	-36.31*	25001	15.77	20.31	1062.9	-36.02
6015	15.88	11.80	1026.4	-26.87*	6013	15.90	9.91	1025.9	-27.22
3017	15.92	20.64	1072.6	-36.60*	6014	15.94	10.91	1027.4	-27.02
6025	15.97	7.90	1027.9	-27.15*	13000	16.05	21.18	1084.6	-35.27
11006	16.15	17.81	1048.8	-33.95*	13010	16.19	20.75	1085.1	-34.55
23014	16.22	12.40	1054.0	-27.03*	6008	16.30	11.47	1025.9	-28.24
11007	16.30	18.25	1048.8	-34.13*	13006	16.30	19.53	1084.6	-33.66
6023	16.31	8.80	1027.9	-27.43*	13005	16.32	20.23	1084.6	-34.16
6009	16.40	10.59	1026.4	-28.05*	6024	16.40	8.17	1025.4	-27.68
3015	16.40	21.02	1108.1	-36.76*	13007	16.54	18.91	1086.1	-33.50
6011	16.58	9.10	1027.4	-27.50*	11005	16.58	17.39	1049.3	-32.11
23013	16.58	13.10	1072.0	-27.82*	6007	16.67	12.30	1026.4	-28.24
24023	16.68	6.01	1040.0	-27.63*	6012	16.70	9.73	1025.4	-28.05
11008	16.70	18.05	1048.8	-32.43*	6006	16.77	11.72	1025.9	-28.69
25015	16.78	20.17	1060.4	-34.56*	11004	16.80	16.72	1049.8	-30.34
11009	16.81	15.69	1051.8	-28.78*	11010	16.87	15.00	1049.8	-28.26
13009	16.88	19.42	1084.1	-33.20*	3013	16.90	21.33	1101.4	-36.86
6004	17.06	10.88	1025.9	-28.40*	906465	17.08	16.18	1049.0	-29.40
905365	17.08	10.15	1025.0	-28.70*	11003	17.09	16.10	1049.8	-28.82
23012	17.10	13.60	1072.0	-27.12*	6010	17.13	9.48	1025.9	-27.57
13008	17.14	19.00	1085.6	-33.35*	24022	17.18	4.61	1044.0	-29.66
3012	17.18	21.48	1093.5	-36.51*	6005	17.20	11.66	1026.4	-28.87
25016	17.25	19.10	1060.4	-32.93*	6003	17.44	11.21	1026.4	-28.11
3011	17.46	21.60	1095.7	-36.37*	10001	17.65	18.81	1058.7	-32.91
11002	17.66	16.38	1048.8	-29.02*	6001	17.70	11.59	1026.9	-28.13
3010	17.74	21.65	1098.3	-36.03*	11011	17.76	14.94	1049.3	-28.08
23011	17.95	13.90	1070.0	-27.21*	6002	18.02	11.30	1026.4	-27.62
10002	18.03	17.90	1055.2	-32.25*	11001	18.05	15.81	1050.3	-28.99
3009	18.05	21.71	1119.7	-35.96*	11014	18.14	15.48	1048.8	-29.47
11013	18.38	14.97	1049.3	-29.89*	10005	18.41	16.62	1054.7	-30.91
11012	18.45	14.32	1049.8	-29.39*	23010	18.49	14.25	1058.0	-29.20
10003	18.54	17.50	1055.7	-32.73*	10004	18.93	17.00	1054.7	-32.86
23009	18.96	14.88	1062.0	-33.08*	3005	19.18	21.21	1121.0	-34.04

G R A V I T Y D A T A L I S T I N G

90 S T A T I O N S

COORDINATES IN UNITS OF 1/2 MILE EAST AND NORTH OF ORIGIN

STATION	EAST	NORTH	ELEV	BOUG	STATION	EAST	NORTH	ELEV	BOUG
3003	19.39	21.70	1115.1	-34.05*	24025	19.58	12.42	1069.0	-31.15
23008	19.60	15.70	1075.0	-35.03*	3001	19.69	22.13	1126.7	-34.46
3105	19.80	22.60	1105.7	-35.52*	3106	19.85	23.04	1107.0	-36.40
23007	20.00	16.55	1106.0	-35.77*	3107	20.20	23.36	1069.9	-35.99
24024	20.35	13.63	1075.0	-34.15*	23006	20.39	17.58	1091.0	-37.16
23003	20.45	19.85	1119.0	-33.45*	23015	20.45	20.55	1109.0	-33.35
1405565	20.60	27.38	1023.0	-46.40*	23004	20.61	18.98	1101.0	-35.07
23002	20.64	21.40	1106.0	-33.82*	3108	20.68	23.52	1051.4	-35.88
23005	20.69	18.40	1100.0	-36.30*	23001	20.87	22.30	1098.0	-33.70
26013	20.90	11.35	1084.0	-27.86*	3109	21.15	23.57	1066.7	-35.54
12023	21.45	14.68	1060.1	-37.26*	12026	21.50	15.97	1058.6	-39.37
3110	21.63	23.63	1077.5	-35.81*	12034	21.68	20.92	1058.6	-31.65
26014	21.70	12.15	1094.0	-28.44*	12022	21.73	14.04	1058.6	-34.11
12033	21.79	20.30	1058.1	-32.14*	946260	21.80	25.28	1099.0	-37.90
171650	21.80	25.52	1095.0	-38.60*	23016	21.81	22.95	1084.0	-34.94
12024	21.85	15.32	1058.1	-36.86*	12032	21.90	19.76	1061.6	-33.02
26012	22.04	10.90	1047.0	-27.49*	3122	22.05	23.19	1104.0	-35.26
3121	22.07	23.63	1091.2	-36.00*	3123	22.08	22.70	1109.2	-34.64
12031	22.12	19.03	1058.1	-33.58*	12025	22.16	15.90	1059.6	-36.97
3124	22.19	22.22	1103.7	-34.07*	12021	22.20	14.62	1058.6	-33.15
3125	22.32	21.84	1062.9	-33.74*	12027	22.33	16.40	1058.6	-38.25
12002	22.36	21.72	1058.6	-33.47*	12029	22.43	17.68	1059.1	-36.28
26015	22.45	11.41	1078.0	-27.66*	12003	22.49	20.91	1059.1	-32.71
3111	22.51	23.60	1105.4	-35.96*	12035	22.53	19.70	1059.6	-32.33
12030	22.55	18.36	1060.1	-33.15*	12020	22.57	15.10	1060.1	-33.51
12005	22.69	20.19	1060.1	-32.82*	12028	22.69	16.79	1059.6	-37.94
12001	22.74	21.42	1058.1	-33.48*	12019	22.80	15.71	1059.1	-33.96
3112	22.86	23.23	1132.6	-34.90*	906565	22.90	17.04	1058.0	-37.90
26011	22.92	10.90	959.0	-30.15*	12015	23.00	18.97	1058.1	-32.30
12004	23.05	20.78	1059.1	-33.32*	905265	23.06	12.70	958.0	-32.50
26009	23.07	12.90	959.5	-31.54*	3113	23.10	22.81	1133.9	-34.69
12007	23.10	19.34	1059.1	-32.80*	12016	23.15	17.97	1058.1	-33.15
26010	23.23	11.20	961.0	-30.56*	12006	23.34	19.81	1058.1	-33.32
3114	23.35	22.41	1138.9	-34.24*	12017	23.40	17.17	1058.6	-34.82
12018	23.42	16.38	1059.1	-34.60*	26006	23.43	10.30	960.0	-30.21
26008	23.45	11.90	959.0	-31.10*	1205265	23.62	6.25	983.0	-28.60
3115	23.72	22.17	1134.5	-34.24*	946060	23.78	24.20	1024.0	-40.20
26005	23.80	9.80	959.5	-30.22*	12008	23.81	19.26	1059.1	-33.03
12009	23.90	18.80	1058.6	-33.20*	26007	23.94	11.00	961.0	-31.13
12011	24.00	19.80	1058.6	-33.65*	3116	24.20	22.10	1074.9	-35.24
26003	24.23	9.45	959.5	-30.28*	12012	24.25	20.01	1058.6	-33.79
26002	24.37	8.90	958.0	-30.15*	26004	24.40	10.30	959.5	-31.13
12013	24.49	19.19	1058.6	-33.69*	12010	24.50	18.42	1059.1	-32.98
26001	24.64	8.00	959.5	-28.06*	3117	24.70	22.10	1018.8	-35.93
12014	24.95	18.71	1058.6	-33.69*	3118	25.16	22.00	967.7	-36.35

********** TOTAL 791 STATIONS **********

MAIN CONTROL PROGRAM FOR GRAVITY EFFECT OF A PRISM

```
C      THREE-DIMENSIONAL MODEL STUDIES OF REGIONAL GRAVITY ANOMALIES.
C      (COORDINATES IN METRES,GRAVITY ANOMALY IN MILLIGALS)
C
       DIMENSIONXI1(100),XI2(100),YI1(100),YI2(100),RHO(100),BOTTOM(100),
      1TOP(100),ISTANO(100)
       COMMONX1,Y1,X2,Y2,X1C,Y1C,X2C,Y2C
  120  READ(5,1) IB, (ISTANO(K),XI1(K),XI2(K),YI1(K),YI2(K),BOTTOM(K),
      1TOP(K),RHO(K),K = 1,IB)
       NPAGE = 1
       IC = 1
       WRITE(6,7)  NPAGE
       DO 100 N = 1,IB
       IF(IC - 25) 25,25,35
   35  NPAGE = NPAGE + 1
       WRITE(6,7)  NPAGE
       IC = 1
   25  WRITE(6,6) N,ISTANO(N),XI1(N),XI2(N),YI1(N),YI2(N),BOTTOM(N) ,
      1TOP(N),RHO(N)
       IC = IC + 1
  100  CONTINUE
   10  READ(5,2) X,Y,DX,DY,L,M,GMAX
       IF(L-999)115,40,115
  115  IF(L)15,120,15
   15  NPAGE = NPAGE + 1
       WRITE(6,9) NPAGE
       WRITE(6,3) X,Y,DX,DY,L,M,IB,GMAX
       IC = 1
       DO 30 I = 1,L
       CX = I-1
       DO 30 J = 1,M
       CY = J-1
       SUM = 0.
       DO 20 K = 1,IB
       X1C = XI1(K) - X - CX*DX
       X1 = ABS (X1C)
       X2C = XI2(K) - X - CX*DX
       X2 = ABS (X2C)
       Y1C = YI1(K) - Y - CY*DY
       Y1 = ABS (Y1C)
       Y2C = YI2(K) - Y - CY*DY
       Y2 = ABS (Y2C)
       HB = BOTTOM(K)
       HT = TOP(K)
       DEL G = (.37056*RHO(K) )*(DEL G5(HB) - DEL G5(HT))
       IF(GMAX)16,20,18
   16  IF(ABS (DEL G) - ABS (GMAX)) 20,17,17
   17  IF(IC - 25) 18,18,50
   50  NPAGE = NPAGE + 1
       WRITE(6,9) NPAGE
       IC = 1
```

MAIN CONTROL PROGRAM FOR GRAVITY EFFECT OF A PRISM

```
18 WRITE(6,4) I,J,ISTANO(K),DELG
   IC = IC + 1
20 SUM = SUM + DEL G
   IF(1 - J) 44,46,46
44 IF(IC - 25) 45,45,46
46 NPAGE = NPAGE + 1
   WRITE(6,9) NPAGE
   IC = 1
45 WRITE(6,5) I,J,SUM
   IC = IC + 1
30 CONTINUE
   GO TO 10
40 CALL EXIT
 1 FORMAT(I5/(I10,5F10.0,F5.0,F5.2))
 2 FORMAT(4F10.0,2I5,F5.1)
 3 FORMAT(14HO ORIGIN   X =F7.0,3X,3HY =F7.0,2X,4HDX =F7.0,2X,4HDY =
  1F7.0,4X,3HL =I3,2X,3HM =I3,3X,14HNO.OF BLOCKS =I3,4X,6HGMAX =F7.1)
 4 FORMAT(1HO,54X,3HI =I3,4X,3HJ =I3,5X,8HBLOCK NO I5,7X,9HDELTA G =
  1F10.5)
 5 FORMAT(1HO,3HI =I3,4X,3HJ =I3,5X,7HDEL G = F10.5)
 6 FORMAT(1HO,I5,7X,I5,2X,6F10.1,F10.2)
 7 FORMAT(1H1,35X,31HCOORDINATES  OF  CORNER  POINTS,47X,4HPAGE I3/
  16H    NO,7X,5HBLOCK,65X,7HDENSITY/1H ,27X,2HX1,8X,2HX2,8X,2HY1,8X,
  22HY2,4X,6HBOTTOM,7X,3HTOP/1HO)
 9 FORMAT(1H1,99X,8X,4HPAGE I3/1HO)
   END
```

SUBROUTINE TO CALCULATE GRAVITY EFFECT OF A PRISM

```
      FUNCTION DEL G5(H1)
      COMMONX1,Y1,X2,Y2,X1C,Y1C,X2C,Y2C
      DIMENSION X(4),Y(4)
      DEL G5 = 0.
      IF(H1)777,510,777
  777 C = 1.5707963
      CONS = .018
      X12 = X1*X1
      X22 = X2*X2
      H2 = H1**2
      Y22 = Y2**2
      Y12 = Y1**2
      R22 = SQRT (X22 + Y22)
      R21 = SQRT (X22 + Y12)
      R12 = SQRT (X12 + Y22)
      R11 = SQRT (X12 + Y12)
      R2 = Y22 + H2
      R1 = Y12 + H2
      R222 = SQRT (X22 + Y22 + H2)
      R212 = SQRT (X22 + Y12 + H2)
      R122 = SQRT (X12 + Y22 + H2)
      R112 = SQRT (X12 + Y12 + H2)
      RO22 = SQRT (R2)
      RO12 = SQRT (R1)
      BN1 = (Y2 + R22)/(Y2 + R222)
      BN2 = (Y1 + R21)/(Y1 + R212)
      BN3 = (Y2 + R12)/(Y2 + R122)
      BN4 = (Y1 + R11)/(Y1 + R112)
      BN5 = (X2 + R22)/(X2 + R222)
      BN6 = (X1 + R12)/(X1 + R122)
      BN7 = (X2 + R21)/(X2 + R212)
      BN8 = (X1 + R11)/(X1 + R112)
      IF(BN1)701,701,702
  702 T1 = ALOG(BN1)
  703 IF(BN2)711,711,712
  712 T2 = ALOG(BN2)
  713 IF(BN3)721,721,722
  722 T3 = ALOG(BN3)
  723 IF(BN4)731,731,732
  732 T4 = ALOG(BN4)
  733 IF(BN5)741,741,742
  742 T5 = ALOG(BN5)
  743 IF(BN6)751,751,752
  752 T6 = ALOG(BN6)
  753 IF(BN7)761,761,762
  762 T7 = ALOG(BN7)
  763 IF(BN8)771,771,772
  772 T8 = ALOG(BN8)
  773 A1 = (R2 + Y2*R222)/((Y2 + R222)*RO22)
      A2 = (R2 + Y2*R122)/((Y2 + R122)*RO22)
```

SUBROUTINE TO CALCULATE GRAVITY EFFECT OF A PRISM

```
      A3 = (R1 + Y1*R212)/((Y1 + R212)*R012)
      A4 = (R1 + Y1*R112)/((Y1 + R112)*R012)
      IF(A1 - 1.)11,12,12
   11 T9  = ATAN (A1/SQRT (1. - A1**2))
   15 IF(A2 - 1.)21,22,22
   21 T10 = ATAN (A2/SQRT (1. - A2**2))
   25 IF(A3 - 1.)31,32,32
   31 T11 = ATAN (A3/SQRT (1. - A3**2))
   35 IF(A4 - 1.)41,42,42
   41 T12 = ATAN (A4/SQRT (1. - A4**2))
   50 IF(Y1C)801,802,801
  801 Q1 = Y1/Y1C
  803 IF(Y2C)811,812,811
  811 Q2 = Y2/Y2C
  813 IF(X1C)821,822,821
  821 Q3 = X1/X1C
  823 IF(X2C)831,832,831
  831 Q4 = X2/X2C
  507 IF(Q1 - Q2 + Q3 - Q4 + 2.)53,501,52
  501 IF(Q1 - Q2)502,503,504
  502 D11 = SQRT (X12 + H2)
      D22 = SQRT (X22 + H2)
      A5 = H1/D22
      A6 = H1/D11
      IF(A5 - 1.)210,211,210
  210 T15 = ATAN (A5/SQRT (1. - A5*A5))
  212 IF(A6 - 1.)220,221,220
  220 T16 = ATAN (A6/SQRT (1. - A6*A6))
  225 IF(X2)230,230,231
  231 T13 = ALOG(X2/D22)
  232 IF(X1)233,233,234
  234 T14 = ALOG(X1/D11)
  235 DEL G5 = CONS*(X2*(T1 + T2 - T13 - T13) - X1*(T3 + T4 - T14 - T14)
     1+ Y2*(T5 - T6) + Y1*(T7 - T8) + H1*(T9 - T10 + T11 - T12
     2- T15 - T15 + T16 + T16))
      GO TO 510
  503 IF(Y2)240,240,241
  241 T17 = ALOG(Y2/SQRT (Y22 + H2))
  242 IF(Y1)243,243,244
  244 T18 = ALOG(Y1/SQRT (Y12 + H2))
  245 DEL G5 = CONS*(X2*(T1 - T2) + X1*(T3 - T4) + Y2*(T5 + T6 -T17-T17)
     1- Y1*(T7 + T8 - T18 - T18) + H1*(T9 + T10 - T11 - T12))
      GO TO 510
  504 WRITE(6,505)
      GO TO 510
   52 DEL G5 = .018*(X2*(T1 - T2) - X1*(T3 - T4) + Y2*(T5 - T6)
     1- Y1*(T7 - T8) + H1*(T9 - T10 - T11 + T12))
  510 DEL G5 = ABS (DEL G5)
      RETURN
   53 X(1) = X1
```

SUBROUTINE TO CALCULATE GRAVITY EFFECT OF A PRISM

```
      IF(X1)251,52,251
  251 IF(X2)252,502,252
  252 IF(Y1)253,503,253
  253 IF(Y2)254,503,254
  254 X(1) = X1
      X(2) = X1
      X(3) = X2
      X(4) = X2
      Y(1) = Y1
      Y(2) = Y2
      Y(3) = Y1
      Y(4) = Y2
      DEL G5 = 0.
      DO 70 M = 1,4
      S1 = SQRT (X(M)**2 + Y(M)**2)
      S2 = SQRT (X(M)**2 + Y(M)**2 + H2)
      D1 = Y(M) + S2
      D2 = X(M) + S2
      D3 = SQRT (X(M)**2 + H2)
      D4 = SQRT (Y(M)**2 + H2)
      RM = Y(M)**2 + H2
      T21 = ALOG((Y(M) + S1)/D1)
      T22 = ALOG(X(M)/D3)
      T23 = ALOG((X(M) + S1)/D2)
      T24 = ALOG(Y(M)/D4)
      A21 = (RM + Y(M)*S2)/(D1*D4)
      A23 = H1/D3
      IF(A21 - 1.)260,261,260
  260 T25 = ATAN (A21/SQRT (1. - A21*A21))
  262 IF(A23 - 1.)263,264,263
  263 T27 = ATAN (A23/SQRT (1. - A23*A23))
   70 DEL G5 = DEL G5 + X(M)*(T21 - T22) + Y(M)*(T23 - T24)
     1+ H1*(T25 - T27)
      DEL G5 = .018*DEL G5
      GO TO 510
   12 T9 = C
      GO TO 15
   22 T10 = C
      GO TO 25
   32 T11 = C
      GO TO 35
   42 T12 = C
      GO TO 50
  701 T1 = 1.
      GO TO 703
  711 T2 = 1.
      GO TO 713
  721 T3 = 1.
      GO TO 723
  731 T4 = 1.
```

```
      GO TO 733
741   T5 = 1.
      GO TO 743
751   T6 = 1.
      GO TO 753
761   T7 = 1.
      GO TO 763
771   T8 = 1.
      GO TO 773
802   Q1 = 1.
      GO TO 803
812   Q2 = 1.
      GO TO 813
822   Q3 = 1.
      GO TO 823
832   Q4 = 1.
      GO TO 507
211   T15 = C
      GO TO 212
221   T16 = C
      GO TO 225
230   T13 = 1.
      GO TO 232
233   T14 = 1.
      GO TO 235
240   T17 = 1.
      GO TO 242
243   T18 = 1.
      GO TO 245
261   T25 = C
      GO TO 262
264   T27 = C
      GO TO 70
505   FORMAT(14HERROR TYPE 504)
      END
```

```
      GRAVRED PROGRAM TO COMPUTE BOUGUER GRAVITY FROM FIELD DATA

      DIMENSION N(500),TM(500),R(500),H(500),TL(500),GL(500),TD(500),
     1TER(500),GR(500),IB(50),G(50),DATE(9)
      DATA N,TM,R,H,TL,GL,TD,TER,GR,IB,G,DATE/500*0,4000*0.,50*0,59*0./
      NUMB = 0
      KN = 0
  100 READ(5,1) DENS,S,BLAT,SCALE,DATE
      IF(DENS.GT. 4.) GO TO 901
      IF(DENS.EQ.0.09) GOTO901
      LOOP = 0
      READ(5,2) IBN,( IB(J),G(J),J=1,IBN)
      WRITE(6,3)
      WRITE(6,4)DATE
      KN= 0
  101 KN= KN+1
      TM3 = 50.
      TM4 = 50.
      IT = KN
      M=0
      D1 = 0.
      D2 = 0.
      R3 = 0.
      R4 = 0.
      NT =0
      DD = 0.
      DT = 0.
      LOOP =LOOP + 1
      READ(5,5) N(KN),TM(KN),R(KN),H(KN),TL(KN),GL(KN),TD(KN),TER(KN)
CARD FOLLOWING MUST BE REMOVED IF TIME BASE IS THE 24 HOUR CLOCK
      IF(TM(KN).LT.8.07) TM(KN)=TM(KN)+12.00
      IF(N(KN).EQ.999999) GO TO 200
      ITM=TM(KN)
      T=ITM
      TM(KN)=T+(TM(KN)-T)/.6
  103 DO102 J=1,IBN
      IF(N(KN)-IB(J)) 102,105,102
  102 CONTINUE
      GO TO 151
  128 IF(M.EQ.3) GOTO 118
      WRITE (6,16) N(KN),LOOP
      M=3
      GO TO 118
  105 R1=R(KN)
      V1=G(J)
      TM1=TM(KN)
      TD1=TD(KN)
      DT=0.
  106 M=1
      GO TO 118
CHECK FOR BASE OR REPEAT STATIONS
  108 DO 107 J=1,IBN
```

```
      IF(N(KN)-IB(J)) 107,109,107
  107 CONTINUE
      JB=KN-1
  130 DO131 J=IT,JB,1
      IF(N(KN)-N(J)) 131,133,131
  131 CONTINUE
      GO TO 106
  120 KN=KN-1
      WRITE(6,7) LOOP,KN
      GOTO200
  133 R3=R(J)
      R4=R(KN)
      TM3=TM(J)
      TM4=TM(KN)
      TD3=TD(J)
      TD4=TD(KN)
      DT=TM4-TM3
      N3= N(KN)
      D2= (R3-R4-(TD4-TD3)/S)/DT
      IF(NT)157,106,157
  157 M=2
      GO TO 118
  109 R2=R(KN)
      V2=G(J)
      TM2=TM(KN)
      TD2=TD(KN)
      D1=(R1-R2-R3+R4-(V1-V2+TD2-TD1)/S)/(TM2-TM1-DT)
      GO TO 110
  151 J=0
      IF(KN.EQ.1)GOTO128
      JB=KN-1
      IF(IT.GT.JB)GOTO154
      DO 152 I=IT,JB,1
      IF(N(KN)-N(I))152,153,152
  153 J = I
  152 CONTINUE
      IF(J)160,154,160
  154 DO155 J=1,IBN
      IF(N(KN)-IB(J)) 155,109,155
  155 CONTINUE
      M=2
  118 KN=KN+1
      IF(M.EQ.3) KN=1
      READ(5,5) N(KN),TM(KN),R(KN),H(KN),TL(KN),GL(KN),TD(KN),TER(KN)
CARD FOLLOWING MUST BE REMOVED IF TIME BASE IS THE 24 HOUR CLOCK
      IF(TM(KN).LT.8.07) TM(KN)=TM(KN)+12.00
      ITM=TM(KN)
      T=ITM
      TM(KN)= T+(TM(KN)-T)/.6
      IF(N(KN)-999999)119,120,119
```

```
  119 GOTO(108,151,103),M
CHECK WHETHER INSIDE OUTSIDE OR INTERLOCKING LOOP
  160 IF(GR(J)) 164,163,164
  163 NT =1
      GO TO 133
C     ALLOW ONLY 3 STATION OVERLAP IN INTERLOCKING LOOPS
  164 IF(KN-J-3)166,166,165
  165 WRITE(6,6) N(KN)
      GO TO 154
  166 V1=GR(J)
      R1=R(J)
      R2=R(KN)
      TM1=TM(J)
      TM2=TM(KN)
      TD1=TD(J)
      TD2=TD(KN)
      V2=GR(J)
      GO TO 110
  110 J=IT-1
  111 J=J+1
      IF(TM(J).LT.TM3)GO TO 112
      IF(TM(J).LT.TM4) GO TO 115
      DA=0.
      DB=0.
      DC=D1
      DD=D1*(TM3-TM1)+D2*(TM4-TM3)
      GO TO 117
  115 DA=0.
      DB=D2
      DC=0.
      DD=D1*(TM3-TM1)
      GO TO 117
  112 DA=D1
      DB=0.
      DC=0.
      DD=0.
      GO TO 117
  117 GR(J)=V1+S*(R(J)-R1+DA*(TM(J)-TM1)+DB*(TM(J)-TM3)+DC*(TM(J)-TM4)
     1+ DD) +TD(J)-TD1
      IF(J.LT.KN)        GO TO 111
      T=TM2-TM1
  147 WRITE(6,8) LOOP,N(IT),N(KN),T
      IF(TM3.LT.50.) WRITE(6,9)N3
      WRITE(6,18) TM1,TM2,TM3,TM4,D1,D2
      WRITE(6,20) R1,R2,V1,V2,IT,KN
      V1=V2
      R1=R2
      TM1=TM2
      TD1=TD2
      DT=0.
```

```
  122 GO TO 101
  200 WRITE(6,13) DENS ,S
      WRITE(6,10)
      KN=KN-1
      IF(BLAT) 300,201,300
  300 LAT= BLAT
      T = LAT
      PHI = (T+(BLAT-T)/.6)*3.14159/180.
      S1=SIN(PHI)
      S2=SIN(2.*PHI)
      ZZ= 978049.
      PP = ZZ+ZZ*.0052884*S1*S1-ZZ*.0000059*S2*S2
      RLE = 1.307*S2
      IF(SCALE.EQ.0.) SCALE=1.
      RLE = RLE*SCALE
  201 DO 400 J=1,KN,1
      IF(TL(J))250,202,250
  250 IF(BLAT) 302,301,302
  301 LAT=TL(J)
      T=LAT
      PHI = (T+(TL(J)-T)/.6)*3.14159/180.
      S1=SIN(PHI)
      S2=SIN(2.*PHI)
      AM=(TL(J)-T)*100.
      ZZ= 978049.
      P   = ZZ+ZZ*.0052884*S1*S1-ZZ*.0000059*S2*S2
      GO TO 350
  202 WRITE(6,11) N(J),GR(J)
      GO TO 400
  302 P=PP+RLE*TL(J)
      A = (BLAT-T)/.6 + TL(J)* SCALE/ 69.13
C    FACTOR 69.13 MILES/DEGREE LATITUDE IS VALID AT 53 TO 54 NORTH
      AB = T+A
      LAT=AB
      T=LAT
      AM=(AB-T)*60.
  350 GB=GR(J)-P+0.09406*H(J)-0.01276*DENS*H(J)+TER(J)
      LG = GL(J)
      GLON= LG
      GLM=(GL(J)-GLON)*100.
      IF(J-IT)351,351,352
  351 C=0.
      IF(G(1)-980000.) 353,353,354
  354 IF(G(1)-982000.) 352,353,353
  353 C=V1- GB
      WRITE(6,21) C
  352 GB=GB+C
      WRITE(6,11) N(J),GR(J),GB,T,AM,GLON,GLM,H(J),J
      IF(BLAT.EQ.0.) GOTO400
C***** NEXT TWO CARDS FOR FLIN FLON AREA ONLY
```

```
      IF(BLAT.EQ.54.4000) TL(J)=TL(J)+11.40
      IF(BLAT.EQ.54.4500) TL(J)=TL(J)+22.80
      IGL=100.*GL(J)+.5
      ITL=100.*TL(J)+.5
      IGB=100.*GB+.5
      WRITE(7,23)N(J),IGL,ITL,IGB
  400 CONTINUE
  401 WRITE(6,12) KN
      NUMB = NUMB + KN
      GOTO100
  900 WRITE(6,14) NUMB
      WRITE(6,17) PHI,S1,S2,PP,P,RLE
      GO TO 902
  901 IF(DENS.EQ.0.09) GO TO 900
      WRITE(6,19) KN
      WRITE(6,15)
    1 FORMAT(F5.2,3F10.5,9A5)
    2 FORMAT(I2,I8,F10.2,3(I10,F10.2)/(4(I10,F10.2)))
    3 FORMAT(1H1,40X,51HSASKATCHEWAN RESEARCH COUNCIL GEOPHYSICS LABORAT
     1ORY  //57X,19HGRAVITY CALCULATION  /)
    4 FORMAT (17X,9A5,/)
    5 FORMAT(I10,3F10.2,2F10.4,2F10.2)
    6 FORMAT(16H REPEAT STATION ,I10,31H NOT USED FOR DRIFT CALCULATION)
    7 FORMAT(30H 999999 CARD FOUND, DRIFT LOOP,I3,11H INCOMPLETE,I10,1X,
     113HSTATIONS READ  )
    8 FORMAT(11H DRIFT LOOP,I3,27H COMPLETE -FIRST STATION IS,I10,16H LA
     1ST STATION IS,I10,13H ELAPSED TIME,F7.3,6H HOURS  )
    9 FORMAT( 8H STATION,I10,31H USED AS BASE FOR INTERIOR LOOP )
   10 FORMAT(45H   STATION   GRAVITY   BOUGUER        LATITUDE,11X,23HLON
     1GITUDE     ELEVATION/13X,66HMGALS       MGALS    DEGREES  MINUTES
     2DEGREES  MINUTES  FT. ASL  )
   11 FORMAT(I10,2F10.2,5X,F5.0,F8.3,6X,F6.0,F8.3,F10.2,4X,I4 )
   12 FORMAT(38H DATA UNDER ONE CONTROL CARD FINISHED ,I10,9H READINGS)
   13 FORMAT(18H BOUGUER DENSITY =,F5.2,28H GRAVIMETER SCALE CONSTANT =,
     1F10.5,29H MILLIGALS PER SCALE DIVISION / )
   14 FORMAT(27H ALL COMPUTATION FINISHED  ,I5, 6H TOTAL  )
   15 FORMAT(49H DENSITY MUST BE SPECIFIED BETWEEN 1.00 AND 4.00   )
   16 FORMAT(42H BASE VALUE MUST BE SPECIFIED FOR STATION ,I10,15H IN DR
     1IFT LOOP   ,I3 )
   17 FORMAT(7H PHI = ,E14.8,6H S1 = ,E14.8,6H S2 = ,E14.8,6H PP =  ,
     1E14.8,10H LAST P = ,E10.8, 7H RLE =  ,E10.8)
   18 FORMAT(7H TM1 = ,E14.8,7H TM2 = ,E14.8,7H TM3 = ,E14.8,7H TM4 =  ,
     1E14.8,6H D1 = ,E14.8,6H D2 = ,F14.8  )
   19 FORMAT(25H CONTROL CARD INCORRECT   ,I4,7HTH CARD  )
   20 FORMAT ( 6H R1 = ,E14.8,6H R2 = ,E14.8,6H V1 = ,E14.8,6H V2 = ,
     1E14.8,16H KN RANGES FROM ,I4,4H TO ,I4)
   21 FORMAT(6H C = ,F14.8)
   22 FORMAT(10H 902 WRITE,I10,I5,I5,F5.2,F10.2,E15.8,E15.8,I5,I5)
   23 FORMAT(1X,I7,2I5,I6)
  902 STOP
```

GRAVRED PROGRAM TO COMPUTE BOUGUER GRAVITY FROM FIELD DATA

END

CALCULATION OF MODEL FAULT CURVES (NORMALIZED) CONTROL PROGRAM

```
C       REQUIRES FUNCTIONS G(X), G1(X), G2(X)
        COMMON D,H
        WRITE(6,11)
   10   FORMAT(7(E15.5))
   11   FORMAT(  105H    X                G PI/2         DG PI/2         D2G
     1PU/2          G PI/3         DG PI/3         D2G PI/3          )
        H = 0.
        DO 1 J=1,401,5
        X = J
        X = (X-201.)/100.
        D = 3.1416/2.
        A = G(X)
        B = G1(X)
        C = G2(X)
        D = 3.1416/3.
        A1 = G(X)
        B1 = G1(X)
        C1 = G2(X)
    1   WRITE(6,10) X,A,B,C,A1,B1,C1
        CONTINUE
        STOP
        END
```

CHARACTERISTIC CURVES FOR A FAULT AT ZERO DEPTH CONTROL PROGRAM

```
C     REQUIRES FUNCTIONS G(X), G1(X), G2(X)
CHARACTERISTIC CURVES FOR A FAULT
      COMMON D,H
      DIMENSION DIS(245), R(245), F(245), RHO(245)
C     D= DIP  H= DEPTH
      H=0.
      DO100 KD=15,90,5
      D=KD
      D=D*3.1415927/180.
      WRITE(6,2) KD
    2 FORMAT(1HO, 16H FAULT FACE DIPS,I4,8H DEGREES//2(57H   (X2-X1)/L
     1X1/X2          G/XS      RHO*L/G      ) )
C      L=THICKNESS IN KILOMETERS
      DO 101 KX= 100,245,5
      X=KX
      X = (X-250.)/100.
C     S1 AND S2 ARE SLOPES OF THE GRAVITY CURVE
      S = G1(X)
      X2 = -1.*X
      X3 = -1.2*X
      S2 = G1(X2)
   50 S3 = G1(X3)
      SM = (S3-S2)/(X3-X2)
      X1 = X2 + (S-S2)/SM
      S1 = G1(X1)
      IF(ABS(S1-S).LT.0.0001  )GOTO200
      X2 = X3
      X3 = X1
      S2 = S3
      GOTO50
  200 F(KX) = (G(X1)-G(X))/(X1-X)/S1
      R(KX) = X/X1
      DIS(KX) = X1-X
      RHO(KX) = 1./3.14159/13.3333/(G(X1)-G(X))
  101 CONTINUE
      WRITE(6,1) (DIS(KX),R(KX),F(KX),RHO(KX) , KX=100,245,5)
  100 CONTINUE
    1 FORMAT (2(1X,4E14.5))
      STOP
      END
```

FUNCTION G(X) TO COMPUTE GRAVITY EFFECT OF FAULT

```
CALCULATION OF GRAVITY EFFECT OF A FAULT
C   D=DIP   H=DEPTH   S=SIN(D)   C=COS(D)
      FUNCTION G(X)
      COMMON D,H,S,C
      W=0.
      B = X - COTAN(D)
      A = B*B+(H+1.)*(H+1.)
      TB = ATAN2(B,(H+1.))
      IF(X.EQ.0.) GO TO 1
      TX = ATAN2(X,H)
      GO TO 2
    1 TX=0.
      IF(H.EQ.0.) W= 10.E-25
    2 G     =1./3.14159 *(1.5708 + (H+1.)*TB - H*TX + (X*S*S + H*S*C)
     1*0.5*ALOG(A/(X*X+H*H+W))-   ( X*S*C+H*C*C)*(TB-TX))
      RETURN
      END
```

```
      FUNCTION G1(X) TO COMPUTE FIRST HORIZONTAL DERIVATIVE FAULT CURVE

CALCULATION OF HORIZONTAL GRADIENT OF GRAVITY DUE TO A FAULT
      FUNCTION  G1(X)
      COMMON D,H
      B = X- COTAN(D)
      A = B*B + (H+1.)*(H+1.)
      C = COS(D)
      S = SIN(D)
      IF(X.EQ.0.) GO TO 1
      TX = ATAN2(X,H)
      GO TO 2
    1 TX = 0.
    2 G1    =1./3.14159 * ((H+1.)*(H+1.)/A +S*S*(X*B/A-1. + 0.5*ALOG
     1(A/(X*X+H*H)))  + S*C*((H*B-H*X-X)/A - ATAN2(B,(H+1.))+TX
     1) - H*C*C*(H+1.)/A )
      RETURN
      END
```

```
      FUNCTION G2(X) TO COMPUTE SECOND HORIZONTAL DERIVATIVE FAULT CURVE


CALCULATION OF D2(G)/DX2 FOR FAULT CONTACT
      FUNCTION G2(X)
      COMMON D,H
      B = X - COTAN(D)
      A = B*B + (H+1.)*(H+1.)
      S = SIN(D)
      C = COS(D)
      G2    =1./3.14159 * (-2.*B*(H+1.)*(H+1.)/A/A +S*S*((X+B)/A-2.*
     1X*B*B/A/A + B/A - X/ (X*X+H*H + 10.E-25)) + S*C*((-A-2.*B*(H*B-
     1H*X-X))/A/A - (H+1.)/((H+1.)*(H+1.)+B*B)+ H/(H*H+X*X+10.E-25))
     1-H*C*C*(-2.*B*(H+1.)/A/A))
      RETURN
      END
```

GRADATIONAL DENSITY CONTRAST

```
      DIMENSION B(51),A(8), G(8,51)
      GNORM(X,H,W) = ((H*H - (X- W)*(X- W))/2. * ALOG(H*H + (X- W)*(X-W
     1)) - 2. * H * (X- W)* ATAN2((X- W),H) + (X- W)*(X- W)*
     10.5 * ALOG((X-W)*(X-W))
     1-(H*H - X*X)/2. * ALOG (H*H + X*X) + 2. * H * X * ATAN2(X,H)
     1- X*X/2.*ALOG (X*X) + 3.14159265 * H )
      W = 1.0
      DO 10K = 1,8
      A(K)=0.5*FLOAT(K)
      H = A(K)
      DO 10 J=1,51
      X = 0.1*FLOAT(J-21)
      X = 0.1E-30 + X
      B(J) = X
      G(K,J) = 6.2831853*A(K)/GNORM(X,H,W)
   10 CONTINUE
      WRITE(6,1) A
    1 FORMAT (3H H=, 8(6X,F6.2,3X))
      WRITE(6,2) ( B(J),(G(K,J),K=1,8),J=1,51)
    2 FORMAT(3H X=,F6.2,8E15.6)
      STOP
      END
```

CHARACTERISTIC CURVES FOR GRADATIONAL DENSITY CONTRAST

```
C       USES SLOPE OF GRAVITY CURVE AT MIDPOINT
        DIMENSION RHO(200),RATIO(200)    ,B(200)
        WRITE(6,4)
      4 FORMAT(1H1,1X,4(30H     X/L      G/2XS    L*RHO/G      ))
        DO1 J=1,200
        X=J
        X=X/100.
        B(J) = 2.*X
        FX=2.*ATAN(X)+    X*ALOG      ((X*X+1.)/(X*X+1.0*10.0**(-30)))
        RATIO(J)=FX/ALOG(SQRT((X*X+1.)/(X*X+1.0*10.0**(-30))))/2./X
      1 RHO(J) = 1./FX/13.333
      2 WRITE(6,3)   (B(K),RATIO(K), RHO(K), K= 1,200)
      3 FORMAT (1H0,4(3F10.6))
        STOP
        END
```